THE MINOR PLANET BULLETIN

BULLETIN OF THE MINOR PLANETS SECTION OF THE ASSOCIATION OF LUNAR AND PLANETARY OBSERVERS

VOLUME 52, NUMBER 3, A.D. 2025 JULY-SEPTEMBER 191.

EDITOR'S NOTE

A few words of appreciation and admiration are appropriate to the author, Eric V. Dose, for more nearly 20 years of contributions to the study of minor planets and high precision photometry of variable stars. For the past five years or so, Mr. Dose has concentrated his attention to measuring and analyzing asteroid lightcurves, contributing nearly two dozen publications as an author or co-author in *The Minor Planet Bulletin*. All of this work has been exemplary in its attention to detail and thorough consideration of results. This appreciation is extended in response to the author noting in his Acknowledgments that he is bringing his astronomical observing career to a conclusion.

LIGHTCURVES OF FOURTEEN ASTEROIDS

Eric V. Dose
3167 San Mateo Blvd NE #329
Albuquerque, NM 87110
mp@ericdose.com

(Received: 2025 March 8)

We present lightcurves and synodic rotation periods for fourteen asteroids, including the lead members for two recognized families: 1332 Marconia and 3811 Karma.

We present asteroid lightcurves obtained via the workflow process described by Dose (2020) and later improved (Dose, 2021a). This workflow applies to each image an ensemble of typically 25-80 nearby comparison ("comp") stars selected from the ATLAS refcat2 catalog (Tonry, 2018). This abundance of comp stars and our custom diagnostic plots allow for rapid identification and removal of outlier, variable, and poorly measured comp stars.

The product of this custom workflow is one night's time series of absolute Sloan r' (SR) magnitudes for one target asteroid. These absolute magnitudes are corrected for instrument transforms, sky extinction, and image-to-image ("cirrus") fluctuations, and thus they represent absolute magnitudes at the top of earth's atmosphere. These magnitudes are imported directly into *MPO Canopus* software (Warner, 2021) where they are adjusted for distance and phase-angle dependence, matched with their corresponding time, fit by Fourier analysis including identifying any aliases, and plotted.

Phase-angle corrections are made by applying a *H-G* model and finding the *G* value that minimizes best-fit RMS error across all nights' data for that apparition. Whenever we cannot estimate *G*, usually due to a narrow range of phase angles, we apply the Minor Planet Center's default value of 0.15. No nightly zero-point adjustments (Delta Comps in *MPO Canopus*) were made to any data presented here, other than by estimating *G*.

Lightcurve Results

Fourteen asteroids were observed from Howling Coyote Remote Observatories at 2295 meters elevation in western New Mexico. Images were acquired with: a 0.50-m PlaneWave OTA on a PlaneWave L-500 mount and equatorial wedge, and a SBIG AC4040M CMOS camera fitted with a Schott GG495 light yellow filter and cooled to -20°C.

This equipment was operated remotely via *ACP* software (DC-3 Dreams), running one-night plan files generated by python scripts (Dose, 2020). Exposure times targeted 2-5 millimagnitudes uncertainty in asteroid instrumental magnitude, subject to a minimum exposure of 90 seconds to ensure suitable comp-star photometry, and to a maximum of 480 seconds.

FITS images were calibrated using temperature-matched, exposure-matched, median-averaged dark images and recent flat images of a flux-adjustable light panel. Calibrated images were plate-solved by *TheSkyX* (Software Bisque), and target asteroids were identified in *Astrometrica* (Herbert Raab). All photometric images were visually inspected; the author excluded images with inadequate tracking or seeing quality, digital artifacts caused by changing CMOS read mode, excessive interference by cloud or moon, or having stars, satellite tracks, cosmic ray artifacts, residual image artifacts, or other apparent light sources within 12 arcseconds of the target asteroid's signal centroid. Images passing these screens were submitted to the workflow.

When using the GG495 light-yellow filter, color transforms are modest in size and essentially linear (first-order), and they yield magnitudes in the standard Sloan r' (SR) passband. In our hands, using this filter (rather than a clear filter or no filter) improves transform linearity and night-to-night magnitude reproducibility to a degree outweighing the minor loss of signal-to-noise ratio caused by ~15% loss of measured flux.

Our workflow employs as comp stars all ATLAS refcat2 entries having: distance of at least 15 arcseconds from image boundaries and from other catalogued flux sources, no catalog VARIABLE flag, SR magnitude within [-2, +1] of the target asteroid's SR magnitude on that night (except that very faint asteroids used comp stars having magnitudes in the range 14 to 16), Sloan r'-i' color value within [0.10, 0.34], and absence of variability as seen in session plots of each comp star's instrumental magnitude vs time.

In this report, "period" denotes an asteroid's synodic rotation period, and "mmag" denotes millimagnitudes (0.001 magnitude). In the lightcurves below, *MPO Canopus* v10 shows "SR" for both Pan-STARRS and Sloan r' values.

562 Salome. This bright, frequently observed, Eos-family asteroid has a complex lightcurve shape that has been denoted both monomodal (6.3501 h, Higgins, 2011web; 6.351 h, Alkema, 2013; 6.35031 h, Hanuš et al., 2016; 6.35030 h, Hanuš et al., 2018a) and bimodal (12.705 h, Bembrick and Allen, 2007; 12.7 h; Behrend, 2005web; 12.7050 h, Hamanowa and Hamanowa, 2011web; 12.699 h, Dose, 2024b) on a 6.35 h monomodal basis. Two other published results (10.4 h, Binzel, 1987; 20.5726 h, Hanuš et al., 2018b) are not clearly related.

Approached simply, our new data can be fit quite suitably as a monomodal lightcurve of period 6.350 ± 0.001 h, that is, of half our own bimodal estimate of 2024. This Fourier fit gives a best G of 0.08 and an RMS error of 11 mmag.

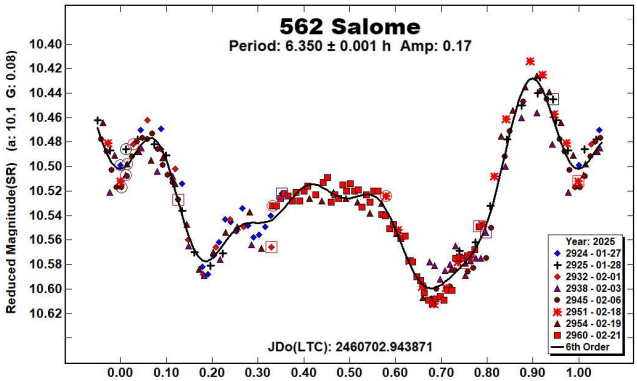

But it is difficult to dismiss the several previously published lightcurves which simply must be interpreted as bimodal, with a period near 12.7 h. So, we then refit our current data while constraining available periods to be near the bimodal period. Because such a bimodal curve will surely be more complex in shape, we increased the Fourier order to 12 and obtained an equally good Fourier fit as obtained for the monomodal case.

This very complex lightcurve shape resembles those of previous reports of period near 12.7 h, including our own of 2024.

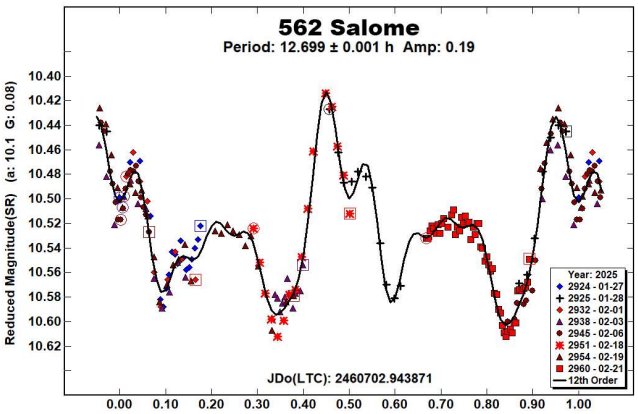

Considered in isolation, this fit might well be considered an over-fitting of our data, even if data coverage were much denser. The RMS error of 10 mmag is close to that of the lower-order fit. The low amplitude cannot help much to choose between monomodal or bimodal interpretations. Our period spectrum produced at Fourier order 6 would indeed support monomodality.

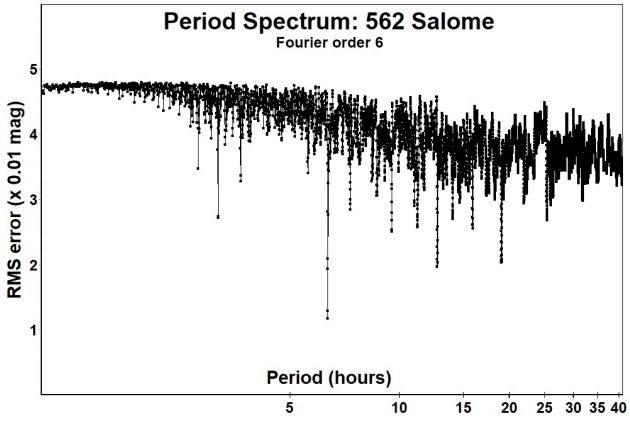

However, a period spectrum on the same data produced at Fourier order 12, suitable to the higher complexity of a bimodal lightcurve, clearly allows for a bimodal interpretation.

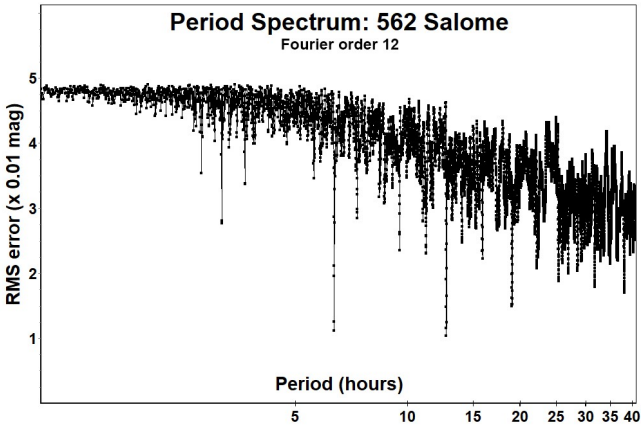

Given these results, and in light of previously published lightcurves, we conclude that the true period of physical rotation of asteroid 562 Salome in space is near our new estimate of 12.699 ± 0.001 h. We further suggest that when observations are taken from certain directions - including that from which this 2025 data but not our 2024 data were taken - the lightcurve shapes repeat in a very nearly exactly manner, every half true rotation, that is, every 6.35 h. Neither period spectrum shows a pronounced signal near previously reported periods of 10.4 h or 20.5726 h.

1332 Marconia. For this namesake asteroid of the Marconia family we find a rotation period of 32.103 ± 0.003 h, in fair to good agreement with three recent results (32.1201 h, Devogèle et al., 2017; 31.34 h, Polakis, 2024; 32.173 h, Dose, 2024b) but differing from two earlier results (19.16 h, Stephens, 2013; 19.2264 h, Ďurech et al., 2016). Our lightcurve is bimodal, and a G value of 0.12 noticeably improved the Fourier fit relative to the MPC default value of 0.15, yielding an RMS error of 13 mmag.

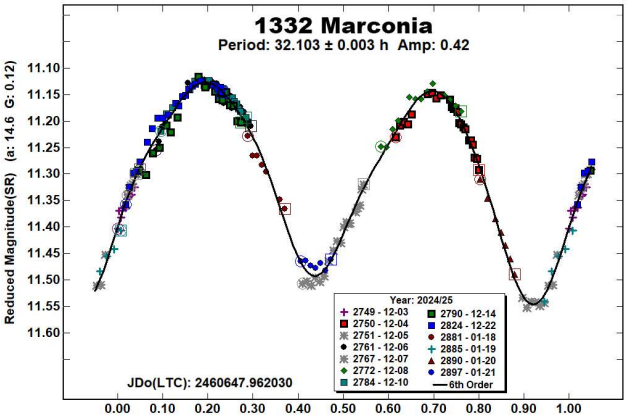

The period spectrum is characteristic of a bimodal lightcurve with similar halves. A relatively minor signal appears near the previously reported results of about 19.2 h, which corresponds to an alias of our result by ½ period per 24 hours.

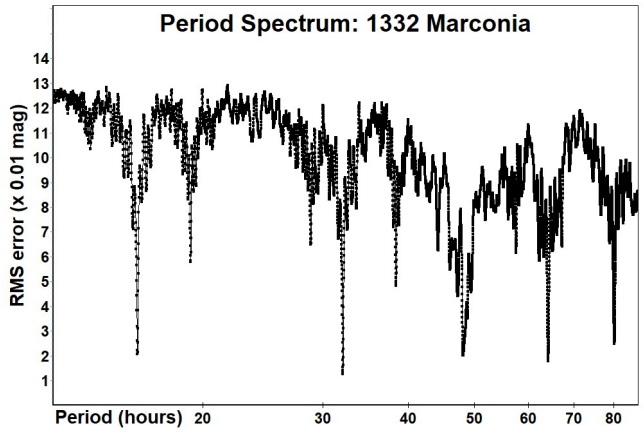

1361 Leuschneria. Previously published period estimates for this outer main-belt asteroid have grouped either near 12.08 h (12.0893 h, Clark, 2016; 12.07463 h, Ďurech et al., 2018; 12.08 h and 12.075 h, Skiff et al., 2019; 12.0421 h, Pál et al., 2020) or near 9.6 h (9.646 h, Casalnuovo, 2016; 9.57 h, Behrend, 2021web) which represents an alias of 12.08 h by ½ rotation per 24 hours.

We report here our new estimate of 12.075 ± 0.002 h and a bimodal lightcurve whose two brightness minima differ in depth and shape. Our phase coverage is incomplete, as common for periods near 12 hours, but the lightcurve shape is very reproducible at all phases where data was taken, and the period spectrum is just that expected for a bimodal lightcurve with similar but visibly differing halves. The narrow range of phase angles over which data were taken allows use of the MPC default G value of 0.15, and our RMS error is 13 mmag.

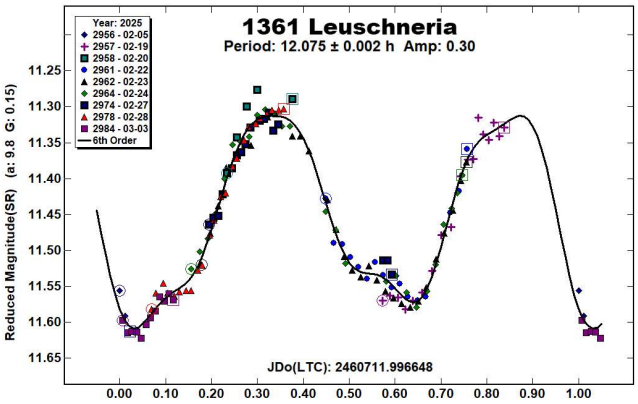

The period spectrum shows only a minor signal near 9.6 h, confirming that our observation data set suffices to disfavor that period solution.

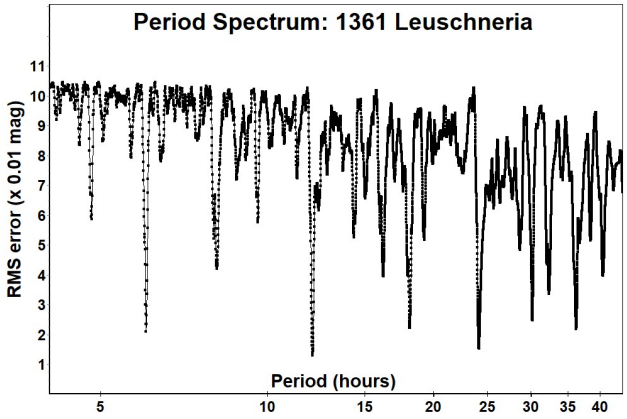

2010 Chebyshev. For this Themis-family asteroid, we report a rotation period of 4.105 ± 0.001 h and a distinctly bimodal lightcurve shape with differing minima and maxima. We know of no previous reports of period or lightcurve for this object. Given the narrow range of phase angles during our observing campaign, we adopt the MPC default G value of 0.15, yielding a Fourier fit RMS error of 17 mmag.

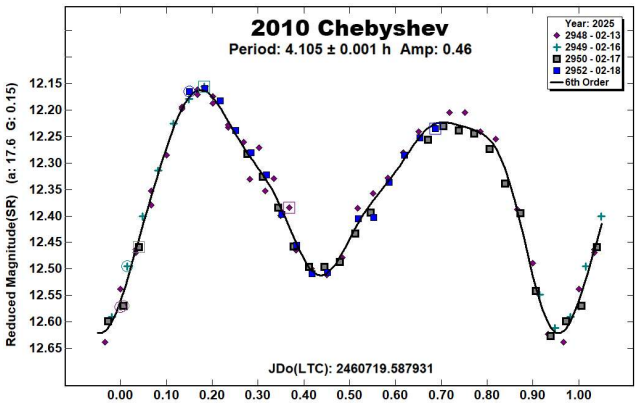

The period spectrum has its major signals at 1, ½, and 2 times our period estimate, consistent with the bimodal lightcurve shape. The large number of minor alias signals is likely due to the period's proximity to 4 hours, and their suppression would likely require more than our four observation sessions and/or sessions of duration longer than about 4 hours.

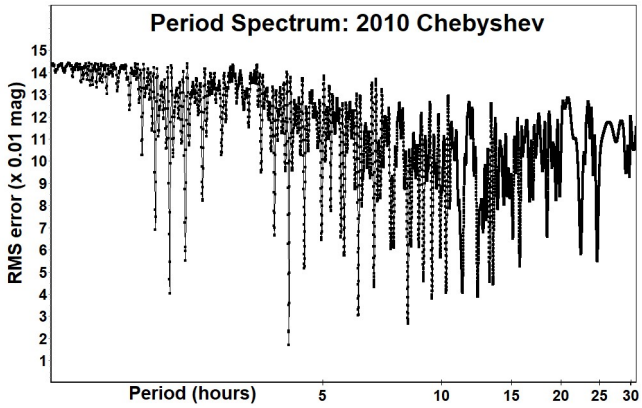

2635 Huggins. We report a rotation period of 3.133 ± 0.001 h for this Flora-family asteroid, in agreement with most (3.129 h, Waszczak et al., 2015; 3.33 h, Chang et al., 2016; 3.1320 h, Benishek, 2022) but not all (9.400 h, Mazzone, 2012web; 48.295 h, Erasmus et al., 2020) previous estimates known to us. We adopt the MPC default G value of 0.15, yielding an RMS error of 19 mmag.

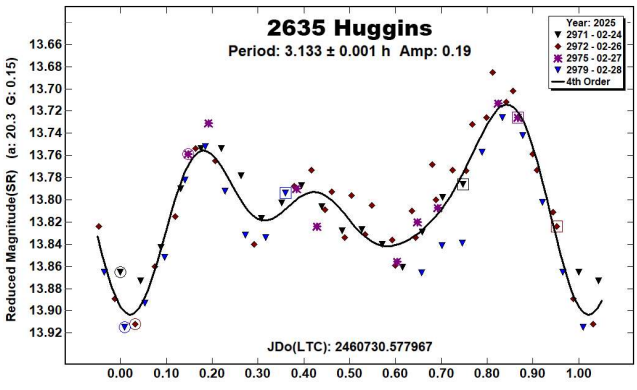

The period spectrum strongly supports our 3.133 h estimate.

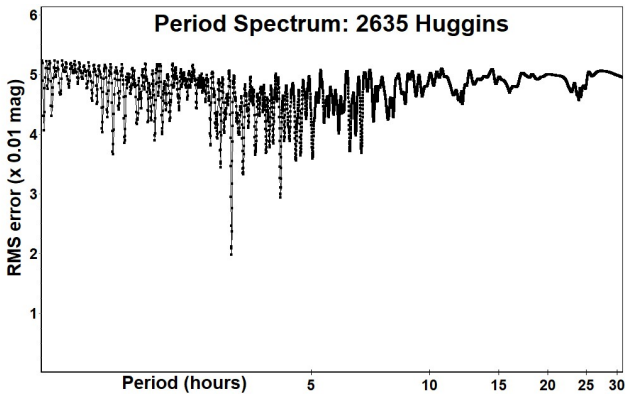

2719 Suzhou. We find a rotation period of 117.38 ± 0.06 h for this inner main-belt asteroid. No previously published period estimate or lightcurve is known to us. Our incomplete phase coverage of this lightcurve is partially compensated by the very large lightcurve amplitude of 0.96 magnitudes. In the end, we find a bimodal lightcurve. A G value (H-G model) of 0.05 improved the Fourier fit, which yielded RMS error of 10 mmag.

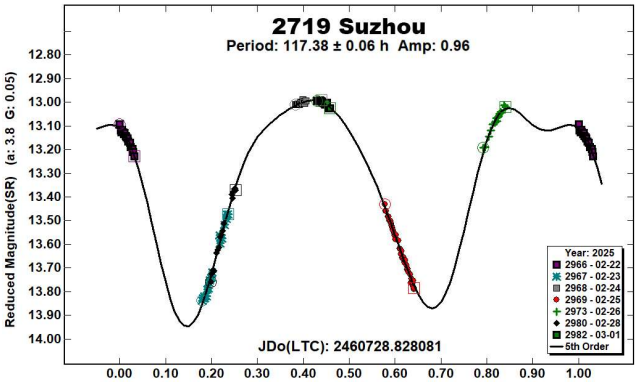

Our period spectrum is imperfect and would surely have been improved by more nights of observation, which unfortunately were unavailable to us. Still, the period spectrum is just what is expected from a sparsely covered, high-amplitude lightcurve of bimodal and typical shape.

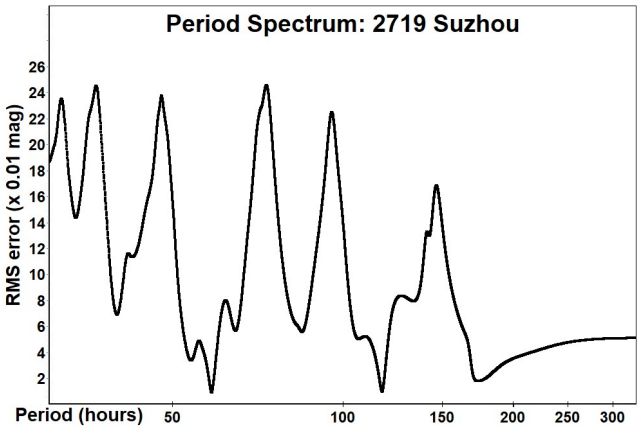

2791 Paradise. For this inner main-belt asteroid, we find an unusual lightcurve shape with rotation period 16.350 ± 0.003 h, in agreement with one published result (16.361 h, Behrend, 2003web) but at variance with three others (9.811 h, Dotto et al., 1992; 9.811 h, Barucci et al., 1994; 9.80729 h, Hanuš et al., 2016). These results near 9.81 h represent an alias of our result by 1 rotation per 24 hours. The MPC default G value of 0.15 sufficed for our narrow range of phase angles, yielding Fourier fit RMS error of 18 mmag.

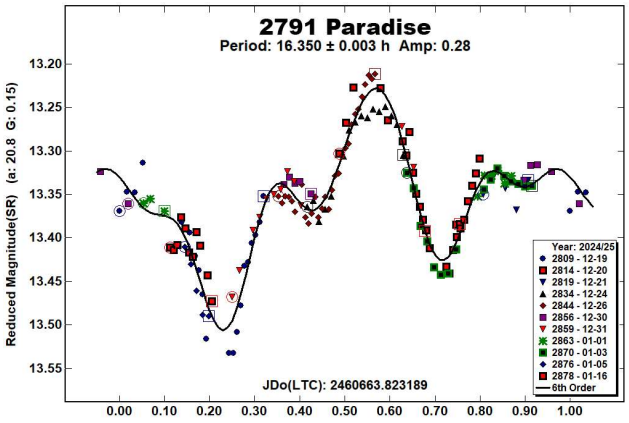

Our campaign benefitted from several observing sessions having duration longer than 6 hours, which allowed us to suppress alias solutions including that of 9.81 h reported three times previously. And indeed, that alias appears only faintly in our period spectrum.

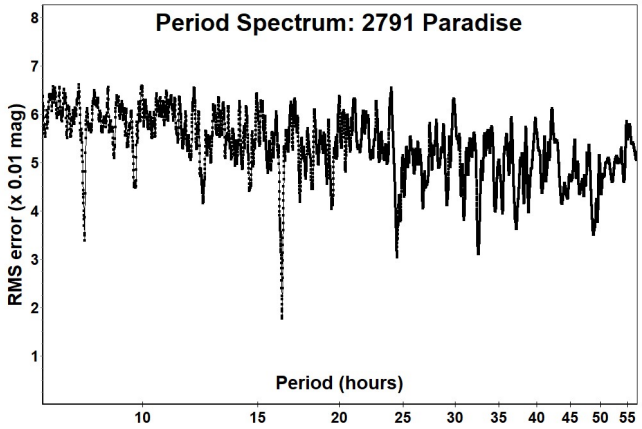

3811 Karma. For this namesake asteroid of the Karma family, we find a rotation period of 14.424 ± 0.001 h and a bimodal lightcurve with similar brightness maxima but with differing minima. Our result agrees with most (14.41 h, Yeh et al., 2020; 14.4234 h, Ďurech et al., 2020; 14.421 h, Dose, 2024a; 14.4262 h, Stone, 2024) but not all (11.52 h, Behrend, 2007web; 13.23 h, Aznar Macías et al., 2016) previously published estimates. A G value of 0.15 optimized the Fourier fit, for which our RMS error is 10 mmag.

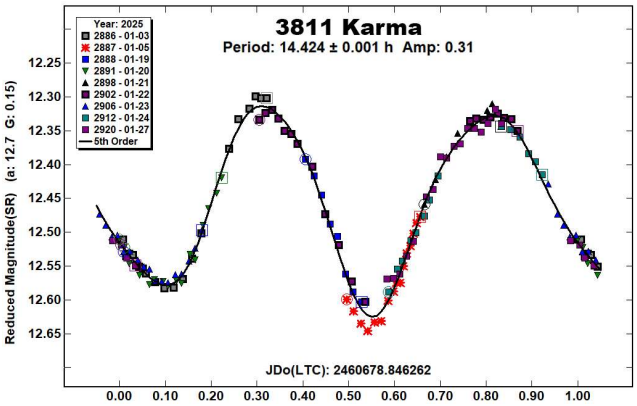

We cannot explain previous estimates of 11.52 h and 13.23 h, and neither appears as a major signal in our own period spectrum.

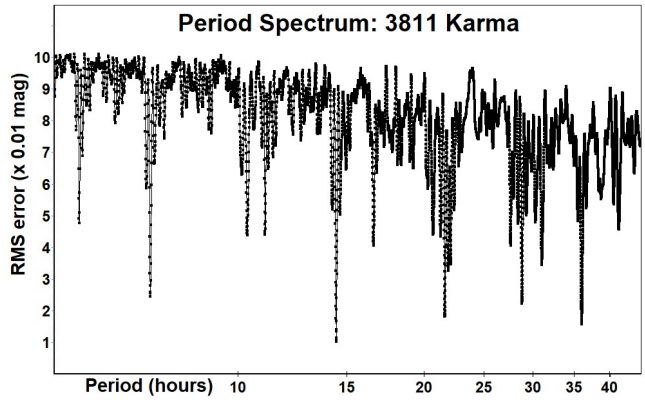

4648 Tirion. From 25 nights of observation (covering ca. 3.6 rotation periods), we estimate the rotation period for this inner main-belt asteroid to be an unusually long 413.00 ± 0.49 h, with a relatively large amplitude of 0.61 magnitudes. We know of no previously published period estimates or lightcurves for this object. A G value (H-G model) of 0.12 optimized the Fourier fit, which has an RMS error of 29 mmag. The large amplitude supports a bimodal interpretation.

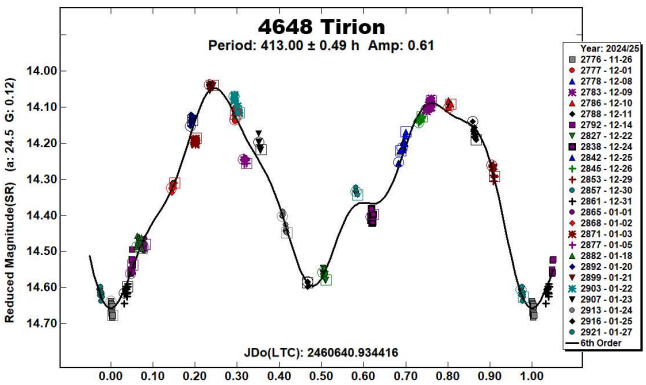

The period spectrum is typical for a well-covered bimodal and long-period lightcurve with similar halves. No competing secondary signals appear.

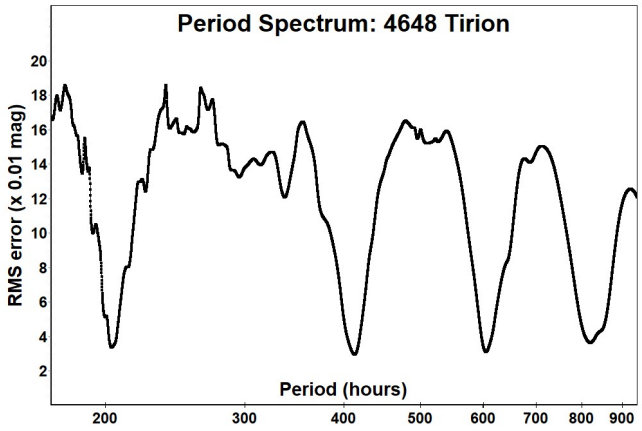

(5534) 1941 UN. We revisit this outer main-belt asteroid with improved equipment and with much more thorough phase coverage, and we obtain a new period estimate of 16.585 ± 0.007 h, which differs from our previous estimate (14.402 h, Dose, 2020). The lightcurve is more complex than previously realized, its shape being supported by several observation sessions of 6 hours' duration or more, as well as by taking long exposures to increase the individual observations' signal-to-noise ratio. A G value of 0.25 improved the Fourier fit; RMS error is 9 mmag.

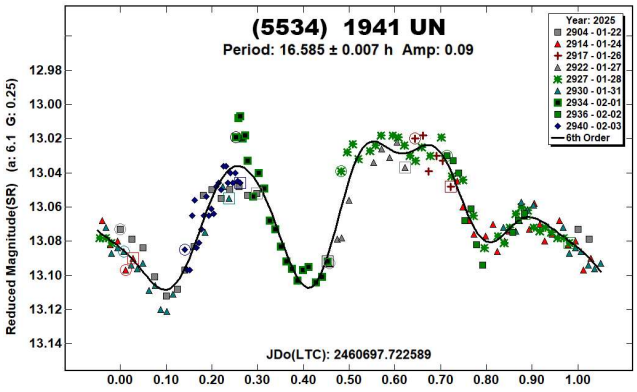

The new period spectrum is unusually clear, and our previous period estimate of 14.402 h does not appear in it.

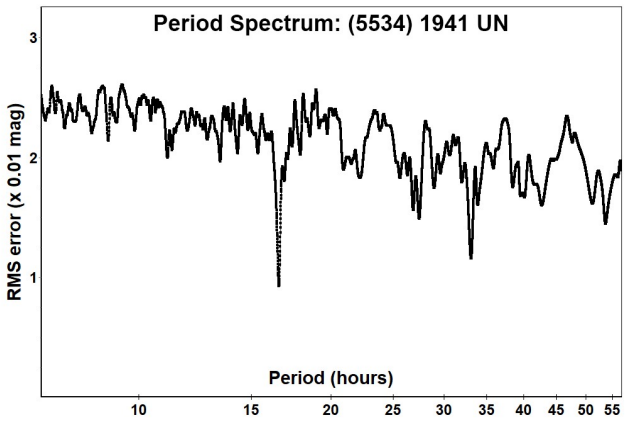

5743 Kato. For this inner main-belt asteroid, we find a rotation period of 14.266 ± 0.001 h, agreeing with one known published result (14.269 h, Waszczak et al., 2015). Our lightcurve is bimodal with reproducibly differing halves. A H-G model G value of 0.27 gave a markedly improved Fourier fit vs the MPC default value of 0.15, yielding an RMS error of 17 mmag.

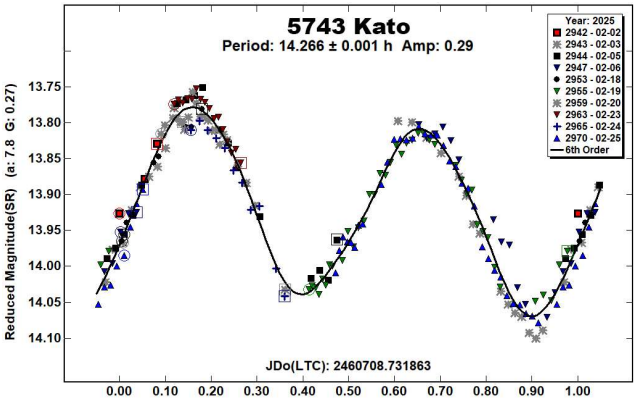

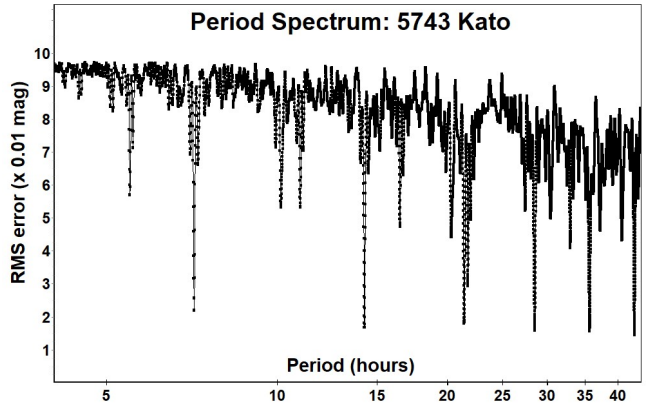

5802 Casteldelpiano. We revisit this inner main-belt asteroid and obtain a new rotation period estimate of 2.971 ± 0.002 h with a very low amplitude of 0.06 magnitudes. This period estimate agrees with all three known published values (2.9710 h, Waszczak et al, 2015; 2.9705 h, Pravec et al., 2018web; 2.9706 h, Dose, 2021b). A G value of 0.33 optimized the Fourier fit, yielding RMS error of 12 mmag.

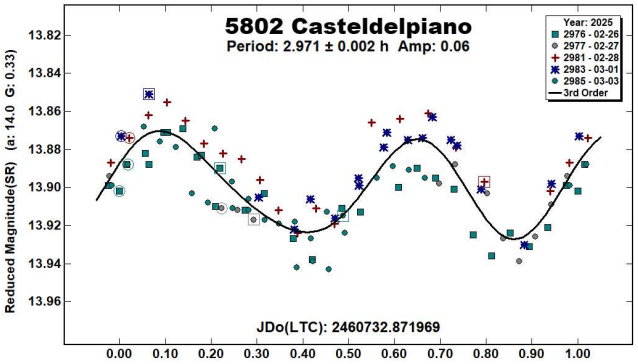

Number	Name	yyyy mm/dd	Phase	L_{PAB}	B_{PAB}	Period(h)	P.E.	Amp	A.E.	Grp
562	Salome	2025 01/27-02/21	10.2 ,4.8	156	13	12.699	0.001	0.19	0.02	EOS
1332	Marconia	2024-5 12/03-01/21	*14.7, 1.5	118	3	32.103	0.003	0.42	0.04	MRC
1361	Leuschneria	2025 02/05-03/03	9.9, 1.9	168	3	12.075	0.002	0.30	0.04	MB-O
2010	Chebyshev	2025 02/13-02/18	17.6,18.4	96	3	4.105	0.001	0.46	0.04	THM
2635	Huggins	2025 02/24-02/28	20.2,21.6	118	3	3.133	0.001	0.19	0.04	FLO
2719	Suzhou	2025 02/22-03/01	*4.1, 0.4	160	0	117.380	0.060	0.96	0.10	MB-I
2791	Paradise	2024-5 12/19-01/16	20.8,22.2	91	38	16.350	0.003	0.28	0.05	MB-I
3811	Karma	2025 01/03-01/27	12.8, 3.5	129	7	14.424	0.001	0.31	0.04	KRM
4648	Tirion	2024-5 11/26-01/27	*24.7, 9.3	111	8	413.000	0.490	0.61	0.08	MB-I
5534	1941 UN	2025 01/22-02/03	6.1, 9.1	121	10	16.585	0.007	0.09	0.03	MB-O
5743	Kato	2025 02/02-02/25	*8.0, 5.6	147	1	14.266	0.001	0.29	0.04	MB-I
5802	Casteldelpiano	2025 02/26-03/03	14.3,11.5	179	2	2.971	0.002	0.06	0.02	MB-I
6827	Wombat	2025 01/18-02/02	*8.2,10.0	120	15	40.287	0.019	0.28	0.04	EUN
44700	1999 SG3	2024-5 12/18-01/18	7.2,21.2	75	-2	17.614	0.002	0.78	0.08	PHO

Table I. Observing circumstances and results. The phase angle is given for the first and last date. If preceded by an asterisk, the phase angle reached an extrema during the period. L_{PAB} and B_{PAB} are the approximate phase angle bisector longitude/latitude at mid-date range (see Harris, 1984). Grp is the asteroid family/group (Warner, 2009).

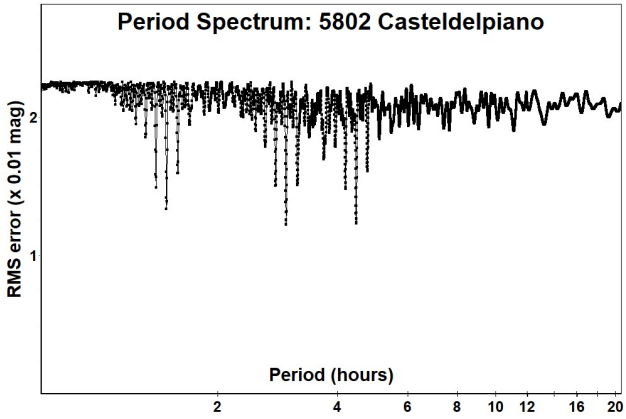

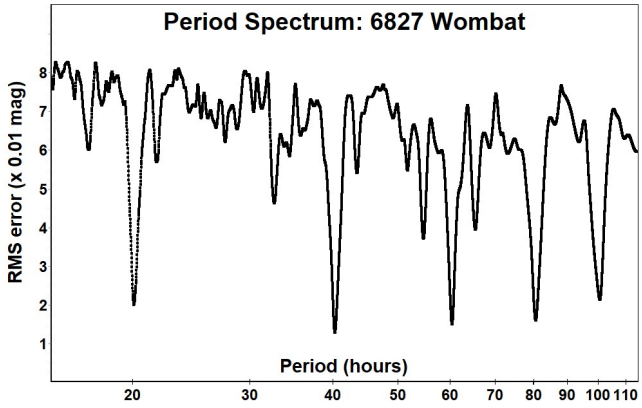

6827 Wombat. For this Eunomia-family asteroid, we find a rotation period of 40.287 h ± 0.019 h, which agrees approximately with one previously published estimate (40.1320 h, Waszczak et al., 2015) but differs from another (64 h, Behrend, 2015web). Our lightcurve is clearly bimodal, with markedly differing halves. For the narrow range of phase angles, the MPC-default G value of 0.15 sufficed, yielding RMS error of 13 mmag.

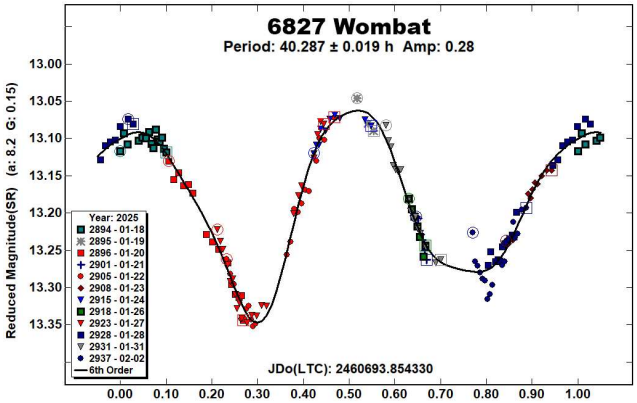

The period spectrum is just that expected for a bimodal lightcurve, with major signals at multiples of ½ period, but absent any major alias signals.

(44700) 1999 SG3. From 16 nights' observations on this Phocaea-family asteroid, we obtain a period estimate of 17.614 ± 0.002 h, in fair agreement with the sole known published estimate (17.8838 h, Pál et al., 2020). The lightcurve is bimodal, with similar halves and a large amplitude. A G value of 0.04 improved the Fourier fit, for which RMS error is 32 mmag.

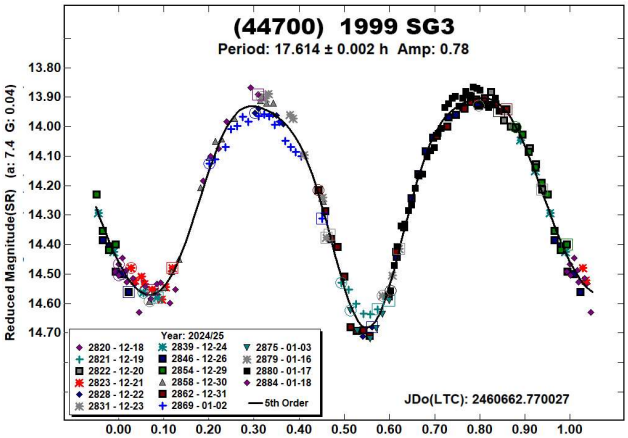

All primary signals within the period spectrum lie at multiples of ½ our period estimate.

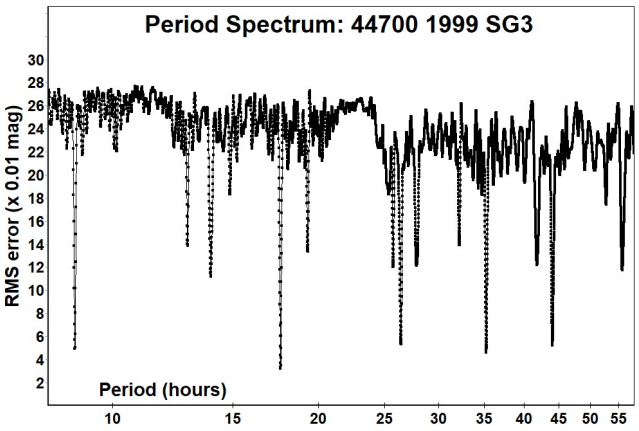

Acknowledgements

The author thanks all contributors to the ATLAS paper (Tonry et al., 2018) for providing openly and without cost the ATLAS refcat2 catalog. Our work also makes extensive use of the python language interpreter and of several supporting packages (notably: astropy, ccdproc, ephem, matplotlib, pandas, photutils, requests, skyfield, and statsmodels), all made available openly and without cost.

Finally, the author thanks all his fellow observers and photometry mentors - far too numerous to catalog here - for their guidance, kindness, and encouragement over the years of his astronomical observing career, which concludes with this manuscript.

References

Alkema, M.S. (2013). "Lightcurve of 562 Salome." *Minor Planet Bull*. **40**, 68.

Aznar Macías, A.; Carreño Garcerán, A.; Arce Mansego, E.; Brines Rodriguez, P.; Lozano de Haro, J.; Fornas Silva, A.; Fornas Silva, G.; Mas Martinez, V.; Rodrigo Chiner, O. (2016). "Twenty-three Asteroids Lightcurves at Observadores de Asteroides (OBAS): 2015 October-December." *Minor Planet Bull*. **43**, 174-181.

Barucci, M.A.; Di Martino, M.; Dotto, E.; Fulchignoni, M.; Rotundi, A.; Burchi, R. (1994). "Rotational Properties of Small Asteroids: Photoelectric Observations of 16 Asteroids." *Icarus* **109**, 267-273.

Behrend, R. (2003web, 2005web, 2007web, 2015web, 2021web). Observatoire de Genève web site. *http://obswww.unige.ch/~behrend/page_cou.html*

Bembrick, C.; Allen, B. (2007). "The Rotation Period of 562 Salome." *Minor Planet Bull*. **34**, 3.

Benishek, V. (2022). "CCD Photometry of 35 Asteroids at Sopot Astronomical Observatory: 2021 November - 2022 July." *Minor Planet Bull*. **49**, 333-341.

Binzel, R.P. (1987). "A photoelectric survey of 130 asteroids." *Icarus* **72**, 135-208.

Casalnuovo, G.B. (2016). "Lightcurve Analysis for Nine Main Belt Asteroids." *Minor Planet Bull*. **43**, 112-115.

Chang, C.-K.; Lin, H.-W.; Ip, W.-H.; Prince, T.A.; Kulkarni, S.R.; Levitan, D.; Laher, R.; Surace, J. (2016). "Large Super-fast Rotator Hunting Using the Intermediate Palomar Transient Factory." *Astrophys. J. Suppl. Series* **227**, 20.

Clark, M. (2016). "Asteroid Photometry from the Preston Gott Observatory." *Minor Planet Bull*. **43**, 2-5.

Devogèle, M. and 53 others (2017). "Shape and spin determination of Barbarian asteroids." *Astron. Astrophys.* **607**, A119.

Dose, E.V. (2020). "A New Photometric Workflow and Lightcurves of Fifteen Asteroids." *Minor Planet Bull*. **47**, 324-330.

Dose, E.V. (2021a). "Lightcurves of Nineteen Asteroids." *Minor Planet Bull*. **48**, 69-76.

Dose, E.V. (2021b). "Lightcurves of Eighteen Asteroids." *Minor Planet Bull*. **48**, 125-132.

Dose, E.V. (2024a). "Lightcurves of Eighteen Asteroids." *Minor Planet Bull*. **51**, 42-49.

Dose, E.V. (2024b). "Lightcurves of Ten Asteroids." *Minor Planet Bull*. **51**, 251-256.

Dotto, E.; Rotundi, A.; De Sanctis, M.C. (1992). "Rotational Properties of Small Asteroids: 1992 Observational Results." Proceedings of the Liège International Astrophysical Colloquium 30, June 24-26, 1992, Institut d'Astrophysique, Liège, 211.

Ďurech, J.; Hanuš, J.; Oszkiewicz, D.; Vančo, R. (2016). "Asteroid models from the Lowell photometric database." *Astron. Astrophys.* **587**, A48.

Ďurech, J.; Hanuš, J.; Alí-Lagoa, V. (2018). "Asteroid models reconstructed from the Lowell Photometric Database and WISE data." *Astron. Astrophys.* **617**, A57.

Ďurech, J.; Tonry, J.; Erasmus, N.; Denneau, L.; Heinze, A.N.; Flewelling, H.; Vančo, R. (2020). "Asteroid models reconstructed from ATLAS photometry." *Astron. Astrophys.* **643**, A59.

Erasmus, N.; Navarro-Meza, S.; McNeill, A.; Trilling, D.E.; Sickafoose, A.A.; Denneau, L.; Flewelling, H.; Heinze, A.; Tonry, J.L. (2020). "Investigating Taxonomic Diversity within Asteroid Families through ATLAS Dual-band Photometry." *Astrophys. J. Suppl. Series* **247**, 13.

Hamanowa, H.; Hamanowa, H. (2011web). As found in LCDB March 5, 2025.

Hanuš, J. and 168 others (2016). "New and updated convex shape models of asteroids based on optical data from a large collaboration network." *Astron. Astrophys.* **586**, A108.

Hanuš, J. and 20 others (2018a). "Spin states of asteroids in the Eos collisional family." *Icarus* **299**, 84-96.

Hanuš, J.; Delbo, M.; Ďurech, J.; Alí-Lagoa, V. (2018b). "Thermophysical modeling of main-belt asteroids from WISE thermal data." *Icarus* **309**, 297-337.

Harris, A.W.; Young, J.W.; Scaltriti, F.; Zappala, V. (1984). "Lightcurves and phase relations of the asteroids 82 Alkmene and 444 Gyptis." *Icarus* **57**, 251-258.

Higgins, D.J. (2011web). As found in LCDB March 5, 2025.

Mazzone, F. (2012web). *www.astrosurf.com/salvador/Fotometria.html*

Pál, A. and 12 others (2020). "Solar System Objects Observed with TESS - First Data Release: Bright Main-belt and Trojan Asteroids from the Southern Survey." *Astrophys. J. Suppl. Series* **247**, 26.

Polakis, T. (2024). "Photometric Results for Twenty Minor Planets." *Minor Planet Bull*. **51**, 126-132.

Pravec, P.; Wolf, M.; Sarounova, L. (2018web) *http://www.asu.cas.cz/~ppravec/neo.htm*

Skiff, B.A.; McLelland, K.P.; Sanborn, J.J.; Pravec, P.; Koehn, B.W. (2019). "Lowell Observatory Near-earth Asteroid Photometric Survey (NEAPS): Paper 3." *Minor Planet Bull*. **46**, 238-265.

Stephens, R.D. (2013). "Asteroids Observed from Santana and CS3 Observatories: 2012 July-September." *Minor Planet Bull*. **40**, 34-35.

Stone, G. (2024). "Lightcurves and Rotation Periods of Asteroids 1861 Komensky, 2096 Vaino 3127 Bagration, 3289 Mitani, 3582 Cyrano, 3589 Loyola, 3811 Karma, 4226 Damiaan, 4458 Oizumi, 6086 Vrchlicky, 6875 Golgi, (18118) 2000 NB24 and 29185 Reich." *Minor Planet Bull*. **51**, 112-116.

Tonry, J.L.; Denneau, L.; Flewelling, H.; Heinze, A.N.; Onken, C.A.; Smartt, S.J.; Stalder, B.; Weiland, H.J.; Wolf, C. (2018). "The ATLAS All-Sky Stellar Reference Catalog." *Astrophys. J.* **867**, A105.

Warner, B.D.; Harris, A.W.; Pravec, P. (2009). "The asteroid lightcurve database." *Icarus* **202**, 134-146. *https://minplanobs.org/MPInfo/php/lcdb.php*

Warner, B.D. (2021). *MPO Canopus* Software. Version 10.8.4.11. BDW Publishing. *http://www.bdwpublishing.com*

Waszczak, A. and 12 others (2015). "Asteroid Light Curves from the Palomar Transient Factory Survey: Rotation Periods and Phase Functions from Sparse Photometry." *Astron. J.*, **150**, 75.

Yeh, T.-S.; Chang, C.-K.; Zhao, H.-B.; Ji, J.-H.; Lin, Z.-Y.; Ip, W.-H. (2020). "The Asteroid Rotation Period Survey Using the China Near-Earth Object Survey Telescope (CNEOST)." *Astron. J.*, **160**, 73.

OBSERVATIONS OF (617) PATROCLUS-MENOETIUS MUTUAL EVENTS BY THE ARISTOTLE UNIVERSITY OF THESSALONIKI

Alexandros Siakas, Ioannis Gkolias, Aggelos Tsiaras, Sotirios Tsavdaridis, Michalis Gaitanas, Kleomenis Tsiganis
Laboratory of Theoretical Mechanics and Astrodynamics
Aristotle University of Thessaloniki (AUTh)
54124, Thessaloniki, GRECEE
asiakas@physics.auth.gr

Georgios Tsirvoulis
Asteroid Engineering Laboratory, Space Systems
Luleå University of Technology
Bengt Hultqvists väg 1, 98192 Kiruna, SWEDEN

(Received: 2025 February 11)

We observed six mutual events in the binary system (617) Patroclus-Menoetius. This report presents the observed lightcurves along with preliminary results regarding the magnitude drop and event timing.

Following the call for observations of the binary system (617) Patroclus and its satellite (617) I Menoetius (Binzel, 2024), we conducted photometric observations of mutual events using two astronomical stations operated by the Section of Astrophysics, Astronomy and Mechanics of AUTh. The observations were carried out between 2024 September 10, and 2024 December 20. The first station (AUTh-2) is located near Taxiarchis in Chalikidiki, Greece, at Longitude: 23° 30' 19.97" E, Latitude: 40° 25' 58.5" N and Elevation: 862 m. It is equipped with a 14" Planewave CDK f/4.75 telescope (with a 0.66× reducer) and a QHY163M CMOS camera, with a QHY-GPSBOX serving as a timing device. The second station (AUTh-3) is located at the SPICA Observatory in Cyprus, at Longitude: 32° 50' 24.6" E, Latitude:34° 55' 55.43" N, Elevation: 1411 m. This station is equipped with an 11" Celestron RASA f/2.2 telescope, also using a QHY163M CMOS camera and a QHY-GPSBOX for timing. A Baader UV/IR-Cut / L-Filter 2" was equipped during the observations.

The observational plan was based on predictions by Brozović et al. (2024). We recorded five Superior events and one Inferior event. Data reduction and relative photometry were performed using the publicly available *Holomon Photometric Software* (HOPS), which has been used extensively for planetary transits (Kokori et al., 2022). For each lightcurve, we determined the mean magnitude of the baseline, measured before or after the phenomenon. The apparent magnitude was then computed by adding the relative instrumental magnitude to this baseline magnitude. No light-time correction was applied.

To estimate the maximum magnitude drop for each event, we calculated the average magnitudes at the maximum and minimum points. This was done by sampling data within ±15 minutes around each peak and trough. The magnitude drop was then determined by subtracting the average minimum magnitude from the average maximum magnitude. Additionally, polynomial fit was used to estimate the event times at the maximum shadowing. In Table I we present the details of each recording. Table II shows the event type along with the calculated magnitude drop. Finally, Table III compares the predicted event times by Brozović et al. (2024) with the estimated times from the observations.

Date	Station	Start (UT)	Stop (UT)	Conditions
2024 Sep 10/11	AUTh-3	20:34	02:19	Partial Clouds
2024 Sep 23/24	AUTh-3	19:30	02:30	Clear
2024 Oct 06	AUTh-3	18:18	23:30	Clear
2024 Oct 23/24	AUTh-3	17:51	23:51	Clear, deteriorated towards the end
2024 Nov 05	AUTh-2	16:44	22:56	Clear
2024 Dec 12	AUTh-3	16:09	20:43	Clear, deteriorated towards the end

Table I: Observation campaigns details.± Observing station, start/end of recording and sky conditions.

Date	Event	Type	Δm
2024 Sep 10/11	Superior	PO, PO+PE, PE	0.41 ± 0.04
2024 Sep 23/24	Superior	PO, PO+PE, PE	0.51 ± 0.05
2024 Oct 06	Superior	PO, PO+PE, TO, PO+PE, PO	0.62 ± 0.03
2024 Oct 23/24	Superior	PE, PO+PE, PO	0.59 ± 0.06
2024 Nov 05	Superior	PE, PO+PE, PO	0.52 ± 0.04
2024 Dec 12	Inferior	PO	0.14 ± 0.03

Table II: Event types and calculated magnitude drops.

Date	Observed (UT)	Predicted (UT)	ΔTime (min)
2024 Sep 10/11	01:09	01:00	+9
2024 Sep 23/24	22:11	21:51	+20
2024 Oct 06	18:51	18:48	+3
2024 Oct 23/24	22:30	22:37	-7
2024 Nov 05	19:31	19:23	+8
2024 Dec 12	19:12	19:11	+1

Table III: Observed and predicted times of maximum drop.

The estimated parameters showed good agreement with the predictions from Brozović et al. (2024), which serves as a guide for these events. We also compared our results with those reported by other observers. Specifically, our observations for the events on 2024 September 10/11 and 2024 September 23/24 were also reported in Hawley et al. (2024). The mutual event on 2024 October 6 was also reported in Hawley et al. (2024) as well as in Brincat (2024). Finally, the mutual event on 2024 October 23/24 was reported by Brincat (2024), Benishek (2024) and Sioulas (2024). Among them, some provided numerical estimations, and their results were generally consistent with ours. For those who did not include explicit estimations, we could only make a qualitative comparison based on their plots, and overall, their findings appear to be in reasonable agreement with ours.

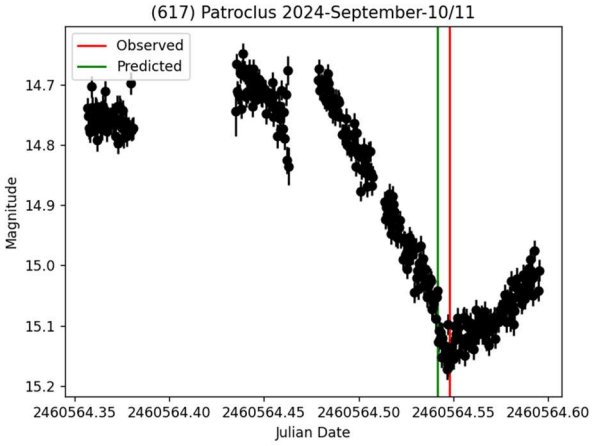

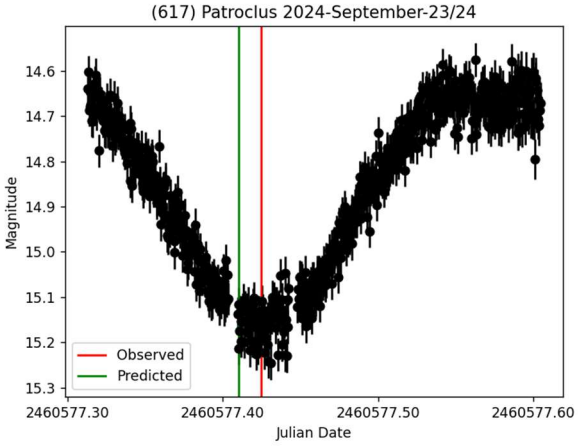

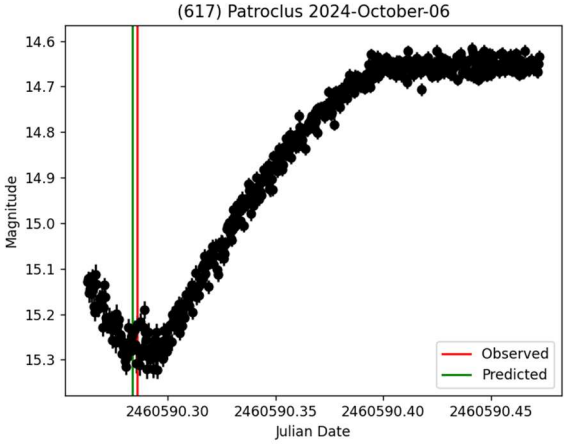

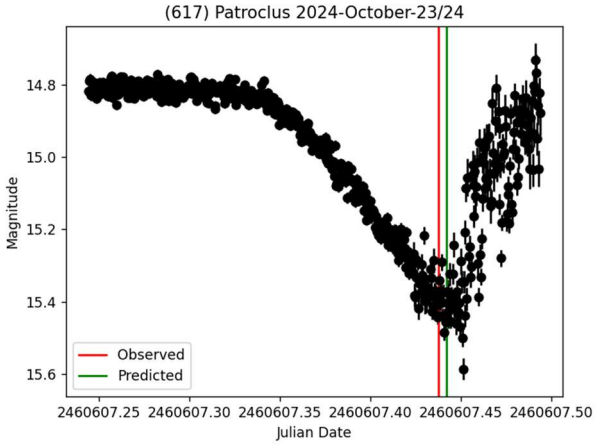

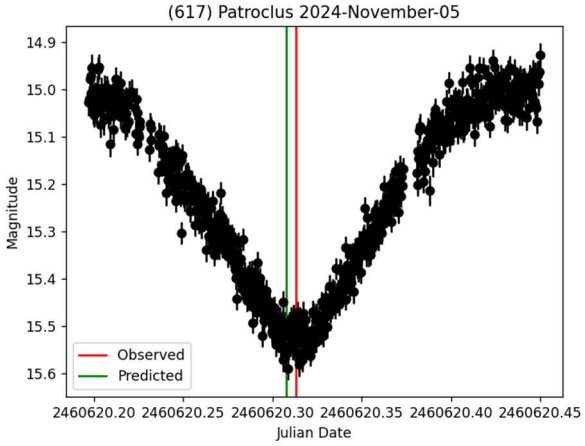

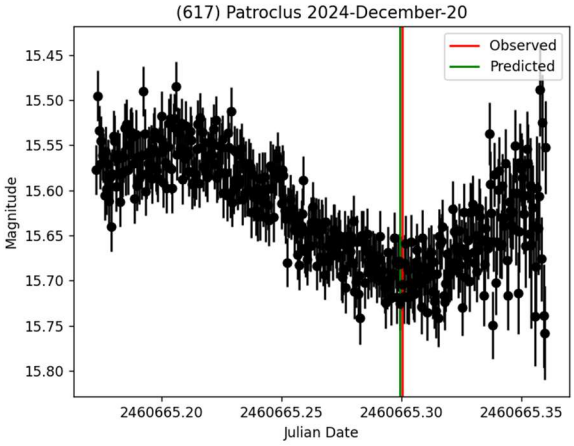

References

Benishek, V. (2024). "Photometric Detection of the 2024 October 23-24 Mutual Event of the Patroclus-Menoetius Binary Jupiter Trojan at SOPOT Astronomical Observatory." *Minor Planet Bull.* **52**, 84.

Binzel, R.P. (2024). "Call for Observations of the Patroclus and Menoetius Mutual Events: Support for the NASA Lucy Mission to the Trojan Asteroids." *Minor Planet Bull.* **51**, 212.

Brincat, S.M. (2024) "Observations of Mutual Events Between 617 Patroclus and Menoetius on September 25, October 6, and October 23, 2024." *Minor Planet Bull.* **52**, 82.

Brozović, M.; Jacobson, R.A.; Park, R.S.; Descamps, P.; Berthier, J.; Pinilla-Alonso, N.; Popescu, M.; Licandro, J. (2024). "Orbit of the Patroclus-Menoetius Binary System and Predictions for the 2024/2025 Mutual Events Season." *Astron. J.* **167**, 104, 12 pp.

Hawley, W.; Armstrong, J.D.; Marshall, J.; DeGroff, K.; Leyland, P.C.; Odeh, M.S.; Oey, J.; Fornas, A.; Gonçalves, R.; Kardasis, E.; Takoudi, A.; Usatov, M.; Drummond, J. (2024). "617 Patroclus-Menoetius Mutual Event Lightcurves." *Minor Planet Bull.* **52**, 70.

Holomon Photometric Sofware (HOPS).
https://github.com/ExoWorldsSpies/hops

Kokori, A.; Tsiaras A.; Edwards B. and 46 colleagues (2022). "ExoClock project: an open platform for monitoring the ephemerides of Ariel targets with contributions from the public." *Exp Astron* **53**, 547-588. *https://doi.org/10.1007/s10686-020-09696-3*

Sioulas, N. (2024). "Patroclus and Menoetius Mutual Events: Support for the NASA LUCY Mission to the Trojan Asteroids." *Minor Planet Bull.* **52**, 86.

PRELIMINARY SPIN-SHAPE MODEL FOR 49 PALES

Lorenzo Franco
Balzaretto Observatory (A81), Rome, ITALY
lor_franco@libero.it

Frederick Pilcher
Organ Mesa Observatory (G50)
4438 Organ Mesa Loop
Las Cruces, NM 88011 USA

Fabio Mortari, Davide Gabellini
Hypatia Observatory (L62), Rimini, ITALY

Giorgio Baj
M57 Observatory (K38), Saltrio, ITALY

Marco Iozzi
HOB Astronomical Observatory (L63)
Capraia Fiorentina, ITALY

(Received: 2025 March 3)

We present a preliminary shape and spin axis model for main-belt asteroid 49 Pales. The model was achieved with the lightcurve inversion process, using combined dense photometric data acquired from seven apparitions between 1977-2024 and sparse data from USNO Flagstaff. Analysis of the resulting data found a sidereal period P = 20.7080 ± 0.0002 hours and two mirrored pole solutions at (λ = 95°, β = -89°) and (λ = 272°, β = -88°) with an uncertainty of ± 30 degrees.

The minor planet 49 Pales was observed mainly by Frederick Pilcher for six oppositions from 2015 to 2024 and, to improve the coverage at various aspect angles, we also used the 1977 data from Asteroid Photometric Catalogue (Lagerkvist et al., 2024) and the sparse data from USNO Flagstaff Station, according Durech et al. (2009). Dense data were downloaded from ALCDEF (ALCDEF, 2021), and sparse data from the Asteroids Dynamic Site (AstDyS-2, 2020).

The observational details of the dense data used are reported in Table I with the reference, the mid-date, number of the lightcurves used for the inversion process, longitude and latitude of phase angle bisector (LPAB, BPAB). The dense data points were binned in order to reduce the overall processing time. The PAB longitude/latitude distribution of the dense and sparse data are shown on Figure 1, while Figure 2 shows the phase curve obtained with the sparse data.

Lightcurve inversion was performed using *MPO LCInvert* v.11.8.4.1 (MPO LCInvert, 2022). For a description of the modeling process see LCInvert Operating Instructions Manual, Durech et al. (2010); and references therein.

In the analysis the processing weighting factor was set, according the data quality, to: 0.5 for the 1977 data, to 1.0 for other dense data and to 0.3 for the sparse data. The "dark facet" weighting factor was set to 1.4 to keep the dark facet area below 1% of total area and the number of iterations was set to 50.

#	Reference	Mid-date (yyyy-mm-dd)	#LCs	LPAB°	BPAB°
1	Schober et al. (1979)	1977-11-18	3	52	3
2	Pilcher et al. (2016)	2015-11-14	8	64	3
3	Pilcher (2017)	2017-02-13	6	160	-3
4	Pilcher (2018)	2018-04-22	7	214	-4
5	Pilcher (2021)	2020-08-19	6	253	4
6	Pilcher (2022)	2022-01-09	6	124	-1
7	Franco et al. (2022)	2022-02-14	5	124	-2
8	Pilcher (2024)	2024-05-20	8	224	-3

Table I. Observational details for the dense data used in the lightcurve inversion process for 49 Pales.

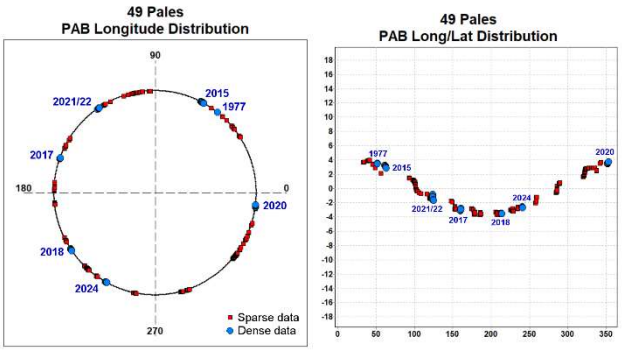

Figure 1. PAB longitude/latitude distribution for the dense and sparse data used in the lightcurve inversion process.

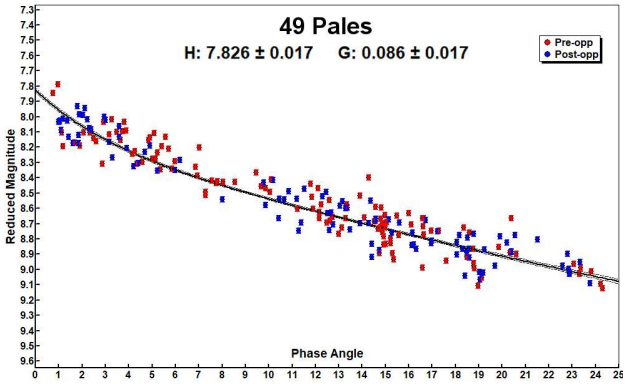

Figure 2. Phase curve obtained from USNO Flagstaff sparse data (reduced magnitude vs phase angle).

In lightcurve inversion work, the most critical step is to find an accurate sidereal rotation period. An inaccurate sidereal period can lead to completely incorrect results, regarding the spin axis and the model. In our work, a scan interval was chosen to cover broadly (40-sigma) the distribution of the observed synodic period values, relating to the dense data used for the inversion process. We found a very close pair of isolated sidereal periods with a Chi-Sq below to the 10% limit for P = 20.70802 h (Figure 3).

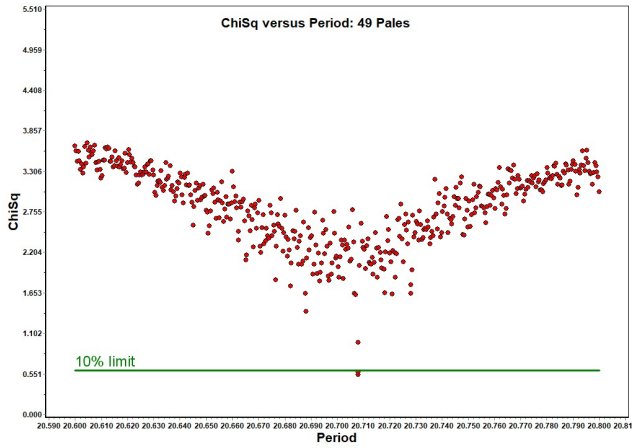

Figure 3. The period scan for 49 Pales shows a very close pair of isolated sidereal periods for P = 20.70802 h, with a Chi-Sq below to the 10% limit.

The pole search was started using the "medium" search option (312 fixed pole position with 15° longitude-latitude steps) and the previously found sidereal period set to "float". From this step we found two mirrored solutions with lower Chi-Sq (Figure 4) separated by 180° in longitude and close to ecliptic longitude-latitude pairs (105°, -90°) and (285°, -90°). Note that the pole search map shows a crowded distribution of potential solutions for ecliptic latitude values close to -90 degrees, without well isolated solutions with the lower Chi-Sq values below the 10% limit, making the two identified pole solutions affected by a not negligible uncertainty.

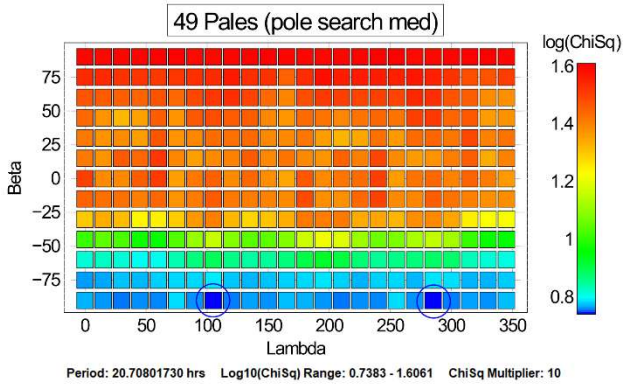

Figure 4. Pole distribution produced by the "medium" search option. The dark blue region indicates the smallest Chi-Sq value while the dark red region indicates the largest. The two mirrored pole solution are centered close to (105°, -90°) and (285°, -90°).

In order to try to refine the two pole positions solutions, a "fine" search option (with 49 fixed pole steps with 10° longitude-latitude pairs and the period set to "float") was started with radius of 30° on the approximate pole positions found previously. Unfortunately, even in this case the search did not show well-isolated pole positions with Chi-Sq values below the 10% limit. The resulting map shows two clustered solutions that had Chi-Sq values within 3% of the lowest value, approximately centered at ecliptic longitude-latitude (99°, -89°) and (273°, -89°) with a radius of 30° in ecliptic longitude (Figure 5).

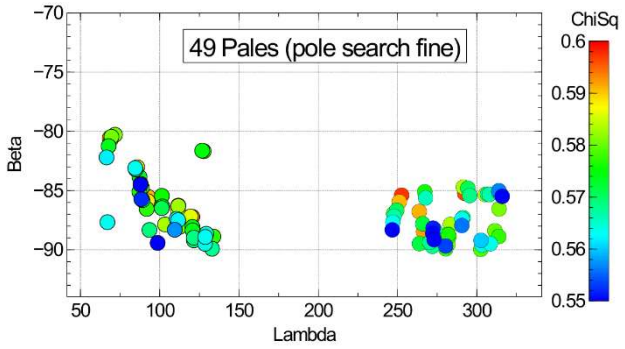

Figure 5. The "fine" pole search shows two clustered solutions (dark blue color) approximately centered near ecliptic longitude-latitude pairs (99°, -89°) and (273°, -89°) with a radius of 30° in lambda and Chi-Sq values within 3% of the lowest value.

Finally, we used the option "none" to get the shape models related to the two mirrored pole solutions found in the previous step. The two solutions are reported in Table II with some statistical data. The reported sidereal period was obtained by averaging the values found into this last step. Typical errors in the pole solution are assumed as ± 30° and the uncertainty in sidereal period has been evaluated as a rotational error of ± 30° over the total time span of the dense data set. We prefer the solution (272°, -88°) which has a lower RMS value.

λ °	β °	Sidereal Period (hours)	RMS	a/b ratio	Ratio of Moments	Angle Phi°
95	-89	20.7080 ± 0.0002	0.0135	1.052	1.0001	+0.8
272	-88		0.0133	1.053	1.0002	+1.9

Table II. The two refined spin axis solutions for 49 Pales (ecliptic coordinates) with an uncertainty of ± 30 degrees. The sidereal period was the average of the two solutions found in the pole search process.

Figure 6 shows the shape model while Figure 7 shows the fit between the model (black line) and observed lightcurves (red points). The fit appears to be good agreement in relation to the low amplitude of the lightcurves (< 0.2 mag) and the poor quality of some data.

The crowding of solutions close to the ecliptic latitude of -90 degrees with not well-isolated pole solutions, advises us to consider this solution as preliminary.

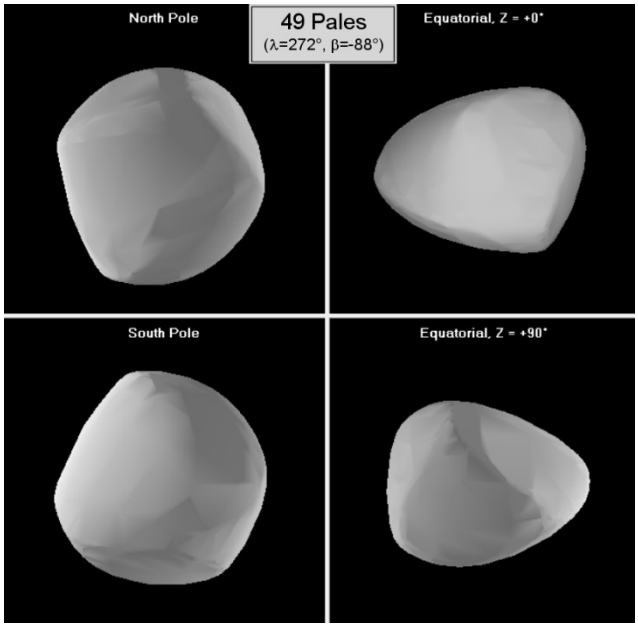

Figure 6. The shape model for 49 Pales (λ = 272°, β = -88°).

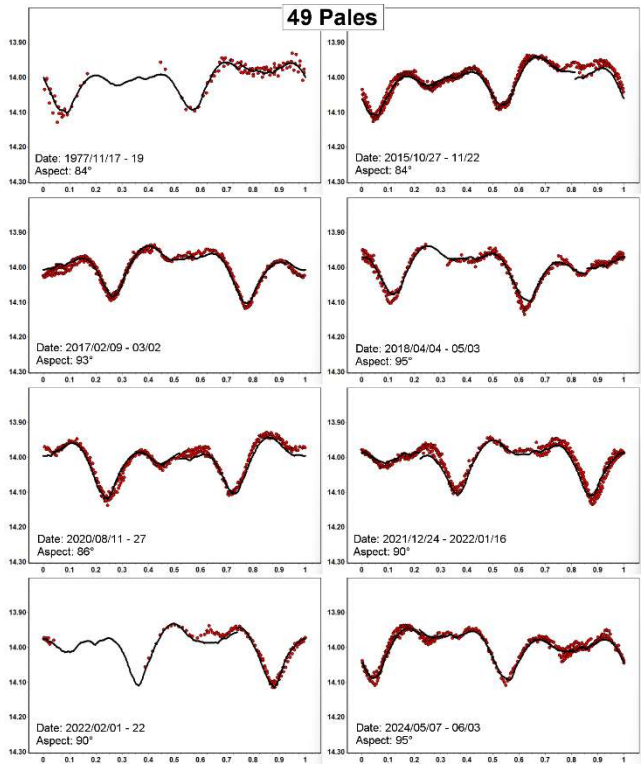

Figure 7. Model fit (black line) versus observed lightcurves (red points) for (λ = 272°, β = -88°) solution.

References

ALCDEF (2021). Asteroid Lightcurve Data Exchange Format web site. *http://www.alcdef.org/*

AstDyS-2 (2020). Asteroids - Dynamic Site. *https://newton.spacedys.com/astdys/*

Durech, J.; Kaasalainen, M.; Warner, B.D.; Fauerbach, M.; Marks, S.A.; Fauvaud, S.; Fauvaud, M.; Vugnon, J.-M.; Pilcher, F.; Bernasconi, L.; Behrend, R. (2009). "Asteroid models from combined sparse and dense photometric data." *A&A* **493**, 291-297.

Durech, J.; Sidorin, V.; Kaasalainen, M. (2010). "DAMIT: a database of asteroid models." *A&A* **513**, A46.

Franco, L.; Marchini, A.; Papini, R.; Iozzi, M.; Scarfi, G.; Mortari, F.; Gabellini, D.; Bacci, P.; Maestripieri, M.; Baj, G.; Galli, G.; Coffano, A.; Marinello, W.; Pizzetti, G.; Aceti, P.; Banfi, M.; Tinelli, L.; Montigiani, N.; Mannucci, M.; Noschese, A.; Mollica, M.; Guido, E.; Ruocco, N.; Bachini, M.; Succi, G. (2022). "Collaborative Asteroid Photometry from UAI: 2022 January-March" *Minor Planet Bulletin* **49**, 200-204.

Lagerkvist, C.-I., Magnusson, P., eds. (2024). Asteroid Photometric Catalog Bundle V1.0, urn:nasa:pds:compil.ast.apc.lightcurves:1.0. NASA Planetary Data System. *https://doi.org/10.26033/xx3z-ed06*

MPO LCInvert (2022). *https://minplanobs.org/BdwPub/php/mpolcinvert.php*

Pilcher, F.; Benishek, V.; Klinglesmith, D.A., III (2016). "Rotation Period, Color Indices, and H-G parameters for 49 Pales." *Minor Planet Bulletin* **43**, 182-183.

Pilcher, F. (2017). "Rotation Period Determinations for 49 Pales, 96 Aegle, 106 Dione 375 Ursula, and 576 Emanuela." *Minor Planet Bulletin* **44**, 249-251.

Pilcher, F. (2018). "New Lightcurves of 33 Polyhymnia, 49 Pales, 289 Nenetta, 504 Cora, and 821 Fanny." *Minor Planet Bulletin* **45**, 356-359.

Pilcher, F. (2021). "Lightcurves and Rotation Periods of 49 Pales, 383 Janina, and 764 Gedania." *Minor Planet Bulletin* **48**, 5-6.

Pilcher, F. (2022). "Lightcurves and Rotation Periods of 49 Pales, 424 Gratia, 705 Erminia, 736 Harvard, 1261 Legia, 1541 Estonia, and 6371 Heinlein." *Minor Planet Bulletin* **49**, 185-188.

Pilcher, F. (2024). "Lightcurves and Rotation Periods of 49 Pales, 62 Erato, 901 Brunsia, 995 Sternberga, and 1114 Lorraine." *Minor Planet Bulletin* **51**, 339-341.

Schober, H.J.; Scaltriti, F.; Zappala, V. (1979). "Photoelectric photometry and rotation periods of three large and dark asteroids: 49 Pales, 88 Thisbe and 92 Undina." *Astronomy and Astrophysics Suppl.* **36**, 1-8.

LIGHTCURVE AND ROTATION OF 55 PANDORA

S.M. Pritchard
125 Grim Hollow Rd.
Red Lion, PA 17356
seth.p@live.com

(Received: 2025 February 23)

A bimodal lightcurve was found for the main-belt asteroid 55 Pandora corresponding to a rotational period of 4.804±0.001 hours with an amplitude of 0.3204±0.0229 mag.

The observations reported here for asteroid 55 Pandora were taken from southern Pennsylvania at 200 meters elevation under Bortle 5 skies. Images were acquired with a 0.2m Celestron C8-N Newtonian reflector on an AVX mount using a ZWO ASI533MM Pro monochrome camera with a V-band Bessel filter. The equipment was operated remotely via the software N.I.N.A. (*Nighttime Imaging 'N' Astronomy*), with off-axis guiding through PHD2 and a ZWO ASI174 mini guide camera. All images were taken with an exposure of 40 seconds at a cadence of 30 seconds between frames.

Image files were calibrated in the standard way using flat field frames and bias frames. flats were taken using a commercial light panel and the "white t-shirt method", and a bespoke set of flats was taken for each observation session. As the ASI533MM does not have any appreciable amp glow, no dark frames were required. Image processing and data analysis was done in *Tycho Tracker Pro* v12.3.1 (Parrott, 2020) using the differential aperture photometry tool. Comp stars were selected for brightness between 13 and 11 mag, a distance of no more than 15 arcmin from the target, and minimal to no variability or scatter in computed mag. A final visual inspection for roundness and lack of aberrations was done by the author.

55 Pandora is a large main-belt asteroid of Tholen spectral type M, with an estimated diameter of 84.8 ± 2.50 km by NEOWISE (Masiero et al., 2012). Martikainen et al. (2021) report a rotation period of 4.804 hours, which is in agreement with results published in the asteroid lightcurve database (Warner et al., 2009). It is not a known member of any asteroid families.

A lightcurve was constructed from image sequences taken on 3 separate nights. On each night sufficient images were taken to capture one complete rotation. A sidereal rotation period of 4.804±0.001 hours was reliably obtained, with an amplitude of 0.3204±0.0229 mag. The SNR of the asteroid between all three image sequences varied between 98.6 and 358.8, with an average of 262.7. The data were corrected for light travel time and with an assumed G value of 0.15.

Acknowledgements

Work on the asteroid lightcurve database (LCDB) was funded in part by National Science Foundation grants AST-1210099 and AST-1507535.

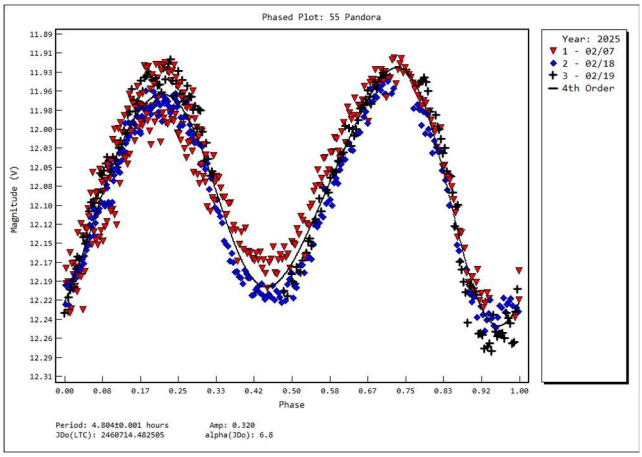

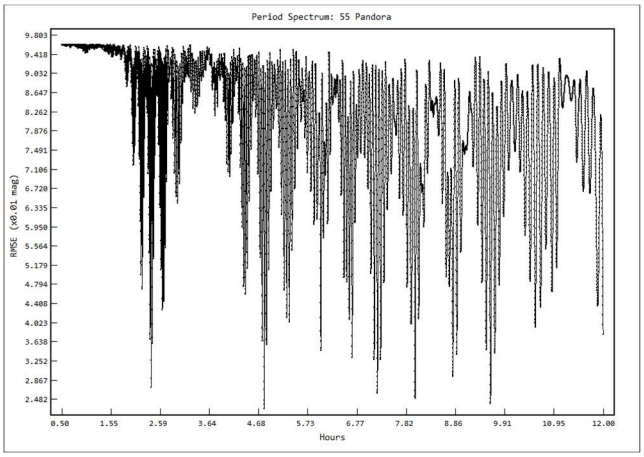

References

Harris, A.W.; Young, J.W.; Scaltriti, F.; Zappala, V. (1984). "Lightcurves and phase relations of the asteroids 82 Alkmene and 444 Gyptis." *Icarus* **57**, 251-258.

Martikainen, J.; Muinonen, K.; Penttila, A.; Cellino, A.; Wang, X.-B. (2021). "Asteroid absolute magnitudes and phase curve parameters from Gaia photometry." *Astron. Astrophys*. **649**, A98.

Masiero, J.R.; Mainzer, A.K.; Grav, T.; Bauer, J.M.; Cutri, R.M.; Nugent, C.; Cabrera, M.S. (2012) "Preliminary Analysis of WISE/NEOWISE 3-Band Cryogenic and Post-Cryogenic Observations of Main Belt Asteroids." *The Astrophysical Journal Letters* **759**, L8.

Parrott, D. (2020). "Tycho Tracker: A New Tool to Facilitate the Discovery and Recovery of Asteroids using Synthetic Tracking and Modern GPU Hardware." *Journal of the American Association of Variable Star Observers (JAAVSO)* **48**, 262.

Warner, B.D.; Harris, A.W.; Pravec, P. (2009). "The Asteroid Lightcurve Database." *Icarus* **202**, 134-146. Updated 2023 Oct 01. *http://www.minorplanet.info/lightcurvedatabase.html*

Number	Name	yyyy mm/dd	Phase	L_{PAB}	B_{PAB}	Period(h)	P.E.	Amp	A.E.	Grp
55	Pandora	2025 02/07-02/19	6.8,10.6	124	8	4.804	0.001	0.3204	0.0229	MB

Table I. Observing circumstances and results. The phase angle is given for the first and last date. If preceded by an asterisk, the phase angle reached an extrema during the period. L_{PAB} and B_{PAB} are the approximate phase angle bisector longitude/latitude at mid-date range (see Harris et al., 1984). Grp is the asteroid family/group (Warner et al., 2009).

THE LIGHTCURVE AND ROTATION PERIOD OF 637 CHRYSOTHEMIS

Frederick Pilcher
Organ Mesa Observatory (G50)
4438 Organ Mesa Loop
Las Cruces, NM 88011 USA
fpilcher35@gmail.com

Eric V. Dose
3167 San Mateo Blvd NE #329
Albuquerque, NM 87110 USA

(Received: 2025 March 13)

We present the first ever published rotation period and amplitude for 637 Chrysothemis: 42.93 ± 0.01 hours and 0.31 ± 0.02 magnitudes, respectively, with an asymmetric bimodal lightcurve.

The only entry for 637 Chrysothemis in the Asteroid Lightcurve Database (Warner et al., 2009), is by Warner (2017) who published a lightcurve with reliability 1 (uncertain value) based on only 4.5 hours of data on a single night. That result, a period of 3.7 hours with an amplitude 0.06 magnitudes, had a scatter of data points exceeding the amplitude of the lightcurve.

To investigate this asteroid, observations by author Pilcher were made at the Organ Mesa Observatory with a Meade 35-cm LX200 GPS Schmidt-Cassegrain, SBIG STL-1001E CCD, 120 second exposures, unguided, clear filter. Image measurement and lightcurve construction were with *MPO Canopus* software with calibration star magnitudes for solar colored stars from the rmag band in the Atlas Refcat 2 catalog. Observations by author Dose were made at the New Mexico Skies Observatory with a 0.50-m PlaneWave OTA on a PlaneWave L-500 mount and equatorial wedge. Images were obtained with an SBIG AC4040M CMOS camera fitted with a Schott GG495 yellow filter. A full description of the measurement and reduction procedure is described in Dose (2025).

Zero-point adjustments of a few ×0.01 magnitude were necessary to make a good fit to the data set combined with sessions by both observers. To reduce the number of data points on the lightcurve and make them easier to read, data points have been binned in sets of 3 with maximum time difference 6 minutes.

A total of 19 sessions by the two observers combined, 2025 Jan. 22 - Feb. 28, provide an excellent fit to an asymmetrical bimodal lightcurve with period 42.93 ± 0.01 hours, amplitude 0.31 ± 0.02 magnitudes.

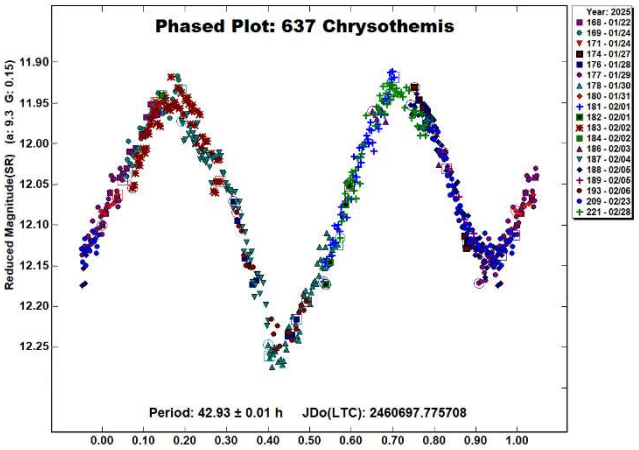

References

Dose, E.V. (2025). "Lightcurves of eight asteroids." *Minor Planet Bull.* **52**, 27-31.

Harris, A.W.; Young, J.W.; Scaltriti, F.; Zappala, V. (1984). "Lightcurves and phase relations of the asteroids 82 Alkmene and 444 Gyptis." *Icarus* **57**, 251-258.

Warner, B.D.; Harris, A.W.; Pravec, P. (2009). "The Asteroid Lightcurve Database." *Icarus* **202**, 134-146. Updated 2023 Oct. *https://minplanobs.org/MPInfo/php/lcdb.php*

Warner, B.D. (2017). "Asteroid lightcurve analysis at the CS3-Palmer Divide Observatory, 2016 July-September." *Minor Planet Bull.* **44**, 12-14.

Number	Name	yyyy/mm/dd	Phase	L_{PAB}	B_{PAB}	Period(h)	P.E	Amp	A.E
637	Chrysothemis	2025/01/22-2025/02/28	*9.3 - 5.6	146	0	42.93	0.01	0.31	0.02

Table I. Observing circumstances and results. The phase angle is given for the first and last dates, where the * indicates that a minimum was reached between these dates. L_{PAB} and B_{PAB} are the approximate phase angle bisector longitude and latitude at mid-date range (see Harris et al., 1984).

BROAD-BAND MONITORING OF 797 MONTANA

Misty C. Bentz
Department of Physics and Astronomy
Georgia State University
25 Park Place, Suite 605
Atlanta, GA 30303 USA
bentz@astro.gsu.edu

Rachel Alahakone, Lexi Azoulay, Emily Burns-Kaurin,
Akshat S. Chaturvedi, Madeline Davis, Karina Kimani-Stewart,
Madison Markham, John P. McGuire, Emma McMullan,
Mahir Patel, Meenakshi Binu Raj, Daijha Sankey,
Abeni Amber-Lee Wilson, Karisa Zdanky
Georgia State University
Atlanta, GA USA

(Received: 2025 April 3)

Broad-band monitoring of asteroid 797 Montana was conducted over the course of four nights in 2025 February. Observations from the first three nights were obtained through a Johnson V filter, while the fourth night was collected as unfiltered observations. We find a best-fit rotation period of 4.545 ± 0.001 h, which agrees with previous measurements, and an amplitude of variability of ΔV = 0.50 ± 0.03 mag, which agrees with an early measurement but is somewhat larger than most studies have reported.

Asteroid 797 Montana was discovered in 1914 by Holger Thiele at Hamburg-Bergedorf Observatory. A main-belt asteroid, 797 Montana is listed in the JPL Small Body Database with a stony S-type classification (JPL, 2025).

Students enrolled in the *Observational Techniques and Instrumentation* class at Georgia State University collected observations of 797 Montana over the course of four nights between 2024 February 07-14 (UT dates here and throughout). They employed the Miller Telescope, a 24-inch Planewave f/6.5 Corrected Dall-Kirkham Astrograph, at GSU's Hard Labor Creek Observatory in Rutledge, GA.

Multiple equipment failures plagued the class this semester. For the first three nights (February 07, 08, and 10), observations were acquired using our backup CCD, an Apogee Alta with 2048 × 2048 pixels. These images were acquired through a Johnson *V* filter, and each image covered a field of view of 26.3 arcmin × 26.3 arcmin with a pixel scale of 0.77 arcsec. On the evening of February 14, the Apogee Alta suffered an electronic short, so an SBIG camera of unknown heritage was unearthed from a closet and mounted on the telescope. Images acquired with the SBIG camera were unfiltered, since the camera could not be used with our existing filter wheel. The SBIG detector provided 1472 × 2184 pixels, and plate solving with astrometry.net (Lang et al., 2010) determined that this corresponded to a field of view of 8.6 arcmin × 12.8 arcmin on the sky with a pixel scale of 0.35 arcsec.

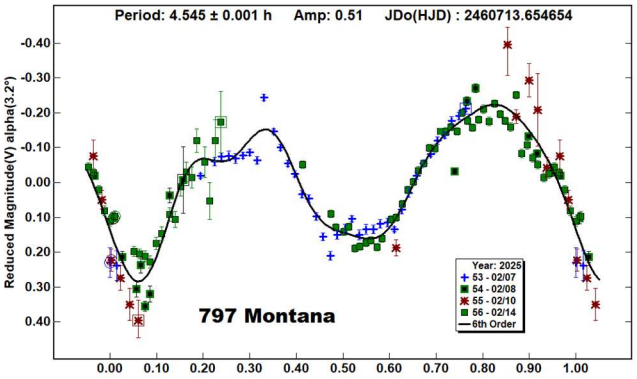

Across the four nights, the weather conditions were mixed, ranging from clear to partly cloudy, and the moon phase ranged from waxing to waning gibbous. Exposure times varied between 150 - 300 s, and all observations were acquired at airmasses < 2.4.

Images from all nights were reduced in *IRAF*. Reductions of the Apogee Alta images included bias and overscan subtraction, dark subtraction, and flat fielding. A leak in the camera seal allowed moisture to collect and condense on the detector, so additional "droplet masks" were created by medianing together several dithered frames to allow most of the remaining droplet pattern to be divided out. The SBIG camera did not suffer from the condensation problem, but also did not provide an overscan region, so reductions were composed of only bias and dark subtraction and flat fielding.

Aperture photometry was carried out in *IRAF*, with measurements of the asteroid and 3-5 field stars acquired from each reduced image. *V*-band measurements of field stars were obtained from the AAVSO Photometric All-Sky Survey (Henden et al., 2009) and were used to convert instrumental magnitudes to calibrated Vega magnitudes for the nights of February 07-10. The unfiltered observations collected on February 14 were adjusted by an offset of ~2 mag to match the calibrated *V*-band observations on the other three nights.

The rotation period and amplitude of variability for 797 Montana were determined using *MPO Canopus*, which implements the Fourier Analysis of Light Curves (FALC) algorithm of Harris et al. (1989). We included 137 measurements and explored fitting orders between 4 and 8 for the period search, with a 6th order fitting solution displayed in the folded lightcurve above. We find that the best-fit period is very stable despite the choice of orders, while the amplitude of variability is somewhat sensitive to this choice. From this analysis, we adopt a final rotation period of 4.545 ± 0.001 h and a *V*-band amplitude of 0.50 ± 0.03 mag.

Our results agree with previous determinations of the rotation period, which include 4.5 h (Angeli et al., 2001), 4.55 ± 0.01 h (Ditteon et al., 2004), 4.5463 ± 0.0002 h (Behrend, 2007web), and 4.54619 ± 0.00005 h (Hanuš et al., 2016). The amplitude of variability that we find agrees with that reported by Angeli et al. (2001) of 0.5 mag, but is somewhat larger than the values reported by Ditteon et al. (2004) of 0.32 ± 0.02 mag and Behrend (2007web) of 0.41 ± 0.01 mag. It is possible that the amplitude of variability

Number	Name	yyyy mm/dd	Phase	L_{PAB}	B_{PAB}	Period(h)	P.E.	Amp	A.E.	Grp
797	Montana	2025 02/07-02/14	1.5,4.9	135	0	4.545	0.001	0.50	0.03	9104

Table I. Observing circumstances and results. The phase angle is given for the first and last date. If preceded by an asterisk, the phase angle reached an extrema during the period. L_{PAB} and B_{PAB} are the approximate phase angle bisector longitude/latitude at mid-date range (see Harris et al., 1984). Grp is the asteroid family/group (Warner et al., 2009).

determined from our lightcurves is slightly inflated by residual noise after attempting to correct for the droplet patterns on the detector. A physical explanation is a more-equatorial aspect for our observations.

Acknowledgements

NOIRLab *IRAF* is distributed by the Community Science and Data Center at NSF NOIRLab, which is managed by the Association of Universities for Research in Astronomy (AURA) under a cooperative agreement with the U.S. National Science Foundation. This research was made possible in part based on data from the AAVSO Photometric All-Sky Survey (APASS), funded by the Robert Martin Ayers Sciences Fund and NSF AST-1412587. The Nova.astrometry.net web service is hosted by the Canadian Advanced Network for Astronomical Research operated by the Canadian Astronomy Data Center, part of the National Research Council of Canada.

References

Angeli, C.A.; Guimarães, T.A.; Lazzaro, D.; Duffard, R.; Fernández, S.; Florczak, M.; Mothé-Diniz, T.; Carvano, J.M.; Betzler, A.S. (2001). "Rotation Periods for Small Main-Belt Asteroids From CCD Photometry." *Astron. J.* **121**, 2245-2252.

Behrend, R. (2007web). "Courbes de rotation d'astéroïdes et de comètes." *http://obswww.unige.ch/~behrend/page_cou.html*

Ditteon, R.; Hirsch, B.; Kirkpatrick, E.; Kramb, S.; Kropf, M.; Meehl, J.; Stanfield, M.; Tollefson, E.; Twarek, A. (2004). "2003-04 winter observing campaign at Rose-Hulman Institute. Results for 797 Montana, 3227 Hasegawa, 3512 Eriepa, 4159 Freeman, 5234 Sechenov, and (5892) 1981 YS1." *Minor Planet Bull.* **31**, 54-56.

Hanuš, J.; Ďurech, J.; Oszkiewicz, D.A.; Behrend, R.; Carry, B.; Delbo, M.; and 163 coauthors. (2016). "New and updated convex shape models of asteroids based on optical data from a large collaboration network." *Astron. Astrophys.* **586**, A108.

Harris, A.W.; Young, J.W.; Scaltriti, F.; Zappala, V. (1984). "Lightcurves and phase relations of the asteroids 82 Alkmene and 444 Gyptis." *Icarus* **57**, 251-258.

Harris, A.W.; Young, J.W.; Bowell, E.; Martin, L.J.; Millis, R.L.; Poutanen, M.; Scaltriti, F.; Zappala, V.; Schober, H.J.; Debehogne, H.; Zeigler, K.W. (1989). "Photoelectric Observations of Asteroids 3, 24, 60, 261, and 863." *Icarus* **77**, 171-186.

Henden, A.A.; Terrell, D.; Levine, S.E.; Templeton, M.; Smith, T.C.; Welch, D.L. (2009). "APASS: The AAVSO Photometric All-Sky Survey." *http://www.aavso.org/apass*

JPL (2025). "Small-Body Database Browser." *https://ssd.jpl.nasa.gov/tools/sbdb_lookup.html*

Lang, D.; Hogg, D.W.; Mierle, K.; Blanton, M.; Roweis, S. (2010). "Astrometry.net: Blind Astrometric Calibration of Arbitrary Astronomical Images." *Astron. J.* **139**, 1782-1800.

Warner, B.D.; Harris, A.W.; Pravec, P. (2009). "The Asteroid Lightcurve Database." *Icarus* **202**, 134-146. Updated 2023 Oct 1. *http://www.MinorPlanet.info/php/lcdb.php*

LIGHTCURVES AND THE ROTATION PERIOD OF THE AMOR-TYPE ASTEROID 887 ALINDA

Frederick Pilcher
Organ Mesa Observatory (G50)
4438 Organ Mesa Loop
Las Cruces, NM 88011 USA
fpilcher35@gmail.com

Jesús Delgado Casal
Observatorio Nuevos Horizontes (Z73)
Camas (Sevilla - SPAIN) CP 41900

Geoffrey Stone
Dimension Point Observatory (V42)
14 Galaxy Point, Mayhill, NM 88339 USA

(Received: 2025 April 8)

We find for the Amor-type asteroid 887 Alinda at its close approach to Earth in 2024-2025 a rotation period of 74.21 ± 0.01 hours, amplitude 0.28 ± 0.02 mag.

The Amor-type asteroid 887 Alinda has orbital elements a =2.479, e=0.567, i=9.353. Prior to the year 2025, the most recent very close approach to Earth was 1974 January at a minimum geocentric distance 0.137 AU. From photometric observations at this occasion, Dunlap and Taylor (1979) published a rotation period of 73h 58m based on incomplete phase coverage. At a moderately close approach to 0.836 AU in 2020 September, Behrend (2020) published an incomplete lightcurve phased to 28.4 hours.

On 2025 January 8, minor planet 887 Alinda passed even closer to Earth, 0.082 AU, than in 1974, and was brighter than magnitude 15 from 2024 October through 2025 March. We present two separate lightcurves and rotation periods that were acquired, respectively, after and before closest approach.

The observations by Pilcher to produce the results reported in this paper were made at the Organ Mesa Observatory with a Meade 35 cm LX200 GPS Schmidt-Cassegrain, SBIG STL-1001E CCD, 60 to 120 second exposures, unguided, clear filter. Observations by Delgado are with an 11-inch Celestron Schmidt-Cassegrain, Atik 4.14 EX CCD, 60 to 120 second exposures. Observations by Stone are with a 0.51m f/8 Ritchey-Chretien mounted on a Paramouont ME-II mount, SBIG AC4040 CMOS camera, Johnson-Cousins R filter, unguided.

For image measurement and lightcurve construction, authors Pilcher and Delgado used *MPO Canopus* software with calibration star magnitudes for solar colored stars from the CMC15 catalog reduced to the Cousins R band. Author Stone used Tycho-Tracker software with near solar colored stars chosen from the ATLAS Refcat 2 with Sloan r' magnitudes. Zero-point magnitudes were adjusted for best fit in the 2025 Feb. 6 - Apr. 1 session set. To reduce the number of data points on the lightcurves and make them easier to read, data points have been binned in sets of 3 with maximum time difference 5 minutes.

A dense lightcurve and robust period were acquired after closest approach. Between 2025 Feb. 6 and Apr. 1, authors Pilcher, Delgado, and Stone acquired data sets on 22 nights, with observing runs seven hours or longer. Their data can be plotted on a dense bimodal phased lightcurve with complete phase coverage and period 74.21 ± 0.01 hours, amplitude 0.28 ± 0.02 magnitudes.

Number	Name	yyyy/mm/dd	Phase	L_{PAB}	B_{PAB}	Period(h)	P.E	Amp	A.E.
887	Alinda	2024/11/06-2024/12/23	26.7 - 40.1	55	-24	74.07	0.02	0.28	0.03
887	Alinda	2025/02/06-2025/04/01	*24.8 - 26.8	154	+18	74.21	0.01	0.28	0.02

Table I. Observing circumstances and results. The phase angle is given for the first and last date, unless a minimum (second value) was reached. L_{PAB} and B_{PAB} are the approximate phase angle bisector longitude and latitude at mid-date range (see Harris et al., 1984).

Before closest approach Geoffrey Stone obtained lightcurves up to four hours on eight nights from 2024 Nov. 6 - Dec. 23. The data from these sessions alone were insufficient to compute an independent period. After the robust post-opposition 74.21-hour period was found from the data by Pilcher et al., a good fit could be made to a period of 74.07 ± 0.02 hours, amplitude 0.28 ± 0.03 magnitudes.

Combined, these observations cover an interval of nearly five months while the target asteroid moved continuously eastward between celestial longitude and latitude 43°, -22°, respectively, on 2024 Nov. 6 to 166°, +16°, respectively, on 2025 April 1. There was no retrograde loop at opposition on 2025 Jan. 9. The 74-hour period published by Dunlap and Taylor (1979) is confirmed, and the 28.4-hour period by Behrend (2020) is ruled out.

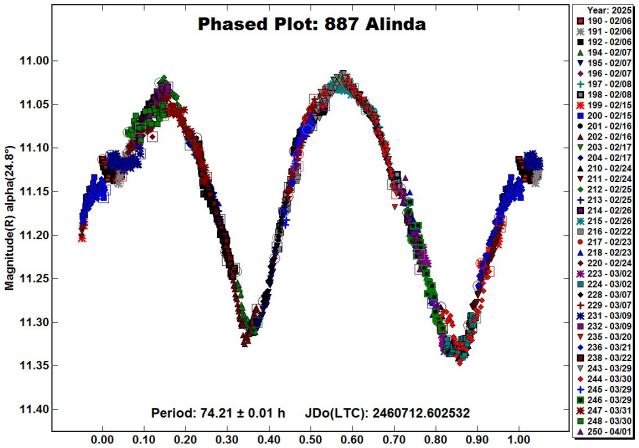

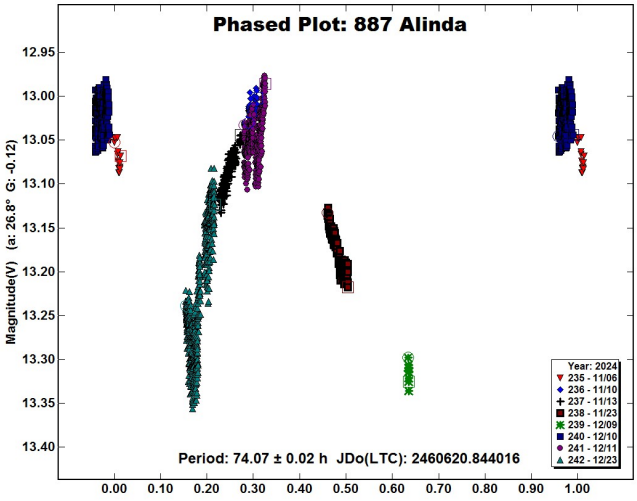

References

Behrend, R. (2020). Observatoire de Geneve web site. *http://*obswww.unige.ch/*~behrend/page_cou.html*

Dunlap, J.L.; Taylor, R.C. (1979). "Minor planets and related and related objects. XXVII. Lightcurves of 887 Alinda." *Astron. J.* **84**, 269-273.

Harris, A.W.; Young, J.W.; Scaltriti, F.; Zappala, V. (1984). "Lightcurves and phase relations of the asteroids 82 Alkmene and 444 Gyptis." *Icarus* **57**, 251-258.

Warner, B.D., Harris, A.W., Pravec, P. (2009). "The Asteroid Lightcurve Database." *Icarus* **202**, 134-146. Updated 2023 Oct. *http://www.minorplanet.info/lightcurvedatabase.html*

LIGHTCURVE ANALYSIS AND ROTATION PERIOD FOR (887) ALINDA

Geovandro Nobre
OARU Observatory (X33)
194 Bela Vista St, Manaus, AM, BRAZIL
oaru.manaus@gmail.com

(Received: 2025 March 5 Revised: 2025 April 4)

Lightcurve observations of NEA (887) Alinda during its closest approach to Earth in late 2024 to early 2025 yield a most likely determination of its synodic rotation period of 73.03 ± 0.01 h. The period estimate is in agreement with the observations of Dunlap and Taylor (1979), whose period was found to be around 74 h, but other periods found could be considered: 71 h and 85.3 h.

Alinda is a mid-sized asteroid whose orbit approaches the orbit of Earth but does not cross it. NASA JPL has classified Alinda as a "Near Earth Asteroid" due to its orbit's proximity to Earth, but it is not considered potentially hazardous because computer simulations have not indicated any imminent likelihood of future collision. Alinda orbits the sun every 1,420 days (3.89 years), coming as close as 1.06 AU and reaching as far as 3.88 AU from the sun. Alinda is about 4.2 kilometers in diameter.

Two rotation periods have been reported for this asteroid: 28.4 h in 2020 (Behrend et al., 2020web), and ~74 h (Dunlap and Taylor, 1979). Here we report that we observed (887) Alinda during its most recent close approach, between 2024 November 17 and 2025 February 28, at the OARU Observatory (X33) in Manaus, Brazil. Observations were carried out using a 200 mm f/5 reflecting telescope equipped with an ASI 294 MC Pro camera. No photometric filters were used, and the exposure time was 30 seconds. All observations were made with 2×2 binning at a plate scale of 1.91 arcsec/pixel. The asteroid and seven comparison stars were measured. Comparison stars were selected with color indices within the range of $0.5 < B\text{-}V < 0.95$, aligning with the typical color range of asteroids.

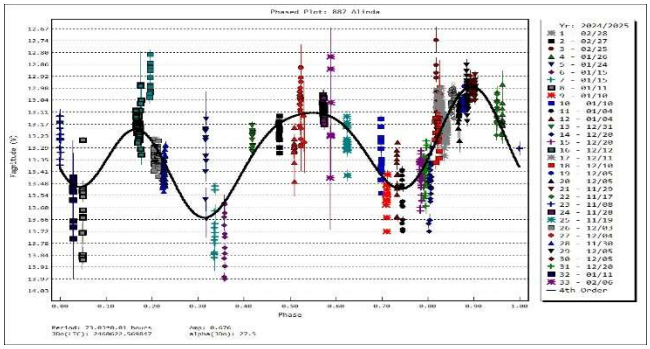

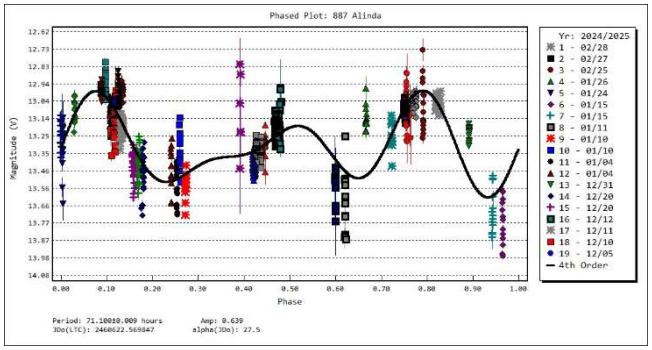

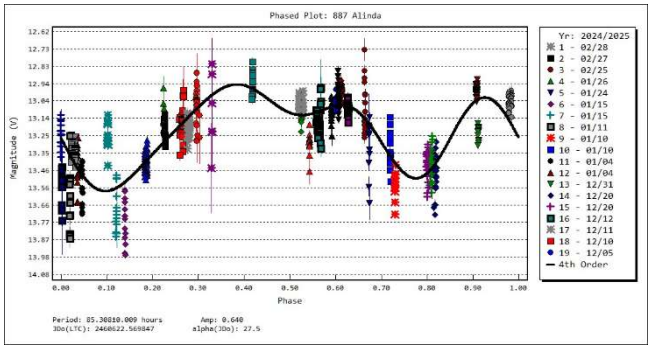

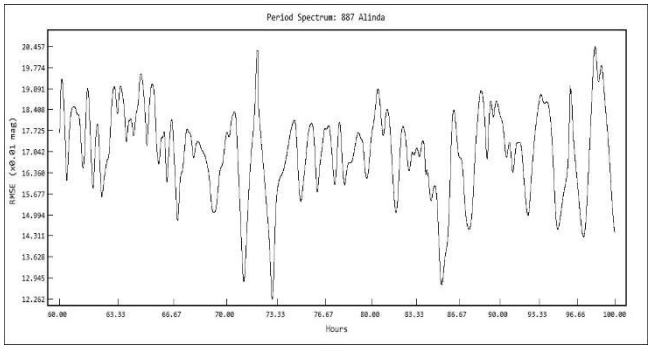

Data reduction and period analysis were performed with *Tycho Tracker Pro* (version 11.7.8) (Parrott, 2020). Three important rotational periods were found in the periodogram, respectively 71h, 73.03h and 85.3h The most likely curve suggests a rotation period of 73.03 ± 0.01 hours, since, in addition to having the lowest RMSE value in the periodogram. This is the one that is most in agreement with the observations of Dunlap and Taylor (1979), whose period was found to be around 73 and 58 minutes. The lightcurve amplitude is approximately 0.67 magnitudes, which indicates a modest elongated shape or albedo variations on the asteroid's surface. More studies will be necessary to complement and accurately determine the rotation period of this asteroid, but the next closest approach to Earth will only occur in January of 2087.

Number	Name	yyyy mm/dd	Phase	L_{PAB}	B_{PAB}	Period(h)	P.E.	Amp	A.E.	Grp
887	Alinda	2024 11/17-2025 02/28	9.2,42.1	81	-12	73.03	0.01	0.67	0.12	NEA

Table I. Observing circumstances and results. The phase angle is given for the first and last date. If preceded by an asterisk, the phase angle reached an extrema during the period. L_{PAB} and B_{PAB} are the approximate phase angle bisector longitude/latitude at mid-date range (see Harris et al., 1984). Grp is the asteroid family/group (Warner et al., 2009).

Acknowledgments

I thank my wife, Andrea Nobre, for accepting my absence during the nights I dedicated to observing this asteroid. I also extend my gratitude to Mr. Richard Binzel, Professor of Planetary Science at the Minor Planet Bulletin for their support in reviewing and publishing these papers.

References

Behrend, R. (2020web). Observatoire de Geneve web site. *https://www.astro.unige.ch/~behrend/page3cou.html#000887*

Dunlap, J.L.; Taylor, R.C. (1979). "Minor planets and related objects. XXVII. Lightcurves for 887 Alinda." *Astron. J.* **84**, 273-279.

Goldstone Radar Observations Planning. *https://echo.jpl.nasa.gov/asteroids/Nov-Dec2024*

Harris, A.W.; Young, J.W.; Scaltriti, F.; Zappala, V. (1984). "Lightcurves and phase relations of the asteroids 82 Alkmene and 444 Gyptis." *Icarus* **57**, 251-258.

Minor Planet Center. *https://www.minorplanetcenter.net*

Parrott, D. (2020). "Tycho Tracker: A New Tool to Facilitate the Discovery and Recovery of Asteroids using Synthetic Tracking and Modern GPU Hardware." *Journal of the American Association of Variable Star Observers (JAAVSO)* **48**, 262.

Pilcher, F. (2024). "An appeal for photometric observations of 887 Alinda." *Minor Planet Bulletin* **51**, 303.

Space Reference. *https://www.spacereference.org/asteroid/887-alinda-a918-aa*

Tycho Tracker Software. *https://www.tycho-tracker.com*

Warner, B.D.; Harris, A.W.; Pravec, P. (2009). "The Asteroid Lightcurve Database." *Icarus* **202**, 134-146. Updated 2016 Sep. *http://www.minorplanet.info/lightcurvedatabase.html*

LIGHTCURVE AND ROTATION PERIOD OF NEAR-EARTH ASTEROID 887 ALINDA DURING THE 2025 CLOSE APPROACH

Timothy C. Brothers
Massachusetts Institute of Technology (MIT)
Department of Earth, Atmospheric and Planetary Sciences
Wallace Astrophysical Observatory (810)
50 Groton Rd., Westford, MA 01886, USA
bro@mit.edu

Fatima Nasir Abbasi
MIT Department of Mathematics
Cambridge, MA 02139, USA

Jayna Ekelmann
MIT Department of Earth, Atmospheric and Planetary Sciences
Cambridge, MA 02139, USA

Michael J. Person
MIT Department of Earth, Atmospheric and Planetary Sciences
MIT Wallace Astrophysical Observatory (810)
Cambridge, MA 02139, USA

Artem Burdanov, Jensen Lawrence, Kaylee Barrera,
Saverio Cambioni, Julien de Wit
MIT Department of Earth, Atmospheric and Planetary Sciences
Cambridge, MA 02139, USA

Pari Rajesh, Emily Albornoz, William Hazell
MIT Department of Aeronautics and Astronautics
Cambridge, MA 02139, USA

Erin Cusson, Jan Toomlaid, Matthew Nunez,
Prajna Nair, Elaine Sheffield
MIT Department of Physics
Cambridge, MA 02139, USA

Zimi Zhang
MIT Department of Mathematics
Cambridge, MA 02139, USA

Amius Marshall-De'Ath
MIT Department of Earth, Atmospheric and Planetary Sciences
Cambridge, MA 02139, USA
and
Imperial College London
London SW7 2AZ, UK

(Received: 2025 April 11)

A month-long global campaign of MIT observers distributed across three telescopes at Wallace Astrophysical Observatory (WAO), USA and three telescopes at Teide Observatory on the island of Tenerife, Spain determined that 887 Alinda has a synodic period of 73.96 ± 0.01 hours and a lightcurve amplitude of 0.23 ± 0.01 magnitudes as measured at a distance of approximately 12.2 million km from Earth.

Number	Name	yyyy mm/dd	Phase	L_{PAB}	B_{PAB}	Period(h)	P.E.	Amp	A.E.	Grp
887	Alinda	2025 01/03-02/06	*25.89,24.77	117	8	73.96	0.01	0.230	0.01	9101

Table I. Observing circumstances and results. The phase angle is given for the first and last date. If preceded by an asterisk, the phase angle reached an extrema during the period. L_{PAB} and B_{PAB} are the approximate phase angle bisector longitude/latitude at mid-date range (see Harris et al., 1984). Grp is the asteroid family/group (Warner et al., 2009).

887 Alinda is an S-type asteroid with a diameter of 6.6 ± 2.0 km diameter (Masiero et al., 2021) belonging to the Amor Near-Earth asteroid family. In January 2025, Alinda passed within 0.082 AU of Earth, its nearest approach since its discovery in 1918 and for the next 500 years (JPL Horizons, 2025). This presented an unprecedented opportunity to measure its rotational amplitude and period.

This observation campaign was initiated in response to the call for Alinda observations in MPB 51-4 (Pilcher, 2024). It was conducted for the purpose of resolving a discrepancy in Alinda's period and amplitude amongst previous attempts by Dunlap and Taylor (1979) and Augustin and Behrend (2020), which determined 73.97 ± 0.05 hours with a 0.35 magnitude amplitude and 28.41 ± 0.05 hours with a 0.123 ± 0.004 magnitude amplitude, respectively. Additionally, according to the Light Curve Database, Tungalog et al. (2002) determined a 73.827-hour period. See Table I for Alinda observation circumstances and results.

Photometry data used for period and amplitude determination were collected in the Sloan r' filter. Supplementary data were taken on the WAO Pier 2 0.35-m telescope in g' and z' filters, although, only the g' data was usable. Over 11,000 images were recorded on six different telescopes with varying apertures, detectors, and methods which are summarized in Table II.

Alinda brightened to at least 8.914 ± 0.023 magnitude (r') on the night of 2025-01-10 UT, two nights after its closest distance to Earth. While the exceptional brightness of the object was advantageous in terms of signal to noise, it did pose saturation issues for the larger telescopes. For the meter-class telescopes in Spain (Teide Observatory, Tenerife, Spain), the solution was to defocus the field, spreading stellar and asteroid signal across more pixels. This required observers to constantly monitor both exposure time and signal levels to account for changing seeing conditions and airmass. In the case of the Elliot 0.6m telescope (Wallace Astrophysical Observatory, Westford, MA, USA) observations were automated using *Voyager* software, meaning a predicted exposure time was required and live adjustments were not possible. Early observations (e.g. 4 Jan 2025) that were near saturation were discarded and exposure times were adjusted to provide more stable imaging on future nights. All WAO data collected on 0.35 robotic telescopes were operated remotely from the MIT campus, 43 km away, by undergraduate student observers. The three Teide Observatory telescopes were operated manually by MIT instructors, graduate students, and undergraduates as part of MIT Course 12.411: *Astronomy Field Camp*.

Photometric analysis was performed using *Tycho Tracker Pro v12.3.1* (Parrott, 2020) for all of the WAO and Telescopio Carlos Sánchez (TCS) data points. Standards were sourced from ATLAS2 r' comparison stars within a color index range of 0.5 < B-V < 0.9. Defocused data obtained at the TCS and Artemis telescopes were analyzed with *AstroImageJ* (Collins et al., 2017*)* using APASS r' calibration stars*,* after which photometry was converted to ALCDEF format.

Site (MPC)	Telescope	Detector filter	Date (2025)	Images Used	M*
MIT-WAO (810)	Elliot 0.6m	16803 CCD r′	01-03	437	A
MIT-WAO (810)	Elliot 0.6m	16803 CCD r′	01-04	323	A
MIT-WAO (810)	Elliot 0.6m	16803 CCD r′	01-05	0	A
MIT-WAO (810)	Elliot 0.6m	16803 CCD r′	01-06	448	A
MIT-WAO (810)	Elliot 0.6m	16803 CCD r′	01-07	322	A
MIT-WAO (810)	Elliot 0.6m	16803 CCD r′	01-08	339	A
MIT-WAO (810)	Pier 2 0.35m	IMX571 CMOS, r′	01-07	0	RR
Teide (954)	IAC80 0.82m	CAMELOT2 r′	01-09	502	R
MIT-WAO (810)	Elliot 0.6m	16803 CCD r′	01-09	325	A
MIT-WAO (810)	Pier 2 0.35m	IMX571 CMOS, r′	01-10	247	RR
MIT-WAO (810)	Pier 3 0.35m	IMX571 CMOS, g′	01-10	33	RR
Teide (Z25)	ARTEMIS 1.0m	BEX2-DD9TW, r′	01-11	155	R
Teide (954)	TCS 1.52m	MUSCAT2 r′	01-15	0	R
Teide (Z25)	ARTEMIS 1.0m	BEX2-DD9TW, r′	01-16	367	R
Teide (Z25)	ARTEMIS 1.0m	BEX2-DD9TW, r′	01-17	0	R
Teide (Z25)	ARTEMIS 1.0m	BEX2-DD9TW, r′	01-19	365	R
Teide (Z25)	ARTEMIS 1.0m	BEX2-DD9TW, r′	01-21	133	R
MIT-WAO (810)	Elliot 0.6m	16803 CCD r′	02-05	600	A
MIT-WAO (810)	Elliot 0.6m	16803 CCD r′	02-06	48	A

Table II. Observational Assets and Data Acquired. M* denotes which method of observation was used: A is automated, R is in-person robotic and RR is remote robotic.

All 14 photometry sets were assembled in *Tycho* in order to determine a best fitting period and amplitude. Figure 1 shows the phased photometric results from all used data sets (as indicated in Table II). Note the close correspondence between data sets of widely disparate nights, such as 7 January 2025 and 4 February 2025. Minor adjustments in magnitude were made to several contributing datasets on the order of a few 10's of mmag to account for variations among standard star magnitudes in differing catalog fields.

Figure 2 plots the resulting periodogram from the combined dataset resulting in our preferred solution of 73.96 ± 0.01 hr and a 0.23 ± 0.01 magnitude amplitude. Aliased multiples (and fractions) of this period can be seen in the periodogram, but our best fitting two-peaked solution is well determined by the data.

A secondary purpose of this observational program was to prepare for future minor planet observation campaigns which will efficiently characterize period, spin axis, and shape by combining photometric light curves observed using optical telescopes with radiometric data obtained from the Haystack 37-m Radio Telescope. As we prepare for upcoming close approaches, this visible-only campaign was a critical step in refining our techniques across a wide variety of telescopes, detectors, software, and methodologies across multiple time zones.

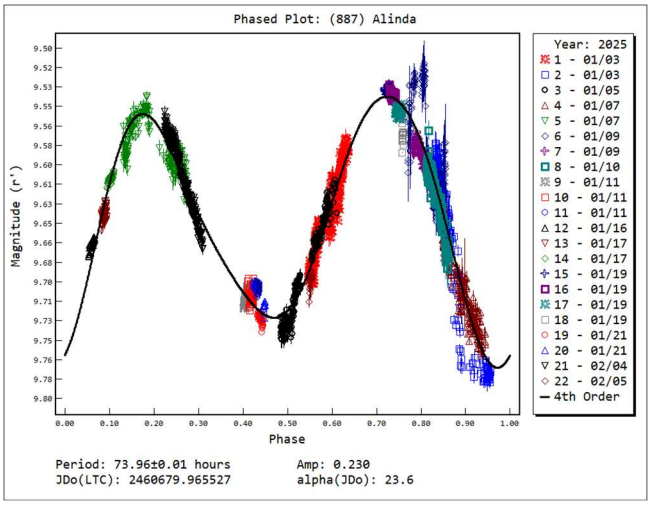

Figure 1. Phased plot of 887 Alinda generated in *Tycho Tracker Pro* (Parrott, 2020). Here we plot all data utilized in the final fitted solutions. Note the close overlap of data from widely distant nights affirming the stability of our final rotation period. (Figure generated by *Tycho Tracker Pro v12.3.1*).

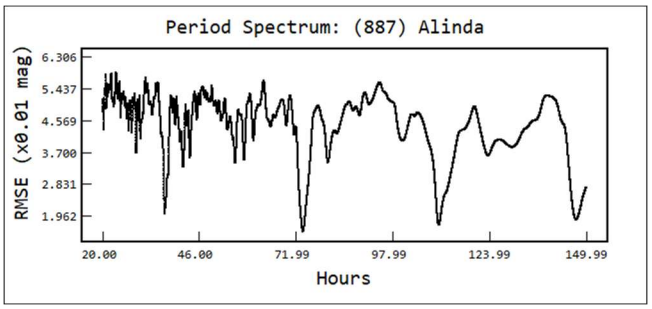

Figure 2. Periodogram generated by *Tycho Tracker Pro*, 4th order fit, showing a strong preference for 73.96 h period. Aliased peaks at multiples and fractions of 74 h are also visible.

To obtain color information on the asteroid, on 9 January 2025 we measured a mean g' magnitude of 9.42 ± 0.01 from 33 images taken with the MIT-WAO (810) Pier 3 0.35-m telescope and a mean r' magnitude of 9.072 ± 0.001 from 247 datapoints on MIT-WAO (810) Pier 2 0.35-m telescope, resulting in a g'-r' color index of 0.35 ± 0.01. These observations spanned a total of approximately 4 hours, a small fraction of the ~74h period, so combination of all data from that period into a single color measurement was deemed warranted.

While the final period found here (73.96 ± 0.01 hours) is consistent with the Dunlap and Taylor (1979) results (73.97 ± 0.05 hours), it is clear from the periodogram in Figure 2 where the radically different results in the literature stem from. This does not rule out the proposed chaotic tumbling behavior noted by Pilcher (2024), but does provide a robust period determination against which future claims of chaotic behavior must be tested.

Acknowledgements

We would like to acknowledge the continued support for WAO by the MIT Department of Earth, Atmospheric and Planetary Sciences. Special thanks are offered to Prof. Richard Binzel and Dr. Stephen Slivan (MIT) for their sage advice on this project. Partial support for student observers was provided by the MIT Undergraduate Research Opportunities Program. Support was also provided by the MIT Department of Earth, Atmospheric and Planetary Sciences for students participating in the MIT Astronomy Field Camp. This article includes observations made with the IAC80 and TCS telescopes operated on the island of Tenerife at the Spanish Observatorio del Teide. Julien de Wit and MIT gratefully acknowledge financial support from the Heising-Simons Foundation, Dr. and Mrs. Colin Masson and Dr. Peter A. Gilman for Artemis, the first telescope of the SPECULOOS network situated in Tenerife, Spain. (Burdanov et al., 2022; Delrez et al. 2013). Utilizing publicly available radio images from NASA's Goldstone Radar (Benner, 2024) proved to be helpful in eliminating spurious period aliases in the *Tycho*-produced periodograms.

References

Augustin, D.; Behrend, R. (2020). "(877) Alinda." CdR&CdL results, p.2. *https://www.astro.unige.ch//~behrend/page2cou.html*

Benner, L.A.M. (2024). Goldstone Radar Observations Planning, 887 Alinda, NASA, 2025 February 22 Update. *https://echo.jpl.nasa.gov/asteroids/Alinda.goldstone.planning.2024.html*

Burdanov, A.Y.; de Wit, J.; Gillon, M. and 14 colleagues (2002). "SPECULOOS Northern Observatory: searching for red worlds in the northern skies." *Publications of the Astronomical Society of the Pacific* **134**(1040), 105001.

Collins, K.A.; Kielkopf, J.F.; Stassun, K.G.; Hessman, F.V. (2017). "AstroImageJ: Image Processing and Photometric Extraction for Ultra-precise Astronomical Light Curves." *Astron. J.* **153**, 77-89.

Delrez, L.; Gillon, M.; Queloz, DS. and 14 colleagues (2018). "SPECULOOS: a network of robotic telescopes to hunt for terrestrial planets around the nearest ultracool dwarfs." Ground-based and airborne telescopes VII. Vol. **10700**. SPIE, 2018.

Dunlap, J.L.; Taylor R.C. (1979)- "Minor planets and related objects. XXVII-Lightcurves of 887 Alinda." *Astronomical Journal* **84**, 269-273.

Harris, A.W.; Young, J.W.; Scaltriti, F.; Zappala, V. (1984). "Lightcurves and phase relations of the asteroids 82 Alkmene and 444 Gyptis." *Icarus* **57**, 251-258.

Masiero, J.R.; Mainzer, A.K.; Bauer, J.M.; Cutri, R.M.; Grav, T.; Kramer, E.; Pittichová, J.; Wright, E.L. (2021). "Asteroid Diameters and Albedos from NEOWISE Reactivation Mission Years Six and Seven." *PSJ* **2**(4),162.

NASA/JPL-Caltech. (2025) JPL Horizons System. *https://ssd.jpl.nasa.gov/horizons/* Accessed March 31, 2025.

Parrott, D. (2020). "Tycho Tracker: A New Tool to Facilitate the Discovery and Recovery of Asteroids using Synthetic Tracking and Modern GPU Hardware." *Journal of the American Association of Variable Star Observers (JAAVSO)* **48**, 262.

Pilcher, F. (2024). "An Appeal for Photometric Observations of 887 Alinda." *Minor Planet Bulletin* **51-4**, 303.

Tungalag, N.; Shevchenko, V.G.; Lupishko, D.F. (2002). "Rotation parameters and shapes of 15 asteroids." *Kinematika i Fizika Nebesnykh Tel* **18**(6), 508-516.

Warner, B.D.; Harris, A.W.; Pravec, P. (2009). "The Asteroid Lightcurve Database." *Icarus* **202**, 134-146. Updated 2016 Sep. *http://www.minorplanet.info/lightcurvedatabase.html*

LIGHTCURVE AND ROTATION PERIOD OF 1318 NERINA

Jiarui Xiong
Xingyuan Observatory
College of Oceanic and Atmospheric Science
Ocean University of China
Songling Rd. 238, Qingdao, Shandong, CHINA
xiongjiarui@stu.ouc.edu.cn

(Received: 2025 April 20)

A single-night observation of asteroid 1318 Nerina was taken by Xingyuan Observatory (MPC Code O40) on 2025 March 19. *Tycho v11.0.1* was used to obtain its lightcurve and rotation period.

Asteroid 1318 Nerina was discovered at Johannesburg on 1934 March 24 by C. Jackson, having a Phocaea-type orbit. On 2025 March 19, Xingyuan observatory used an f/4 0.2m reflector and an ASI6200MM CCD to measure its magnitude. After analysis with the software *Tycho v11.0.1* (Parrott, 2020) this work suggests Nerina's rotation period as 2.5352 hours and the maximum amplitude as 0.061 mag. Considering Nerina's sky motion and brightness, the exposure time selected was 180 seconds with the sensor temperature set at -20 degrees Celsius. All of the frames were taken under L band (unfiltered).

In pre-processing, the frames were calibrated using bias, flat, and dark frames, then aligned. In measurement, the reference stars' information was read from the V band of the APASS catalog. According to ALCDEF's data (Warner et al., 2009), (1318) Nerina's mean absolute magnitude $H = 12.32$ mag and the assuming slope parameter $G = 0.2$. After the light-time correction and the (H-G) correction, the lightcurve was obtained. The fitting used 4th order can be seen in the Figure. The fitting result is a period of $P = 2.5352 \pm 0.004$ hours (for JD 2460336.0), and the maximum amplitude of $A = 0.061 \pm 0.014$ mag. It is noticeable that the errors are calculated automatically by *Tycho*. Detailed data for further study are available from the author upon request.

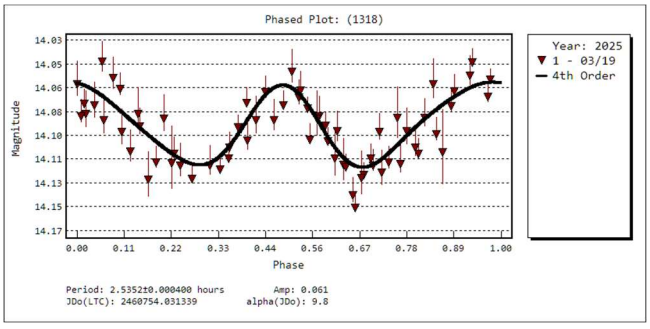

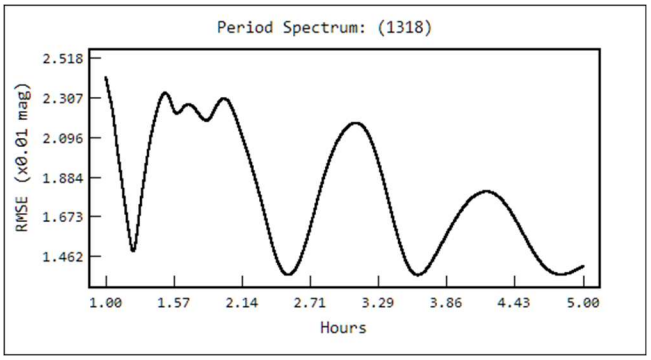

Acknowledgements

This work is supported by Xingyuan College of Ocean University of China. This work is possible in part based on data from AAVSO Photometric All-Sky Survey (APASS) and software *Tycho v11.0.1* developed by Daniel Parrott. We want to express our special thanks to Dr. Ye Yuan in Pulper Mount Observatory and Astronomical Associations of the Ocean University of China. Thanks to my colleges Yue Lu, Chenyang Guo, and Boyu Ai for their support.

References

Harris, A.W.; Young, J.W.; Scaltriti, F.; Zappala, V. (1984). "Lightcurves and phase relations of the asteroids 82 Alkmene and 444 Gyptis." *Icarus* **57**, 251-258.

Parrott, D. (2020). "Tycho Tracker: A New Tool to Facilitate the Discovery and Recovery of Asteroids using Synthetic Tracking and Modern GPU Hardware." *Journal of the American Association of Variable Star Observers (JAAVSO)* **48**, 262.

Warner, B.D.; Harris, A.W.; Pravec, P. (2009). "The Asteroid Lightcurve Database." *Icarus* **202**, 134-146. Updated 2016 Sep. *http://www.minorplanet.info/lightcurvedatabase.html*

Number	Name	yyyy mm/dd	Phase	L_{PAB}	B_{PAB}	Period(h)	P.E.	Amp	A.E.	Grp
1318	Nerina	2025 03/19	9.8,9.9	166	5	2.5352	0.0004	0.061	0.014	Phocaea

Table I. Observing circumstances and results. The phase angle is given for the first and last date. If preceded by an asterisk, the phase angle reached an extrema during the period. L_{PAB} and B_{PAB} are the approximate phase angle bisector longitude/latitude at mid-date range (see Harris et al., 1984). Grp is the asteroid family/group (Warner et al., 2009).

LIGHTCURVE AND PERIOD OF KORONIS FAMILY MEMBER (2837) GRIBOEDOV

Francis P. Wilkin
Union College
Department of Physics and Astronomy
807 Union St.
Schenectady, NY 12308
wilkinf@union.edu

(Received: 2025 April 13)

For Koronis family member (2837) Griboedov we derive a synodic period of 3.9498 ± 0.0002 h.

We continue our observational program on Koronis family objects (Wilkin et al., 2022; 2024) to increase the sample of known spins (Slivan et al., 2003; 2023). Observational planning used the Koronis family web tool (Slivan, 2003). Observations were made using the 0.61-m Ritchey-Chretien telescope CHI-1 operated by Telescope.Live in Rio Hurtado, Chile using a QHY 600 Pro (CMOS) camera. Its 9576×6382×3.8µm array yields image scale 0.39"/pix and 31'×21' FOV. We used *AstroImageJ* (Collins et al., 2017) to perform photometry on all images. Corrections for light travel time were made using ephemerides from the JPL Horizons web app (JPL, 2024).

No published periods or lightcurves for Griboedov were found in the LCDB based on densely-sampled data. Previously-published periods based upon sparse survey data were given by two studies. Erasmus et al. (2020) give period 3.950 h from ATLAS data, and Ďurech and Hanuš (2023) give 3.94987 h from Gaia DR3 data. We observed Griboedov on six nights from 2024 May 16 to Jun 7 with total span of 23 nights. The relatively large amplitude 0.68 ± 0.05 excludes the possibility that the lightcurve is quadruply-periodic (Harris et al., 2014). The resulting doubly-periodic lightcurve yields synodic period 3.9498 ± 0.0002 h, in agreement with the prior published periods from sparse-in-time survey photometry.

Acknowledgments

Remote observations were made possible by the Union College Faculty Research Fund to F. Wilkin. We thank Dimitris Vasileilos Zora for the use of his lightcurve formatting template.

References

Collins, K.A.; Kielkopf, J.F.; Stassun, K.G.; Hessman, F.V. (2017). "AstroImageJ: Image Processing and Photometric Extraction for Ultra-precise Astronomical Light Curves." *Astron. J.* **153**, 77-89.

Ďurech, J.; Hanuš, J. (2023). "Reconstruction of asteroid spin states from Gaia DR3 photometry." *Astron. Astrophys.* **675**, A24.

Erasmus, N.; Navarro-Meza, S.; McNeill, A.; Trilling, D.E.; Sickafoose, A.A.; Denneau, L.; Flewelling, H.; Heinze, A.; Tonry, J.L. (2020). "Investigating Taxonomic Diversity within Asteroid Families through ATLAS Dual-band Photometry." *Astrophys. J. Suppl.* **247**, 13.

Harris, A.W.; Pravec, P.; Gálad, A.; Skiff, B.A.; Warner, B.D.; Világi, J.; Gajdoš, Š.; Carbognani, A.; Hornoch, K.; Kušnirák, P.; Cooney, Jr., W.R.; Gross, J.; Terrell, D.; Higgins, D.; Bowell, E.; Koehn, B.W. (2014). "On the maximum amplitude of harmonics of an asteroid lightcurve." *Icarus* **235**, 55-59.

Harris, A.W.; Young, J.W.; Scaltriti, F.; Zappala, V. (1984). "Lightcurves and phase relations of asteroids 82 Alkmene and 444 Gyptis." *Icarus* **57**, 251-258.

JPL (2024). "Horizons System." *https://ssd.jpl.nasa.gov/horizons/app.html#/*

Slivan, S.M. (2003). "A Web-based tool to calculate observability of Koronis program asteroids." *Minor Planet Bull.* **30**, 71-72.

Slivan, S.M.; Binzel, R.P.; Crespo de Silva, L.D.; Kaasalainen, M.; Lyndaker, M.M.; Krčo, M (2003) "Spin vectors in the Koronis family: comprehensive results from two independent analyses of 213 rotation lightcurves." *Icarus* **162**, 285-307.

Slivan, S.M.; Hosek Jr., M.; Kurzner, M.; Sokol, A.; Maynard, S.; Payne, A.V.; Radford, A.; Springmann, A.; Binzel, R.P.; Wilkin, F.P.; Mailhot, E.A.; Midkiff, A.H.; Russell, A.; Stephens, R.D.; Gardiner, V.; Reichart, D.E.; Haislip, J.; LaCluyze, A.; Behrend, R.; Roy, R. (2023). "Spin vectors in the Koronis family: IV. Completing the sample of its largest members after 35 years of study." *Icarus* **394**, A115397.

Warner, B.D.; Harris, A.W.; Pravec, P. (2009). "The Asteroid Lightcurve Database." *Icarus* **202**, 134-146. Updated 2023 Oct. *http://www.MinorPlanet.info/php/lcdb.php*

Wilkin, F.P.; AlMassri, Z.; Bowles, P.; Pargiello, M.; Sindoni, J. (2022). "Lightcurves for three Koronis Family Asteroids from the Union College Observatory." *Minor Planet Bull.* **49**, 267-268.

Wilkin, F.P.; Castro, E.; Magno, M.; Petrauskas, R.; Zora, D.-V. (2024) "Lightcurves for Three Koronis Family Asteroids." *Minor Planet Bull.* **51**, 180-181.

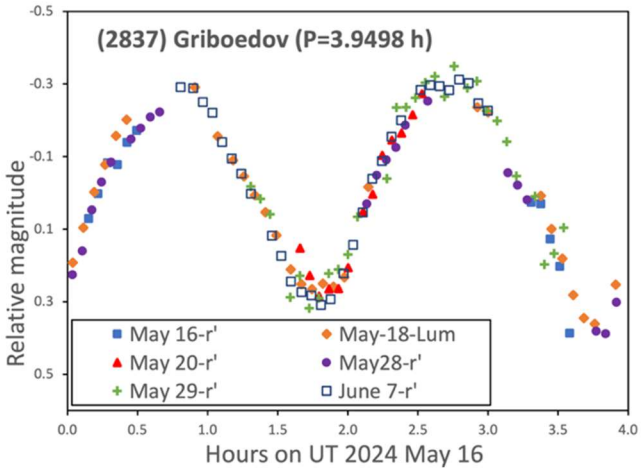

Number	Name	yyyy mm/dd	Phase	L_{PAB}	B_{PAB}	Period(h)	P.E.	Amp	A.E.	Grp
2837	Griboedov	2024 5/16-6/7	*3.4,4.9	244	0	3.9498	0.0002	0.68	0.05	Kor

Table I. Observing circumstances and results. The phase angle is given for the first and last dates. If preceded by an asterisk, the phase angle reached an extremum during the period. L_{PAB} and B_{PAB} are the approximate phase angle bisector longitude/latitude at mid-date range (see Harris et al., 1984). Grp is the asteroid family/group (Warner et al., 2009).

LIGHTCURVE AND ROTATION PERIOD OF 46925 BRADYHARAN

Daniel P. Bamberger
Northolt Branch Observatories
Alfred-Wegener-Straße 34
35039 Marburg, GERMANY
danielpeter1204@aol.com

Sam Deen
Deep Random Survey (MPC: X09)
Simi Valley, CA, USA

K. Ly
University of California, Los Angeles
Los Angeles, CA, USA

Elvis Oliveira Mendes
Instituto de Física, Universidade Federal Fluminense
Niterói, Rio de Janeiro, BRAZIL

Arndt Schnabel
Deep Random Survey
GERMANY

Guy Wells
Northolt Branch Observatories
Northolt, ENGLAND

(Received: 2025 February 24 Revised: 2025 March 24)

Unfiltered CCD photometric observations of 46925 Bradyharan were obtained in Rio Hurtado, Chile, in February 2025. We report a synodic rotation period of 9.0322 ± 0.0015 h and an amplitude of 0.29 ± 0.02 mag.

46925 Bradyharan is a 16-km main belt asteroid (JPL, 2025). It was discovered by the Catalina Sky Survey in 1998. It was named on 2025 February 3, following a suggestion by the lead author of this paper (Haran, 2025). The asteroid belongs to the small Brucato family. The LCDB (Warner et al., 2009) gives a spectral type of CX, and the JPL SBDB gives an albedo of 0.044 based on data from the WISE spacecraft (Mainzer et al., 2019).

The LCDB listed no periods for Bradyharan. In 2023, Ďurech and Hanuš (2023) reported a period of 9.0363 h, as well as a pole solution (λ=352°, β=-68°) that indicates that this is a retrograde rotator. Using Gaia DR3 photometry, they derived a shape model that is distinctly triangular. We suggest that the angular shape is responsible for our triple-peaked lightcurve.

The observations we report here were made with the PlaneWave CDK400 at Deep Random Survey (MPC: X09) in Rio Hurtado, Chile, on eight separate nights in February 2025. The data is available in the Asteroid Lightcurve Photometry Database (ALCDEF). Our period results are in agreement with prior reports.

Acknowledgements

We thank David Rankin at the Catalina Sky Survey for his support, and for his valuable comments.

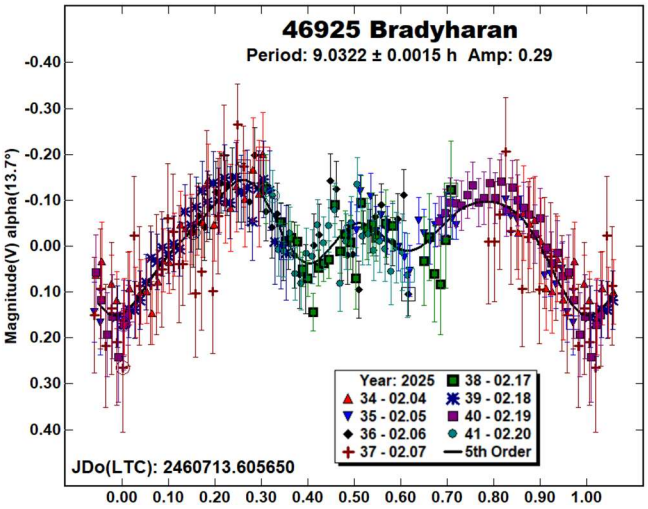

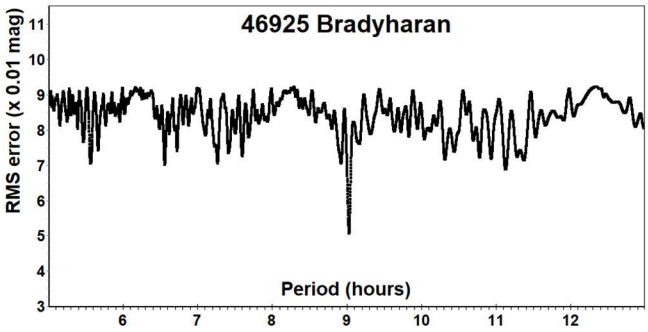

References

Ďurech, J.; Hanuš, J. (2023). "Reconstruction of asteroid spin states from Gaia DR3 photometry." *A&A* **675**, A24. July 2023. *https://astro.troja.mff.cuni.cz/projects/damit/asteroid_models/view/12401*

Haran, B.J. (2025). "An Asteroid named Bradyharan." Sixty Symbols. *https://www.youtube.com/watch?v=VLLrHQVMx64*

Harris, A.W.; Young, J.W.; Scaltriti, F.; Zappala, V. (1984). "Lightcurves and phase relations of the asteroids 82 Alkmene and 444 Gyptis." *Icarus* **57**, 251-258.

JPL (2025). Small-Body Database Lookup. *https://ssd.jpl.nasa.gov/tools/sbdb_lookup.html#/?sstr=46925*

Mainzer, A.K.; Bauer, J.M.; Cutri, R.M.; Grav, T.; Kramer, E.A.; Masiero, J.R.; Sonnett, S.; Wright, E.L. (2019). "NEOWISE Diameters and Albedos V2.0." NASA Planetary Data System. *https://doi.org/10.26033/18S3-2Z54*

Warner, B.D.; Harris, A.W.; Pravec, P. (2009). "The Asteroid Lightcurve Database." *Icarus* **202**, 134-146. Updated 2023 Oct. 1. *https://www.minorplanet.info/php/lcdb.php*

Number	Name	yyyy/mm/dd	Phase	L_{PAB}	B_{PAB}	Period(h)	P.E.	Amp	A.E.	Grp
46925	Bradyharan	2025/02/04-02/20	13.7,17.7	103	9	9.0322	0.0015	0.29	0.02	BRU

Table I. Observing circumstances and results. The phase angle is given for the first and last date. If preceded by an asterisk, the phase angle reached an extrema during the period. L_{PAB} and B_{PAB} are the approximate phase angle bisector longitude/latitude at mid-date range (see Harris et al., 1984). Grp is the asteroid family/group (Warner et al., 2009).

PHOTOMETRIC OBSERVATIONS OF ASTEROIDS 229 ADELINDA, 5802 CASTELDELPIANO AND (27174) 1999 BB2

Alessandro Marchini, Riccardo Papini, Lorenzo Pierguidi,
Joao Pedro Savino, Sabina Schintu
Astronomical Observatory, University of Siena (K54)
Via Roma 56, 53100 - Siena, ITALY
marchini@unisi.it

(Received: 2025 April 10)

Photometric observations of three main-belt asteroids were conducted to verify or determine their synodic rotation periods. We found: for 229 Adelinda P = 6.599 ± 0.001 h with A = 0.28 ± 0.02 mag; for 5802 Casteldelpiano, P = 2.970 ± 0.001 h with A = 0.07 ± 0.02 mag; for (2714) 1992 BB2, P = 4.820 ± 0.001 h with A = 0.05 ± 0.02 mag.

CCD photometric observations of three main-belt asteroids were carried out in February-April 2025 at the Astronomical Observatory of the University of Siena (K54). We used a 0.30-m *f*/5.6 Maksutov-Cassegrain telescope, SBIG STL-6303E NABG CCD camera; the pixel scale was 2.30 arcsec when binned at 2×2 pixels. We used a Clear filter and 300 seconds of exposure time.

Data processing and analysis were done with *MPO Canopus* (Warner, 2018). All images were calibrated with dark and flat-field frames and the instrumental magnitudes converted to R magnitudes using solar-colored field stars from a version of the CMC-15 catalogue distributed with *MPO Canopus*. Table I shows the observing circumstances and results.

A search through the asteroid lightcurve database (LCDB; Warner et al., 2009) indicates that our result may be the first reported lightcurve observations and results for (27174) 1999 BB2.

229 Adelinda (A882 QB) was discovered by J. Palisa at Vienna on 1888 August 22. It is an outer main-belt asteroid with a semi-major axis of 3.423 AU, eccentricity 0.136, inclination 2.077°, and an orbital period of 6.33 years. Its absolute magnitude is H = 9.35 (JPL, 2025). The NEOWISE satellite infrared radiometry survey (Mainzer et al., 2019) found a diameter D = 105.912 ± 1.779 km using an absolute magnitude H = 9.13.

Observations were conducted over three nights and collected 159 data points. The period analysis confirms a rotational period of P = 6.599 ± 0.001 h with an amplitude A = 0.28 ± 0.02 mag, in good agreement with the previously results published in the LCDB (Lagerkvist et al., 2001; Ďurech et al., 2020).

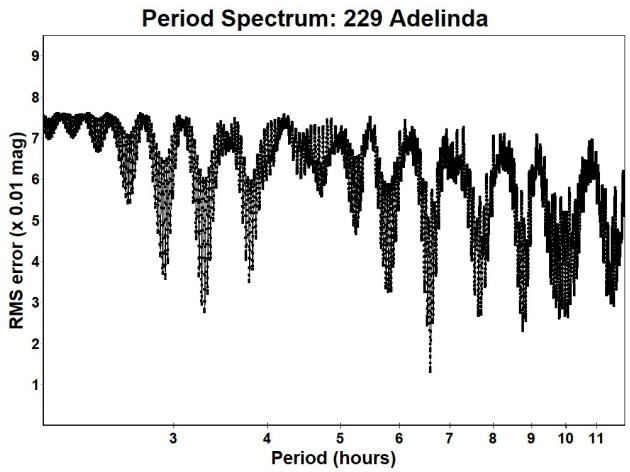

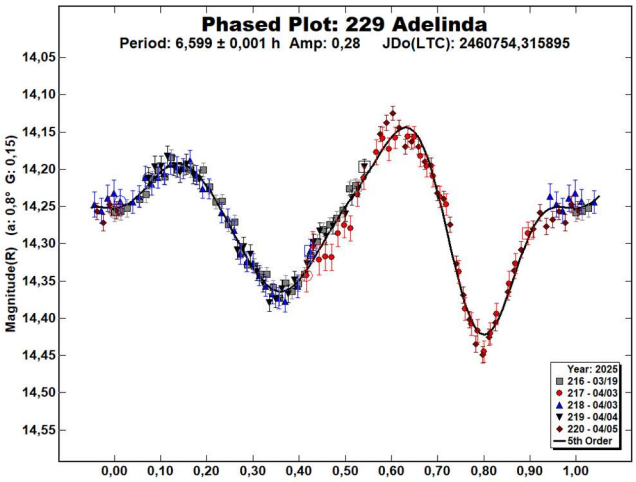

5802 Casteldelpiano (1984 HL1) was discovered on 1984 April 27 by V. Zappala at the European Southern Observatory and dedicated to Castel del Piano, an ancient castle near Carrara, Tuscany, Italy, that has been restored by Sabina Ruffaldi and Andrea Ghigliazza, two great lovers of astronomy and friends of the discoverer. It is an inner main-belt asteroid with a semi-major axis of 2.272 AU, eccentricity 0.155, inclination 2.396°, and an orbital period of 3.42 years. Its absolute magnitude is H = 13.43 (JPL, 2025). The NEOWISE satellite infrared radiometry survey (Nugent et al., 2016) found a diameter D = 4.894 ± 1.073 km using an absolute magnitude H = 13.63.

Observations were conducted over four nights and collected 143 data points. The period analysis shows a rotational period of P = 2.970 ± 0.001 h with an amplitude A = 0.07 ± 0.02 mag, in good agreement with the previously results published in the LCDB (Waszczak et al., 2015; Dose, 2021).

Number	Name	2025/mm/dd	Phase	L_{PAB}	B_{PAB}	Period(h)	P.E.	Amp	A.E.	Grp
229	Adelinda	03/19-04/05	*0.8,4.4	181	1	6.599	0.001	0.28	0.02	MB-O
5802	Casteldelpiano	03/19-04/03	*1.5,7.4	182	1	2.970	0.001	0.07	0.02	MB-I
27174	1999 BB2	02/15-03/06	2.8,11.9	144	2	4.820	0.001	0.05	0.02	MB-M

Table I. Observing circumstances and results. The phase angle is given for the first and last date. If preceded by an asterisk, the phase angle reached an extremum during the period. L_{PAB} and B_{PAB} are the approximate phase angle bisector longitude/latitude at mid-date range (see Harris et al., 1984). Grp is the asteroid family/group (*Warner et al.,* 2009).

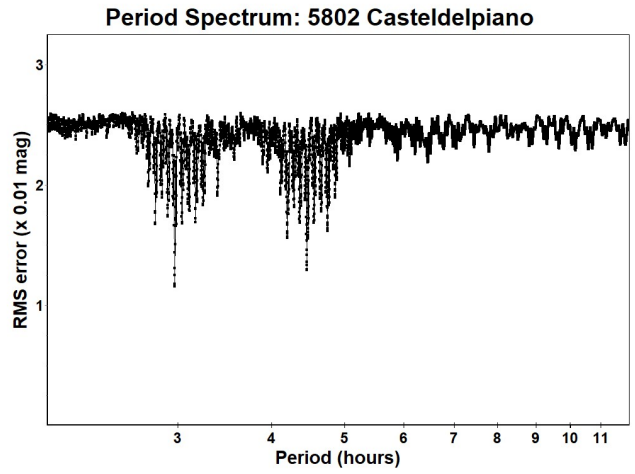

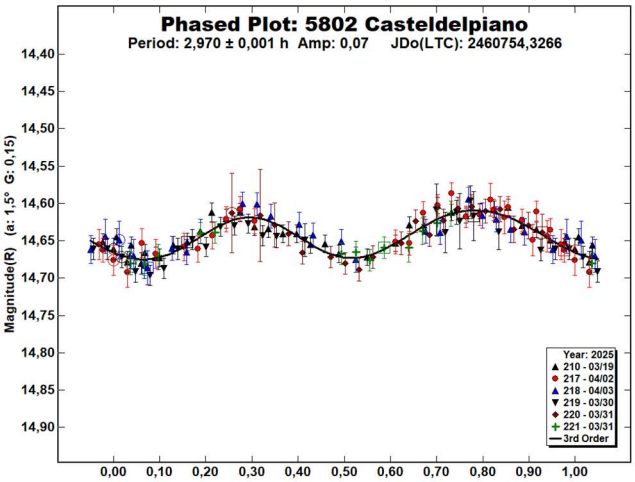

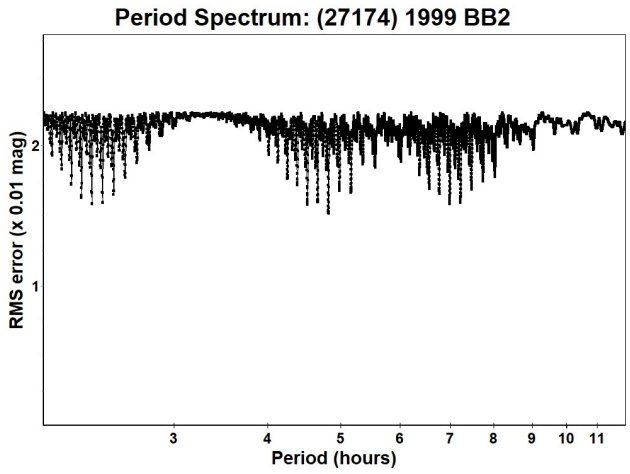

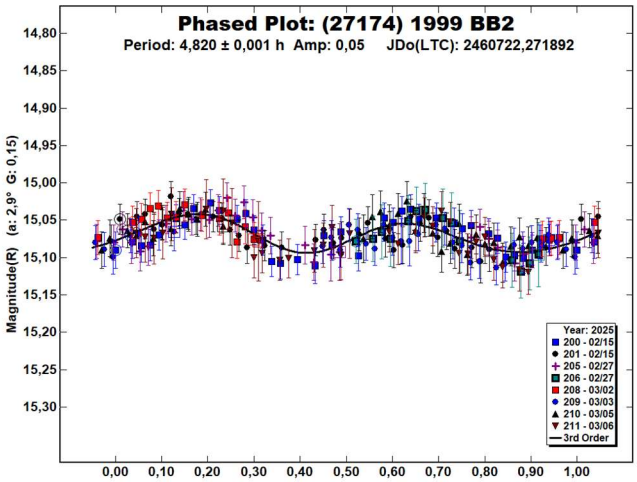

(27174) 1999 BB2 was discovered on 1999 January 19 at Črni Vrh Observatory. It is a middle main-belt asteroid with a semi-major axis of 2.650 AU, eccentricity 0.270, inclination 12.130°, and an orbital period of 4.31 years. Its absolute magnitude is H = 13.15 (JPL, 2025). The NEOWISE satellite infrared radiometry survey (Mainzer et al., 2019) found a diameter D = 7.753 ± 0.338 km using an absolute magnitude H = 12.4.

Observations were conducted over four nights and collected 234 data points. Unluckily, due to the bad weather we couldn't collect more data and the asteroid faded below the magnitude threshold of our telescope. Despite the small amplitude A = 0.05 ± 0.02 mag, the period analysis shows a rotational period of P = 4.820 ± 0.001 h as the most likely bimodal solution. Further observations are strongly encouraged to nail down the actual period.

Acknowledgements

Lorenzo Pierguidi, Joao Pedro Savino and Sabina Schintu are students of the course in Physics and Advanced Technologies at the University of Siena. They collaborated in images acquisition and further light curve analysis during their internship in our observatory and appear deservedly as authors.

References

Dose, E.V. (2021). "Lightcurves of Eighteen Asteroids" *Minor Planet Bull.* **48**, 125-132.

Ďurech, J.; Tonry, J.; Erasmus, N.; Denneau, L.; Heinze, A.N.; Flewelling, H.; Vančo, R. (2020). "Asteroid models reconstructed from ATLAS photometry." *A&A* **643**, A59.

Harris, A.W.; Young, J.W.; Scaltriti, F.; Zappala, V. (1984). "Lightcurves and phase relations of the asteroids 82 Alkmene and 444 Gyptis." *Icarus* **57**, 251-258.

JPL (2025). Small Body Database Search Engine. *https://ssd.jpl.nasa.gov*

Lagerkvist, C.I.; Erikson, A.; Lahulla, F.; De Martino, M.; Nathues, A.; Dahlgren, M. (2001). "A Study of Cybele Asteroids. I. Spin Properties of Ten Asteroids." *Icarus* **149(1)**, 190-197.

Mainzer, A.K.; Bauer, J.M.; Cutri, R.M.; Grav, T.; Kramer, E.A.; Masiero, J.R.; Sonnett, S.; Wright, E.L. (2019). "NEOWISE Diameters and Albedos V2.0." *NASA Planetary Data System, https://doi.org/10.26033/18S3-2Z54*.

Nugent, C.R.; Mainzer, A.; Bauer, J.; Cutri, R.M.; Kramer, E.A.; Grav, T.; Masiero, J.; Sonnett, S.; Wright, E.L. (2016). "NEOWISE Reactivation Mission Year Two: Asteroid Diameters and Albedos." *AJ* **152**, 63.

Warner, B.D.; Harris, A.W.; Pravec, P. (2009). "The Asteroid Lightcurve Database." *Icarus* **202**, 134-146. Updated 2023 Oct. *https://minplanobs.org/mpinfo/php/lcdb.php*

Warner, B.D. (2018). MPO Software, MPO Canopus v10.7.7.0. Bdw Publishing. *http://bdwpublishing.com/*

Waszczak, A.; Chang, C.-K.; Ofek, E.O.; Laher, R.; Masci, F.; Levitan, D.; Surace, J.; Cheng, Y.-C-; Ip, W.-H.; Kinoshita, D.; Helou, G.; Prince, T.A.; Kulkarni, S. (2015). "Asteroid Light Curves from the Palomar Transient Factory Survey: Rotation Periods and Phase Functions from Sparse Photometry." *AJ* **150**, 75.

LIGHTCURVES AND ROTATION PERIODS OF 229 ADELINDA, 413 EDBURGA, 1101 CLEMATIS, 1342 BRABANTIA, AND 1343 NICOLE

Frederick Pilcher
Organ Mesa Observatory (G50)
4438 Organ Mesa Loop
Las Cruces, NM 88011 USA
fpilcher35@gmail.com

(Received: 2025 April 2)

Synodic rotation periods and amplitudes are found for 229 Adelinda 6.5992 ± 0.0002 hours, 0.26 ± 0.02 magnitudes; 413 Edburga 15.770 ± 0.001 hours, 0.52 ± 0.02 magnitudes; 1101 Clematis 8.598 ± 0.001 hours, 0.19 ± 0.02 magnitudes with an irregular lightcurve; 1342 Brabantia 4.1752 ± 0.0001 hours, 0.19 ± 0.01 magnitudes; and 1343 Nicole 14.771 ± 0.001 hours, amplitude 0.21 ± 0.01 magnitudes.

The new observations to produce the results reported in this paper were made at the Organ Mesa Observatory with a Meade 35-cm LX200 GPS Schmidt-Cassegrain, SBIG STL-1001E CCD, 60 to 120 second exposures, unguided, clear filter. Image measurement and lightcurve construction were with *MPO Canopus* software with calibration star magnitudes for solar colored stars from the CMC15 catalog reduced to the Cousins R band. Zero-point adjustments of a few × 0.01 magnitude were made for best fit. To reduce the number of data points on the lightcurves and make them easier to read, data points have been binned in sets of 3 with maximum time difference 5 minutes.

229 Adelinda. The only previously published lightcurve is by Lagerkvist et al. (2001) which presents an approximate period of 6.6 hours. New observations on five nights 2025 Feb. 22 - Mar. 24 provide a good fit to an asymmetrical bimodal lightcurve with period 6.5992 ± 0.0002 hours, amplitude 0.26 ± 0.02 magnitudes (Fig. 1). This value is consistent with Lagerkvist et al. (2001) and greatly improves the accuracy of their period.

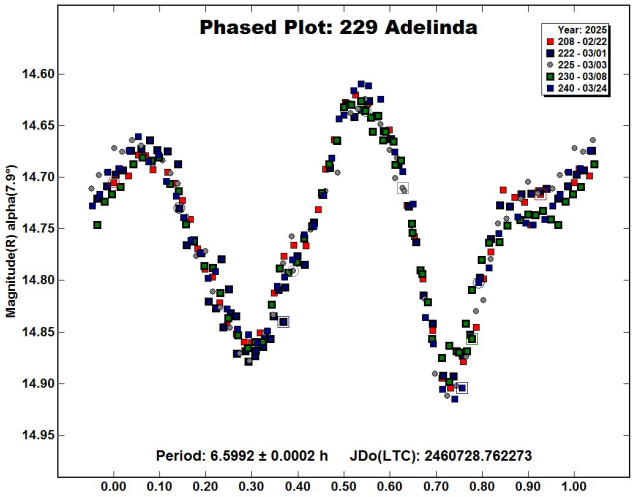

Fig. 1. Lightcurve of 229 Adelinda phased to a period of 6.5992 hours.

413 Edburga. Previously published periods are by Hainaut-Rouelle et al., (1995), 15 hours; Behrend (2006web), 12.1 hours; Warner (2010b), 15.773 hours; and Warner (2012), 15.78 hours. All authors found amplitudes between 0.36 and 0.53 magnitudes. New observations on five nights 2025 Jan. 20 - Mar. 5 provide an excellent fit to a synodic period of 15.770 ± 0.001 hours, amplitude 0.52 ± 0.02 magnitudes (Fig. 2). This period is consistent with Warner (2010b) and Warner (2012) and differs considerably from the other published periods. The amplitude is within the range of all published amplitudes.

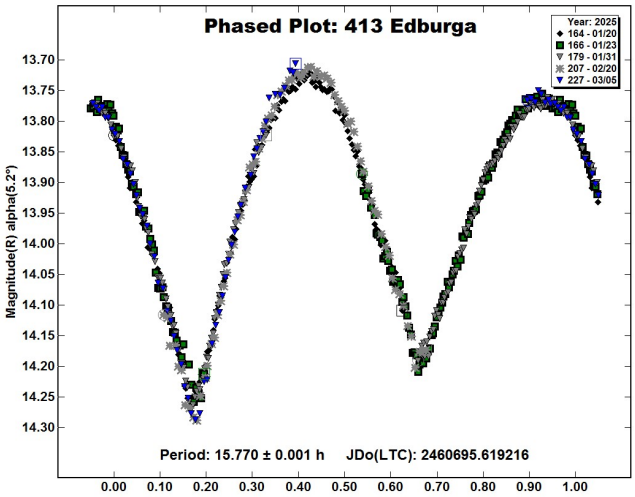

Fig. 2. Lightcurve of 413 Edburga phased to a period of 15.770 hours.

1101 Clematis. Previously published periods are by Behrend (2002web), 8.61 hours; Stephens (2004), 12.68 hours; Behrend (2009web), 8.5994 hours; Warner (2010a), 34.3 hours; and Pál et al. (2020), 8.61332 hours. New observations on six nights 2025 March 10 - April 1 provide a good fit to an irregular bimodal lightcurve with period 8.598 ± 0.001 hours, amplitude 0.19 ± 0.02 magnitudes (Fig. 3). This value is consistent with all previously published periods except for those by Stephens (2004) and by Warner (2010a), which are now ruled out.

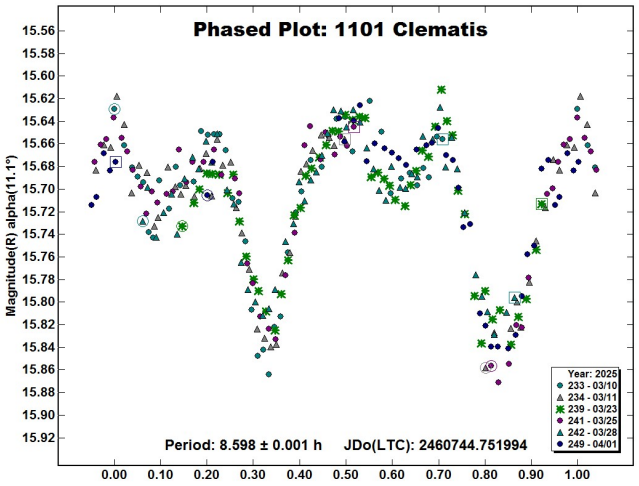

Fig. 3. Lightcurve of 1101 Clematis from this study, phased to a period of 8.598 hours.

Pál et al. (2020) obtained data points at 0.5-hour intervals continuously for six days 2019 March 28 - April 2 with the TESS (Transiting Exoplanet Survey Satellite). The author downloaded their data from the Asteroid LightCurve Data Exchange Format website *www.ALCDEF.org*, deleted a few highly discordant data points, from which an excellent lightcurve with period 8.599 ± 0.002 hours, amplitude 0.20 ± 0.03 magnitudes (Fig. 4) could be drawn. The lightcurve by Pál et al. (2020) was obtained with the target only sixteen degrees away in the sky from its location at the current study. As one would expect, the two lightcurves are similar in both period and shape.

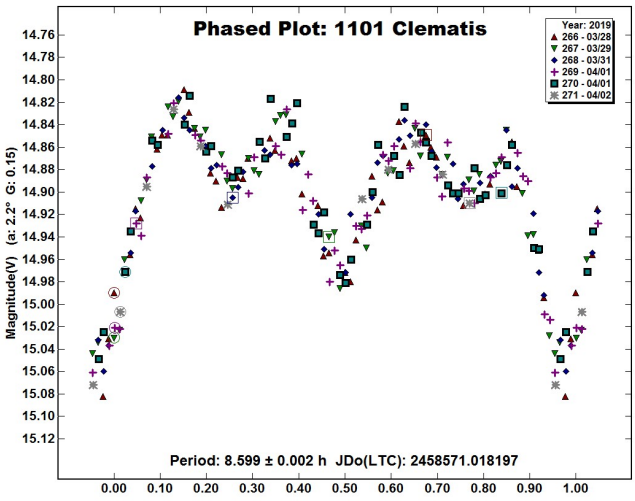

Fig. 4. Lightcurve of 1101 Clematis from Pál et al. (2020) phased to a period of 8.599 hours.

1342 Brabantia. Eight previously periods published in the "Asteroid Lightcurve Database," Warner et al. (2009), updated 2023 October, are all between 4.16 and 4.184 hours. New observations on five nights 2025 Jan. 25 - Mar. 4 provide a good fit to an irregular lightcurve with period 4.1752 ± 0.0001 hours, amplitude 0.19 ± 0.01 magnitudes (Fig. 5). This value is consistent with many other published periods.

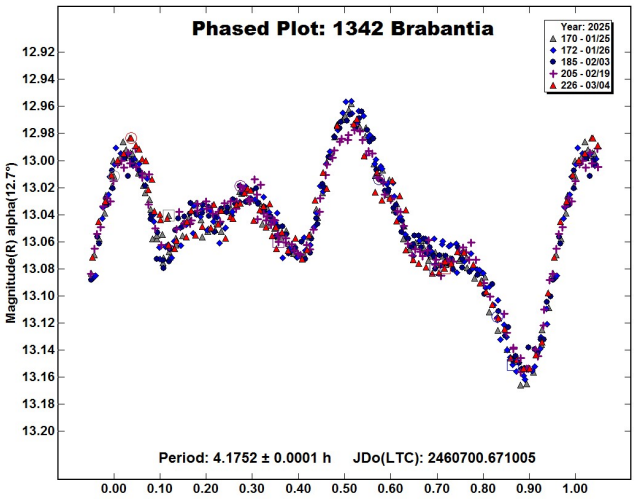

Fig. 5. Lightcurve of 1342 Brabantia phased to a period of 4.1752 hours.

Number	Name	yyyy/mm/dd	Phase	L_{PAB}	B_{PAB}	Period(h)	P.E	Amp	A.E.
229	Adelinda	2025/02/22-2025/03/24	7.9 - 0.7	182	1	6.5992	0.0002	0.26	0.02
413	Edburga	2025/01/20-2025/03/05	* 5.1 - 13.1	128	11	15.770	0.001	0.52	0.02
1101	Clematis	2019/03/28-2019/04/02	2.4 - 1.8	191	-5	8.599	0.001	0.20	0.03
1101	Clematis	2025/03/10-2025/04/01	11.1 - 4.4	204	-1	8.598	0.001	0.18	0.02
1342	Brabantia	2025/01/25-2025/03/04	*12.7 - 14.2	145	-7	4.1752	0.0001	0.19	0.01
1343	Nicole	2024/12/31-2025/01/28	* 4.1 - 9.4	122	7	14.771	0.001	0.21	0.01

Table I. Observing circumstances and results. The phase angle is given for the first and last date, unless a minimum (second value) was reached. L_{PAB} and B_{PAB} are the approximate phase angle bisector longitude and latitude at mid-date range (see Harris et al., 1984).

1343 Nicole. Previously published periods and amplitudes are by Behrend (2005web), 70 hours, 0.29 magnitudes; Wasczak et al. (2015), 14.778 hours, 0.42 magnitudes; Aznar et al. (2016), 14.76 hours, 0.38 magnituides; and Colazo et al. (2023), 14.773 hours, 0.4 magnitudes. New observations on six nights 2024 Dec. 31 - 2025 Jan. 28 provide a good fit to a synodic period of 14.771 ± 0.001 hours, amplitude 0.21 ± 0.01 magnitudes (Fig. 6). The amplitude is smaller than any amplitudes previously observed. The period is consistent with all previously published periods, except Behrend (2005web), whose 70-hour period is now ruled out.

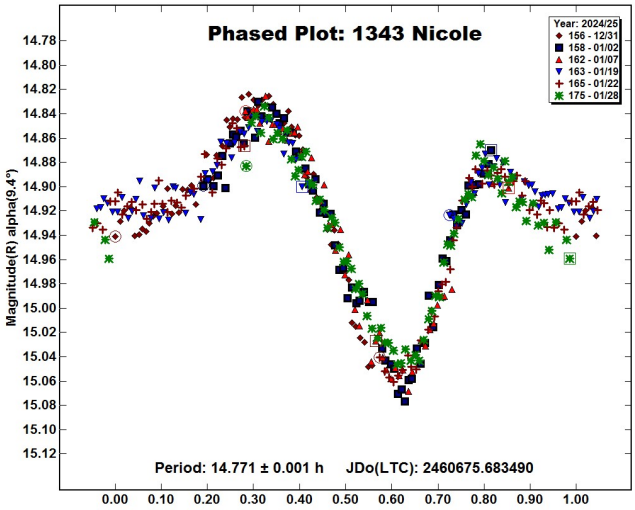

Fig. 6. Lightcurve of 1343 Nicole phased to a period of 14.771 hours.

References

Aznar, A.; Garceran, A.C.; Mansego, E.A.; Rodriguez, P.B.; Lozano de Haro, J.; Fornas Silva, A.; Fornas Silva, G.; Martinez, V.M.; Chiner, O.R. (2016). "Twenty-three asteroids lightcurves at Observadores de Asteroides (OBAS): 2015 October-December." *Minor Planet Bull.* **43**, 174-181.

Behrend, R. (2002web, 2005web, 2006web, 2009web). Observatoire de Geneve web site. *http://*obswww.unige.ch/*~behrend/page_cou.html*

Colazo, M.; Scotta, D.; Melia, R.; Ciancia, G.; Fornari, C.; Morales, M.; Monteleone, B.; Wilberger, A.; Santos, F.; García, A.; Suárez, N.; Belocchino, E.; Chapman, A.; Nolte, R.; Martini, M.; Mottino, A.; Colazo, C. (2023). "Asteroid photometry and lightcurve." *Minor Planet Bull.* **50**, 51-53.

Hainaut-Rouelle, M.-C.; Hainaut, O.R.; Detal, A. (1995). "Lightcurves of selected minor planets." *Astron. Astrophys. Suppl. Ser.* **112**, 125-142.

Harris, A.W.; Young, J.W.; Scaltriti, F.; Zappala, V. (1984). "Lightcurves and phase relations of the asteroids 82 Alkmene and 444 Gyptis." *Icarus* **57**, 251-258.

Lagerkvist, C.-I.; Erikson, A.; Lahulla, F.; De Martino, M.; Nathues, A.; Dahlgren, M. (2001). "A study of Cybele asteroids. I. Spin properties of ten asteroids." *Icarus* **149**, 190-197.

Pál, A.; Szakáts, R.; Kiss, C.; Bódi, A.; Bognár, Z.; Kalup, C.; Kiss, L.L.; Marton, G.; Molnár, L.; Plachy, E.; Sárneczky, K.; Szabó, G.M.; Szabó, R. (2020). "Solar System Objects Observed with TESS - First Data Release: Bright Main-belt and Trojan Asteroids from the Southern Survey." *Ap. J.* **247**, A26.

Stephens, R.D. (2004). "Photometry of 683 Lanzia, 1101 Clematis, 1499 Pori, 1507 Vaasa, and 3893 DeLaeter." *Minor Planet Bull.* **31**, 4-6.

Warner, B.D. (2010a). "Analysis of the lightcurve of 1101 Clematis." *Minor Planet Bull.* **37**, 73-74.

Warner, B.D. (2010b). "Asteroid lightcurve analysis at the Palmer Divide Observatory, 2010 March-June." *Minor Planet Bull.* **37**, 161-165.

Warner, B.D. (2012). "Asteroid lightcurve analysis at the Palmer Divide Observatory, 2011 September-December." *Minor Planet Bull.* **39**, 69-80.

Warner, B.D.; Harris, A.W.; Pravec, P. (2009). "The Asteroid Lightcurve Database." *Icarus* **202**, 134-146. Updated 2023 Oct. *https://minplanobs.org/MPInfo/php/lcdb.php*

Waszczak, A.; Chang, C.-K.; Ofeck, E.O.; Laher, F.; Masci, F.; Levitan, D.; Surace, J.; Cheng, Y-C.; Ip, W-H.; Kinoshita, D.; Helou, G.; Prince, T.A.; Kulkarni, S. (2015). "Asteroid light curves from the Palomar transient factory survey: rotation periods and phase functions from sparse photometry." *The Astonomical Journal 150(3), 75pp. https://dx.doi.org/10.1088/0004-6256/150/3/75.*

PHOTOMETRY OF SUSPECTED AND CONFIRMED BINARY ASTEROIDS

Tom Polakis
Command Module Observatory
121 W. Alameda Dr.
Tempe, AZ 85282 USA
tpolakis@cox.net

(Received: 2025 April 3 Revised: 2025 May 13)

CCD photometric observations of seven suspected and three confirmed binary asteroids were made from 2024 December through 2025 March. Mutual events were not detected for any of the seven suspected binary asteroids. Phased lightcurves were created for all ten asteroids. All the data have been submitted to the ALCDEF database.

CCD photometric observations of ten main-belt asteroids were performed at Command Module Observatory (MPC V02) in Tempe, AZ. The purpose of the observations was to look for mutual events, i.e., lightcurve attenuations due to occultations and/or eclipses in a binary system, and if detected, compute orbital period solutions.

The majority of binary asteroids were discovered with photometric observations by detecting mutual events. Direct imaging by spacecraft or radar for nearby asteroids has shown companion bodies. In rare cases, stellar occultations have revealed a companion as two separate disappearances and reappearances.

Liberato et al. (2024) pursued an approach that incorporated searching for "wobble" in astrometric observations. Knowing the precise orbits, they used 34 months of *Gaia* DR3 observations to search for periodicity in the residuals of observed asteroid positions. A total of 361 binary candidates were found by this method, some of which are known binaries.

Their table of binary candidates was filtered to include only those with a signal-to-noise ratio flag of 1, bringing the total down to 115 candidates. Further, the table was sorted to look particularly for asteroids with short wobble periods. From this list, seven candidates were found that were sufficiently bright and well-placed for observations.

Three additional known binary asteroids culled from to table maintained by Johnston (2025), were added.

Images were taken at V02 using a 0.32-m *f*/6.7 Modified Dall-Kirkham telescope, SBIG STXL-6303 CCD camera, and a 'clear' glass filter. Exposure time for the images was 2 minutes. The image scale after 2×2 binning was 1.76 arcsec/pixel.

Table I shows the observing circumstances and results. All of the images of these asteroids were obtained between 2024 December and 2025 March.

Images taken at V02 were calibrated using a dozen bias, dark, and flat frames. Flat-field images were made using an electroluminescent panel. Image calibration and alignment was performed using *MaxIm DL* (Diffraction Limited, 2017) software.

The data reduction and period analysis were done using *Tycho* (Parrott, 2025). In these fields, the asteroid and three to five comparison stars were measured. Comparison stars were selected with colors within the range of $0.5 < B\text{-}V < 0.95$ to correspond with color ranges of asteroids. In order to reduce the internal scatter in the data, the brightest stars of appropriate color that had peak ADU counts below the range where chip response becomes nonlinear were selected. *Tycho* plots instrumental vs. catalog magnitudes for solar-colored stars, which is useful for selecting comp stars of suitable color and brightness.

The clear-filtered images were reduced to Pan-STARRS r′ to minimize error with respect to a color term. Comparison star magnitudes were obtained from the ATLAS catalog (Tonry et al., 2018), which is incorporated directly into *Tycho*. The ATLAS catalog derives Pan-STARRS *griz* magnitudes using a number of available catalogs. The consistency of the ATLAS comp star magnitudes and color-indices allowed the separate nightly runs to be linked often with no zero-point offset required or shifts of only a few hundredths of a magnitude in a series.

Data reduction for V02 images used a 9-pixel (16 arcsec) diameter measuring aperture for asteroids and comp stars. It was typically necessary to employ star subtraction to remove contamination by field stars.

For the asteroids described here, the RMS scatter on the phased lightcurves is noted, which gives an indication of the overall data quality including errors from the calibration of the frames, measurement of the comp stars, the asteroid itself, and the period-fit. Period determination was done using the *Tycho* Fourier-type FALC fitting method (Harris et al., 1989). Phased lightcurves show the maximum at phase zero. Magnitudes in these plots are apparent and scaled by *Tycho* to the first night. In four of the 10 cases, the curve was better fit with a departure of the phase-slope parameter *G* from the default value of 0.15. When present, this is noted in each section.

The Asteroid Lightcurve Database (LCDB; Warner et al., 2009) was consulted to locate previously published results. All the new data for these asteroids can be found in the Asteroid Lightcurve Data Exchange Format (ALCDEF) database.

Observing mutual events requires favorable geometry, in which the observer is situated near the companion's orbital plane. Pravec et al. (2012) showed that there is preference for orbits of asteroid companions to lie near the ecliptic plane. This improves the prospects for detecting mutual events.

Mutual events were not found in any of the seven candidates, and only one of the three confirmed binaries showed such events. This one binary has a matching orbital period. Therefore, orbital periods are not included in Table I.

Non-detection can be attributed to several causes. In four of the seven candidates, the wobble period closely matched the known rotation period. It is possible that the wobble is simply due to the offset between the barycentric and astrometric center of a single body. Binary detection by astrometric wobble is most favorably observed for orbits that are out of the ecliptic plane; the opposite is true for photometry. Some actual binaries may not show mutual events due to unfavorable geometry. Finally, observations at V02 were conducted with a small telescope at an urban site, so photometric precision may have not been sufficient for capturing mutual events with small amplitudes.

90 Antiope was discovered by Robert Luther in 1866 at Dusseldorf. It is a well-characterized synchronous binary. The most recent period determination was made by Bartczak et al. (2014), who computed 16.505046 ± 0.000005 h. During four nights, 477 images were obtained to determine a synodic period of 16.504 ± 0.002 h. The lightcurve has an amplitude of 0.54 mag, and an RMS error on the fit of 0.02 mag. The lightcurve shows clear signs of synchronous binary asteroid behavior, with sharp V-shaped troughs from mutual events overlaid on the gentler rotational signature.

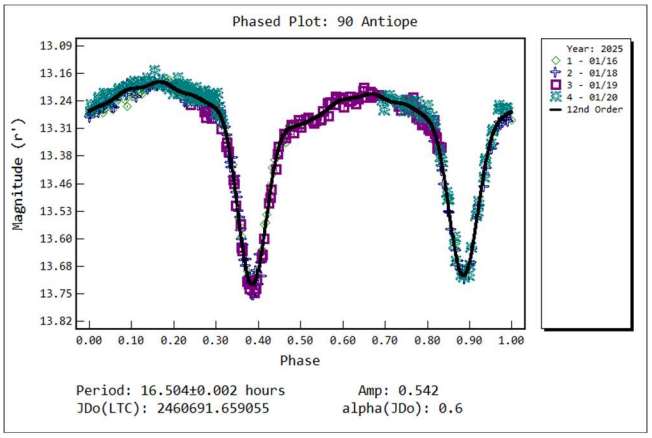

238 Hypatia. Viktor Knorr discovered this asteroid at Berlin in 1884. Per Liberato et al. (2024), it exhibited a wobble period of 9.852 ± 0.010 h. Franco et al. (2024) published a rotation period of 8.873 ± 0.001 h, in line with previous values. In five nights, 444 data points were acquired, yielding a period solution of 8.874 ± 0.002 h. The amplitude is 0.06 ± 0.01 mag. The best fit was accomplished with $G = 0.11$.

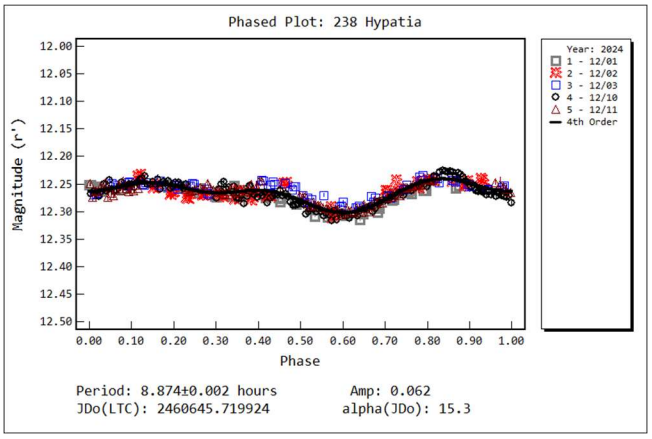

247 Eukrate was discovered by Robert Luther at Dusseldorf in 1865. It has an astrometric wobble period of 12.098 ± 0.060 h, which corresponds with the rotation period of 12.09480 ± 0.00005, determined by Hanuš et al. (2016). At V02, the asteroid was observed on three nights, and 694 images were gathered. The resulting period is 12.101 ± 0.004 h, with an amplitude of 0.11 ± 0.01 mag.

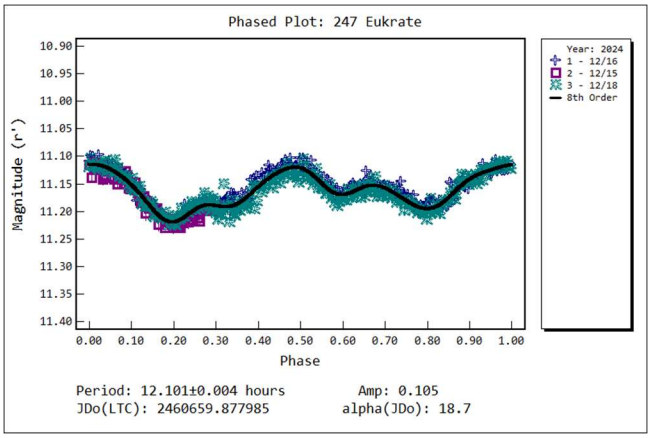

488 Kreusa is one of Max Wolf's many discoveries from Heidelberg. Its wobble period is 16.369 ± 0.005 h. Pilcher (2019) computed a rotation period of 32.645 ± 0.001 h. During 11 nights, 1815 data points were acquired, resulting in a period of 32.656 ± 0.013 h, with an amplitude of 0.05 ± 0.01 mag. G was set to 0.23 to optimize the fit.

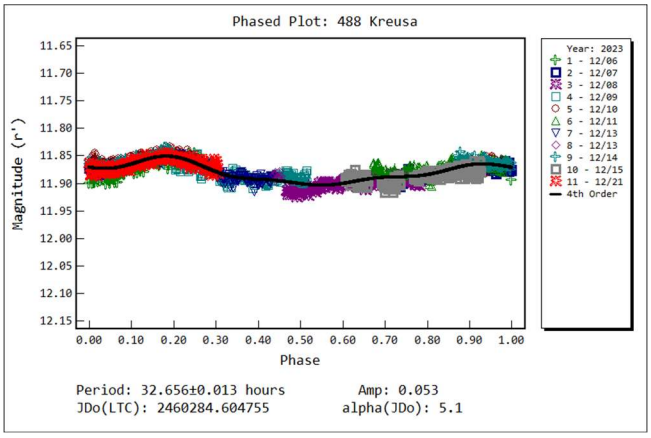

504 Cora. This outer main-belt asteroid was discovered in 1902 at Arequipa by Solon Irving Baily. It exhibited a wobble period of 11.332 ± 0.005 h. The LCDB shows many agreeing period solutions, the most recent being Pilcher (2021) with 7.5872 ± 0.002 h. A total of 410 images were taken on three nights. The resulting synodic rotation period is 7.589 ± 0.003 h, agreeing best with previous values. The amplitude of the lightcurve is 0.20 mag, with an RMS error on the fit of 0.02 mag. The curve was best fit with G increased to 0.50.

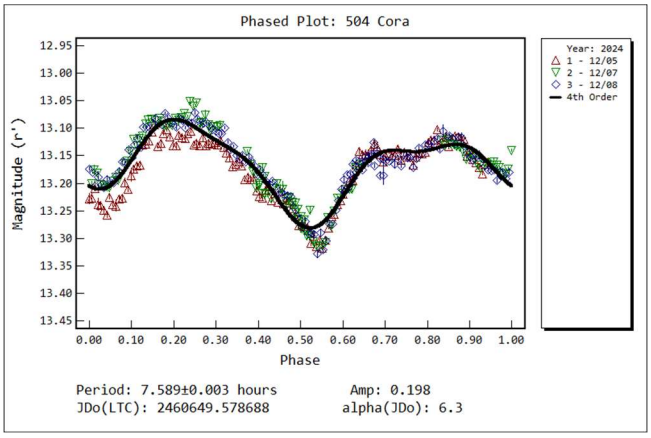

Number	Name	yy/mm/dd	Phase	L_{PAB}	B_{PAB}	Period(h)	P.E.	Amp	A.E.	Grp
90	Antiope	25/01/16-01/20	0.6,1.5	116	2	16.604	0.002	0.54	0.02	THM
238	Hypatia	24/12/01-12/11	15.3,12.6	108	-15	8.874	0.002	0.06	0.01	MB-O
247	Eukrate	24/12/16-12/18	18.7,18.5	91	-34	12.101	0.004	0.11	0.01	MB-O
488	Kreusa	24/12/06-12/21	20.0,21.1	179	11	32.656	0.013	0.05	0.01	MB-O
504	Cora	24/12/05-12/08	6.3,7.1	66	-10	7.589	0.003	0.20	0.02	MB-O
542	Susanna	24/12/01-12/03	16.6,16.2	118	-10	10.076	0.010	0.19	0.02	MB-O
674	Rachelle	23/11/07-11/10	22.2,22.4	147	13	30.861	0.042	0.16	0.01	MB-O
1127	Mimi	24/12/01-12/04	21.7,20.6	107	-11	12.748	0.003	0.78	0.01	MB-I
1626	Sadeya	25/01/15-01/20	13.2,16.3	98	-4	3.421	0.001	0.12	0.01	MB-I
2577	Litva	25/03/27-03/30	9.4,8.1	197	7	2.816	0.002	0.19	0.08	HUN

Table I. Observing circumstances and results. The phase angle is given for the first and last date. If preceded by an asterisk, the phase angle reached an extrema during the period. L_{PAB} and B_{PAB} are the approximate phase angle bisector longitude/latitude at mid-date range (see Harris et al., 1984). Grp is the asteroid family/group (Warner et al., 2009).

542 Susanna was discovered in 1904 at Heidelberg by Paul Götz. Liberato et al. (2024) show a wobble period of 10.02 ± 0.02 h. The most recent of agreeing period solutions is by Polakis (2024), who published a value of 10.091 ± 0.008 h. During three nights, 170 images were obtained. The computed rotation period is 10.076 ± 0.010 h, with an amplitude of 0.19 ± 0.02 mag.

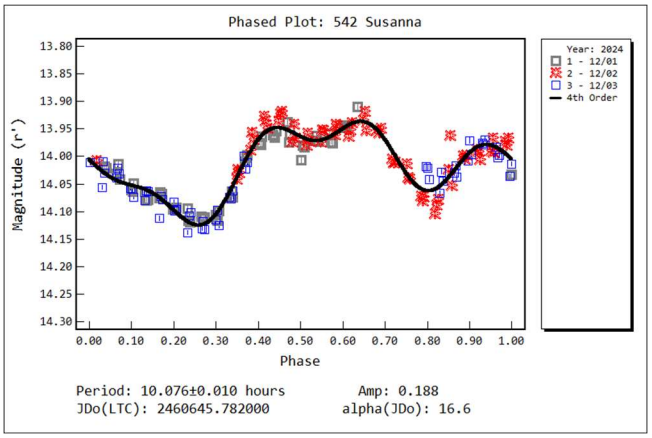

674 Rachel. This outer main-belt asteroid was discovered by Wilhelm Lorenz at Heidelberg in 1908. It showed a wobble period of 10.558 ± 0.070 h. Durech et al. (2020) published a sidereal rotation period of 30.9753 ± 0.0008 h. A total of 956 data points were obtained during four nights, producing a computed rotation period of 30.861 ± 0.042 h. The amplitude is 0.16 ± 0.01 mag.

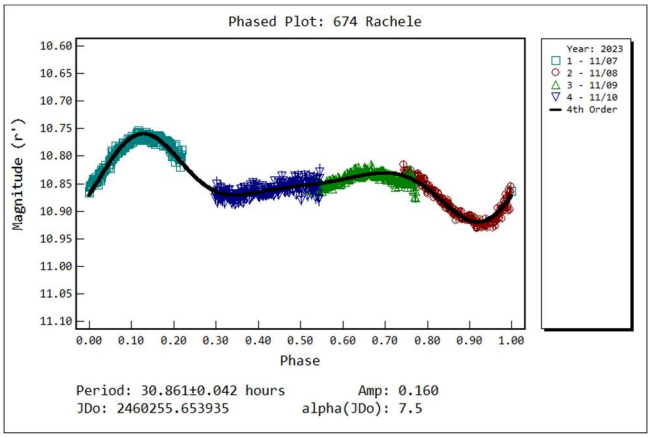

1127 Mimi was discovered by Sylvain Arrend at Uccle in 1929. Its wobble period is shown as 12.774 ± 0.11 h. Hanuš et al. (2018) published a rotation period of 12.74555 ± 0.00002 h. After four nights, 347 data points were used to compute a synodic period of 12.748 ± 0.003 h. The amplitude of the lightcurve is 0.78 ± 0.01 mag.

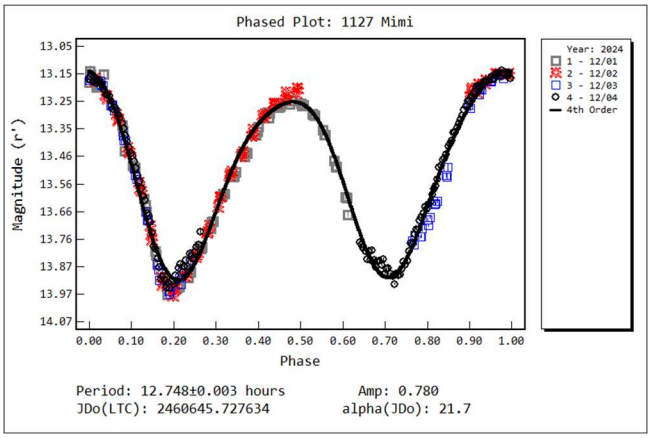

1626 Sadeya. This minor planet was discovered by Josep Comas i Solà at Barcelona in 1927. It is a confirmed binary, with an orbital period determined by Benishek (2020) of 51.3 ± 0.2 h. Benishek also reported a rotation period of 3.4202 ± 0.0002 h. Observations were made for five nights, during which time 503 images were obtained. The calculated rotation period is 3.421 ± 0.001 h, with an amplitude of 0.12 ± 0.01 mag. The optimal curve fit appeared with G = 0.22. Mutual events are not apparent in the lightcurve.

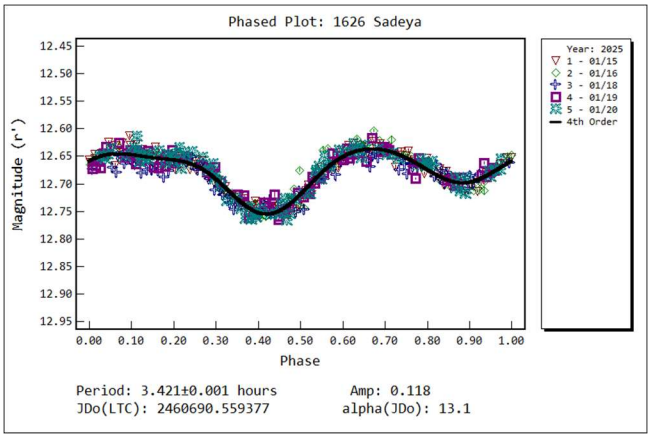

2577 Litva is a Hungaria-type asteroid that was discovered by Lyudmila Chernykh at Nauchnyj in 1975. Warner and Stephens (2011) reported an orbital period of the companion of 35.88 ± 0.01 h, and a primary rotation period of 2.81288 ± 0.0005 h. A total of 492 images were obtained in three nights, producing a rotation period of 2.816 ± 0.002 h. The amplitude is 0.19 ± 0.08 mag. A solution for mutual events or a secondary rotation period could not be disentangled in the light curve, but it is likely that one or both caused the poor fit.

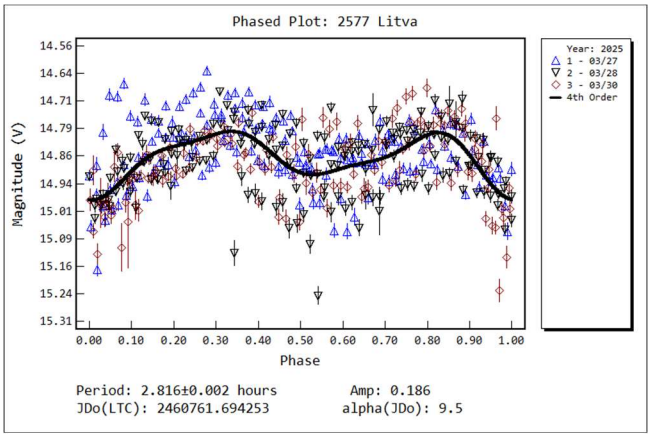

Acknowledgments

The author would like to express his gratitude to Brian Skiff for his indispensable mentoring in data acquisition and reduction. Thanks also go out to Daniel Parrott for support of his *Tycho* software package.

References

Bartczak, P.; Michałowski, T.; Santana-Ros, T.; Dudziński, G. (2014). "A new non-convex model of the binary asteroid 90 Antiope obtained with the SAGE modelling technique." *MNRAS* **443**, 1802-1809.

Benishek, V. (2020). **CBET**, 4893.

Diffraction Limited (2017). *MaxIm DL* software. *https://diffractionlimited.com/product/maxim-dl/*

Durech, J.; Tonry, J.; Erasmus, N.; Denneau, L.; Heinze, A.N.; Flewelling, H.; Vanco, R. (2020). "Asteroid models reconstructed from ATLAS photometry." *Astron. Astrophys.* **643**, A59.

Franco, L. and 19 additional co-authors (2024). "Collaborative Asteroid Photometry from UAI: 2023 July-September." *Minor Planet Bull*. **51**, 56-61.

Hanuš, J. and 19 additional co-authors (2016). "New and updated convex shape models of asteroids based on optical data from a large collaboration network." *Astron. Astrophys*. **586**, 108-131.

Hanuš, J.; Delbo', M.; Ďurech, J.; Alí-Lagoa, V. (2018). "Thermophysical modeling of main-belt asteroids from WISE thermal data." *Icarus* **309**, 297-337.

Harris, A.W.; Young, J.W.; Scaltriti, F.; Zappala, V. (1984). "Lightcurves and phase relations of the asteroids 82 Alkmene and 444 Gyptis." *Icarus* **57**, 251-258.

Harris, A.W.; Young, J.W.; Bowell, E.; Martin, L.J.; Millis, R.L.; Poutanen, M.; Scaltriti, F.; Zappala, V.; Schober, H.J.; Debehogne, H.; Zeigler, K.W. (1989). "Photoelectric Observations of Asteroids 3, 24, 60, 261, and 863." *Icarus* **77**, 171-186.

Johnston, W.R. (2025). "Asteroids With Satellites." *https://www.johnstonsarchive.net/astro/asteroidmoons.html*

Liberato, L.: Tanga, P.; Mary, D.; Minker, K.; Carry, B.; Spoto, F.; Bartczak, P.; Sicardy, B.; Oszkiewicz, D.; Desmars, J. (2024). "Binary asteroid candidates in Gaia DR3 astrometry." *Astron. Astrophys*. **688**, 50-73.

Parrott, D. (2025). *Tycho* software. *https://www.tycho-tracker.com/*

Pravec, P. and 41 additional co-authors (2012). "Binary asteroid population. 2. Anisotropic distribution of orbit poles of small, inner main-belt binaries." *Icarus* **218**, 125-143.

Pilcher, F. (2019). "Rotation Period Determinations for 58 Concordia, 384 Burdigala, 464 Megaira, 488 Kreusa, and 491 Carina." *Minor Planet Bull* **46**, 360-363.

Pilcher, F. (2021). "Lightcurves and Rotation Periods of 47 Aglaja, 504 Cora 527 Euryanthe, 593 Titania, and 594 Mireille." *Minor Planet Bull*. **48**, 217-218.

Polakis, T. (2024). "Photometric Results for Twenty Minor Planets." *Minor Planet Bull*. **51**, 126-132.

Tonry, J.L.; Denneau, L.; Flewelling, H.; Heinze, A.N.; Onken, C.A.; Smartt, S.J.; Stalder, B.; Weiland, H.J.; Wolf, C. (2018). "The ATLAS All-Sky Stellar Reference Catalog." *Astrophys. J.* **867**, A105.

Warner, B.D.; Harris, A.W.; Pravec, P. (2009). "The Asteroid Lightcurve Database." *Icarus* **202**, 134-146. Updated 2023 Oct. *http://www.minorplanet.info/lightcurvedatabase.html*

Warner, B.; Stephens, R. (2011). "On Confirmed and Suspected Binary Asteroids Observed at the Center for Solar System Studies." *Minor Planet Bull*. **48**, 40-49.

LIGHTCURVE RESULTS FOR EIGHT MAIN-BELT ASTEROIDS

Gonzalo Fornas (J57)
Asociación Valenciana de Astronomía
(Centro Astronómico Alto Turia)
C/ Profesor Blanco 16. 46014 Valencia, SPAIN
gon@iicv.es

Alvaro Fornas (J57)
Asociación Valenciana de Astronomía (CAAT)

Alfonso Carreño (Y76)
Nova Canet Observatory

Fernando Huet (Z93)
Asociación Valenciana de Astronomía.
Polop Observatory

Enrique Rathmann (Y78)
Asociación Valenciana de Astronomía
Tros Alt Observatory

Enrique Arce (J67)
Asociación Valenciana de Astronomía
Vallbona Observatory

Vicente Mas, AVA –J57, CAAT
Centro Astronómico del Alto Turia, SPAIN

(Received: 2025 April 8)

Photometric observations for eight main-belt asteroids allowed us to derive the following rotational synodic periods: 2663 Miltiades, 3.95796 ± 0.00007 h; 3539 Weimar, 8.7059 ± 0.0007 h; 9014 Svyatorichter, 3.7635 ± 0.0008 h; 13441 Janmerlin, 23.0840 ± 0.0007 h; (14488) 1994 TF15, 2.8761± 0.0001 h; (15138) 2000 EQ93, 16.4228 ± 0.0023 h; (18489) 1996 BV2, 2.9317 ± 0.0014 h; (18513) 1996 TS5, 9.7437 ± 0.0028 h.

We report on the photometric analysis for eight-belt asteroids by Asociación Valenciana de Astronomía (AVA). The data were obtained during the last quarter of 2024 and first months of 2025. We present graphic results of data analysis, mainly lightcurves, with the plot phased to a given period. We managed to obtain several accurate and complete lightcurves and calculating as accurately as possible their rotation periods.

Observatory	Telescope (meters)	CCD
C.A.A.T. J57	17" DK	QHY- 600
C.A.A.T. J57	10" NW	ZWO ASI 1600
Z93	SC 8"	SBIG ST8300
J67	SC 10"	SBIG ST7
Y78	SC 8"	ZWO ASI 294 MM PRO
Y76	SC 9..25"	ATIK 314L+

Table I. List of instruments used for the observations.

We focused on asteroids with no reported period and those where the reported period was poorly established and needed confirmation. The targets were selected from the Collaborative Asteroid Lightcurve (CALL) website (*http://www.minorplanet.info/call.html),* the Minor Planet Center (*http://www.minorplanet.net*) and Brian D. Warner et at. (2024). The Asteroid Lightcurve Database (LCDB; Warner et al., 2009) was consulted to locate previously published results.

Images were measured using *MPO Canopus* (Bdw. Publishing) with a differential photometry technique. The comparison stars were restricted to near solar-color to minimize color dependencies, especially at larger air masses. The lightcurves show the synodic rotation period. The amplitude (peak-to-peak) that is shown is that for the Fourier model curve and not necessarily the true amplitude.

2663 Miltiades. This inner main-belt asteroid was discovered on 1960 Sep 24 at Palomar by PLS. We made observations on 2025 Jan 7 to Feb 4. From our data we derive a synodic rotation period of 3.95796 ± 0.00007 h and an amplitude of 0.88 mag. Durech et al. (2018) found a sidereal period of 3.957489 h and Martikainen et al. (2021) found a sidereal period of 3.957490 h. All of them are consistent with our calculation.

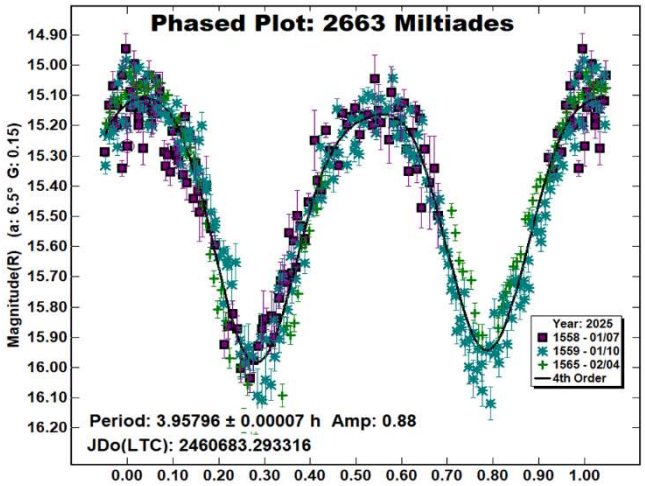

3539 Weimar. This outer main-belt asteroid of the Eunea family was discovered on 1967 Apr 11 at Thuringia State Observatory Tautenburg by F. Börngen. We made observations on 2024 Jul 7 to Aug 1. From our data we derive a synodic rotation period of 8.7059 ± 0.0007 h and an amplitude of 0.50 mag. Garlitz (2011web) got a period of 7.29 h.

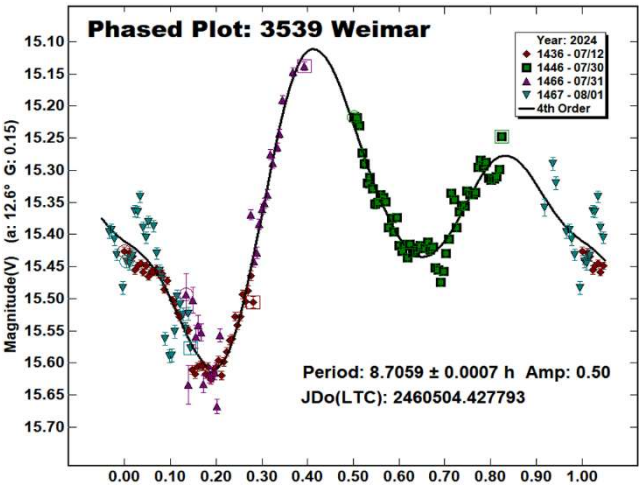

9014 Svyatorichter. This inner main-belt asteroid was discovered on 1985 Oct. 22 at Nauchnij by L.V. Zhuravleva. We made observations on 2024 Dec 21 - 25. From our data we derive a synodic rotation period of 3.7635 ± 0.0008 h and an amplitude of 0.33 mag. We have no previous information about its rotation period.

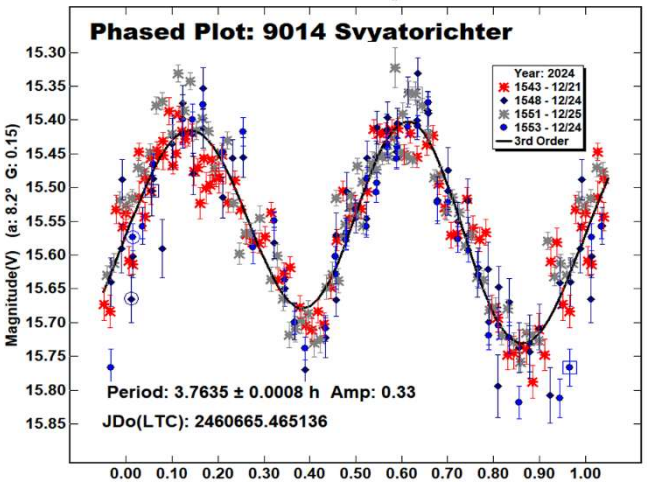

13441 Janmerlin. This middle main-belt asteroid was discovered on 1960 Sep. 24 at Palomar by PLS. We made observations on 2024 Sep 30 to Dec 21. From our data we derive a synodic rotation period of 23.0840 ± 0.0007 h and an amplitude of 0.74 mag. The period is close to 24 hours and we have not obtained the complete lightcurve but only one of the halves. In any case, the result of the period calculation is accurate enough. Our results match with Marchini and Papini (2025) who got a period of 23.087 h.

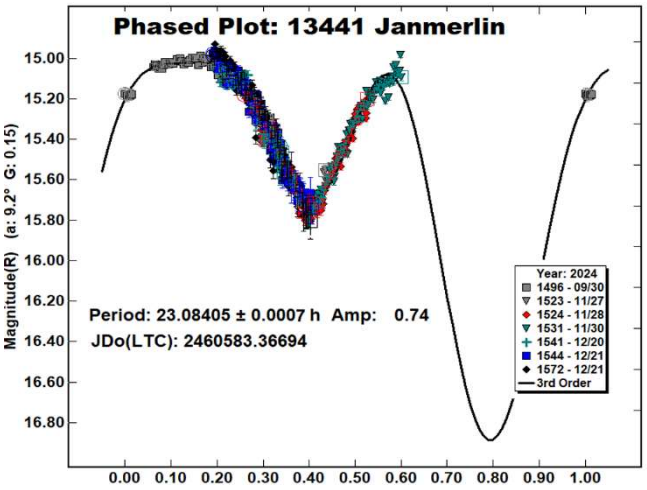

(14488) 1994 TF15. This inner main-belt asteroid was discovered on 1994 Oct 13 at Kiyosato Observatory by S. Otomo. We made observations on 2024 Oct 4 to Nov 9. From our data we derive a synodic rotation period of 2.8761 ± 0.0001 h and an amplitude of 0.24 mag. We have no previous information about its rotation period.

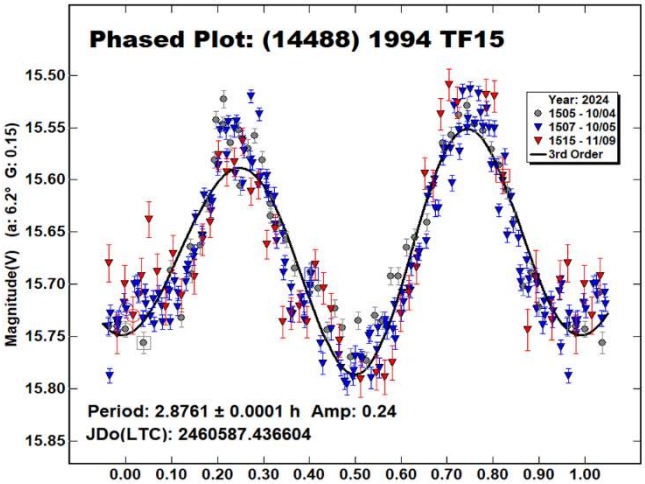

(15138) 2000 EQ93. This middle main-belt asteroid was discovered on 2000 March 9 at SOCORRO by LINEAR. We made observations on 2024 Sep 5 to Oct 5. From our data we derive a synodic rotation period of 16.4228 ± 0.0023 h and an amplitude of 0.14 mag. We have no previous information about its rotation period.

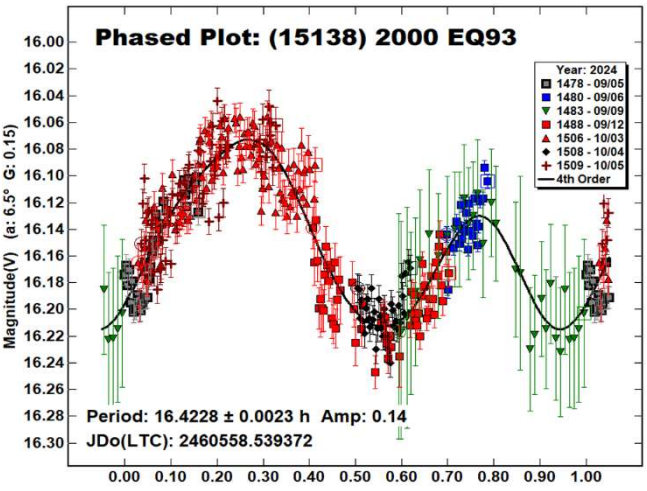

Number	Name	yyyy mm/dd	Phase	L_{PAB}	B_{PAB}	Period(h)	P.E.	Amp	A.E.	Grp
2663	Miltiades	2025 01/07-02/04	6.4,18.6	105.5	9.0	3.95796	0.00007	0.88	0.05	MB-I
3539	Weimar	2024 07/12-08/01	5.7,10.6	290.9	8.9	8.7059	0.0007	0.5	0.05	MB-O
9014	Svyatorichter	2024 12/21-12/24	8.7,10.5	76.1	1.8	3.7635	0.0008	0.33	0.05	MB-I
13441	Janmerlin	2024 09/30-12/21	8.6,25.6	26.1	-4.5	23.0840	0.0007	0.74	0.05	MB-M
14488	1994 TF15	2024 10/04 11/09	6.1,15.7	20.4	3.4	2.8761	0.0001	0.24	0.05	MB-I
15138	2000 EQ93	2024 09/05-10/05	6.5,13.8	350.3	9.8	16.4228	0.0023	0.14	0.03	MB-M
18489	1996 BV2	2025 02/01-02/04	7.1, 6.1	142.7	9.0	2.9317	0.0014	0.15	0.03	MB-M
18513	1996 TS5	2025 02/02-02/05	14.3,16.0	111.8	-1.3	9.7437	0.0028	0.75	0.05	MB-I

Table I. Observing circumstances and results. The phase angle is given for the first and last date. If preceded by an asterisk, the phase angle reached an extrema during the period. L_{PAB} and B_{PAB} are the approximate phase angle bisector longitude/latitude at mid-date range (see Harris et al., 1984). Grp is the asteroid family/group (Warner et al., 2009).

(18489) 1996 BV2. This middle main-belt asteroid was discovered on 1996 Jan 26 at Kashihara by F. Uto. We made observations on 2025 Feb 1 to 4. From our data we derive a synodic rotation period of 2.9317 ± 0.0014 h and an amplitude of 0.15 mag. We have not previous information about its rotation period.

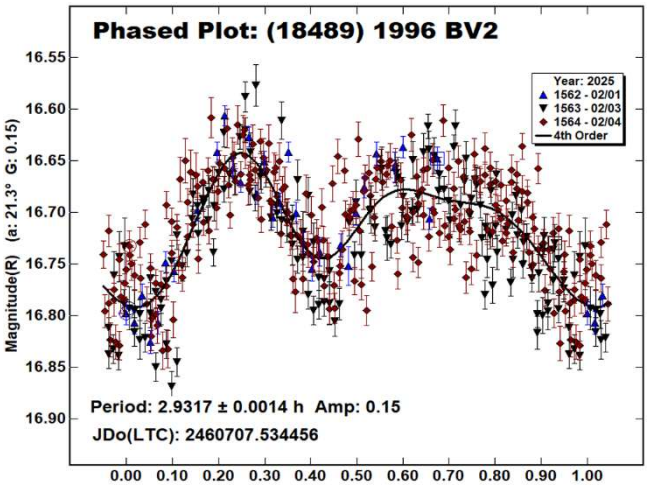

(18513) 1996 TS5. This inner main-belt asteroid of the Phocaea family was discovered on 1996 Oct 7 at Catalina Station by T.B. Spahr. We made observations on 2025 Feb 1 to 4. From our data we derive a synodic rotation period of 9.7437 ± 0.0028 h and an amplitude of 0.75 mag. We have no previous information about its rotation period.

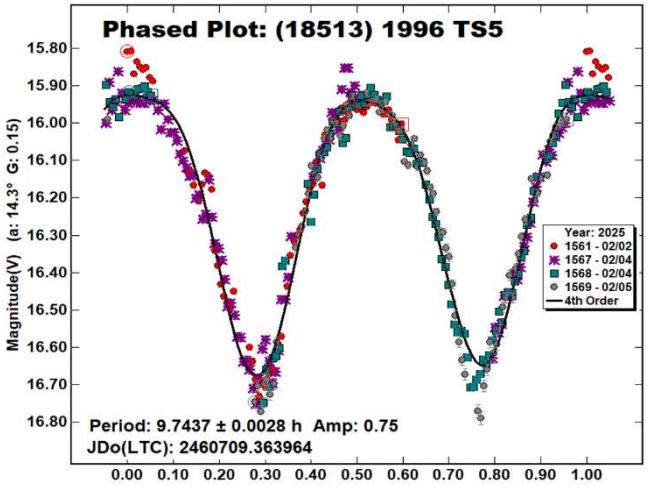

References

Durech, J.; Hanus, J.; Ali-Lagoa, V. (2018). "Asteroid models reconstructed from the Lowell Photometric Database and WISE data." *Astron. Astrophys.* **617**, A57.

Garlitz (2011web). (unknown link).

Harris, A.W.; Young, J.W.; Scaltriti, F.; Zappala, V. (1984). "Lightcurves and phase relations of the asteroids 82 Alkmene and 444 Gyptis." *Icarus* **57**, 251-258.

Marchini, A; Papini, R. (2025). "13441 Janmerlin, an Asteroid with an Earth Commensurate Rotation Period." *Minor Planet Bull.* **52**, 7-8.

Martikainen, J.; Muinonen, K.; Penttila, A.; Cellino, A.; Wang, X.-B. (2021). "Asteroid absolute magnitudes and phase curve parameters from Gaia photometry." *Astron. Astrophys.* **649**, A98.

Warner, B.D.; Harris, A.W.; Pravec, P. (2009). "The Asteroid Lightcurve Database." *Icarus* **202**, 134-146. Updated 2016 Sep. *http://www.minorplanet.info/lightcurvedatabase.html*

Warner, B.D.; Harris, A.W.; Durech J.; Lance A.M. (2024). "Lightcurve Photometry Opportunities: 2024 July - September." *Minor Planet Bull*. **51**, 293-296.

LIGHTCURVES OF TWENTY ASTEROIDS

Geoffrey Stone
Dimension Point Observatory
14 Galaxy Point
Mayhill, NM 88339
geoff@first-light-systems.com

(Received: 2025 April 8)

We present lightcurves and synodic rotation periods for twenty asteroids observed from December 2024 through March 2025 at Dimension Point Observatory.

Photometric observation of these minor planets were conducted from January 2025 through March 2025 at Dimension Point Observatory (V42).

Images were acquired using a 0.61-m f/6.5 Corrected Dall-Kirkham telescope with Finger Lakes Instrumentation Kepler KL400 back-illuminated CMOS camera and a 0.51-m f/8 Ritchey-Chrétien telescope with SBIG AC4040 CMOS camera. The equipment was operated remotely using *ACP Expert* (Denny, 2024) and *MaximDL* (George et al., 2024). Time was synchronized using a local stratum 1 time source and Meinberg NTP client software. Exposures were typically 120 seconds unfiltered or through a yellow blue-blocking long-pass filter with cutoff at 500nm.

Target selection and observation planning was performed using the authors own Python scripts. Orbital elements, ephemeris and other information were obtained from the Minor Planet Center (MPC) website (*http://www.minorplanet.net*), the JPL Solar System Dynamics website (*http://ssd.jpl.nasa.gov*) (Giorgini et al., 1996), the Lowell Observatory Minor Planet Services website (*http://asteroid.lowell.edu*) (Moskovitz, 2022) and the LCDB database (Warner et al., 2009).

Image calibration, plate solving, measurement and period analysis were performed using *Tycho-Tracker* V12.3 (Parrott 2020). Calibration masters were prepared using *AstroImageJ* (Collins et al., 2017). Comparison stars of near solar color were chosen from the ATLAS refcat2 star catalog using Sloan r′ magnitudes (Tonry et al., 2018). Additional period analysis was carried out using *MPO Canopus* V10.8.4.1 (Warner, 2020).

1887 Virton. We observed this member of the Eos family on sixteen nights in 2024 December and 2025 January. There were prior reports from Dose (2024) of 70.071 ± 0.011, Polakis (2024) of 69.64 ± 0.08 and Hawley et al. (2024) of 70.165 ± 0.003. We found 70.18 ± 0.04 hours with an amplitude of 0.3239 ± 0.0197 mag, in agreement with Hawley.

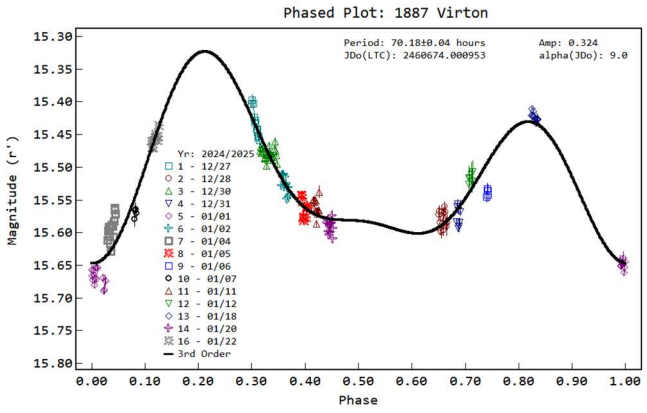

1890 Konoshenkova is named after Olga Petrovna Konoshenkova, who was schoolmistress at the Crimean Observatory School. We found a period of 14.526 ± 0.012 hours with an amplitude of 0.227 ± 0.0237 mag. We found no prior rotation period reports.

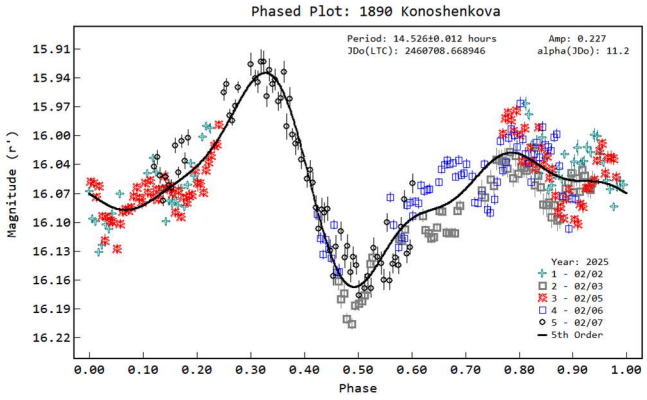

2010 Chebyshev. We found a period of 4.097 ± 0.001 hours with an amplitude of 0.435 ± 0.0242 mag. A search of the LCDB found no prior reports for this member of the Themis family.

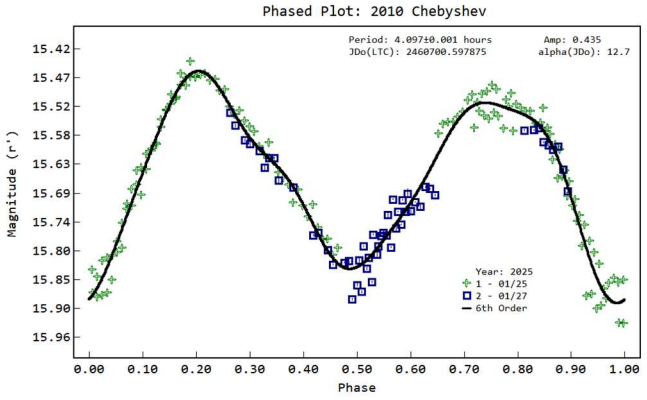

Number	Name	yyyy mm/dd	Phase	L_{PAB}	B_{PAB}	Period(h)	P.E.	Amp	A.E.	Grp
1887	Virton	2024 12/27-01/21	10.0, 3.4	121	9	70.18	0.04	0.32	0.02	Eos
1890	Konoshenkova	2025 02/02-02/07	11.2,12.8	106	8	14.526	0.012	0.23	0.02	MB-O
2010	Chebyshev	2025 01/25-01/27	12.7,13.4	94	3	4.097	0.001	0.44	0.02	Themis
2194	Arpola	2025 02/16-03/25	*12.5,14.4	158	11	110.78	0.07	0.50	0.02	MB-I
2225	Serkowski	2025 02/26-03/03	9.3,11.1	135	3	2.764	0.003	0.33	0.03	Koronis
2244	Tesla	2025 02/21-03/22	9.4, 4.0	177	9	37.65	0.04	0.38	0.03	MB-O
2316	Jo-Ann	2025 01/21-02/08	14.9, 8.9	160	0	33.850	0.025	0.24	0.04	Massalia
2719	Suzhou	2025 01/20-02/08	29.8,11.9	158	0	118.30	0.04	1.13	0.04	MB-I
3368	Duncombe	2025 01/03-02/08	*8.7, 7.6	124	20	34.030	0.007	0.25	0.02	MB-O
3909	Gladys	2025 02/04-03/20	13.6,20.8	104	-14	25.48	0.01	0.50	0.05	Eunomia
4099	Wiggins	2024 12/22-01/22	*9.4, 9.4	105	-10	10.994	0.006	0.15	0.03	Maria
4350	Shibecha	2025 02/23-02/25	18.0,17.3	188	10	2.890	0.004	0.10	0.02	MB-M
5424	Covington	2025 01/23-01/24	17.6,17.3	159	-3	5.460	0.007	0.30	0.02	MB-I
6735	Madhatter	2025 01/29-02/05	4.4, 2.4	136	4	8.550	0.004	0.14	0.02	MB-I
6950	Simonek	2025 02/20-02/25	9.8,11.4	138	15	3.298	0.002	0.11	0.03	Eunomia
9010	Candelo	2025 02/26-03/26	12.5,23,8	138	3	5.015	0.001	0.11	0.03	MB-I
13352	Gyssens	2025 03/10-03/29	9.1,11.6	173	16	3.041	0.001	0.20	0.02	Eunomia
13542	1991 VC5	2025 01/18-02/08	8.4,17.3	107	9	52.807	0.023	0.40	0.04	Vesta
24863	Cheli	2024 12/25-02/04	4.7,20.7	89	8	16.716	0.005	0.17	0.04	MB-M
27736	Ekaterinburg	2025 01/20-02/01	20.5,21.4	94	15	5.604	0.001	0.55	0.03	MB-O

Table I. Observing circumstances and results. The phase angle is given for the first and last date. If preceded by an asterisk, the phase angle reached an extrema during the period. L_{PAB} and B_{PAB} are the approximate phase angle bisector longitude/latitude at mid-date range (see Harris et al., 1984). Grp is the asteroid family/group (Warner et al., 2009).

2194 Arpola. We found a period of 110.78 ± 0.07 hours with an amplitude of 0.50 ± 0.02 mag. We observed this middle main-belt asteroid on fifteen nights in 2024 February and March. We were unable to find any prior rotation period reports.

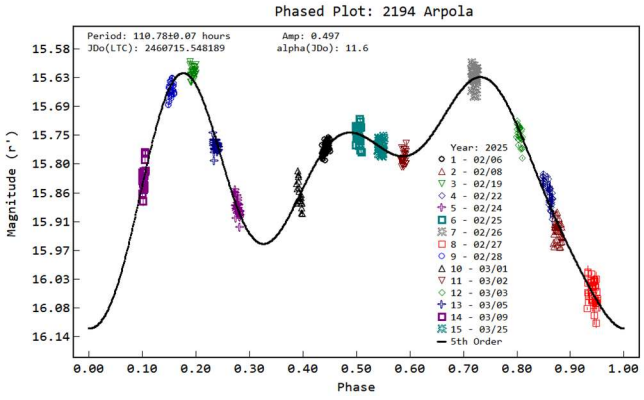

2225 Serkowski is a member of the Koronis family named after Krzysztof Serkowski, a Polish American astronomer. We found a period of 2.764 ± 0.003 hours with an amplitude of 0.333 ± 0.03 mag. We found no prior rotation period reports.

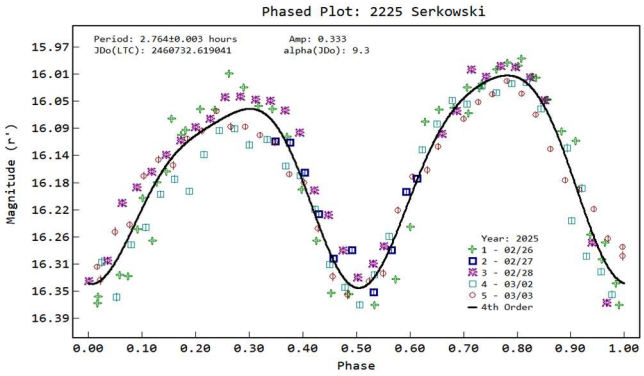

2244 Tesla was discovered in 1952 by Protitch at Belgrade and is named for Nikila Tesla. There are prior reports from Polakis (2024) of > 300 hours, Marchini and Papini (2024) of 24.65 hours, and Farfán et al. (2024) of 18.45 hours. We found a best fit of 37.65 ± 0.04 hours with an amplitude of 0.382 ± 0.03 mag, disagreeing with prior reports.

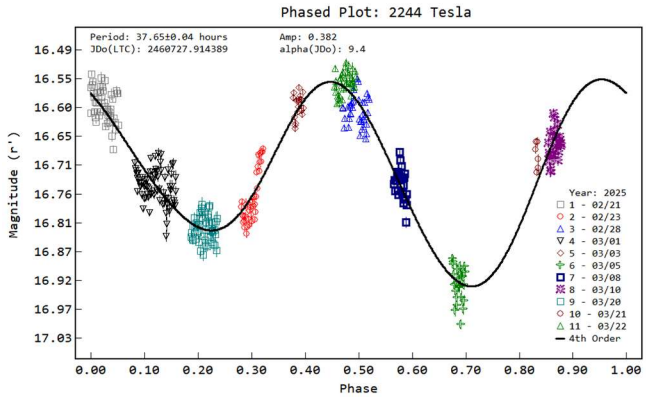

2316 Jo-Ann was discovered by Ted Bowell in 1980 at Anderson Mesa. It is named in honor of his wife, Jo-Ann. We found one prior survey report from Chang et al. (2014) of 33.0 ± 2.0 hours. Analysis of our data resulted in a period of 33.850 ± 0.025 hours with an amplitude of 0.2376 ± 0.0417 mag, consistent with the survey result.

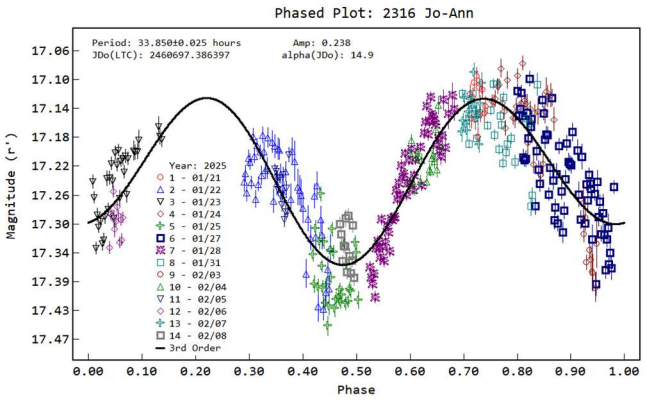

2719 Suzhou was discovered at Purple Mountain Observatory in 1965. It is named for the city of Suzhou, China. We found a period of 118.30 ± 0.04 hours with an amplitude of 1.129 ± 0.0383 mag. We found no prior rotation period reports.

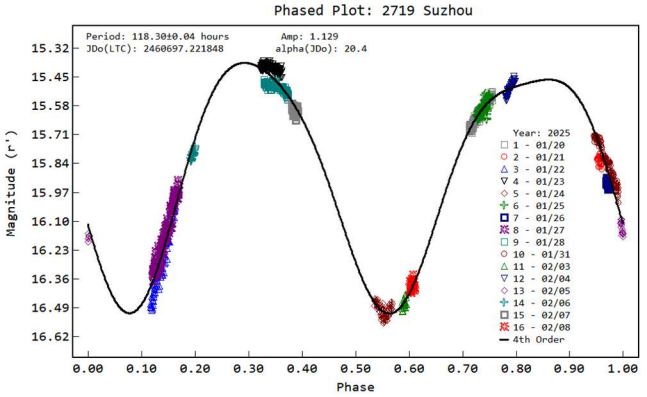

3368 Duncombe. Discovered in 1985 by Ted Bowell at Anderson Mesa, it is named in honor of Dr. Raynor Lockwood Duncombe (1917-2013), a former director of the U.S. Naval Observatory and professor at the University of Texas at Austin. We found a period of 34.030 ± 0.007 hours with an amplitude of 0.2513 ± 0.0249 mag. We found no prior rotation period reports.

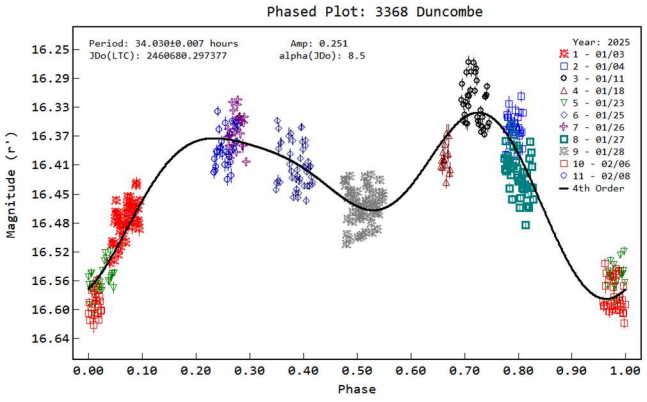

3909 Gladys. This member of the Eunomia family was discovered in 1988 by Kenneth Zeigler at Flagstaff. It is named after his mother, Gladys Marie Zeigler (1921-1988). We observed it on fourteen nights in 2025 February and March. We found two prior reports from Behrend (2006web) of 3.596 hours and from Angeli and Barucci (1996) of 6.83 hours. Analysis of our data resulted in a best fit of 25.48 ± 0.01 hours with an amplitude of 0.504 ± 0.05 mag, differing with the prior reports. Coverage is not complete so this result could be wrong.

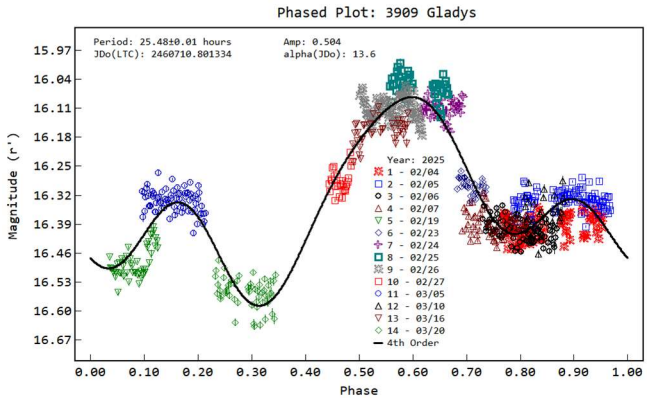

4099 Wiggins. This member of the Maria family was discovered in 1988 by H. Debehogne at ESO. It is named after Patrick Wiggins, a NASA/JPL Solar System Ambassador.

We found a prior report from Hawley et al. (2024) of 10.985 ± 0.001 9hours. Analysis of our data resulted in a best fit of 10.994 ± 0.006 hours with an amplitude of 0.1526 ± 0.0292 mag, close to but slightly longer than the report from Hawley.

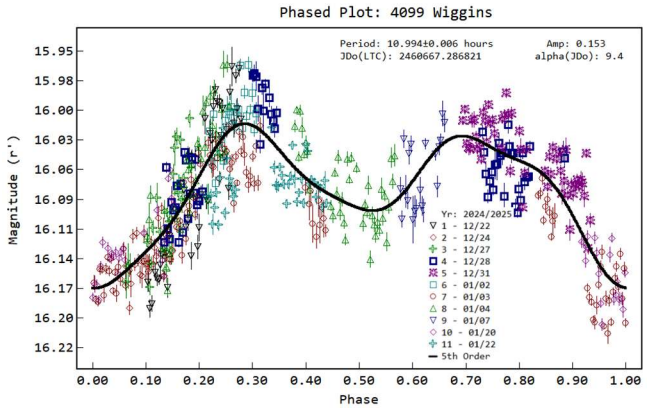

4350 Shibecha is a middle main-belt asteroid discovered in 1989 by Ueda and Kandeda at Kushiro. It is named after the city of Shibecha on the island of Hokkaido, Japan.

There is a prior survey report from Pál et al. (2020) of 2.88958 along with reports from Ferrero (2012) of 2.890 and Strabla et al. (2012) of 2.89. The LCDB quality score U was 2+. We found a period of 2.890 ± 0.004 hours with an amplitude of 0.10 ± 0.02 mag, in agreement with prior reports.

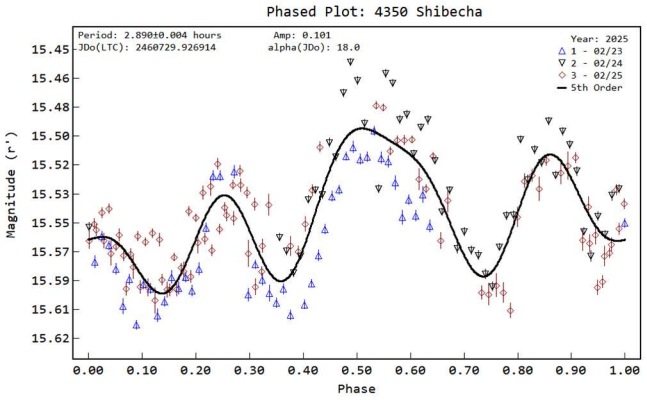

5424 Covington. This inner main-belt asteroid was discovered by Ted Bowell at Flagstaff in 1983. It is named after Arthur Edwin Covington, the first Canadian radio astronomer, who discovered that the sun emits large amounts of microwaves in the 10.7 cm wavelength. There was one prior report from Behrend (2006web) of 5.0 ± 0.6 hours with an ALCDEF quality score U of 2. We found 5.4595 ± 0.007 hours with an amplitude of 0.299 mag. Our data covers multiple cycles, so we consider this result secure.

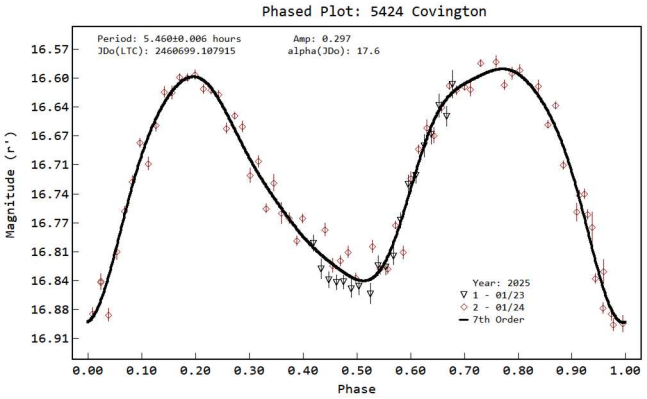

6950 Simonek is a member of the Eunomia family discovered in 1982 by F. Dossin at Haute Provence. It is named after Simone Ek, wife of the discover.

There are two prior survey reports from Waszczak et al. (2015) of 3.083 and Pál et al. (2020) of 3.29607. We found a period of 3.298 ± 0.002 hours with an amplitude of 0.106 ± 0.03 mag, in agreement with Pál.

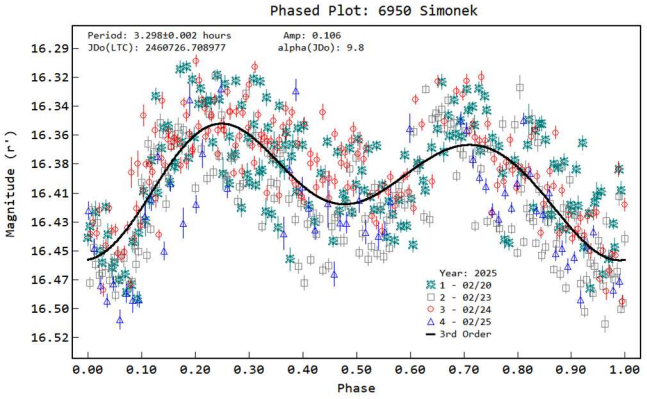

6735 Madhatter was discovered in 1992 by T. Urata at Nihondaira Observatory. It is named after the character in Lewis Carroll's *Alice's Adventures in Wonderland*. We found a period of 8.550 ± 0.004 hours with an amplitude of 0.136 ± 0.169 mag. We were unable to find any prior rotation period reports.

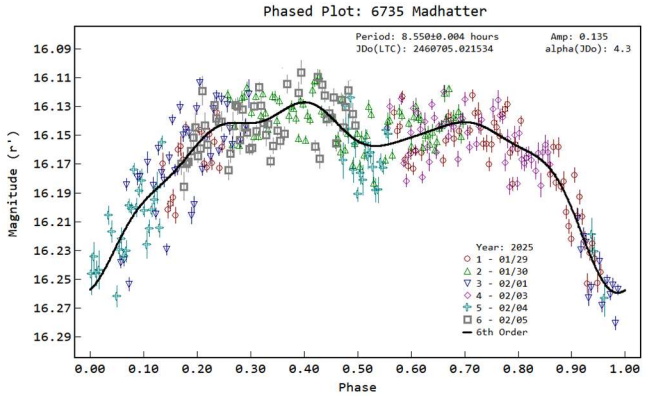

9010 Candelo. We found a period of 5.016 ± 0.001 hours with an amplitude of 0.112 ± 0.0278 for this inner main-belt asteroid. We found no prior rotation period reports.

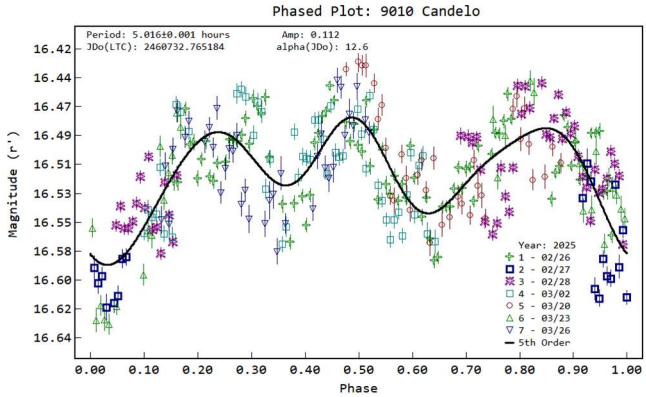

13352 Gyssens. Pál et al. (2020) reported 3.040 hours for this member of the Eunomia family. The LCDB quality score U was 2. We found 3.041 ± 0.001 hours with an amplitude of 0.196 ± 0.016 mag, in agreement with Pál.

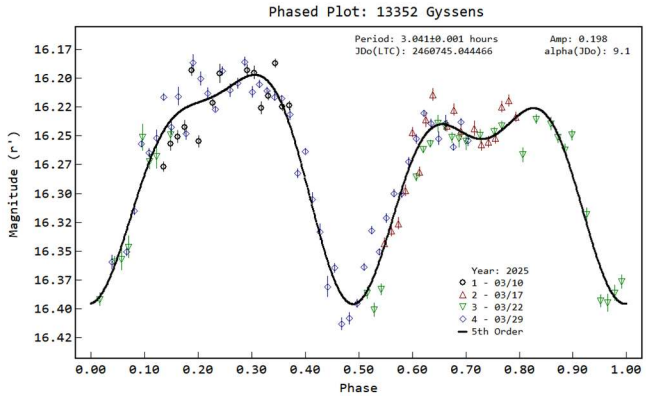

(13542) 1991 VC5 was discovered by Otomo at Kiyosata. We found a period of 52.807 ± 0.023 hours with an amplitude of 0.398 ± 0.0371 mag. We found no prior rotation period reports.

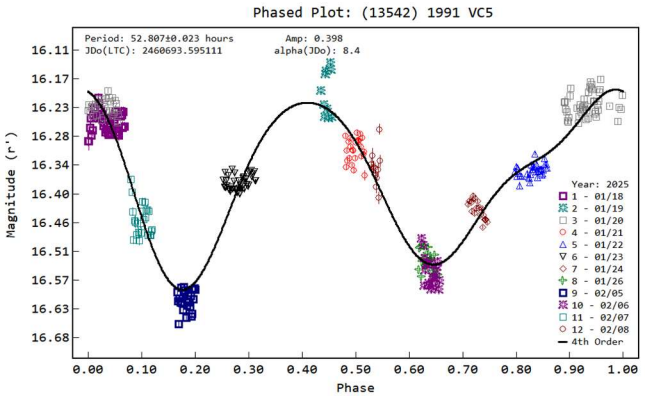

24863 Cheli was discovered in 1996 by d'Isonzo at Farra d'Isonzo. It is named for Italian astronaut Maurizio Cheli. We observed it on fifteen nights in 2024 December through 2025 February, finding a period of 16.716 ± 0.005 with an amplitude of 0.1646 ± 0.0393 mag. We found no prior rotation period reports.

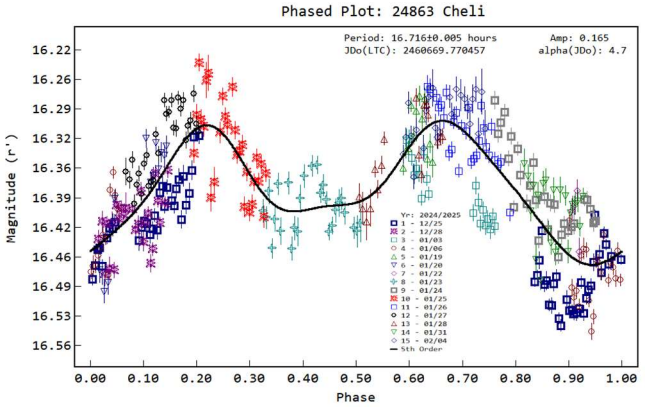

27736 Ekaterinburg. We found a period of 5.6036 ± 0.0011 hours with an amplitude of 0.552 ± 0.0342 mag. We found no prior rotation period reports.

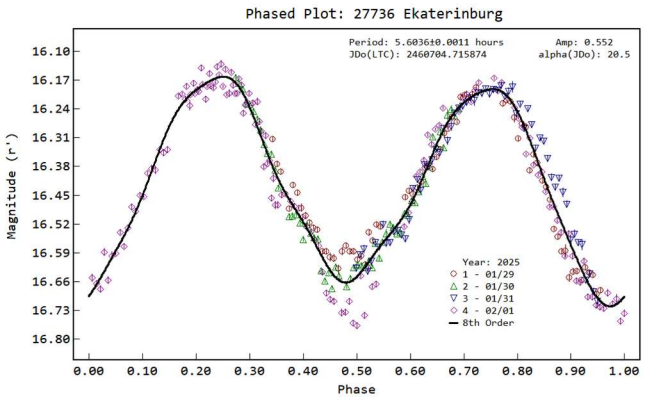

Acknowledgements

The author gratefully acknowledges the generosity of Dr. Richard Post for ongoing use of one of his domes to house one of the author's telescopes. This research made use of the *Python* language interpreter (van Rossum, 1995) along with the *Skyfield* (Rhodes, 2019), *astropy* (Astropy Collaboration, 2022), *astroplan* (Morris et al., 2018), *matplotlib* (Hunter, 2007), and *NumPy* (Harris et al., 2020) libraries. This research used data from the Asteroid Terrestrial-impact Last Alert System (ATLAS) project, funded through NASA grants NN12AR55G, 80NSSC18K0284, and 80NSSC18K1575. The ATLAS science products have been made possible through the contributions of the University of Hawaii Institute for Astronomy, the Queen's University Belfast, the Space Telescope Science Institute, and the South African Astronomical Observatory. Funding for PDS observations, analysis, and publication was provided by NASA grant NNX13AP56G. Work on the asteroid lightcurve database (LCDB) was funded in part by National Science Foundation grants AST-1210099 and AST-1507535. Data from the MPC's database is made freely available to the public. Funding for this data and the MPC's operations comes from a NASA PDCO grant (80NSSC22M0024), administered via a University of Maryland - SAO subaward (106075-Z6415201). The MPC's computing equipment is funded in part by the above award, and in part by funding from the Tamkin Foundation. This research used data found on the JPL Solar System Dynamics Website. The JPL Solar System Dynamic group's ephemeris development, maintenance, and improvement tests are part of NASA's Advanced Multi-Mission Operations System, which is funded by NASA's Science Mission Directorate, Planetary Science Division.

References

Angeli, C.A.; Barucci, M.A. (1996). "CCD observations: rotational properties of 13 small asteroids." *Planetary and Space Science* **44**(3), 181-186.

Astropy Collaboration (2022). "The Astropy Project: Sustaining and Growing a Community-oriented Open-source Project and the Latest Major Release (v5.0) of the Core Package." *The Astrophysical Journal* **935**(2), id. 167, 20pp.

Behrend, R. (2006web). Observatoire de Geneve web site. *http://obswww.unige.ch/~behrend/page_cou.html*

Chang, C.-K.; Ip, W.-H.; Lin, H.-W.; Cheng, Y.-C.; Ngeow, C.-C.; Yang, T.-C.; Waszczak, A.; Kulkarni, S.R.; Levitan, D.; Sesar, B.; Laher, R.; Surace, J.; Prince, T.A. (2014). "313 New Asteroid Rotation Periods from Palomar Transient Factory Observations." *The Astrophysical Journal* **788**(1), id. 17, 21.

Collins, K.; Kielkopf, J.; Stassun, K.; Hessmane, F. (2017). "AstroImageJ: Image Processing and Photometric Extraction for Ultra-Precise Astronomical Light Curves." *The Astronomical Journal* **153**(2), 13.

Denny, R. (2024). *ACP Expert* software, version 9.1. DC-3 Dreams. *https://acpx.dc3.com*

Dose, E.V. (2024). "Lightcurves of Eighteen Asteroids." *The Minor Planet Bulletin* **51**(1), 42-49.

Farfán, R.G.; Garcáa de la Cuesta, F.; Martínez, F.L.; Lorenz, E.R.; Albá, C. Botana; Casal, J.D.; De Elias Cantalapiedra, J.; Saura, A.M.; Mañanes, E.F.; Ribes, N.G.; Fernández, J.R.; Fernández, J.M.; Nogues, R.N.; Santos Álamo, F.M. (2024). "Analysis and Lightcurves of 22 Asteroids." *The Minor Planet Bulletin* **51**(3), 259-263.

Ferrero, A. (2012). "Lightcurve Photometry of Six Asteroids." *Minor Planet Bull*. **39**, 138-139.

George, D.; Sharratt, G.; Benson, E.; Browne, H.; Browne, P.; Creery, C.; Boltwood, P.; Mussar, R.; Waring, J.; Lawrence, O.; Robichaud, A. (2024). Maxim DL V6.50. *https://diffractionlimited.com/*

Giorgini, J.; Yeomans, D.; Chamberlin, A.; Chodas, P.; Jacobson, R.; Keesey, M.; Lieske, J.; Ostro, S.; Standish, E.; Wimberly, R. (1996). "JPL's On-Line Solar System Data Service." *Bulletin of the American Astronomical Society* **28**(3), 1158.

Harris, A.W.; Young, J.W.; Scaltriti, F.; Zappala, V. (1984). "Lightcurves and phase relations of the asteroids 82 Alkmene and 444 Gyptis." *Icarus* **57**, 251-258.

Harris, C.R.; Millman, K.J.; van der Walt, S.J.; Gommers, R.; Virtanen, P. and 21 colleagues (2020). "Array programming with NumPy." *Nature* **585**, 357-362.

Hawley, W.; Miles, R.; Wiggins, P.; McCormick, J.; Watkins, A.; Kardasis, E.; Pilcher, F.; Arnold, S. (2024). "Lightcurve and Rotation Period Analysis of 1887 Virton and 4099 Wiggins." *The Minor Planet Bulletin* **51**(2), 166-168.

Hunter, J.D. (2007) "Matplotlib: A 2D Graphics Environment." *Computing in Science & Engin*eering **9**(3), 90-95.

Marchini, A.; Papini, R. (2024). "Photometric Observations of Asteroids 1631 Kopff, 2244 Tesla, 2967 Vladisvyat and 9628 Sendaiotsuna." *Minor Planet Bull*. **5**1, 158-160.

Morris, B.; Tollerud, E.; Sipőcz, B.; Diel, C.; Douglas, S.; Moskovitz, N.; Wasserman, L.; Burt, B.; Schottland, R.; Bowell, E.; Bailen, M.; Granvik, M. (2022). "The astrob database at Lowell Observatory." *Astronomy and Comput*ing **41**, 19.

Moskovitz, N.; Wasserman, L.; Burt, B.; Schottland, R.; Bowell, E.; Bailen, M.; Granvik, M. (2022). "The astrob database at Lowell Observatory." *Astronomy and Comput*ing **41**, id. 100661.

Pál, A.; Sazkáta, R.; Kiss, C.; Bódi, A.; Bognár, Z.; Kalup, C.; Kiss, L.; Marton, G.; Molnár, L.; Plachy, E.; Sárneczky, K.; Szabó, G.; Szabó, R. "Solar System Objects Observed with TESS - First Data Release: Bright Main-belt and Trojan Asteroids from the Southern Survey." *The Astrophysical Journal Supplement Series* **247**(1), id. 26. 9pp. *axXiv:2001.05822*

Parrott, D. (2020). "Tycho Tracker: A New Tool to Facilitate the Discovery and Recovery of Asteroids Using Synthetic Tracking and Modern GPU Hardware." *The Journal of the American Association of Variable Star Observers* **48**(2), 262. *http://www.tycho-tracker.com*

Polakis, T. (2024). "Photometric Results for Twenty Minor Planets." The Minor Planet Bull. **51**, 126-132.

Rhodes, B. (2019). Skyfield: High precision research-grade positions for planets and Earth satellites generator, *Astrophysics Source Code Library*, record ascl: 1907.024, July 2019 *http://rhodesmill.org/skyfield*

Strabla, L.; Quadri, U.; Girelli, R. (2012). "Lightcurve Analysis for Eight Minor Planets at Bassan Bresciano Observatory." *Minor Planet Bull*. **39**, 177-179.

Tonry, J.; Denneau, L.; Flewelling, H.; Heinze, A.; Onken, C.; Smartt, S.; Stalder, B.; Weiland, H.; Wolf, C. (2018). "The ATLAS All-Sky Stellar Reference Catalog." *The Astrophysical Journal* **867**(2), id. 105, 16.

van Rossum, G. (1995). Python tutorial, technical report CS-R9526, *Centrum voor Wiskunde en Informatica (CWI)*, Amsterdam, May 1995. *http://www.python.org*

Warner, B.D.; Harris, A.W.; Pravec, P. (2009). "The asteroid lightcurve database." *Icarus* **202**, 134-146. Updated 2023 April 24. *https://www.alcdef.org*

Warner, B.D. (2020). MPO Canopus Software. Canopus version 10.8.4.1. Bdw Publishing. *https://minplanobs.org/bdwpub/php/displayhome.php*

Waszczak, A.; Chang, C.-K.; Ofek, E.O.; Laher, R.; Masci, F.; Levitan, D.; Surace, J.; Cheng, Y.-C.; Ip, W.-H.; Kinoshita, D.; Helou, G.; Prince, T.A.; Kulkarni, S. (2015). "Asteroid Light Curves from the Palomar Transient Factory Survey: Rotation Periods and Phase Functions from Sparse Photometry." *Astron. J.* **150**, A75.

COLLABORATIVE ASTEROID PHOTOMETRY FROM UAI: 2025 JANUARY - MARCH

Lorenzo Franco
Balzaretto Observatory (A81), Rome, ITALY
lor_franco@libero.it

Alessandro Marchini, Riccardo Papini
Astronomical Observatory, University of Siena (K54)
Via Roma 56, 53100 - Siena, ITALY

Gianni Galli
GiaGa Observatory (203), Pogliano Milanese, ITALY

Giulio Scarfi
Iota Scorpii Observatory (K78), La Spezia, ITALY

Nico Montigiani, Massimiliano Mannucci
Osservatorio Astronomico Margherita Hack (A57)
Lastra a Signa, ITALY

Luca Buzzi
Schiaparelli Observatory (204), Varese, ITALY

Paolo Bacci, Martina Maestripieri
GAMP - San Marcello Pistoiese (104), Pistoia, ITALY

Marco Iozzi
HOB Astronomical Observatory (L63)
Capraia Fiorentina, ITALY

Nello Ruocco
Osservatorio Astronomico Nastro Verde (C82), Sorrento, ITALY

Matteo Lombardo
Zen Observatory (M26), Scandicci, ITALY

Giorgio Baj
M57 Observatory (K38), Saltrio, ITALY

Luciano Tinelli
GAV (Gruppo Astrofili Villasanta), Villasanta, ITALY

(Received: 2025 April 14)

Photometric observations of seven asteroids were made in order to acquire lightcurves for shape/spin axis modeling. Lightcurves were acquired for 862 Franzia, 1318 Nerina, 1342 Brabantia, 4133 Heureka, 6239 Minos, (137126) 1999 CF9, and (137805) 1999 YK5.

Collaborative asteroid photometry was done inside the Italian Amateur Astronomers Union (UAI, 2024) group. The targets were selected mainly in order to acquire lightcurves for shape/spin axis modeling. Table I shows the observing circumstances and results.

The CCD observations were made in 2025 January-March using the instrumentation described in the Table II. Lightcurve analysis was performed at the Balzaretto Observatory with *MPO Canopus* (Warner, 2023). All the images were calibrated with dark and flat frames and converted to standard magnitudes using solar colored field stars from CMC15 and ATLAS catalogues, distributed with *MPO Canopus*. For brevity, "LCDB" is a reference to the asteroid lightcurve database (Warner et al., 2009).

862 Franzia is a S-type (Bus and Binzel, 2002) middle main-belt asteroid. Collaborative observations were made over nine nights. The period analysis shows a synodic period of $P = 7.522 \pm 0.001$ h with an amplitude $A = 0.14 \pm 0.03$ mag, close to the previously published results in the LCDB. For the H-G parameters, the half peak-to-peak R band magnitude of each session has been evaluated and converted to V band, using the color index found by Franco et al. (2024; 0.46 ± 0.01). We found $H = 10.09 \pm 0.05$ and $G = 0.37 \pm 0.08$.

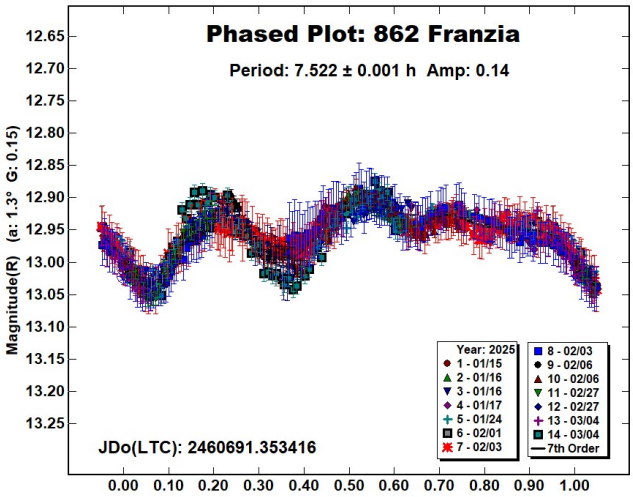

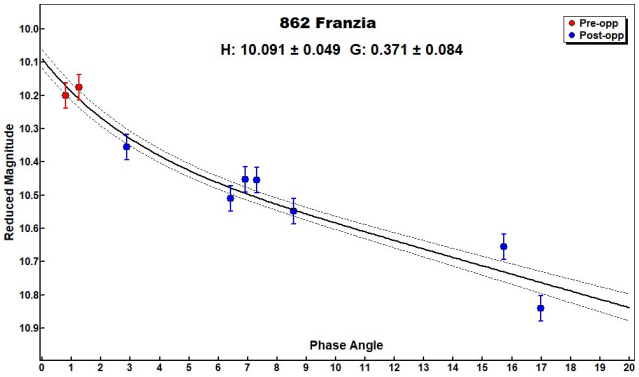

1318 Nerina is a medium albedo inner main-belt asteroid. Collaborative observations were made over seven nights. The period analysis shows a synodic period of $P = 2.5276 \pm 0.0001$ h with an amplitude $A = 0.08 \pm 0.03$ mag.

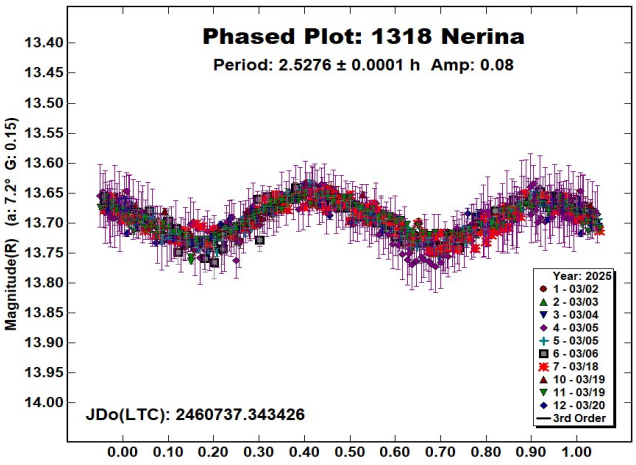

The period is close to the previously published results in the LCDB. Multiband photometry, obtained by N. Montigiani and M.

Mannucci (A57) on 2025 March 19, shows color indices B-V = 0.67 ± 0.04; V-R = 0.41 ± 0.04, both close to a M-type asteroid (Shevchenko and Lupishko, 1998; 0.72 ± 0.09; 0.42 ± 0.04).

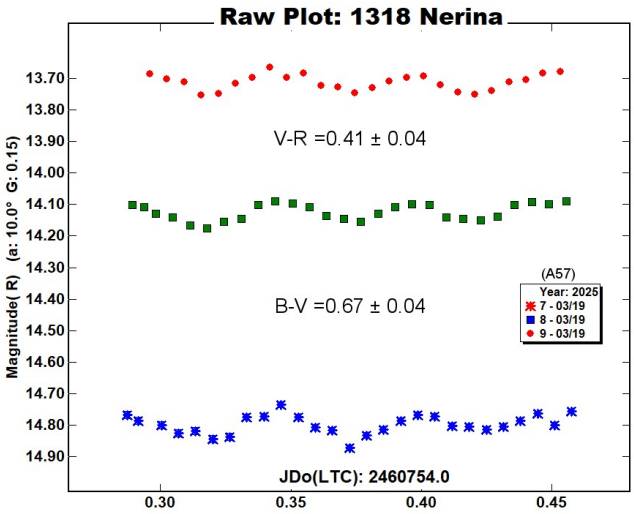

1342 Brabantia is a X-type (Tholen, 1984) inner main-belt asteroid. Collaborative observations were made over six nights. The period analysis shows a synodic period of P = 4.1750 ± 0.0002 h with an amplitude A = 0.18 ± 0.02 mag. The period is close to the previously published results in the LCDB.

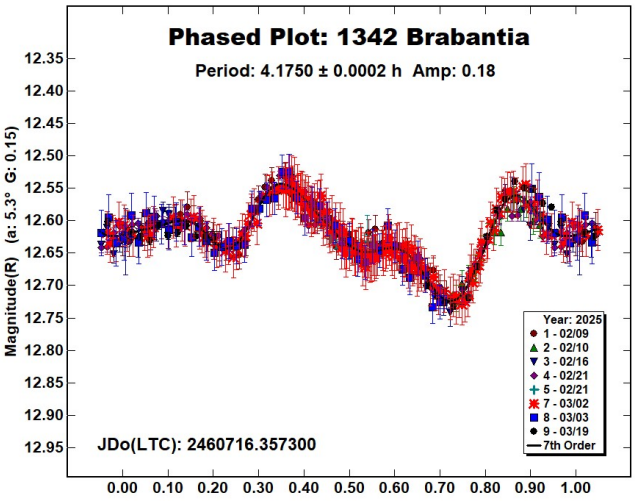

4133 Heureka is a medium-albedo middle main-belt asteroid. Collaborative observations were made over four nights. The split halves plot shows almost identical halves; we prefer the quadrimodal solution with P = 3.730 ± 0.001 h and an amplitude A = 0.13 ± 0.03 mag, below the spin barrier of 2.2 hours. This solution is close to Chelius (2023; 3.726 h ± 0.001). Multiband photometry was acquired by P. Bacci and M. Maestripieri (104), and by N.Montigiani and M. Mannucci (A57) on 2025 February 15, respectively in the V, R and B, V, R bands. We found the color indices B-V = 0.82 ± 0.07; V-R = 0.48 ± 0.05. This last is the result of averaging the two independent values. Both color indices are close to a S-type asteroid (Shevchenko and Lupishko, 1998; 0.86 ± 0.04; 0.49 ± 0.05).

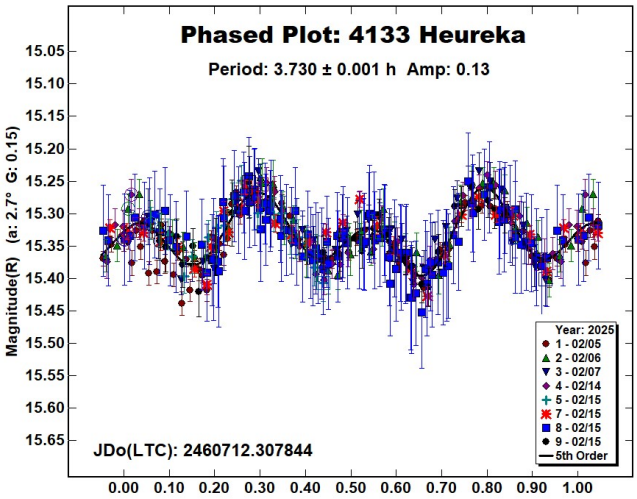

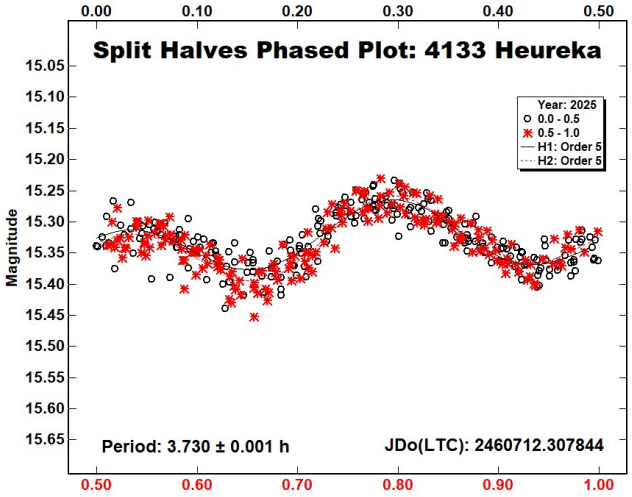

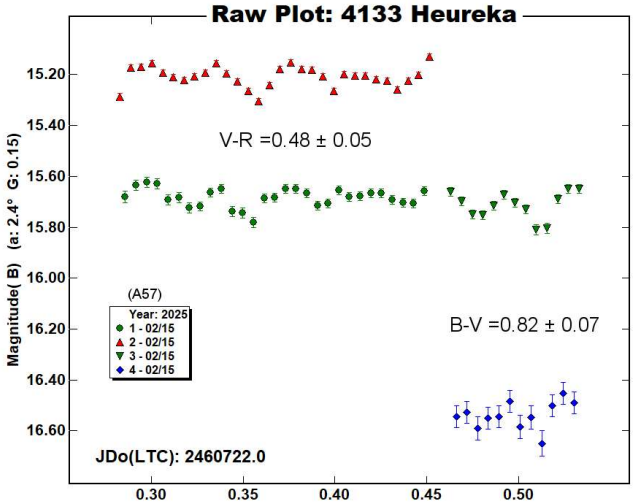

6239 Minos is an Apollo Near-Earth asteroid, classified as a Potentially Hazardous Asteroid (PHA). Observations by L. Buzzi were made over one night at the Schiaparelli Observatory (204). We found a synodic period of P = 3.55 ± 0.02 h and an amplitude A = 0.09 ± 0.03 mag. The period is close to the previously published results in the LCDB.

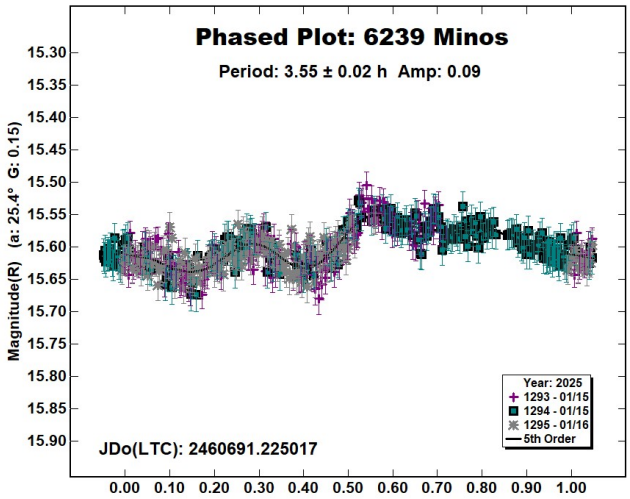

(137126) 1999 CF9 is an Apollo Near-Earth asteroid, classified as a Potentially Hazardous Asteroid (PHA). Collaborative observations were made over three nights. We found a bimodal solution with a synodic period of $P = 6.67 \pm 0.01$ h and an amplitude $A = 0.96 \pm 0.04$ mag. No others periods were found in the LCDB.

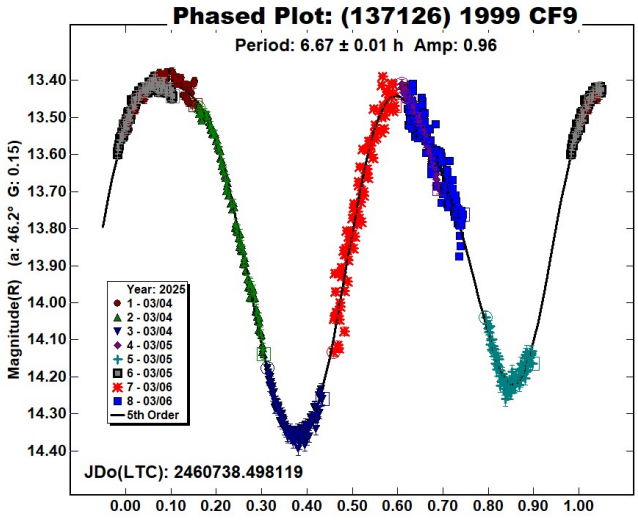

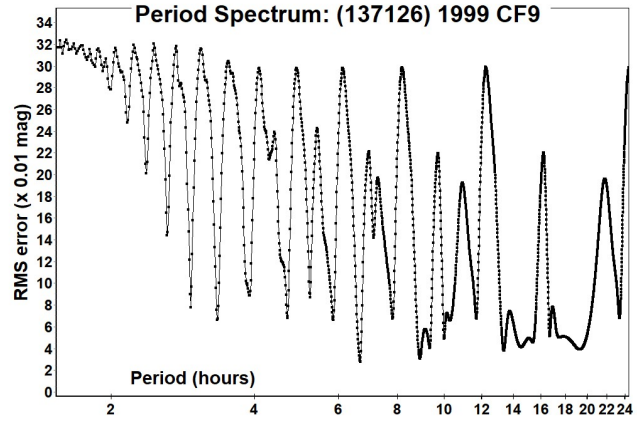

(137805) 1999 YK5 is an Aten Near-Earth asteroid. Observations by L. Buzzi were made over two nights at the Schiaparelli Observatory (204). We found a quadrimodal solution with a synodic period of $P = 6.91 \pm 0.1$ h and an amplitude $A = 0.21 \pm 0.07$ mag. This period is almost double compared to the previously published results in the LCDB.

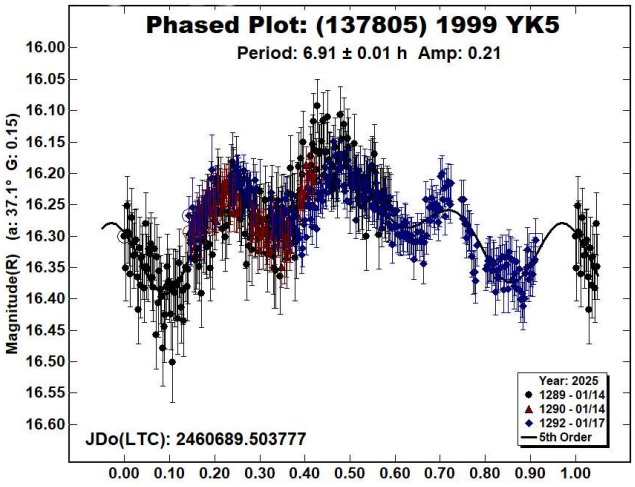

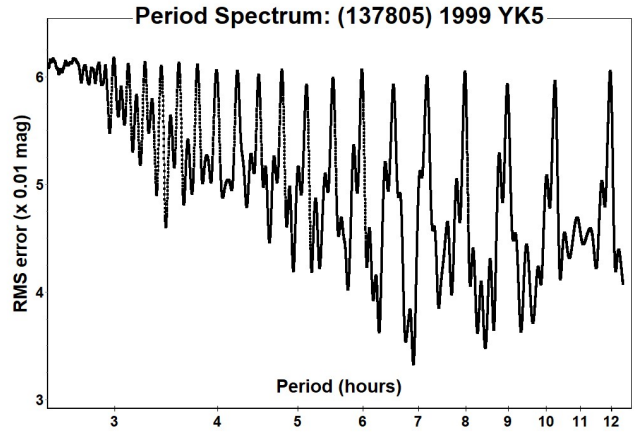

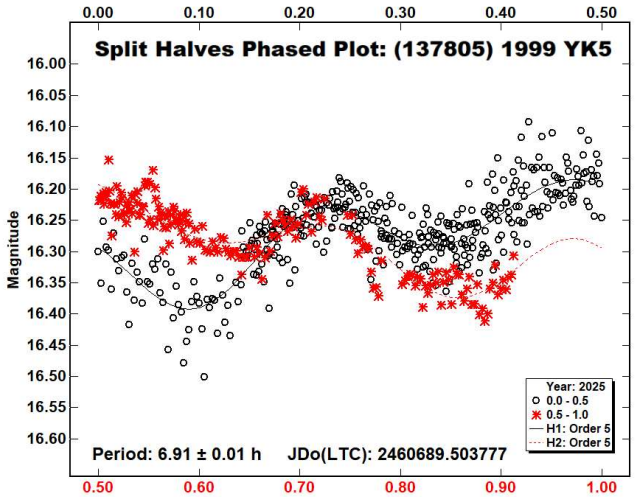

Number	Name	2025 mm/dd	Phase	L_{PAB}	B_{PAB}	Period(h)	P.E.	Amp	A.E.	Grp
862	Franzia	01/15-03/04	*1.2,16.9	118	-1	7.522	0.001	0.14	0.03	MB-M
1318	Nerina	03/02-03/20	*7.2,10.5	166	7	2.5276	0.0001	0.08	0.03	MB-I
1342	Brabantia	02/09-03/19	*5.2,22.2	146	-10	4.1750	0.0002	0.18	0.02	MB-I
4133	Heureka	02/05-02/15	*2.7,2.5	142	1	3.730	0.001	0.13	0.03	MB-M
6239	Minos	01/15-01/15	25.3,25.9	105	13	3.55	0.02	0.09	0.03	NEA
137126	1999 CF9	03/04-03/06	46.1,62.0	192	10	6.67	0.01	0.96	0.04	NEA
137805	1999 YK5	01/14-01/17	37.1,37.7	111	33	6.91	0.01	0.21	0.07	NEA

Table I. Observing circumstances and results. The first line gives the results for the primary of a binary system. The second line gives the orbital period of the satellite and the maximum attenuation. The phase angle is given for the first and last date. If preceded by an asterisk, the phase angle reached an extrema during the period. L_{PAB} and B_{PAB} are the approximate phase angle bisector longitude/latitude at mid-date range (see Harris et al., 1984). Grp is the asteroid family/group (Warner et al., 2009).

Observatory (MPC code)	Telescope	CCD	Filters	Observed Asteroids (#Sessions)
Astronomical Observatory, University of Siena (K54)	0.30-m MCT f/5.6	SBIG STL-6303e (bin 2×2)	Rc,C	862(3), 1318(1), 1342(3), 4133(1)
GiaGa Observatory (203)	0.36-m SCT f/5.8	Moravian G2-3200	Rc,C	862(3), 1318(2), 4133(1)
Iota Scorpii(K78)	0.40-m RCT f/6.1	CMOS QHY 268 (bin 4x4)	Rc	862(2), 1318(1), 1342(1), 4133(1)
Osservatorio Astronomico Margherita Hack (A57)	0.35-m SCT f/8.3	SBIG ST10XME (bin 2x2)	B,V,Rc	1318(2), 4133(2)
Schiaparelli Observatory (204)	0.84-m NRT f/3.5	Moravian C3-61000 PRO (bin 4×4)	C	6239(1), 137805(3)
San Marcello Pistoiese Observatory (104)	0.60-m NRT f/4.0	Apogee Alta	V,Rc,C	4133(1), 137126(2)
HOB Astronomical Observatory (L63)	0.20-m SCT f/6.0	ATIK 383L+ (bin 2x2)	C	1318(1), 1342(1)
Osservatorio Astronomico Nastro Verde (C82)	0.35-m SCT f/6.3	SBIG ST10XME (bin 2x2)	C	1318(2)
Zen Observatory (M26)	0.30-m RCT f/7.4	ATIK 383L+ (bin 2x2)	C	137126(1)
M57 (K38)	0.35-m RCT f/5.5	SBIG STT1603ME	Rc	862(1)
GAV	0-20-m SCT f/6.3	QSI683 (bin 2x2)	Rc	1342(1)

Table II. Observing Instrumentations. MCT: Maksutov-Cassegrain, NRT: Newtonian Reflector, RCT: Ritchey-Chretien, SCT: Schmidt-Cassegrain.

References

Bus S.J.; Binzel, R.P. (2002). "Phase II of the Small Main-Belt Asteroid Spectroscopic Survey - A Feature-Based Taxonomy." *Icarus* **158**, 146-177.

Chelius, T. (2023). "Lightcurve Analysis of Three Asteroids." *Minor Planet Bulletin* **50**, 41-42.

Franco, L.; Scarfi, G.; Baj, G.; Iozzi, M.; Lombardo, M.; Marchini, A.; Papini, R.; Falco, C.; Nastasi, A.; Fini, P.; Betti, G.; Arangio, J.; Bacci, P.; Maestripieri, M.; Montigiani, N.; Mannucci, M.; Coffano, A.; Marinello, W.; Aceti, P.; Banfi, M. (2024). "Collaborative Asteroid Photometry from UAI: 2023 July - September." *Minor Planet Bulletin* **51**, 56-61.

Harris, A.W.; Young, J.W.; Scaltriti, F.; Zappala, V. (1984). "Lightcurves and phase relations of the asteroids 82 Alkmene and 444 Gyptis." *Icarus* **57**, 251-258.

Shevchenko, V.G.; Lupishko, D.F. (1998). "Optical properties of Asteroids from Photometric Data." *Solar System Research* **32**, 220-232.

Tholen, D.J. (1984). "Asteroid taxonomy from cluster analysis of Photometry." Doctoral Thesis. University Arizona, Tucson.

UAI (2024). "Unione Astrofili Italiani" web site. *https://www.uai.it*

Warner, B.D.; Harris, A.W.; Pravec, P. (2009) "The asteroid lightcurve database." *Icarus* **202**, 134-146. Updated 2025 April 8. *https://minplanobs.org/alcdef/index.php*

Warner, B.D. (2023). MPO Software. MPO Canopus v10.8.6.20. Bdw Publishing. *http://minorplanetobserver.com*

SYNODIC ROTATION PERIODS AND LIGHTCURVES FOR 26 ASTEROIDS FROM SOPOT ASTRONOMICAL OBSERVATORY: 2024 OCTOBER – 2025 MARCH

Vladimir Benishek
Belgrade Astronomical Observatory
Volgina 7, 11060 Belgrade 38, SERBIA
vlaben@yahoo.com

(Received: 2025 April 14)

Synodic rotation periods and lightcurves established for 26 asteroids observed at the Sopot Astronomical Observatory in the time span 2024 October - 2025 March are summarized in this paper.

Photometric observations of 26 asteroids were conducted at Sopot Astronomical Observatory (SAO) from 2024 October through 2025 March in order to determine the asteroids' synodic rotation periods. For this purpose, two 0.35-m *f*/6.3 Meade LX200GPS Schmidt-Cassegrain telescopes were employed. The telescopes are equipped with a SBIG ST-8 XME and a SBIG ST-10 XME CCD cameras. The exposures were unfiltered and unguided for all targets. Both cameras were operated in 2×2 binning mode, which produces image scales of 1.66 arcsec/pixel and 1.25 arcsec/pixel for ST-8 XME and ST-10 XME cameras, respectively. Prior to measurements, all images were corrected using dark and flat field frames.

Photometric reduction was conducted using *MPO Canopus* (Warner, 2018). Differential photometry with up to five comparison stars of near solar color ($0.5 \leq$ B-V ≤ 0.9) was performed using the Comparison Star Selector (CSS) utility. This helped ensure a satisfactory quality level of night-to-night zero-point calibrations and correlation of the measurements within the standard magnitude framework. Field comparison stars were calibrated using standard Cousins R magnitudes derived from the Carlsberg Meridian Catalog 15 (VizieR, 2024) Sloan r' magnitudes using the formula: R = r' - 0.22 in all cases presented in this paper. In some instances, small zero-point adjustments were necessary in order to achieve the best match between individual data sets in terms of achieving the most favorable statistical indicators of Fourier fit goodness.

Lightcurve construction and period analysis was performed using *Perfindia* custom-made software developed in the R statistical programming language (R Core Team, 2024) by the author of this paper. The essence of its algorithm is reflected in finding the most favorable solution for rotational period by minimizing the *residual standard error* of the lightcurve Fourier fit.

In summary, it represents a sequence of the following numerical and statistical procedures applied over a combined photometric dataset covering a range of solar phase angles for which the rotational lightcurve does not undergo significant shape changes:

The original data are prepared by applying appropriate light-time and apparent magnitude corrections to compensate for the effects of finite velocity light propagation and changes of apparent magnitude due to the asteroid's solar phase angle change over the course of observations.

The light-time correction values (τ) are subtracted from the initial observation times in Julian days:

$$\tau = 0.0057755183\,\Delta \qquad (1)$$

Δ is the geocentric distance of a target in astronomical units.

For magnitude corrections (Δm) to achieve better initial alignment of individual data sets from different nights along the intensity axis, the formula given in Zeigler and Hanshaw (2016) is applied:

$$\Delta m = -2.5\ log\ \frac{\Delta_i^2\, r_i^2}{\Delta_0^2\, r_0^2} \qquad (2)$$

where Δ_i and Δ_o, r_i and r_0 are the mean geocentric and heliocentric distances of a target on the i-th night and the initial night of observation, respectively.

The linear regression method incorporated in the R programming language is applied upon the data previously prepared in the above-described manner to fit the entire series of Fourier models represented by equation (3) for different rotation period guesses over a user-selected interval [P_0, P_0 + k ΔP] and with a predefined step (resolution) ΔP and a predefined number of steps (k) for the inital value of a period P_0.

$$m(\varphi) = m_0 + \sum_{n=1}^{l}(a_n \cos\ n\varphi + b_n \sin\ n\varphi) + \epsilon \qquad (3)$$

Here, φ is the rotational phase, defined as follows:

$$\varphi = 2\pi\left[\frac{t-t_0}{P_i} - Int\left(\frac{t-t_0}{P_i}\right)\right] \qquad (4)$$

t is the time of individual observation, t_0 is the time of the first observation in the combined data set, P_i is one of rotational period guesses from a predefined interval of period values representing an individual Fourier model. m_0 in (3) is the mean apparent magnitude corresponding to the solar phase angle of the initial observation. a_n and b_n are the Fourier coefficients of the n-th order. Setting the maximum value of the Fourier order ($n = l$) in (3) is not limited by the program, but in practice it is most often not the case to take values greater than 15.

ϵ is an error term independent of the sine and cosine terms, representing some random error of the model.

One of the common ways to determine the regression model random error dispersion in the R statistical programming language is to calculate ***residual standard error (RSE)*** as a measure of the standard deviation of the residuals ϵ.

The regression model residual standard error is calculated according to the following formula:

$$RSE = \sqrt{\frac{RSS}{RDF}} = \sqrt{\frac{\sum_i (m_i - m_{pred.})^2}{n-k-1}} \qquad (5)$$

where the *RSS* is the *residual sum of squares* or *deviance*, which represents the sum of the squares of the vertical deviations of the magnitudes of the individual data points (m_i) from the values predicted by the Fourier fit ($m_{pred.}$), and *RDF* (*residual degrees of freedom*) is calculated as n-k-1, where n is total number of observations and k is the total number of model parameters that corresponds to the total number of Fourier coefficients a_n and b_n in (3).

The *Perfindia* algorithm aims to find the value of a period ***P*** in the above-mentioned user-preset period range that corresponds to the model with minimal RSE, generating a whole series of models (3) associated with their corresponding periods P_i for which the inherent RSEs are determined. In other words, a period spectrum is generated (i.e. dependence of the RSE on the period) from which a period with the *minimum* RSE value is extracted. The model with minimum RSE should correspond to the best Fourier fit

representation of the rotational lightcurve in a predefined period range, and the corresponding period extracted from the entire set of values should represent the most plausible synodic rotation period value in the given period range.

Subsequent refinement of the obtained period (model) is certainly possible by iteratively searching an increasingly narrow range around the initially found period value by reducing the "scanning" steps ΔP. The program also has the ability to gradually automatically vertically shift each individual data set of choice in a narrow interval around the most favorable period value until the lowest ultimate RSE is found.

The lightcurve plots presented in this paper show so-called 2% error for rotational periods, i.e. an error that would cause the last data point in a combined data set by date order to be shifted by 2% (Warner, 2012a) and represented by the following formula:

$$\Delta P = \frac{0.02 \cdot T}{P^2} \qquad (6)$$

where P and T are the rotational period and the total time span of observations, respectively. Both of these quantities must be expressed in the same units.

Table I gives the observing circumstances and results.

Observations and results

1205 Ebella. A search of the Asteroid Lightcurve Database records (LCDB; Warner et al., 2009) shows no previous rotation period determination results for this asteroid. Photometric observations carried out in 2024 October over 6 nights indicate a bimodal lightcurve with a period of $P = 3.0019 \pm 0.0007$ h as the statistically most favorable solution.

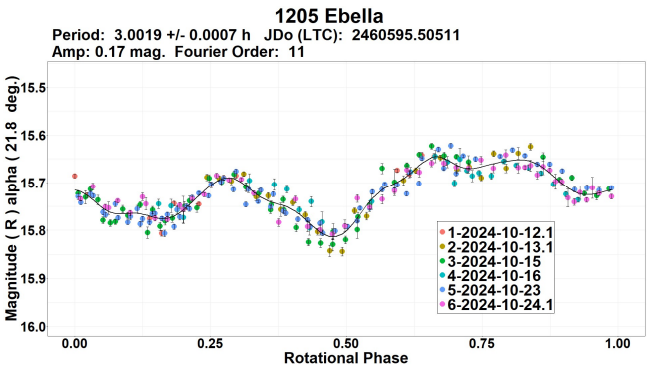

2738 Viracocha. Stone (2024) finds 2.639 h for the rotational period. A bimodal period solution ($P = 2.6391 \pm 0.0004$ h) obtained from SAO observations in 2025 March is quite identical to the only previously found result.

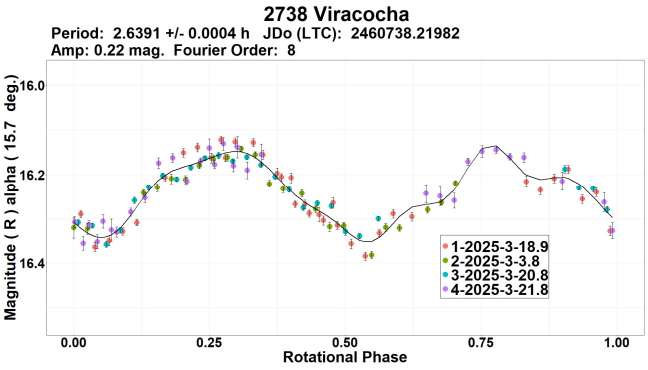

3486 Fulchignoni. Rotation period of $P = 2.8076 \pm 0.0003$ h, found from the SAO data obtained in 2024 October on 4 nights matches well with the only previously determined rotation period result by Erasmus et al. (2020) of 2.808 h.

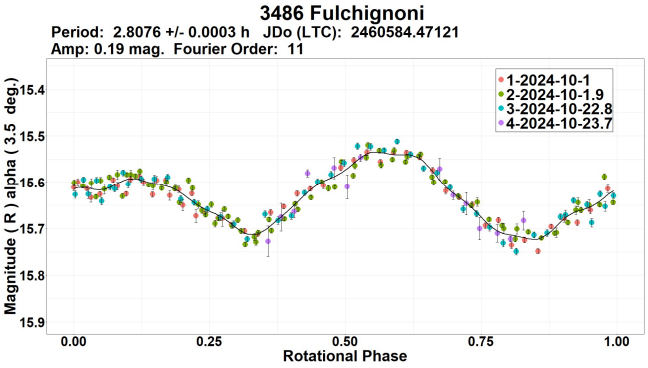

3583 Burdett. No previous rotation period determinations are known for this asteroid. Observations conducted over 5 nights in 2024 October-November indicate a bimodal rotational period of $P = 2.7191 \pm 0.0004$ h.

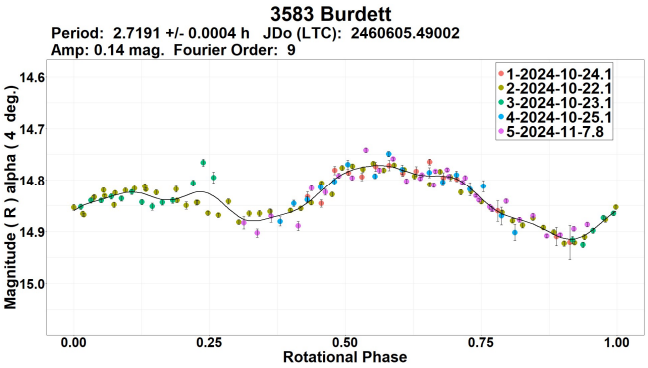

4031 Mueller. A period of $P = 2.944 \pm 0.006$ h, obtained from a dense combined photometric dataset acquired over two consecutive nights in 2024 November is in excellent agreement with virtually all previously reported rotation period determinations listed in the LCDB, some of which are as follows: 2.9420 h (Warner, 2009), 2.944 h (Warner, 2012b), 2.942 h (Warner, 2017), 2.940 h (Behrend, 2020web), 2.9413 h (Behrend, 2023web).

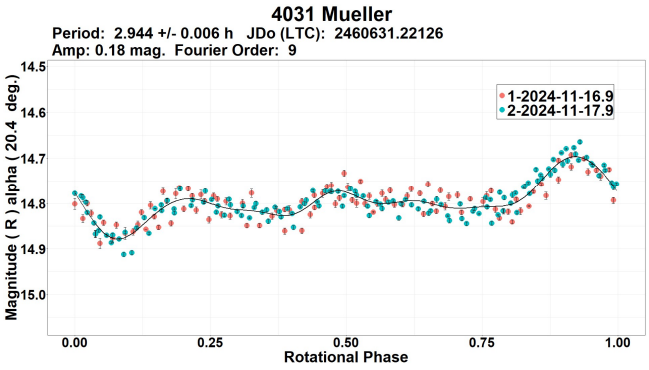

4133 Heureka. The obtained period result of P = 3.7295 ± 0.0008 h is very close to the only previously reported period of 3.726 h by Chelius (2023).

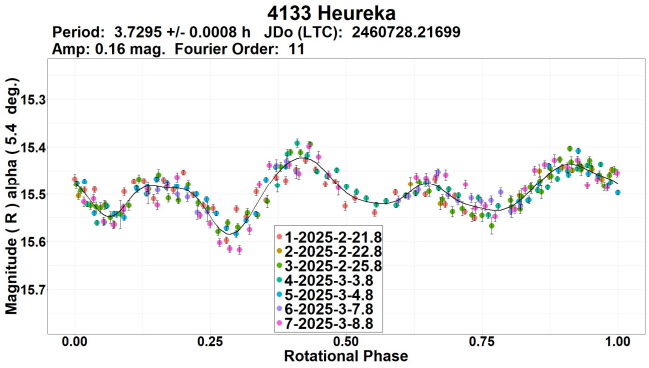

4159 Freeman. In this case as well, observations made at SAO on 3 consecutive nights in 2024 November led to a result (P = 4.399 ± 0.009 h) that is in line with virtually all previously reported values listed in the LCDB: Ditteon et al. (2004, 4.4021 h), Behrend (2009web, 4.405 h), Waszczak et al. (2015, 4.399 h and 4.403 h), Behrend (2022web, 4.393 h).

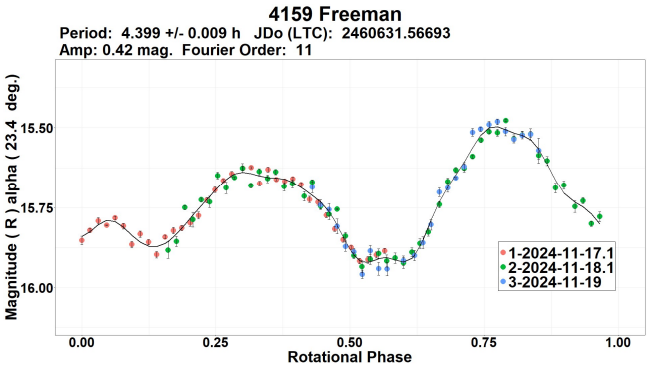

4225 Hobart. Dense photometric data collected at SAO over 3 nights in 2024 October show statistically unambiguous bimodal solution for period of P = 2.7737 ± 0.0006 h. There is no indication of any deviations in the lightcurve indirectly noted by Behrend (2023web) on the "Observatoire de Geneve" website, which states the triple period shown here (8.320152 h), with the comment that rotational cycles do not repeat identically, which may indicate some deviations present in the lightcurve.

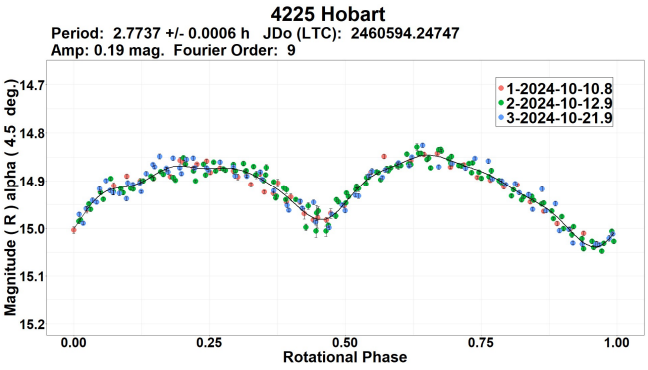

4706 Dennisreuter. Analysis of dense photometric data obtained on 9 nights shows an unequivocal rotation period of P = 2.4599 ± 0.0002 h, different from the previous results presented in the LCDB, among which the closest is the one obtained by Waszczak et al. (2015) of 2.578 h.

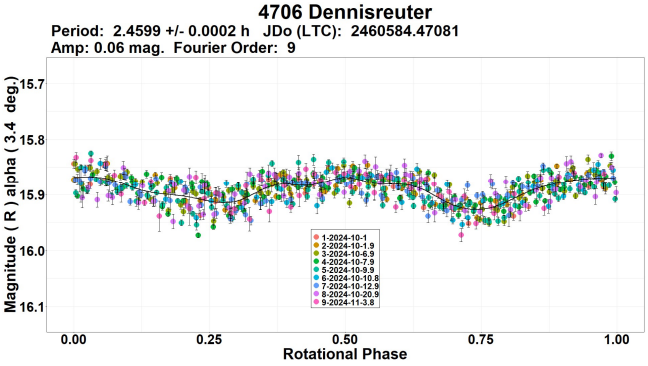

4789 Sprattia. Observations on 3 nights in 2024 October-November show a bimodal rotation period result of P = 3.1341 ± 0.0009 h, statistically identical to the only previously obtained result by Waszczak et al. (2015) of 3.136 h, which is in very good agreement with the result presented here.

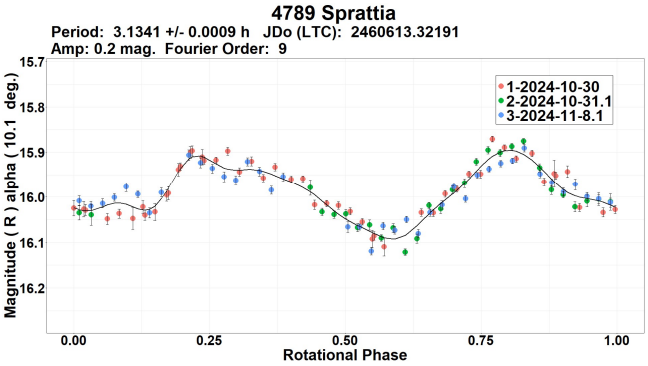

5491 Kaulbach. According to the LCDB records, this is another asteroid with no previously known rotation period. Combined dense photometric data obtained over 4 nights in 2024 late October - early November yielded an unambiguous period solution of P = 2.7777 ± 0.0008 h.

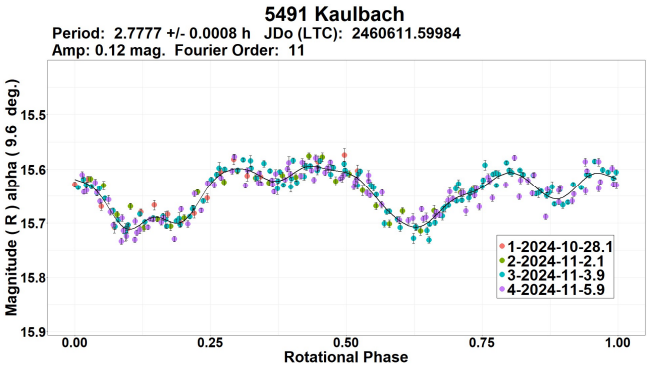

5668 Foucault. The found period value (P = 2.5739 ± 0.0002 h) is quite close to the only previously reported one of 2.5540 h (Pravec, 2018web).

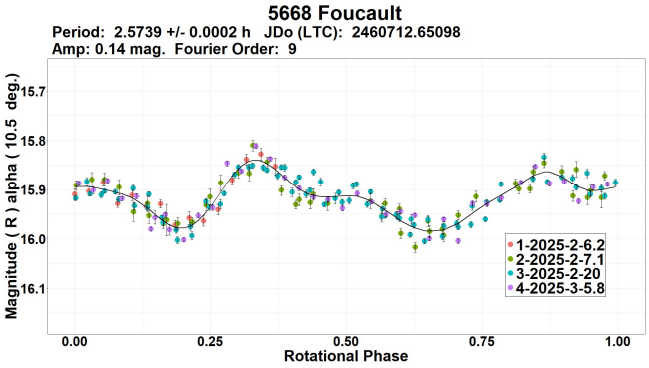

5802 Casteldelpiano. The 2025 February - March data show a low-amplitude bimodal lightcurve phased to a period of P = 2.9708 ± 0.0004 h as the most favorable unequivocal solution, which is highly consistent with the values present in the LCDB: 2.971 h (Waszczak et al., 2015), 2.9705 h (Pravec, 2018web), and 2.971 h (Dose, 2021).

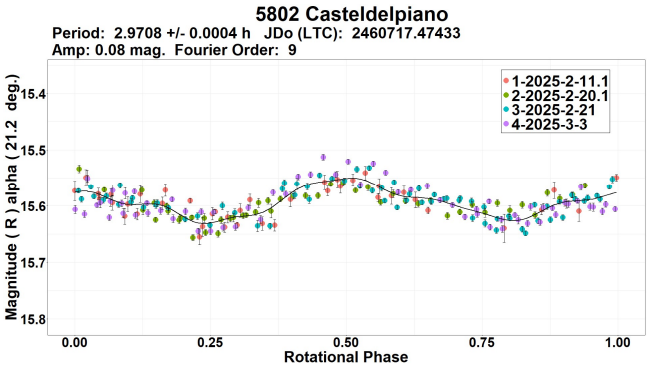

6171 Uttorp. No prior rotation period determinations were found for this asteroid. Observations over 5 nights in 2024 October - November show a bimodal lightcurve with a period of P = 3.687 ± 0.003 h as the most favorable solution resulting from the period analysis.

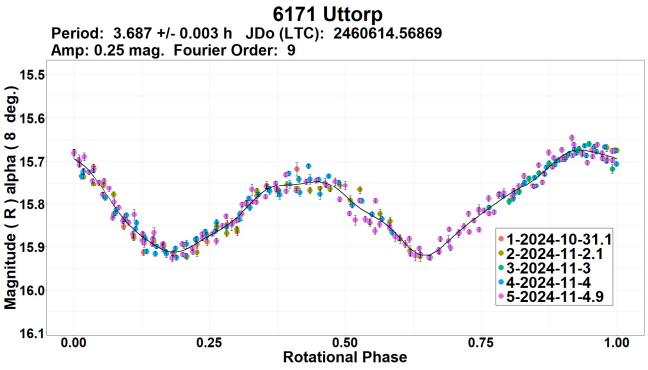

6243 Yoder. Previous reports on rotation period determinations are not known in this case as well. Three nights of observations in 2025 February-March yielded a bimodal lightcurve of relatively large amplitude (0.24 mag.) at low solar phase angles with a period of P = 2.9526 ± 0.0007 h.

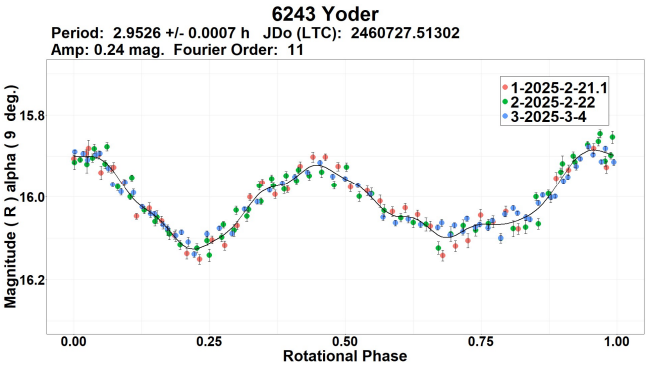

(6348) 1995 CH1. A dense photometric dataset from 3 nights in 2024 October - November shows a period of P = 3.083 ± 0.001 h, which is in a good agreement with two previously found values of 3.09 h (Chang et al., 2015) and 3.085 h (Waszczak et al., 2015).

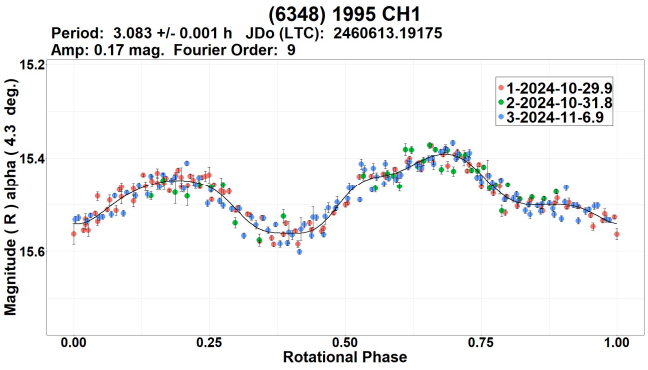

(6634) 1987 KB. Stephens (2014) and Pal et al. (2020) found following values for rotation periods: 5.333 h and 5.32762 h, respectively. The period value found from dense data obtained on 2 consecutive nights at SAO gives a period of P = 5.34 ± 0.03 h, which is in good agreement with two aforementioned results. Behrend (2002web, 2020web), on the other hand, finds two very close to each other, but significantly different values for period compared to the other results: 7.251 h (2002) and 7.159 h (2020). It should be noted that these latter results are derived from data that only partially cover the rotational cycle (in the older dataset) or are very sparse and noisy.

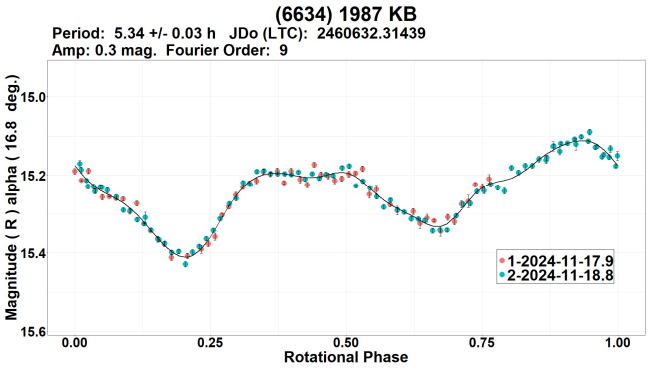

6821 Ranevskaya. A bimodal period solution of P = 2.811 ± 0.004 h was found from data obtained during 3 consecutive nights in 2024 December. The only previously found period of 2.81 h (Carbo et al., 2009) fully agrees with the newly established one.

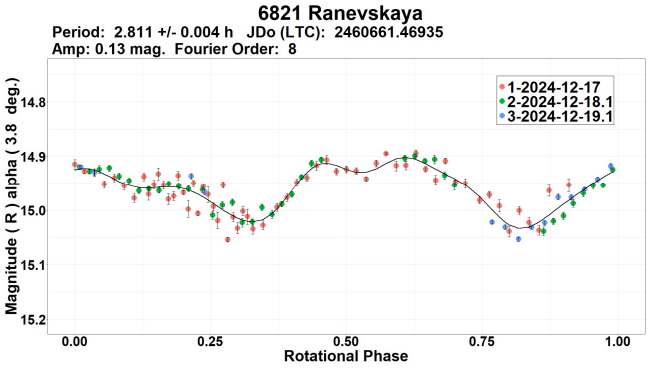

(6858) 1990 ST10. Prior reports on rotation period determinations for this asteroid do not exist. Five nights of observations in 2025 January - February resulted in a bimodal lightcurve with a period of P = 2.8009 ± 0.0003 h.

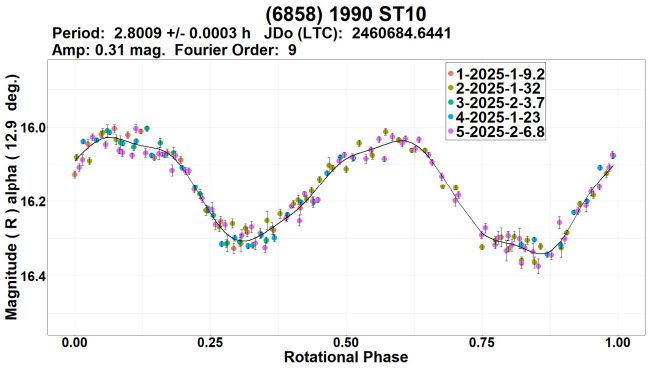

(13819) 1999 SX5. The newly established rotation period (P = 2.586 ± 0.002 h) is in accordance with previously found ones: 2.5848 h (Behrend, 2020web) and 2.592 h (Skiff et al., 2023).

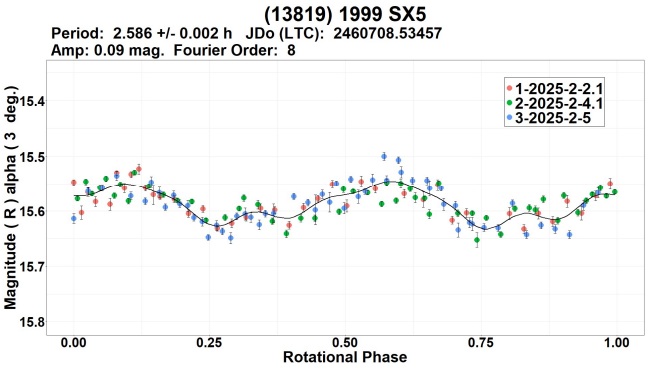

(17485) 1991 RP9. There are no previous period determination records in the LCDB for this one. Dense photometric data collected over more than a month of observations from late 2024 November to 2025 early January point out a bimodal solution for rotational period of P = 2.8073 ± 0.0002 h.

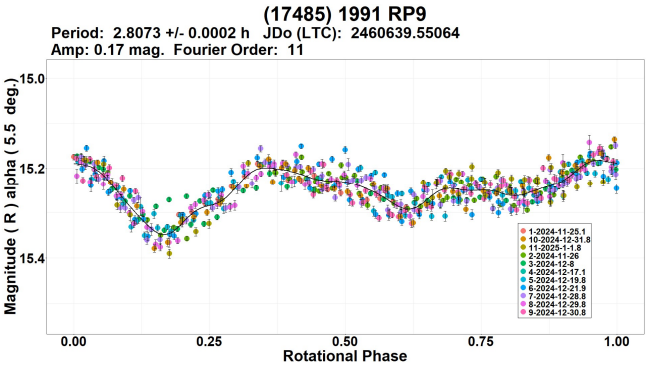

(18489) 1996 BV2. According to the LCDB records this is the first rotation period determination for this asteroid. Observations made on 4 consecutive nights in late 2025 January reveal a period of P = 2.935 ± 0.003 h.

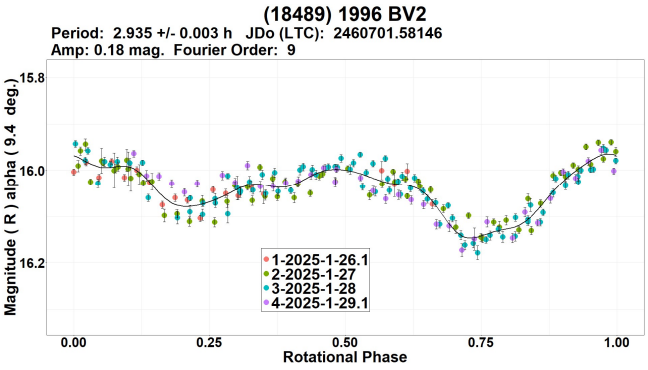

(21755) 1999 RE190. Observed for 3 nights in early 2025 January. The found unique bimodal solution for a period of P = 2.979 ± 0.002 h is distinctly different from the four results obtained by Erasmus et al. (2018, 2019), all of which are between 1.9 and 1.97 h.

Number	Name	20yy/mm/dd	Phase	L_{PAB}	B_{PAB}	Period (h)	P.E.	Amp	A.E.	Grp
1205	Ebella	24/10/12-24/10/24	21.8,16.2	54	5	3.0019	0.0007	0.17	0.02	MB-I
2738	Viracocha	25/03/03-25/03/21	9.9,16.7	143	-1	2.6391	0.0004	0.22	0.03	MB-O
3486	Fulchignoni	24/09/30-24/10/23	*3.5, 9.9	14	-2	2.8076	0.0003	0.19	0.02	HER
3583	Burdett	24/10/21-24/11/07	*5.3, 4.8	38	0	2.7191	0.0004	0.14	0.02	HER
4031	Mueller	24/11/16-24/11/18	20.4,20.9	38	23	2.944	0.006	0.18	0.03	HUN
4133	Heureka	25/02/21-25/03/08	5.4,12.4	142	-1	3.7295	0.0008	0.16	0.03	EUN
4159	Freeman	24/11/17-24/11/19	23.4,23.3	132	8	4.399	0.009	0.42	0.03	MB-I
4225	Hobart	24/10/10-24/10/21	4.5,10.3	12	-4	2.7737	0.0006	0.19	0.02	MB-I
4706	Dennisreuter	24/09/30-24/11/03	*3.4,15.7	13	-4	2.4599	0.0002	0.06	0.03	MB-I
4789	Sprattia	24/10/29-24/11/08	10.1, 4.6	53	-1	3.1341	0.0009	0.20	0.03	MB-I
5491	Kaulbach	24/10/28-24/11/06	9.6, 5.6	47	7	2.7777	0.0008	0.12	0.02	FLOR
5668	Foucault	25/02/06-25/03/05	*10.5, 7.8	154	7	2.5739	0.0002	0.14	0.03	FLOR
5802	Casteldelpiano	25/02/10-25/03/03	21.2,11.4	179	2	2.9708	0.0004	0.08	0.03	MB-I
6171	Uttorp	24/10/31-24/11/05	8.0, 5.1	50	4	3.687	0.003	0.25	0.02	MB-I
6243	Yoder	25/02/21-25/03/04	9.0, 3.2	167	-3	2.9526	0.0007	0.24	0.03	MB-I
6348	1995 CH1	24/10/29-24/11/07	4.3, 6.5	36	7	3.083	0.001	0.17	0.03	MB-I
6634	1987 KB	24/11/17-24/11/18	16.8,17.2	26	7	5.34	0.03	0.30	0.02	MB-I
6821	Ranevskaya	24/12/16-24/12/19	3.8, 5.0	79	-1	2.811	0.004	0.13	0.02	MB-I
6858	1990 ST10	25/01/09-25/02/06	*12.9, 5.7	132	10	2.8009	0.0003	0.31	0.03	EUN
13819	1999 SX5	25/02/02-25/02/05	3.0, 1.2	138	-1	2.586	0.002	0.09	0.03	PHO
17485	1991 RP9	24/11/25-25/01/01	*5.5,16.2	70	9	2.8073	0.0002	0.17	0.03	MAR
18489	1996 BV2	25/01/26-25/01/29	9.4, 8.2	143	8	2.935	0.003	0.18	0.03	MB-I
21755	1999 RE190	25/01/05-25/01/09	11.6, 9.8	121	-9	2.979	0.002	0.31	0.03	MB-I
24260	Krivan	25/01/05-25/01/09	11.6,10.7	118	18	3.319	0.003	0.34	0.03	EUN
30839	1991 GH1	25/03/05-25/03/09	8.8, 7.2	179	5	3.503	0.004	0.16	0.03	NP
56086	1999 AA21	24/10/18-24/10/21	18.0,18.1	26	28	2.775	0.003	0.15	0.03	PHO

Table I. Observing circumstances and results. Phase is the solar phase angle given at the start and end of the date range. If preceded by an asterisk, the phase angle reached an extrema during the period. L_{PAB} and B_{PAB} are the average phase angle bisector longitude and latitude. Grp is the asteroid family/group (Warner et al., 2009): MB-I = main-belt inner, MB-O = main-belt outer, MAR = Maria, PHO = Phocaea, HER = Hertha, FLOR = Flora, NP = Nysa-Polana, EUN = Eunomia, HUN = Hungaria.

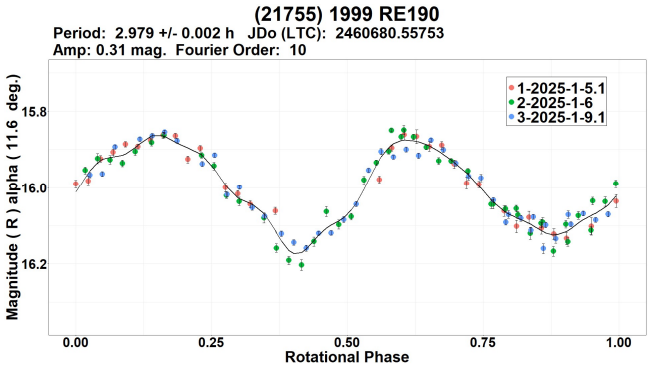

24260 Krivan. The only previous reference by Brinsfield (2012, 3.318 h) is fully consistent with the newly established bimodal solution of P = 3.319 ± 0.003 h, obtained from 2 nights of observations in 2025 January.

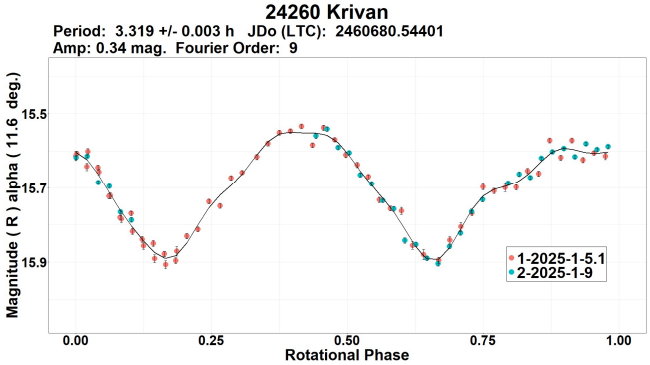

(30839) 1991 GH1. A unique period result of P = 3.503 ± 0.004 h was established based on data from 3 nights of observations in 2025 March. This is the first period determination for this asteroid.

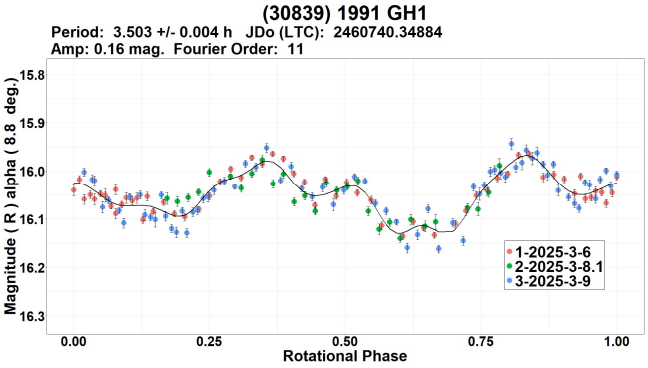

(56086) 1999 AA21. The newly determined rotation period of P = 2.775 ± 0.003 h from 3 nights of observations in 2024 October is completely in line with previously found values by Pal et al. (2020, 2.76957 h), Stephens and Warner (2021, 2.77037 h) and Benishek (2021, 2.7699 h).

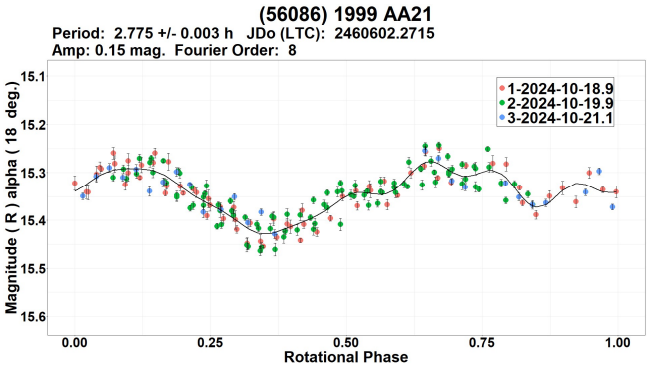

Acknowledgements

Observational work at Sopot Astronomical Observatory is generously supported by Gene Shoemaker NEO Grants awarded by the Planetary Society in 2018 and 2022.

References

Behrend, R. (-2002web, -2009web, -2020web, -2022web, -2023web). Observatoire de Geneve web site. *http://obswww.unige.ch/~behrend/page_cou.html*

Benishek, V. (2021). "Photometry of 30 Asteroids at Sopot Astronomical Observatory: 2020 February - October." *Minor Planet Bull.* **48**, 77-83.

Brinsfield, J.W. (2012). "Asteroid Lightcurve Analysis at the Via Capote Observatory: 2011 Apr-Dec." *Minor Planet Bull.* **39**, 55-57.

Carbo, L.; Green, D.; Kragh, K.; Krotz, J.; Meiers, A.; Patino, B,; Pligge, Z.; Shaffer, N.; Ditteon, R. (2009). "Asteroid Lightcurve Analysis at the Oakley Southern Sky Observatory: 2008 October thru 2009 March." *Minor Planet Bull.* **36**, 152-157.

Chang, C-K.; Ip, W.-H.; Lin, H.-W.; Cheng, Y.-C.; Ngeow, C.-C.; Yang, T.-C.; Waszczak, A.; Kulkarni, S.R.; Levitan, D.; Sesar, B.; Laher, R.; Surace, J.; Prince, T.A. (2015). "Asteroid Spin-rate Study Using the Intermediate Palomar Transient Factory." *Astrophys. J. Suppl. Series* **219**, id. 27.

Chelius, T. (2023). "Lightcurve Analysis of Three Asteroids." *Minor Planet Bull.* **50**, 41-42.

Ditteon, R.; Hirsch, B.; Kirkpatrick, E.; Kramb, S.; Kropf, M.; Meehl, J.; Stanfield, M.; Tollefson, E.; Twarek, A. (2004). "2003-04 winter observing campaign at Rose-Hulman Institute. Results for 797 Montana, 3227 Hasegawa, 3512 Eriepa, 4159 Freeman, 5234 Sechenov, and (5892) 1981 YS1." *Minor Planet Bull.* **31**, 54-56.

Dose, E.V. (2021). "Lightcurves of Eighteen Asteroids." *Minor Planet Bull.* **48**, 125-132.

Erasmus, N.; McNeill, A.; Mommert, A.; Trilling, D.E.; Sickafoose, A.A.; van Gend, C. (2018). "Taxonomy and Light-curve Data of 1000 Serendipitously Observed Main-belt Asteroids." *Astrophys. J. Suppl. Series* **237**, id. 19.

Erasmus, N.; McNeill, A.; Mommert, A.; Trilling, D.E.; Sickafoose, A.A.; Paterson, K. (2019). "A Taxonomic Study of Asteroid Families from KMTNET-SAAO Multiband Photometry." *Astrophys. J. Suppl. Series* **242**, id. 15.

Erasmus, N.; Navarro-Meza, S.; McNeill, A.; Trilling, D.E.; Sickafoose, A.A.; Denneau, L.; Flewelling, H.; Heinze, A.; Tonry, J.L. (2020). "Investigating Taxonomic Diversity within Asteroid Families through ATLAS Dual-band Photometry." *Astrophys. J. Suppl. Ser.* **247**, A13.

Pal, A.; Szakáts, R.; Kiss, C.; Bódi, A.; Bognár, Z.; Kalup, C.; Kiss, L.L.; Marton, G.; Molnár, L.; Plachy, E.; Sárneczky, K.; Szabó, G.M.; Szabó, R. (2020). "Solar System Objects Observed with TESS - First Data Release: Bright Main-belt and Trojan Asteroids from the Southern Survey." *Ap. J. Supl. Ser.* **247**, 26-34.

Pravec, P. (2018web). Photometric Survey for Asynchronous Binary Asteroids web site. *http://www.asu.cas.cz/~ppravec/newres.txt*

R Core Team (2024). "R: A language and environment for statistical computing. " R Foundation for Statistical Computing. Vienna, Austria. *https://www.R-project.org/*

Skiff, B.A.; McLelland, K.P.; Sanborn, J.J.; Koehn, B.W. (2023). "Lowell Observatory Near-Earth Asteroid Photometric Survey (NEAPS): Paper 5." *Minor Planet Bull.* **50**, 74-101.

Stephens, R.D. (2014). "Asteroids Observed from CS3: 2013 October-December." *Minor Planet Bull.* **41**, 92-95.

Stephens, R.D.; Warner, B.D. (2021). "Main-belt Asteroids Observed from CS3: 2020 July to September." *Minor Planet Bull.* **48**, 56-69.

Stone, G. (2024). "Lightcurves and Rotation Periods of 1292 Luce, 1340 Yvette, 2738 Viracocha 2841 Puijo, 4362 Carlisle, and 9911 Quantz." *Minor Planet Bull.* **51**, 3-5.

VizieR (2024). *http://vizier.u-strasbg.fr/viz-bin/VizieR*

Warner, B.D. (2009). "Asteroid Lightcurve Analysis at the Palmer Divide Observatory: 2008 September - December." *Minor Planet Bull.* **36**, 70-73.

Warner, B.D.; Harris, A.W.; Pravec, P. (2009). "The Asteroid Lightcurve Database." *Icarus* **202**, 134-146. Updated 2023 Oct 01. *http://www.minorplanet.info/lightcurvedatabase.html*

Warner, B.D. (2012a). *The MPO Users Guide: A Companion Guide to the MPO Canopus/PhotoRed Reference Manuals*. BDW Publishing, Eaton, CO.

Warner, B.D. (2012b). "Asteroid Lightcurve Analysis at the Palmer Divide Observatory: 2011 December - 2012 March." *Minor Planet Bull.* **39**, 158-167.

Warner, B.D. (2017). "Asteroid Lightcurve Analysis at CS3-Palmer Divide Station: 2016 July - September." *Minor Planet Bull.* **44**, 12-19.

Warner, B.D. (2018). MPO Canopus software. Version 10.7.11.3. *http://www.bdwpublishing.com*

Waszczak, A.; Chang, C.-K.; Ofek, E.O.; Laher, R.; Masci, F.; Levitan, D.; Surace, J.; Cheng, Y.-C.; Ip, W.-H.; Kinoshita, D.; Helou, G.; Prince, T.A.; Kulkarni, S. (2015). "Asteroid Light Curves from the Palomar Transient Factory Survey: Rotation Periods and Phase Functions from Sparse Photometry." *Astron. J.* **150**, A75.

Zeigler, K.; Hanshaw, B. (2016). "Photometric Observations of Asteroids 3829 Gunma, 6173 Jimwestphal and (41588) 2000 SC46." *Minor Planet Bull.* **43**, 199-200.

REVIEW OF ROTATION CURVES AND PERIODS OF 32 ASTEROIDS

Rafael González Farfán (Z55)
Observatorio Uraniborg
Écija, Sevilla, SPAIN
uraniborg16@gmail.com

Faustino García de la Cuesta (J38)
La Vara, Valdés, Asturias, SPAIN

Jesús Delgado Casal (Z73)
Observatorio Nuevos Horizontes
Camas, Sevilla, SPAIN

Esteban Reina Lorenz (232)
Masquefa, Can Parellada
Barcelona, SPAIN

Carlos Botana Albá (Y85)
Observatorio en Magalofes
Fene, A Coruña, SPAIN

Javier De Elías Cantalapiedra (L46)
Observatorio en Majadahonda
Madrid, SPAIN

Javier Ruiz Fernández (J96)
Observatorio de Cantabria
Cantabria, SPAIN

Fernando Limón Martínez (Z50)
Observatorio Mazariegos
Mazariegos, Palencia, SPAIN

José M. Fernández Andújar (Z77)
Observatorio Inmaculada del Molino
Sevilla, SPAIN

Esteban Fernández Mañanes (Y90),
Noelia Graciá Ribes
Observatorio Estelia
Ladines, Asturias, SPAIN

Juan Collada Bárcena (945),
Alfonso Coya Lozano
Observatorio Monte Deva
Gijón, SPAIN

Javier Polancos Ruiz
Observatorio La Portilla
Llanes, Asturias, SPAIN

José Manuel Cores
Observatorio de Pedreña
Pedreña, Cantabria, SPAIN

(Received: 2025 February 12 Revised: 2025 May 10)

We assess data for 32 asteroids to investigate whether or not there have been significant changes in the previously published results for their rotation periods. A secondary goal is to contribute to the creation of 3D models. The 32 asteroids studied were: 77 Frigga (9.005 h), 79 Eurynome (5.975 h), 174 Phaedra (5.746 h), 247 Eukrate (12.091 h), 291 Alice (4.316 h), 321 Florentina (2.870 h), 350 Ornamenta (9.182 h), 402 Chloe (10.668 h), 416 Vaticana (5.370 h), 504 Cora (7.587 h), 511 Davida (5.129 h), 513 Centesima (4.792 h), 534 Nassovia (9.476 h), 575 Renate (3.676 h), 620 Drakonia (5.488 h), 675 Ludmilla (7.717 h), 766 Moguntia (4.817 h), 802 Epyaxa (4.392 h), 811 Nauheima (4.002 h), 966 Muschi (5.353 h), 1120 Cannonia (3.811 h), 1260 Walhalla (3.858 h), 1514 Ricouxa (10.415 h), 1664 Felix (3.345 h), 1808 Bellerophon (4.149 h), 1925 Franklin-Adams (2.979 h), 2195 Tengstrom (2.821 h), 2693 Yan'an (3.841 h), 3654 AAS (3.549 h), 3672 Stevedberg (2.778 h), 4440 Tchantches (2.788 h) and 5598 Carlmurray (2.923 h).

Introduction. Through a broad collaboration we report recent lightcurve observations summarized in Table I. The images obtained were calibrated in the conventional mode, without photometric filter, and with the application of darks, bias and flats. Data analysis and processing were performed using *FotoDif* (2021), *Tycho Tracker* (2023) and *Periodos* (2020) software. In addition, all data were light-time corrected. The results are summarized below. Individual lightcurve plots along additional comments as required are also presented.

77 Frigga. One of the most recent observations of this asteroid was made by Raoul Behrend in 2021 (Behrend, 2021web). Our observations were made in the early days of February 2025, resulting in a light curve and data that allowed us to deduce a rotation period of 9.005 ± 0.006 hours and an amplitude of 0.080 ± 0.008 units. These values are very close to those obtained by Raoul Behrend and those published in ALCDEF (9.0032 h).

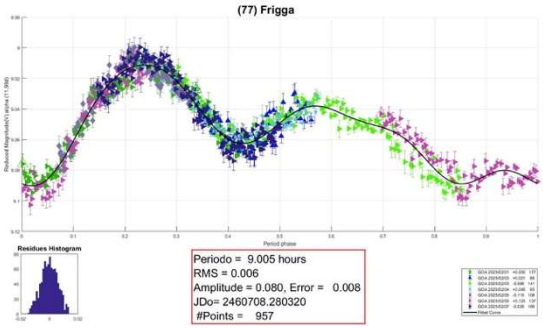

79 Eurynome. Although our study and follow-up of this asteroid began in April 2022, it had to be resumed at the end of January 2025 and completed at the beginning of February of the same year. The result obtained for its rotation period does not differ significantly from the previous one, which is widely published in the literature (v.g. Scaltriti and Zappala 1976). The curve we plotted, with just over 1700 points, allowe,d us to deduce a period P = 5.975 ± 0.011 hours, and an amplitude of A = 0.200 ± 0.016.

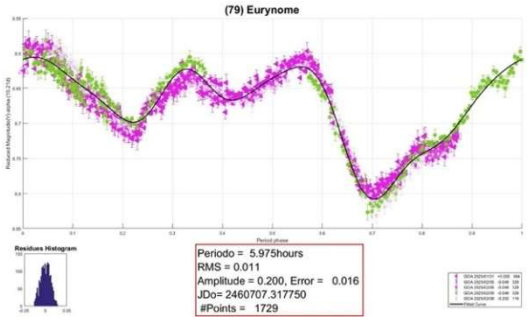

174 Phaedra. Discovered on 1877 September 2 from the United States, our observations were made between late January and early February 2025. The data obtained allowed us to deduce a rotation period of 5.746 ± 0.014 hours, and an amplitude of A = 0.260 ± 0.020. These data are in acceptable agreement with those recently published in 2018 by Raoul Behrend (Behrend, 2018web).

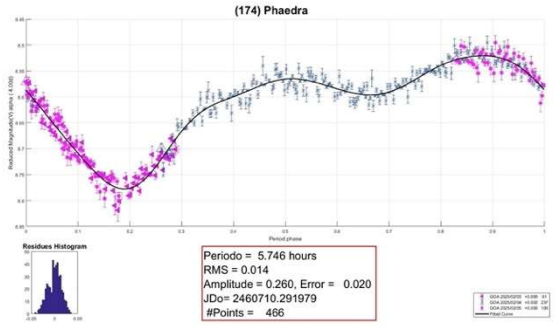

247 Eukrate. Between mid-December 2024 and early January 2025, we made observations of this main belt asteroid. The obtained curve and data allowed us to deduce a rotation period P = 12.091 ± 0.008 hours, and an amplitude of 0.100 ± 0.011. These results are consistent with those recently published in 2016 by Hanus et al. (2016).

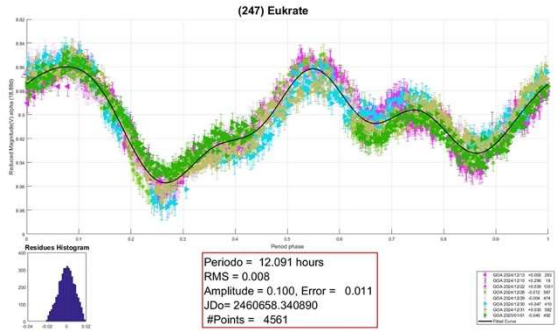

291 Alice. There is an extensive bibliography and results on this asteroid. One of the most recent is from 2019 (Ruthroff, 2019). Ours were carried out between November and December 2024 and allowed us to deduce a rotation period of 4.316 ± 0.017 hours and an amplitude of 0.120 ± 0.025. These results are in agreement with previously published results.

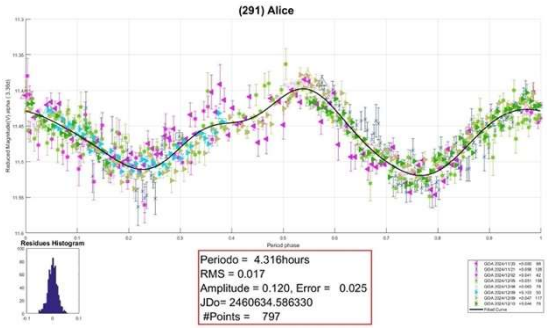

321 Florentina. This asteroid, which belongs to the main asteroid belt and was discovered on 1891 October 15 by Johann Palisa of the Vienna Observatory, has been a much-studied asteroid since 1958. One of the last follow-up observations was made in 2022 by Wilkin et al. (2022). Our observations were made between November and December 2024. The data obtained and the light curve produced allowed us to deduce a rotation period of 2.870 ± 0.025 hours, and A = 0.340 ± 0.035.

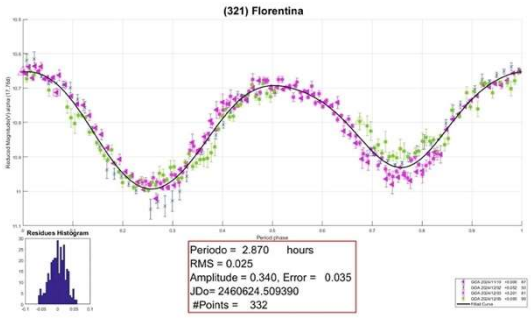

350 Ornamenta. Discovered in 1892 by the Nice Observatory, Ornamenta is a main belt asteroid with a diameter of almost 130 km. Its rotation period has been extensively studied since 1993 by Schober et al. (1993). Our studies of this asteroid were carried out at the end of December 2024. We were able to derive a rotation period of 9.182 ± 0.009 hours and an amplitude of 0.230 ± 0.012.

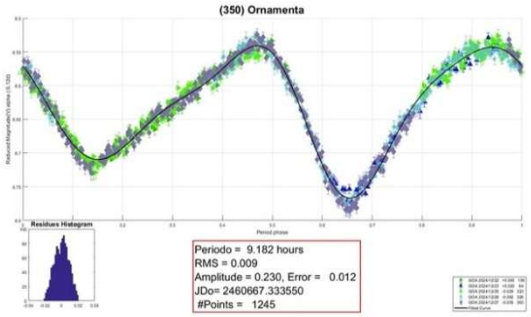

402 Chloe. Raoul Behrend's 2022 observations (Behrend, 2022web) are one of the latest to be published. Ours were made between November and December 2024 and allowed us to deduce a rotation period of 10.668 ± 0.013 hours and an amplitude of 0.300 ± 0.019.

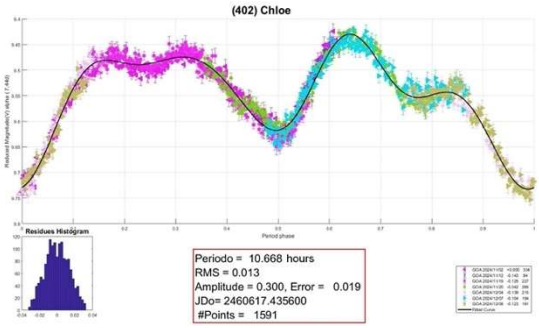

416 Vaticana. In December 2024, we made observations of this asteroid. We were able to construct a complete curve that allowed us to deduce a rotation period of 5.370 ± 0.009 hours, and A = 0.080 ± 0.012 units.

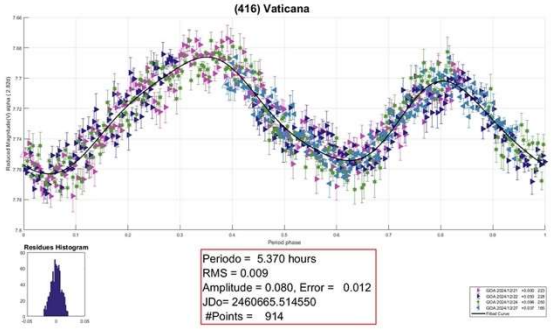

504 Cora. The images obtained of this asteroid, and the light curve constructed from them, allowed us to obtain a rotation period in perfect agreement with the latest published measurements (Pilcher, 2021). Our results, P = 7.587 ± 0.015 hours, and A = 0.160 ± 0.021.

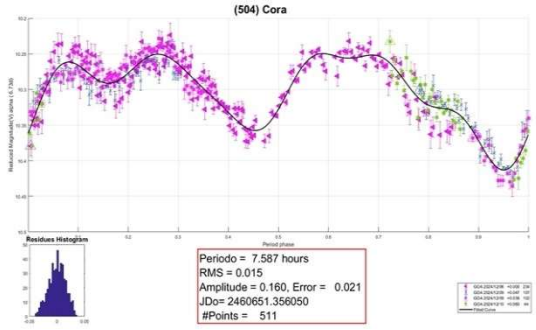

511 Davida. There is a long list of publications on this main belt asteroid, starting in 1954, of which 2021 is one of the most recent (Vernazza et al., 2021). Our observations were carried out during the month of November 2024 and allowed us to obtain a rotation period data in excellent agreement with the existing ones. We obtained P = 5.129 ± 0.008 hours and A = 0.260 ± 0.016.

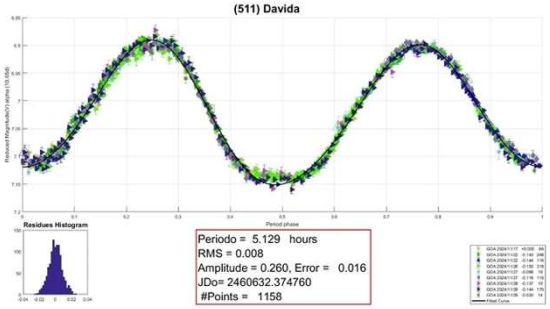

513 Centesima. With a diameter of almost 50 km, this main belt asteroid has also been studied on several occasions, one of the most recent being by Polakis in 2022 (Polakis, 2022). Ours took place in November 2024 and allowed us to deduce a rotation period of 4.792 ± 0.019 hours, and A = 0.310 ± 0.027, in perfect agreement with the most recent previous studies.

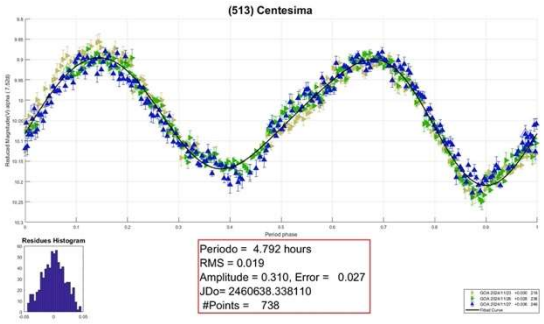

534 Nassovia. There are numerous references in the ALCDEF database for this asteroid, giving it a rotation period of 9.382 hours. However, our observations, made in December 2024, differ slightly from this result. We obtained a period of 9.476 ± 0.011 hours and an amplitude A = 0.100 ± 0.016.

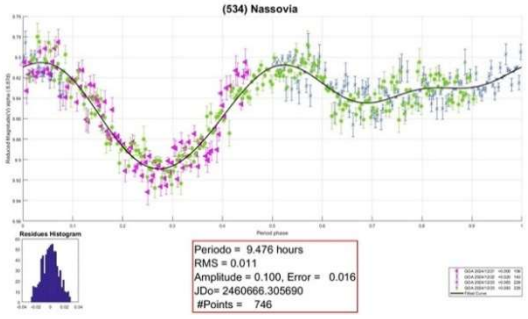

575 Renate. Belonging to the main asteroid belt, and discovered in September of 1905. ALCDEF has a published rotation period of 3,676 hours. During the month of November 2024, we tracked this asteroid, and we were able to deduce a rotation period in perfect agreement with the above data. Our result was P = 3.676 ± 0.016 hours, and A = 0.180 ± 0.022.

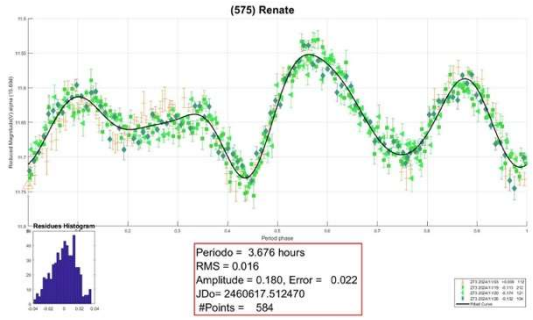

620 Drakonia. During the month of December 2024, we observed this main belt asteroid and were able to deduce a rotation period of P = 5.488 ± 0.021 hours and an amplitude of A = 0.540 ± 0.030.

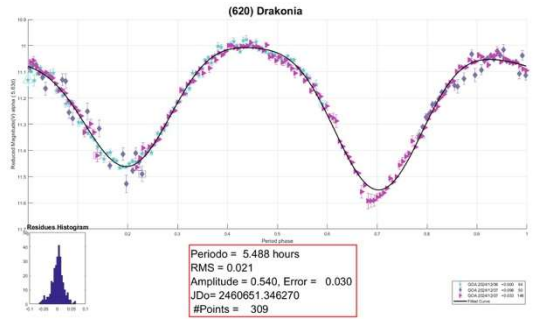

675 Ludmilla. One of the most recent publications of the rotation period and amplitude for this asteroid can be found in Martikainen et al. (2021). They give a result of 7.717 hours. Our results, obtained in late December 2024 and early January 2025, give the same value: P = 7.717 ± 0.013 hours, and A = 0.440 ± 0.019.

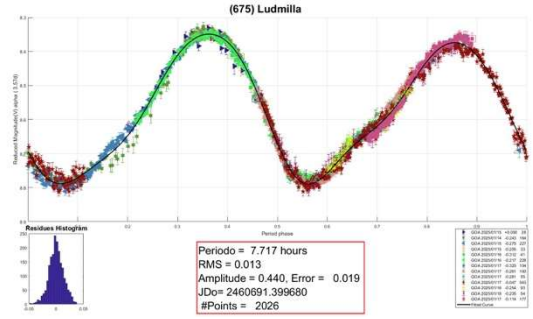

766 Moguntia. We have not found many publications in the literature with results on the rotation period of this asteroid. One of them (Behrend, 2010web), gives a value of 4,816 hours. The value obtained by our measurements, in December 2024, is practically the same: P = 4.817 ± 0.014 hours, A = 0.180 ± 0.020.

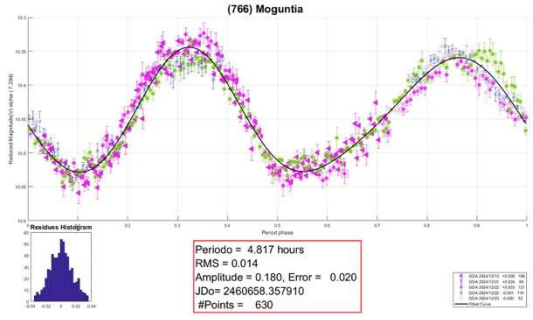

802 Epyaxa. The rotation period published for this asteroid in ALCDEF is exactly the same as the one we obtained with our measurements last December 2024. We measured P = 4.392 ± 0.026 hours, and A = 0.500 ± 0.037.

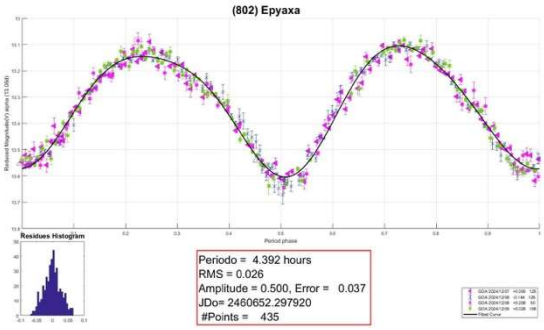

811 Nauheima. The observations we have found in the literature for this asteroid date from 2008. They give it a rotation period of 4.001 hours. In the month of December 2024, our measurements allowed us to obtain a very similar value: P = 4.002 ± 0.025 hours, and A = 0.210 ± 0.035.

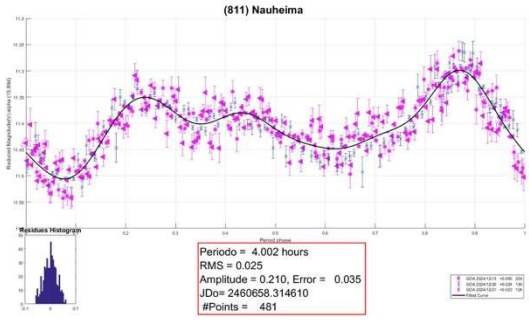

966 Muschi. Discovered in November 1921, this main belt asteroid has a published rotation period of 5.355 hours in 2020 (Durech et al., 2020). Just over 4 years later, in December 2024, our observations gave a similar result. P = 5.353 +/- 0.017 hours, and A = 0.380 +/- 0.025.

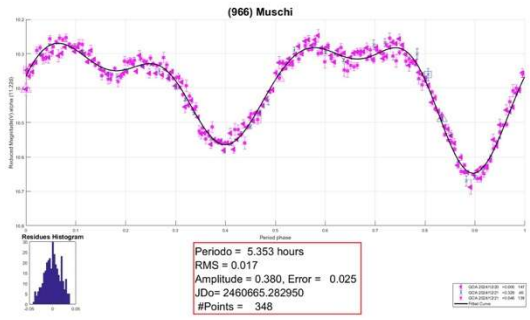

1120 Cannonia. Franco et al. (2020) published for this asteroid a result for the rotation period of 3.810 hours. Our result, from December 2024, gave an almost identical value: P = 3.811 ± 0.021 hours, and A = 0.140 ± 0.029.

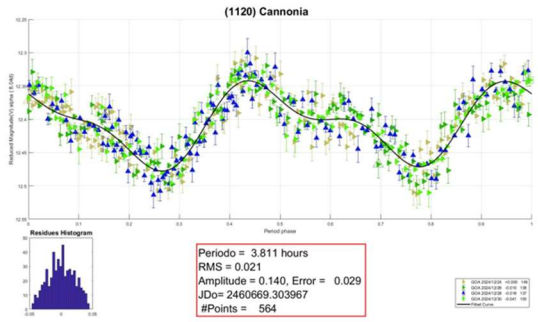

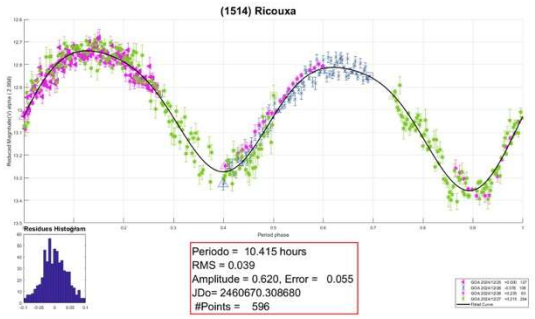

1260 Walhalla. We have not found any data on the rotation period of this asteroid in the usual literature. Walhalla is a main-belt asteroid discovered in January 1933 by the astronomer Karl Wilhelm Reinmuth of the Heidelberg Observatory, and initially designated as 1933 BW. Our observations in October 2024 gave a period of P = 3.858 ± 0.027 hours and an amplitude of 0.200 ± 0.039. The periodogram is shown here.

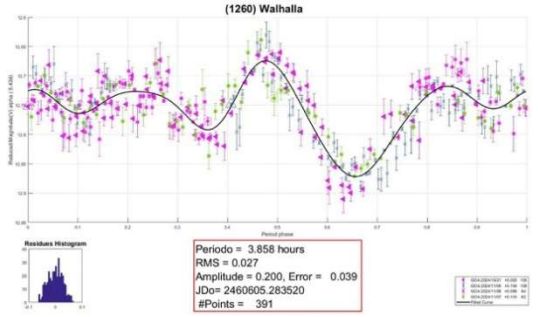

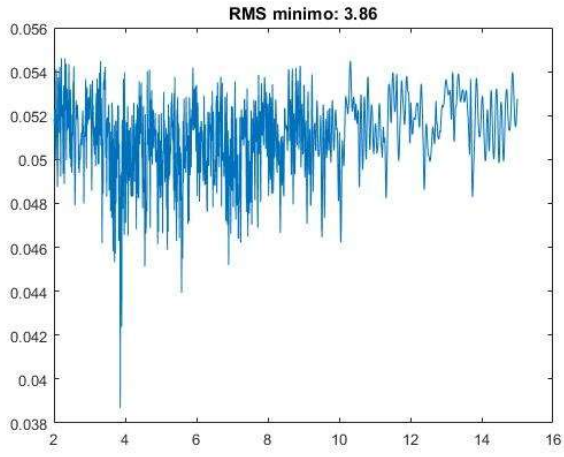

1514 Ricouxa. The published rotation period data in ALCDEF (10.438 h) is slightly higher than that obtained by our team in late December 2024 and early January 2025. Our results are P = 10.415 ± 0.039 hours, and A = 0.620 ± 0.055.

1664 Felix. Discovered by Eugène Joseph Delporte at the Royal Observatory of Belgium in February 1929, this asteroid has a published rotation period of 3,345 hours. Our observations in November 2024 confirmed this value, as we found P = 3.345 ± 0.035 hours, and A = 0.330 ± 0.050.

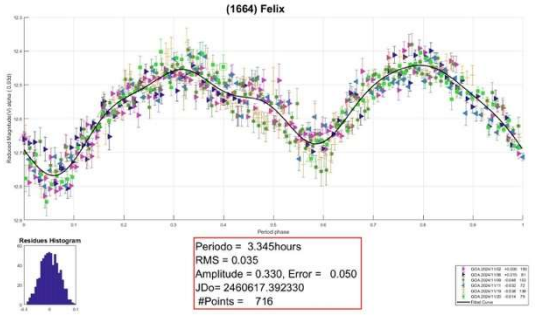

1808 Bellerophon. There are not many published observations and results for the rotation period of this asteroid, so the original JPL figure of 3.820 hours had to be confirmed or not. On the other hand, ALCDEF shows a different result of 4,147 hours. Our team observed it in December 2024 and obtained a result more in line with ALCDEF. We measured P = 4.149 ± 0.032 hours, A = 0.130 ± 0.045.

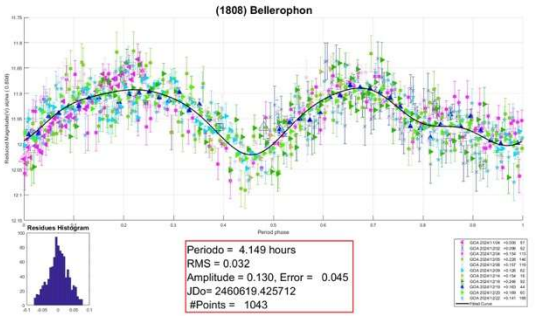

1925 Franklin-Adams. This asteroid, which belongs to the asteroid belt and was discovered by Hendrik van Gent on 1934 September 9 from the Leiden South Station in Johannesburg, South Africa, has a rotation period that has been extensively studied since 2005. It is one of the so-called short-period asteroids, with a published period of 2.978 hours (ALCDEF). In December 2024, our team was able to obtain its light curve and confirm the result of P = 2.979 ± 0.029 hours and A = 0.290 ± 0.041.

Number	Asteroid	20yy mm/dd	Phase	Period(h)	P.E.	Amp	A.E.
77	Frigga	25/02/01-25/02/05	12.0 - 13.6	9.005	0.006	0.080	0.008
79	Eurynome	25/01/31-25/02/08	10.3 - 19.6	5.975	0.011	0.200	0.016
174	Phaedra	25/02/03-25/02/04	4.0 - 4.4	5.746	0.014	0.260	0.020
247	Eukrate	24/12/13-25/01/01	18.9 - 18.4	12.091	0.008	0.100	0.011
291	Alice	24/11/19-24/12/10	3.4 - 9.3	4.316	0.017	0.120	0.025
321	Florentina	24/11/09-24/12/03	17.9 - 11.3	2.870	0.025	0.340	0.035
350	Ornamenta	24/12/20-24/12/27	5.2 - 7.9	9.182	0.009	0.230	0.012
402	Chloe	24/11/02-24/12/08	7.5 - 14.6	10.668	0.013	0.300	0.019
416	Vaticana	24/12/20-24/12/27	2.7 - 4.4	5.370	0.009	0.080	0.012
504	Cora	24/12/06-24/12/10	6.7 - 8.0	7.587	0.015	0.160	0.021
511	Davida	24/11/17-24/11/28	10.7 - 13.5	5.129	0.017	0.310	0.024
513	Centesima	24/11/23-24/11/27	7.6 - 9.0	4.792	0.027	0.310	0.027
534	Nassovia	24/12/21-24/12/23	8.9 - 9.7	9.476	0.011	0.100	0.016
575	Renate	24/11/02-24/11/26	15.7 - 9.5	3.676	0.016	0.180	0.022
620	Drakonia	24/12/06-24/12/07	5.7 - 5.9	5.488	0.021	0.540	0.030
675	Ludmilla	24/11/15-25/01/18	23.1 - 4.6	7.717	0.013	0.440	0.019
766	Moguntia	24/12/13-24/12/23	7.3 - 5.6	4.817	0.014	0.180	0.020
802	Epyaxa	24/12/07-24/12/09	13.1 - 14.1	4.392	0.026	0.500	0.037
811	Nauheima	24/12/13-24/12/21	15.9 - 17.4	4.002	0.025	0.210	0.035
966	Muschi	24/12/20-24/12/21	11.3 - 11.6	5.353	0.017	0.380	0.025
1120	Cannonia	24/12/24-24/12/30	8.1 - 11.2	3.811	0.021	0.140	0.029
1260	Walhalla	24/10/21-24/11/07	5.4 - 10.8	3.858	0.027	0.200	0.039
1514	Ricouxa	24/12/25-25/01/02	2.9 - 6.1	10.415	0.039	0.620	0.055
1664	Felix	24/11/02-24/11/11	0.9 - 5.6	3.345	0.035	0.330	0.050
1808	Bellerophon	24/12/02-24/12/22	13.8 - 20.7	4.419	0.032	0.130	0.045
1925	Franklin-Adams	24/12/24-24/12/30	15.7 - 17.5	2.979	0.029	0.290	0.041
2195	Tengstrom	24/11/19-24/11/27	5.8 - 2.5	2.821	0.017	0.280	0.023
2693	Yan'an	24/12/02-24/12/04	15.9 - 16.9	3.841	0.021	0.140	0.029
3654	AAS	24/09/29-24/11/07	0.9 - 21.9	3.549	0.020	0.120	0.029
3672	Stevedberg	24/12/08-24/12/10	8.1 - 9.0	2.778	0.018	0.200	0.025
4440	Tchantches	25/01/15-25/02/04	9.1 - 14.4	2.788	0.051	0.280	0.072
5598	Carlmurray	24/12/20-24/12/29	4.4 - 1.7	2.923	0.043	0.270	0.060

Table I. Observing circumstances and results. Phase is the solar phase angle given at the start and end of the date range. If preceded by an asterisk, the phase angle reached an extrema during the period.

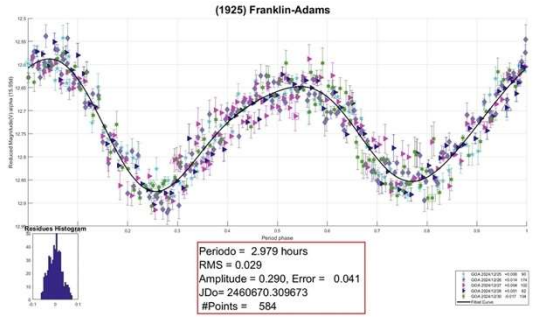

2195 Tengstrom. One of the most recent data for the synodic rotation period of this asteroid was obtained by Pravec and Sarounova in 2022 (Pravec et al., 2022web), who published a value of 2.821 hours. This result is in complete agreement with that obtained by our team in November 2024: P = 2.821 ± 0.017 hours, and A = 0.280 ± 0.023.

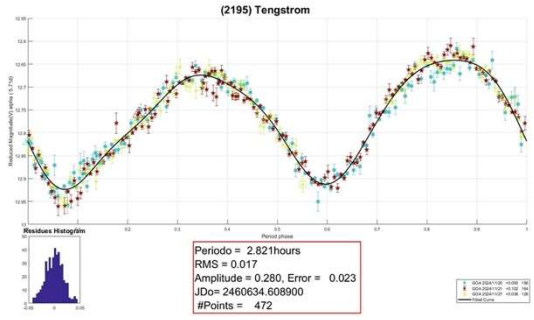

2693 Yan'an. During the month of December 2024, we had the opportunity to study this main belt asteroid discovered in November 1977 by the Purple Mountain Observatory team from the Purple Mountain Observatory, Nanjing, (China). The data obtained allowed us to determine a rotation period of 3.841 ± 0.021 hours and an amplitude of 0.140 ± 0.029. These data are in good agreement with those reported in the literature for this short-period asteroid (ALCDEF).

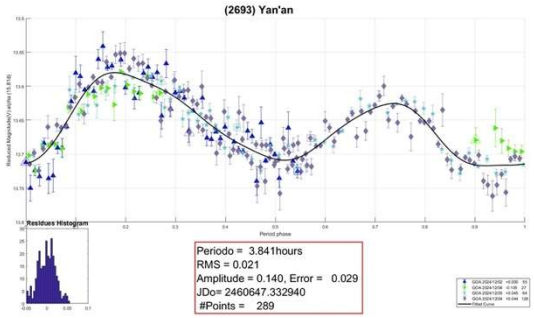

3654 AAS. Also known as 1949 QH1, this main belt asteroid, only 4.3 km in diameter, was discovered on 21 August 1949 by the Indiana Asteroid Program team at the Goethe Link Observatory in Brooklyn (USA). It is a short-period asteroid with an orbital period of 3.548 hours (ALCDEF), although no data were available from JPL at the time of our observations. However, in MPB-52 there were two articles by Vladimir Benishek (Benishek, 2025) and Geoffrey Stone (Stone, 2025) with observations of this asteroid on dates similar to ours. Our measurements gave a value almost

identical to those of these authors: P = 3.549 ± 0.020 hours and A = 0.120 ± 0.029 hours.

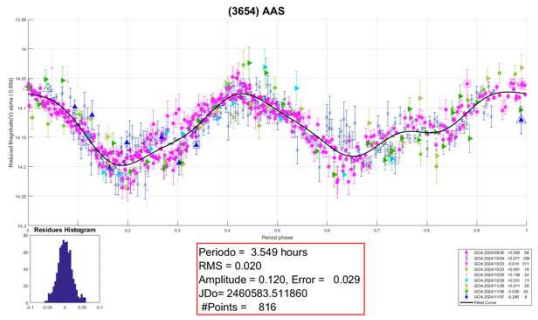

3672 Stevedberg. A short-period asteroid in the main belt, there are many publications on its synodic period. Virtually all of them agree on a value of 2.778 hours. Our measurements in December 2024 were also in agreement: P = 2.778 ± 0.018 hours, A = 0.200 ± 0.025.

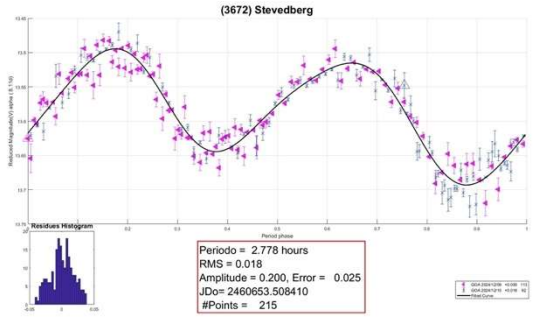

4440 Tchantches. Although it is a small main belt asteroid, there are studies suggesting that it may be a binary asteroid (Warner, 2013). The main rotation period recorded in ALCDEF is 2.788 hours. In January 2025, we carried out a study of this asteroid and obtained a synodic rotation value equal to the published one: P = 2.788 ± 0.051 hours, A = 0.280 ± 0.072.

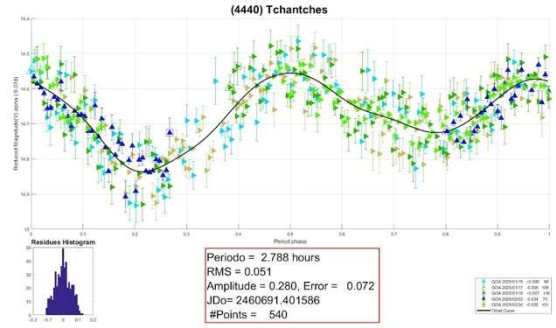

5598 Carlmurray. In December 2024 we measured and followed this main belt asteroid. We were able to obtain a synodic rotation period very close to that previously published (ALCDEF, 2.9226 h) of P = 2.923 ± 0.043 hours, A = 0.270 ± 0.060.

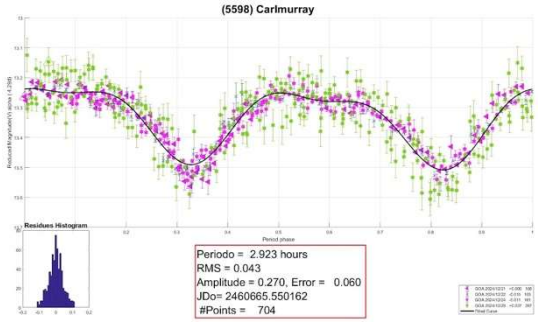

References

ALCDEF. Asteroid Lightcurve Data Exchange Format web site. *http://alcdef.org*

Behrend, R. (2010web, 2018web, 2021web, 2022web) Observatoire de Geneve web site, *htttp://obswww.unige.ch/~behrend/page_cou.html*

Benishek, V. (2025). "Photometry of 24 Asteroids from Sopot Astronomical Observatory: 2024 March - October." *Minor Planet Bull.* **52**, 45-52.

Durech, J.; Tonry, J.; Erasmus, N.; Denneau, L.; Heinze, A.N.; Flewelling, H.; Vanco, R. (2020). "Asteroid models reconstructed from ATLAS photometry." *Astron. Astrophys.* **643**, A59.

Franco, L.; Marchini, A.; Papini, R.; Iozzi, M.; Scarfi, G. and 20 colleagues (2022). "Collaborative Asteroid Photometry from UAI: 2022 January-March." *Minor Planet Bull.* **49**, 200-204.

FotoDif (2021) software. *http://astrosurf.com/orodeno/fotodif/index.htm*

Hanus, J.; Durech, J.; Oszkiewicz, D.A.; Behrend, R.; Carry, B. and 164 colleagues (2016). "New and updated convex shape models of asteroids based on optical data from a large collaboration network." *Astron. Astrophys.* **586**, A108.

JPL. Small-Body Database Lookup *https://ssd.jpl.nasa.gov/tools/sbdb_lookup.html#/?sstr=52768*

Martikainen, J.; Muinonen, K.; Penttila, A.; Cellino, A.; Wang, X.-B. (2021). "Asteroid absolute magnitudes and phase curve parameters from Gaia photometry." *Astron. Astrophys.* **649**, A98.

Períodos (2020) software.
http://www.astrosurf.com/salvador/Programas.html

Pravec, P.; Wolf, M.; Sarounova, L. (2022web)
http://www.asu.cas.cz/~ppravec/neo.htm]

Pilcher, F. (2021). "Lightcurves and Rotation Periods of 47 Aglaja, 504 Cora, 527 Euryanthe, 593 Titania, and 594 Mireille." *Minor Planet Bull.* **48**, 217-218.

Polakis, T. (2022). "Lightcurves for Sixteen Minor Planets." *Minor Planet Bull.* **49**, 298-303.

Ruthroff, J. (2019). "Low Phase Angle Observations of Asteroid 291 Alice." *Minor Planet Bull.* **46**, 319-320.

Scaltriti, F.; Zappala, V. (1976). "The similarity of the opposition effect among asteroids." *Astron. Astrophys. Suppl. Ser.* **23**, 167-179.

Schober, H.J.; Erikson, A.; Hahn, G.; Lagerkvist, C.-I. (1993). "Physical studies of asteroids. XXVIII. Lightcurves and photoelectric photometry of asteroids 2, 14, 51, 105, 181, 238, 258, 369, 377, 416, 487, 626, 679, 1048 and 2183." *Astron. Astrophys. Suppl. Ser.* **101**, 499-505.

Stone, G. (2025). "Lightcurves of Twenty-two Asteroids." *Minor Planet Bull.* **52**, 51-58.

Tycho Tracker (2023) software.
https://www.tycho-tracker.com

Vernazza, P.; Ferrais, M.; Jorda, L.; Hanuš, J.; Carry, B. and 62 colleagues (2021). "VLT/SPHERE imaging survey of the largest main-belt asteroids: Final results and synthesis." *Astron. Astrophys.* **654**, A56.

Warner, B.D. (2010). "A Tale of Two Asteroids: (35055) 1984 RB and (218144) 2002 RL66." *Minor Planet Bull.* **37**, 112-118.

Warner, B.D. (2013). "Something Old, Something New: Three Binary Discoveries from the Palmer Divide Observatory." *Minor Planet Bull*. **40**, 119-121.

Wilkin, F.P.; AlMassri, Z.; Bowles, P.; Pargiello, M.; Sindoni, J. (2022). "Lightcurves for Three Koronis Family Asteroids from the Union College Observatory." *Minor Planet Bull.* **49**, 267-268.

DETERMINING THE ROTATIONAL PERIODS AND LIGHTCURVES OF FIVE ASTEROIDS

Zelie-Louise Bradicich
Caitlin Bell
Lydia Bullock
Kent Montgomery
East Texas A&M University
P.O. Box 3011
Commerce, TX 75429-3011
Kent.Montgomery@tamuc.edu

(Received: 2025 April 15)

Aperture photometry using 1-meter class telescopes was performed to find lightcurves and rotation periods for the following five asteroids: 1833 Shmakova, 3.838 ± 0.001 h; 2305 King, 2.975 ± 0.001 h; 8168 Rogerbourke, 7.035 ± 0.003 h; (25283) 1998 WU, 2.634 ± 0.001 h; and (66251) 1999 GJ2, 2.462 ± 0.001 h.

This research was conducted to create lightcurves and determine the rotation periods for the following asteroids: 1833 Shmakova, 2305 King, 8168 Rogerbourke, (25283) 1998 WU, and (66251) 1999 GJ2. These asteroids were found using the Collaborative Asteroid Lightcurve Link (CALL) website with several filters: an asteroid's declination needed to be positive, and its apparent magnitude was required to be between 14 and 16. These asteroids were also chosen to have opposition dates around two weeks prior to the date of observation.

Asteroid 1833 Shmakova was discovered by L. Chernykh at the Crimean Astrophysical Observatory in Nauchnyj in 1969. This asteroid has a semi-major axis of 2.63 AU, an orbital eccentricity of 0.114, and an absolute magnitude of 11.83 (JPL, 2025). Asteroid 2305 King was discovered in 1980 at the Harvard College Observatory's Agassiz Station. It has a semi-major axis of 2.79 AU, an orbital eccentricity of 0.030, and an absolute magnitude of 11.77 (JPL, 2025). Asteroid 8168 Rogerbourke was discovered in 1991 at Palomar Observatory by E.F. Helin. It has a semi-major axis of 2.40 AU, eccentricity 0.288, and absolute magnitude 13.80 (JPL, 2025). Asteroid (25283) 1998 WU was discovered at Oizumi Observatory in 1998 by T. Kobayashi. This asteroid has a semi-major axis of 2.63 AU. Its orbital eccentricity is 0.250 and it has an absolute magnitude of 13.70 (JPL, 2025). The asteroid (66251) 1999 GJ2 was discovered by LINEAR (Lincoln Near-Earth Asteroid Research) at Socorro, New Mexico, in 1999. It has a semi-major axis of 1.54 AU, eccentricity of 0.198, and absolute magnitude of 17.04 (JPL, 2025).

Number	Name	yyyy mm/dd	Phase	L_{PAB}	B_{PAB}	Period(h)	P.E.	Amp	A.E.	Grp
1833	Shmakova	2024 06/07-06/11	17.2,16.5	129.7	1	3.838	0.001	0.35	0.02	MB-M
2305	King	2024 01/31-02/06	18.7,19.8	82.3	-2	2.975	0.001	0.20	0.03	MB-M
8168	Rogerbourke	2023 12/04-12/06	4.6,3.7	80.3	-2.3	7.035	0.003	0.29	0.02	MB-I
25283	1998 WU	2023 09/10-09/19	8.5,10.2	139.5	-1	2.634	0.001	0.13	0.05	MB-M
66251	1999 GJ2	2024 09/28-10/02	16.3,17.7	334.2	-1.5	2.462	0.001	0.10	0.04	NEA

Table I. Observing circumstances and results. The phase angle is given for the first and last date. If preceded by an asterisk, the phase angle reached an extrema during the period. L_{PAB} and B_{PAB} are the approximate phase angle bisector longitude/latitude at mid-date range (see Harris et al., 1984). Grp is the asteroid family/group (Warner et al., 2009).

Methods

Images of each target's field were taken using the Planewave CDK 700 0.7-m telescope at the East Texas A&M University (ETAMU) Observatory and the Southern Association for Research in Astronomy Consortium's 0.9-m telescope (SARA-KP) located in Kitt Peak, Arizona. All images were taken through a luminance filter that blocked both infrared and ultraviolet light, with each image having an exposure time of 180 seconds. The detectors were Andor CCD cameras which were thermoelectrically cooled to a temperature between -20°C and -50°C at the ETAMU Observatory and between -70°C and -110°C for SARA-KP to reduce thermal noise. The telescopes were refocused every hour, with observations for each asteroid being collected over several nights.

Three types of calibration images were taken every night of observation: bias frames, dark frames, and flat field images. Between 20-30 bias frames were taken with no exposure time at the beginning of the night, and 2-3 dark frames were taken with a 180-second exposure time. The flat field images were taken against the twilight sky, with a varying exposure time. Depending on the night, between 13-20 flat field images were obtained. Master images were then created from all the calibration images using *Maxim DL* (Diffraction Limited), which was also used to calibrate and align the images.

Aperture photometry was performed on the calibrated images using *MPO Canopus* v.10.8.1.1 software (Warner, 2019). Five comparison stars were chosen based on their magnitude and relative position to the target. The difference in brightness between the asteroid and the average brightness of the reference stars was determined for each image. The resulting magnitudes were then plotted against time to produce the asteroid's lightcurve. Finally, a Fourier transform of the lightcurve was taken to determine the asteroid's best rotation period and its amplitude.

Results

1833 Shmakova was observed for two nights, with a total of 191 images obtained. The first night of observation was 2024 June 7 using the ETAMU Observatory's 0.7-m telescope. 67 images were collected on the first night. The second night was 2024 June 11 using the SARA-KP 0.9-m telescope, during which 124 images were obtained. Analysis of the resulting lightcurve shows a rotation period of 3.838 ± 0.001 h, with an amplitude of 0.35 mag. This is close to the results of a previous study by Monson and Kipp (2004), who found a similar period of 3.934 ± 0.003 h and an amplitude of 0.38 mag.

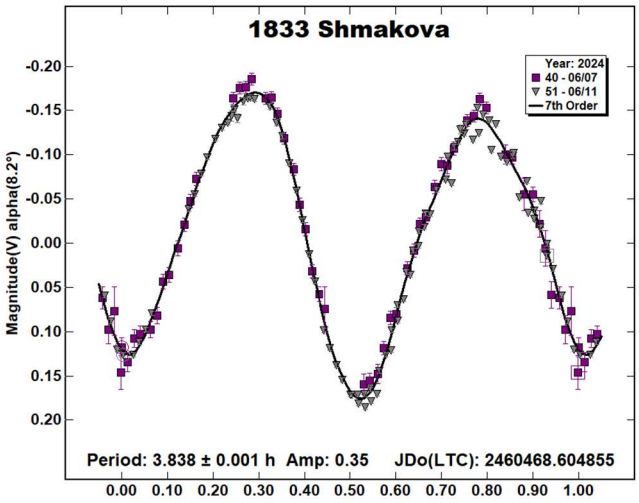

2305 King. Images were taken over two nights using the ETAMU Observatory's 0.7-m telescope, yielding a total of 144 images. The first night of observation on 2024 January 31 produced 73 images, with a second night on 2024 February 6 producing another 71 images. The resulting lightcurve has a period of 2.975 ± 0.001 h, and an amplitude of 0.20 mag. Odden et al. (2019) found a similar rotation period of 3.0368 ± 0.0005 h and an amplitude of 0.19 mag.

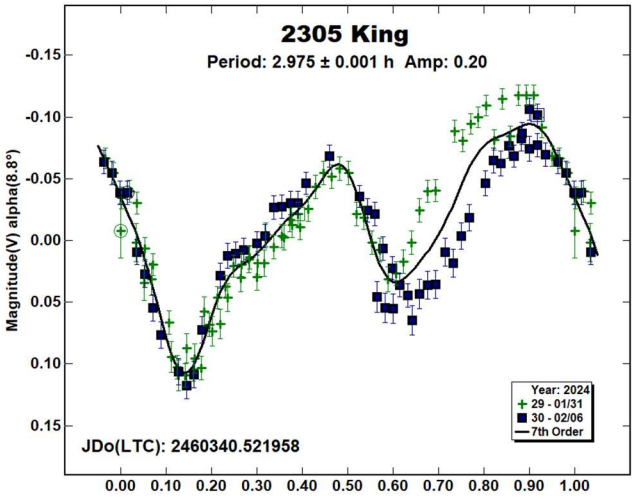

8168 Rogerbourke. In total, 413 images were collected for the asteroid 8168 Rogerbourke over three consecutive nights of observation. The first 150 images were obtained on 2023 December 4, with another 113 images on 2023 December 5, and the final 150 images on 2023 December 6. The ETAMU 0.7-m telescope was used for all nights of observation. Analysis of the obtained lightcurve for 8168 Rogerbourke shows a period of 7.035 ± 0.003 h and an amplitude of 0.29 mag. The Minor Planet Lightcurve Database (Warner et al., 2009) and the JPL Small-Body Database (JPL, 2025) did not show any previous rotational period results for the asteroid 8168 Rogerbourke.

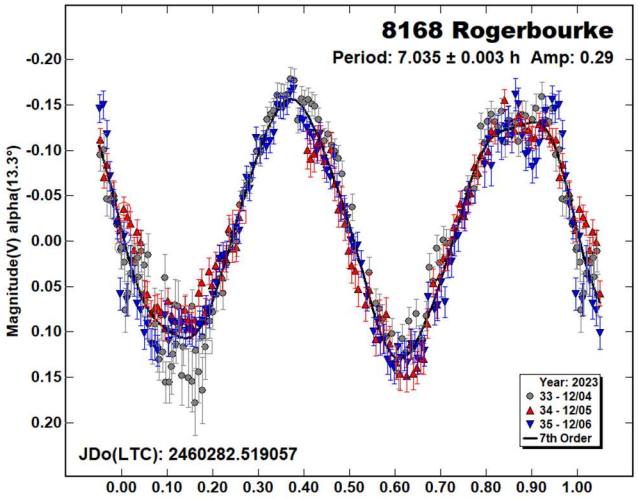

(25283) 1998 WU. Three nights were spent observing the asteroid (25283) 1998 WU with the ETAMU 0.7-m telescope. A total of 300 images were obtained over these three nights. 100 images were collected on each of the nights of 2023 September 10, 2023 September 18, and 2023 September 19. The resulting lightcurve has a rotational period of 2.634 ± 0.001 h and an amplitude of 0.13 mag. No previous results for the rotational period were found in the JPL Small-Body Database (NASA, n.d.) and the Minor Planet Light Curve Database (Warner et al., 2009).

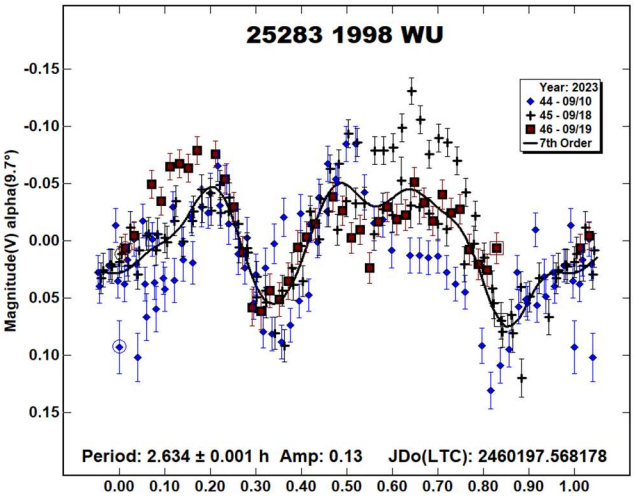

(66251) 1999 GJ2 was observed for three nights using the ETAMU Observatory's 0.7-m telescope. A total of 229 images were collected. The first night of data collection was 2024 September 28, with 89 images obtained. The second night was 2024 September 29, with 40 images obtained. The final night of observation was 2024 October 2, with a total of 100 images obtained. Analysis of the resulting lightcurve shows a rotational period of 2.462 ± 0.001 h with an amplitude of 0.10 mag. This agrees with the results of a previous study by Farfan et al. (2025) that reported a period of 2.463 ± 0.018 h and an amplitude of 0.10 mag. This is also similar to the rotational period of 2.461 ± 0.002 h and amplitude of 0.11 mag that were found by Benishek (2025).

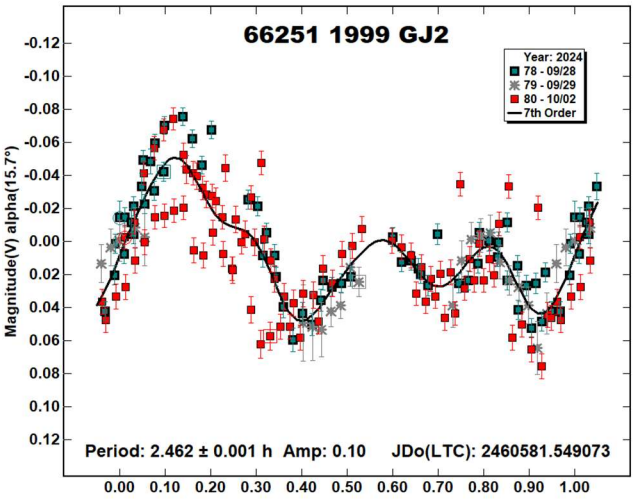

References

Benishek, V. (2025). "Photometry of 24 Asteroids from Sopot Astronomical Observatory." *Minor Planet Bull.* **52**, 45-50.

Collaborative Asteroid Lightcurve Link (CALL): Potential Lightcurve Targets. *http://www.minorplanet.info/PHP/call_OppLCDBQuery.php*

Diffraction Limited MaxIm DL - Astronomy and Scientific Imaging Software. *https://diffractionlimited.com/product/maxim-dl/*

Farfan, R.; Cuesta, F.; Lorenz, E.; Alba, C.; Cantalapiedra, J.; Fernandez, J.; Martinez, F.; Pinilla, F.; Andujar, J. (2025). "Analysis and Review of Rotation Curves and Periods of 12 Asteroids." *Minor Planet Bull.* **52**, 35-37.

Harris, A.W.; Young, J.W.; Scaltriti, F.; Zappala, V. (1984). "Lightcurves and phase relations of the asteroids 82 Alkmene and 444 Gyptis." *Icarus* **57**, 251-258.

JPL (2025). Small-Body Database Search Engine. *http://ssd.jpl.nasa.gov/sbdb.cgi*

Monson, A.; Kipp, S. (2004). "Rotational Periods of Asteroids 1165 Imprinetta, 1299 Mertona, 1645 Waterfield, 1833 Shmakova, 2313 Aruna, and (13856) 1999 XZ105." *Minor Planet Bull.* **31**, 71-73.

Odden, C.; Abruzzese, Z.; Beckwith, R.; Chandran, R.; El Alam, Z.; Glover, E.; Kacergis, J.; Lazaro, I.; Julia, C.; Nyiha, I.; Solomon, H.; Wang, J.; Yu, Z.; Zhu, J. (2019). "Lightcurve Analysis of Asteroid 2305 King." *Minor Planet Bull.* **46**, 363-364.

Warner, B.D.; Harris, A.W.; Pravec, P. (2009). "The Asteroid Lightcurve Database." Icarus **202**, 134-146. Updated 2023 Oct. *http://www.MinorPlanet.info/php/lcdb.php*

Warner, B.D. (2019). MPO Canopus software. Version 10.8.1.1. Bdw Publishing. *http://www.minorplanetobserver.com/*

LIGHTCURVE ANALYSIS FOR NINE NEAR-EARTH ASTEROIDS OBSERVED IN FEBRUARY 2010 AND JANUARY - APRIL 2025

Peter Birtwhistle
Great Shefford Observatory
Phlox Cottage, Wantage Road
Great Shefford, Berkshire, RG17 7DA
UNITED KINGDOM
peter@birtwhistle.org.uk

(Received: 2025 April 14)

Lightcurves and amplitudes for nine near-Earth asteroids observed from Great Shefford Observatory during close approaches in February 2010 and between January and April 2025 are reported. All but one are small objects with rotation periods 0.5 hour or shorter and three are identified as having tumbling rotation.

Photometric observations of near-Earth asteroids during close approaches to Earth in February 2010 and between January and April 2025 were made at Great Shefford Observatory using a 0.40-m Schmidt-Cassegrain and Apogee Alta U47+ CCD camera. All observations were made unfiltered and with the telescope operating with a focal reducer at f/6. The 1K×1K, 13-micron CCD was binned 2×2 resulting in an image scale of 2.16 arcsec/pix. All the images were calibrated with dark and flat frames and *Astrometrica* (Raab, 2024) was used to measure photometry using G band data from the DR3 catalogue. *MPO Canopus* (Warner, 2023), incorporating the Fourier algorithm developed by Harris (Harris et al., 1989) was used for lightcurve analysis.

No previously reported results have been found in the Asteroid Lightcurve Database (LCDB) (Warner et al., 2009), from searches via the Astrophysics Data System (ADS, 2025) or from wider searches unless otherwise noted. All size estimates are calculated using H values from the Small-Body Database Lookup (JPL, 2025b), using an assumed albedo for NEAs of 0.2 (LCDB readme.pdf file) and are therefore uncertain and offered for relative comparison only.

(484976) 2009 UN3. This is a relatively large Apollo (*H = 18.5, D ~590 m*) discovered by the Siding Spring Survey on 2009 Oct 19 (McNaught et al., 2009) which made an approach to 14 Lunar Distances (LD) from Earth on 2010 Feb 9.3 UTC. It is classified by the Minor Planet Center as a potentially hazardous asteroid due to its size and Earth Minimum Orbital Intersection Distance (MOID) of 0.025 AU (= 10 LD) and was observed by radar from Goldstone on 2010 Feb 8 and 9 (JPL 2025c). Photometry was obtained starting on 2010 Feb 10.00 UTC for 1.7 h and again the next night starting on 2010 Feb 10.94 UTC for a further 2.5 h. A raw plot (with discontinuous time axis) shows that a partial rotation was captured on each night, with slightly different maxima and a phased solution determined the best-fit period to be 4.091 ± 0.001 h with amplitude 0.50 ± 0.03. The period spectrum shows a number of other potential solutions between 1.9 and 5.6 h with only slightly inferior RMS values, though all of these have issues with the resultant fitted Fourier curves, where the amplitude or shape of the calculated curves are either rather unlikely in the phase ranges where observational gaps occur, or do not follow the observed direction of slope in places.

(484976) 2009 UN3 was reported by Hicks et al. (2010) with a period of 4.123 h and amplitude of 0.5 from observations on 2010 Feb 15 and Polishook (2012) reported a partial lightcurve with estimated period 4.0 ± 0.5 h and amplitude 0.45 ±0.05 from observations on 2010 Feb 18. The results presented here agree well with both previous papers.

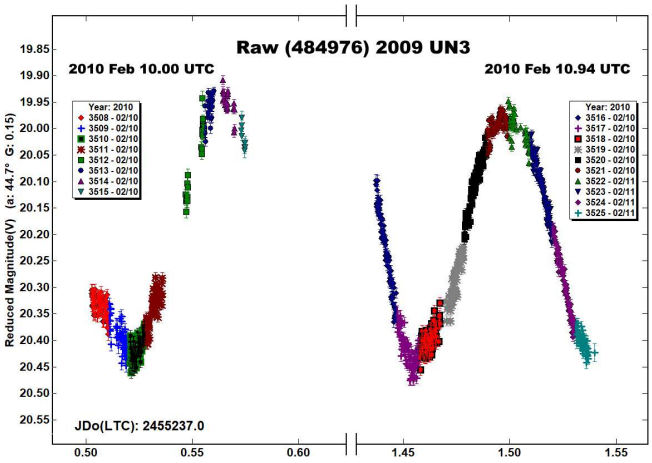

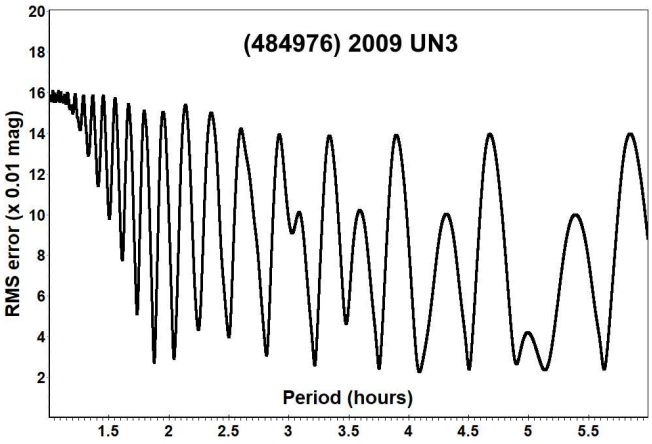

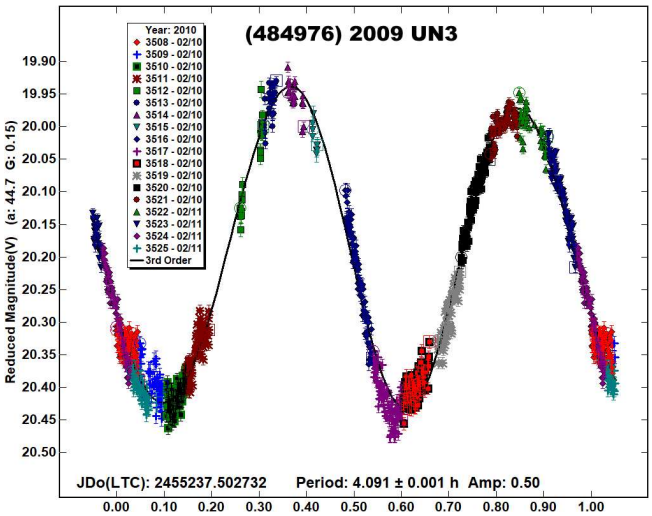

2025 AB. The Catalina Sky Survey discovered this Aten (*H = 27.1, D ~11 m*) on 2025 Jan 1.3 UTC (Kowalski et al., 2025a) and it made a very close approach, to 0.4 LD from Earth on 2025 Jan 3.3 UTC. Both Sentry (JPL, 2025a) and NEODyS (NEODyS, 2025) list 2025 AB as a virtual impactor with single very low probability events in 2122 and 2105 respectively. It was observed for 2.4 h starting on 2025 Jan 2.89 UTC as it approached from 1.0 to 0.8 LD, With the apparent speed reaching 226 arcsec/min exposures were reduced from 3.9 to 2.3 s to keep image trailing within the photometry measurement aperture utilised in *Astrometrica*.

Three sets of regularly spaced minima, at small integer multiples of 0.0286 h (~1.7 m), 0.0170 h (~1.0 m) and 0.0242 h (~1.5 m) are identified on a linearly plotted period spectrum and are strong indicators that non-principal axis rotation (NPAR), or tumbling, may be present. The *MPO Canopus* Dual Period Search function was used to isolate potential NPAR solutions for rotation and precession, lightcurves for the best-fit pair of periods found are given, labelled P1 and P2, where:

P1 = 0.057151 ± 0.000008 h (~3.4 min), amplitude 1.2
P2 = 0.034019 ± 0.000004 h (~2.0 min), amplitude 0.5

A weaker solution, consisting of the same dominant P1 period but with a secondary period of:

P3 = 0.048454 ± 0.00001 h (~2.9 min), amplitude 0.4

was also located, but it is noted that the frequency of the P3 period is just a linear combination of the frequencies of P1 and P2, where: 2/P2 – 1/P1 = 2/P3. Solutions with similar RMS fits are also obtained using the P1 period and half the P2 or P3 periods.

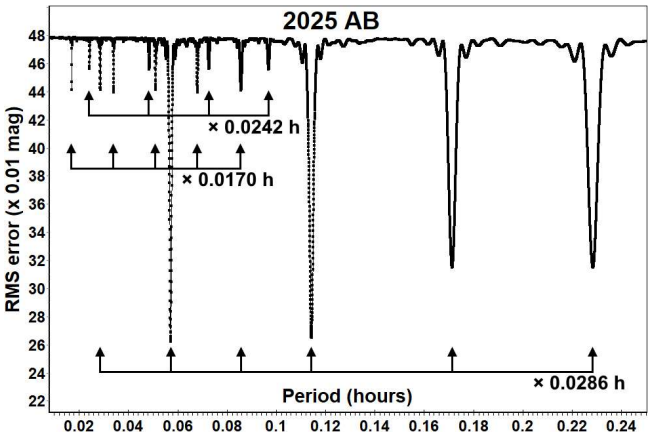

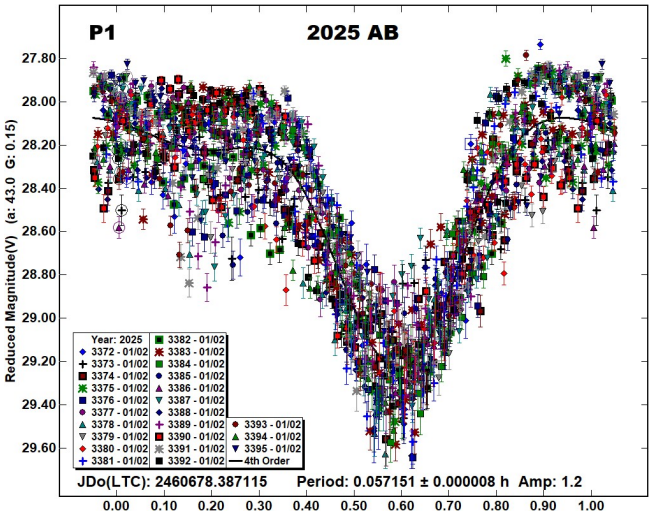

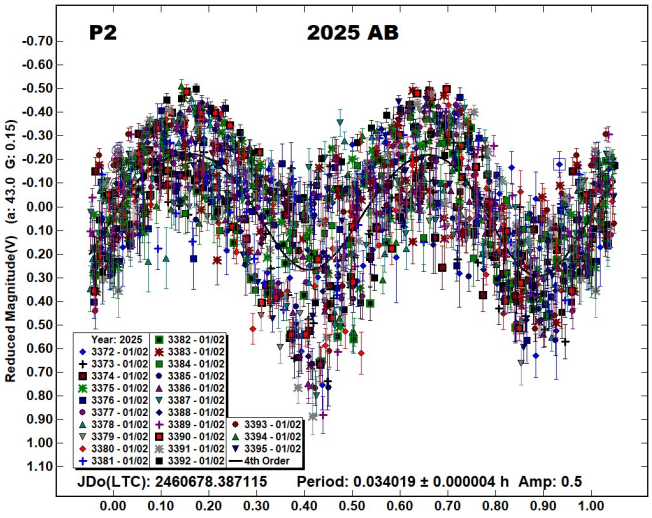

It is not possible to determine from this analysis whether the main apparent frequencies are the real frequencies of rotation and precession for the tumbler or just linear combinations of them. However, it is expected that 2025 AB may be rated as PAR = -3 on the scale defined in Pravec et al., (2005) where NPA rotation is reliably detected with the two periods resolved. An ambiguity of the period's solution may be tolerated provided the resulting spectrum of frequencies with significant signal is the same for the different solutions. (Petr Pravec, personal communication). The NPAR solution indicates the full amplitude of the tumbling rotation was 1.7 mag. 2025 AB completed 42 rotations of the P1 period and 71 rotations of the P2 period during the 2.4 h it was under observation.

2025 AC. This is a very small Apollo (*H = 29.0, D ~5 m*) discovered by ATLAS-HKO, Haleakala on 2025 Jan 1.5 UTC (Kowalski et al., 2025b). It also made a very close approach to 0.4 Lunar Distances (LD) from Earth on 2025 Jan 2.9 UTC, about 8 h before 2025 AB. Observations were made for 1.9 h starting at 2025 Jan 2.73 UTC and its apparent speed increased from 320 to 360 arcsec/min, with exposures being reduced equivalently from 1.6 to 1.4 s to reduce image trailing. The period spectrum again reveals signs of NPA rotation, with two sets of regularly spaced minima, at small integer multiples of 0.0025 h (~9 s) and 0.0039 h (~14 s).

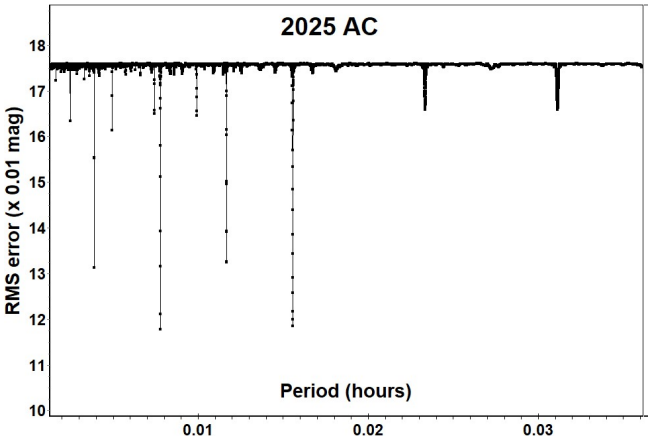

The *MPO Canopus* Dual Period Search function determined the best-fit pair of periods to be:

P1 = 0.0077818 ± 0.0000003 h (~28 sec), amplitude 0.4
P2 = 0.0049569 ± 0.0000001 h (~18 sec), amplitude 0.3

No other significant aliases of these two periods were located. Corresponding lightcurves are here labelled P1 and P2:

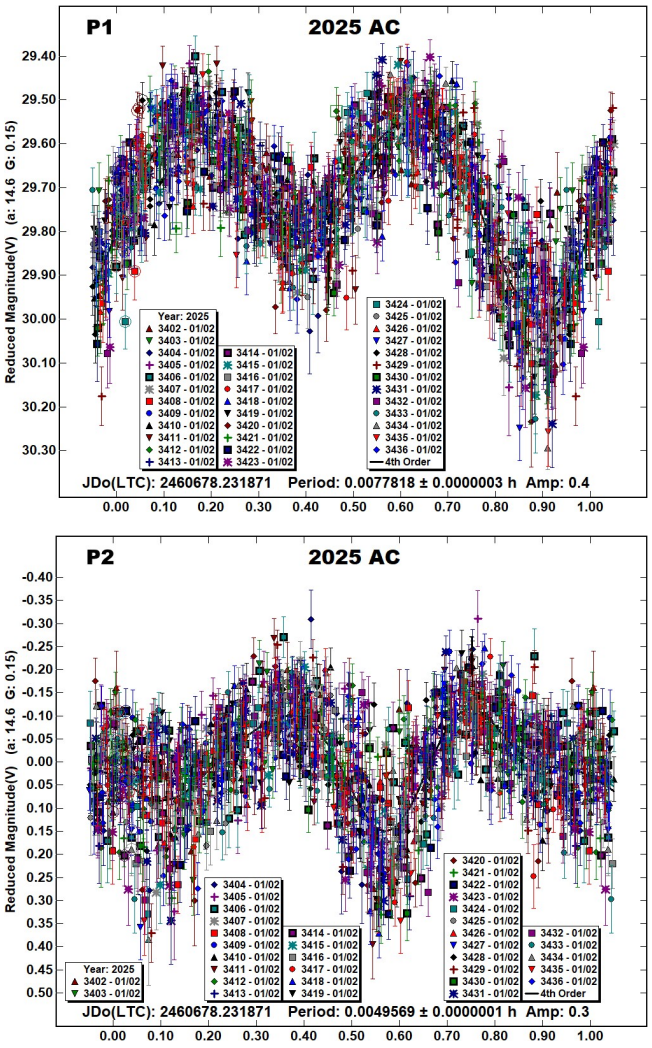

Both of the rotation periods in the NPAR solution are very short (28 and 18 sec), raising the possibility that the lightcurves may be affected by lightcurve smoothing. The optimum exposure length for a detection of the second harmonic (generally the strongest harmonic in most lightcurves) for an asteroid in principal axis rotation is determined by Pravec et al. (2000) to be 0.185 × rotation period, so for an 18 s period, optimum exposure length = 3.3 s. With longer exposure lengths lightcurve smoothing would start to reduce the apparent amplitude and increasingly deform the lightcurve shape (Birtwhistle, 2021). However, for a tumbling asteroid, the transition from maximum to minimum light, or vice versa can occur faster than might be inferred from either of the individual related NPAR periods, causing an exposure to 'average out' the change in intensity. To investigate whether an exposure length of 1.6 s may have caused lightcurve smoothing for this NPA rotation, an empirical analysis of the calculated NPAR lightcurve for 2025 AC during the time it was under observation was calculated. This indicated that the largest difference between consecutive extrema was 0.62 mag and the fastest transition with at least half this maximum value took ~3.6 s, with most of the transitions being smaller and slower. Assuming a worst case where 2 maxima and 2 minima occur at this fastest rate, equivalent to a bimodal lightcurve rotation period of 3.6 × 4 = 14.4 s, the optimal exposure length would be 0.185 × 14.4 = 2.7 s. Due to the fast apparent motion of 2025 AC, exposure lengths were limited to 1.6 s or shorter and therefore it is unlikely that either the P1 or P2 lightcurves for 2025 AC are significantly affected by lightcurve smoothing.

It is noted that the calculated ephemeris magnitude in the H-G system, using an assumed value of G = 0.15 predicts 2025 AC fading by about 0.13 mags during the 1.9 h of observation as the phase angle increased from 14 to 23°, but the observed magnitude actually brightened linearly throughout by about 0.07 mag, suggesting an issue with the assumed value of G. The NPAR lightcurve solution given here uses G = 0.15 with small zero-point adjustments to each of the 35 sessions to remove the brightness trend, minimising the overall RMS of the fit. However, to investigate the phase effect, an hour of photometry (6 sessions) from the previous night 2025 Jan 1.95 UTC was measured when 2025 AC was 2 mags fainter, together with 10 minutes of photometry (4 sessions) obtained on 2025 Jan 3.04 UTC, making a total of 45 sessions spanning phase angles from 14 - 56°. All the images were taken with no filter and measured using G-band comparison star mags. The photometry was reduced to unit distance and each session then averaged. Due to the superfast rotation, most of the sessions cover 3 or more P2 rotations, effectively reducing the lightcurve amplitude to zero. The full amplitude from NPAR solutions on the 1st and 2nd nights are similar, at 0.73 and 0.70 mags respectively and an adjustment of half the amplitude, -0.36 mags was made to each session to make the values equivalent to the maximum brightness of the lightcurve. One further adjustment of 0.28 mag was made using the MPC V-band correction for G to approximate mag V (MPC, 2025b). All the 45 data points were then entered into the *MPO Canopus* H/G Calculator, resulting in a best-fit H/G relationship of:

H = 29.75 ± 0.10, G = 1.24 ± 0.18

indicating that the asteroid has an unusually shallow phase function with a high value for G. Forcing G = 0.15 gives a much poorer fit:

H = 28.81 ± 0.25, G = 0.15 ± 0.20 (assumed)

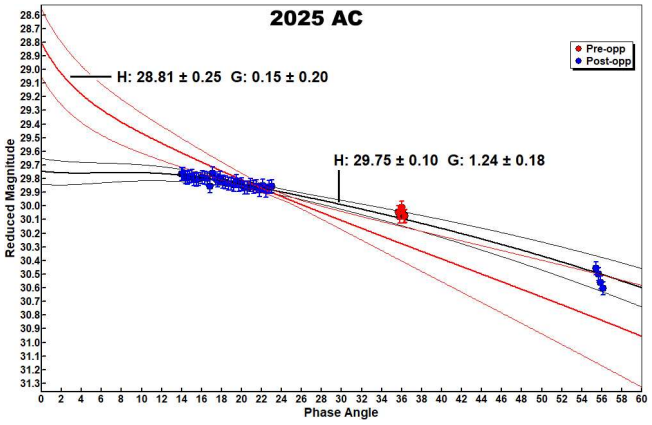

This compares with:

H = 29.03, G = 0.15 (assumed) (JPL, 2025b)
H = 29.02, G = 0.15 (assumed) (MPC, 2025a)

The H = 29.75 value suggests the physical size of 2025 AC may be only ~60% of that expected from the JPL and MPC H values which are both presumed calculated from lightcurve mean rather than maximum values.

It is expected that 2025 AC may be rated as PAR = -3 where NPA rotation has been reliably detected with the two periods resolved. (Petr Pravec, personal communication). The NPAR solution indicates the full amplitude of the tumbling rotation was 0.7 mag. During the 1.9 h of observation used for these lightcurves, 2025 AC completed 249 rotations of the P1 period and 391 rotations of the P2 period.

2025 CF. Another very small Apollo (*H = 29.9, D ~3 m*), this one was discovered by the Mt. Lemmon Survey on 2025 Feb 2.29 UTC, just 19 hours before it passed Earth at a distance of 0.3 LD (Coffano et al., 2025). It was observed for 36 minutes starting at 2025 Feb 2.89 UTC when it was at 0.6 LD and 16th mag. With very fast apparent motion (360 increasing to 440 arcsec/min) exposures were reduced from 1.5 to 1.2 s and measurements correspondingly have rather poor SNr. A period spectrum shows three well defined minima, with the best-fit being at 0.1062 ± 0.0005 h (~6.4 min) and is shown in the phased plot to represent a bimodal lightcurve with an amplitude of 0.4. 2025 CF completed 5.7 rotations while under observation.

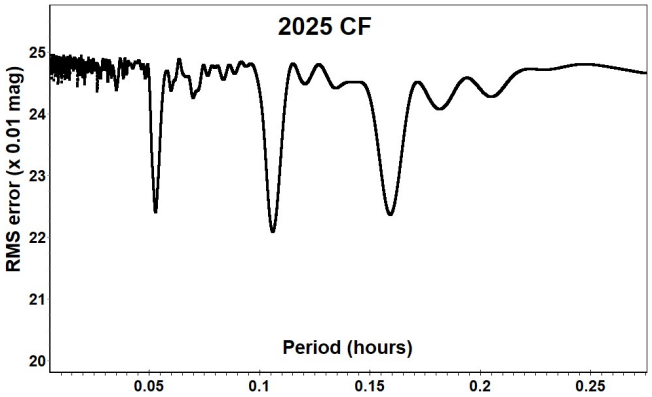

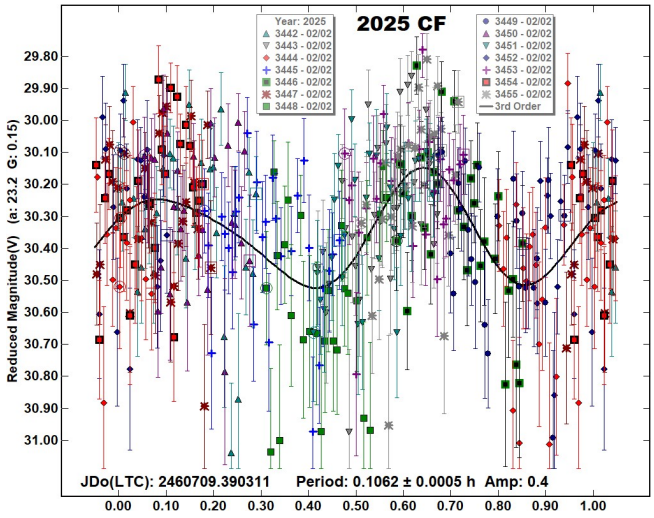

2025 CQ1. Discovered by ATLAS-HKO, Haleakala on 2025 Feb 5.4 UTC, this Apollo (*H = 26.2, D ~17 m*) passed Earth at 2.3 LD 8 hours later (Manca et al., 2025). It was observed for 80 minutes starting at 2025 Feb 5.96 UTC, a few hours after closest approach, when it was at 2.5 LD and 16th mag. Again, the fast apparent motion of 200 arcsec/min limited exposures to 2.4 - 2.6 sec to reduce image trailing. The best-fit solution from the period spectrum is at 0.406 ± 0.002 h (~24 min) and indicates that 3.3 rotations were completed during the time it was under observation.

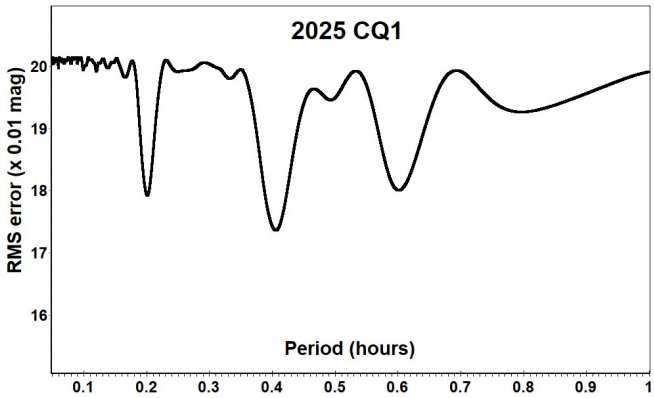

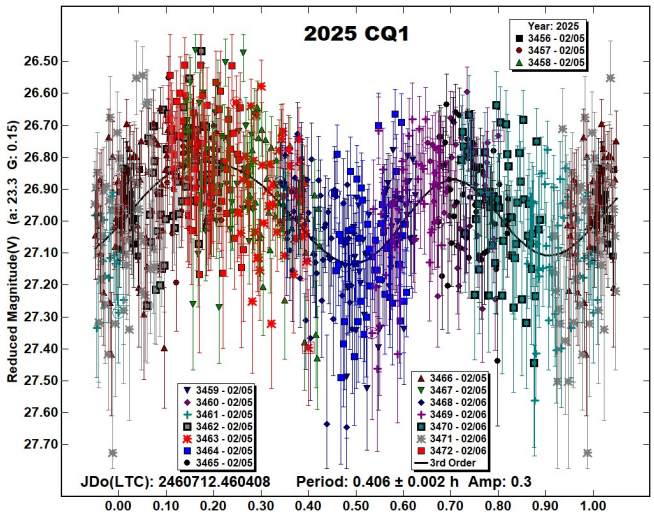

2025 DJ22. This is a small Apollo (*H = 27.0, D ~12 m*) discovered by the Mt. Lemmon Survey on 2025 Feb 27 and which passed closest to Earth on 2025 Mar 1.5 UTC at 1.5 LD (Fumagalli et al., 2025). It was followed for 3.2 h starting at 2025 Feb 28.90 UTC when it was at 2 LD and with apparent speed accelerating to 170 arcsec/min. Exposures were reduced from 4.4 to 3.4 sec to keep trailing within the *Astrometrica* measurement annulus. A linearly scaled period spectrum shows a number of very sharply defined minima and again these reveal signs of NPA rotation, with two sets of regularly spaced minima, this time at small integer multiples of 0.00656 h (~24 s) and 0.01037 h (~37 s). Analysis with the *MPO Canopus* Dual Period Search function determined the 24 s and 37 s values represent monomodal lightcurves and that the best fit periods give bimodal lightcurves at double those values, where:

P1 = 0.013112 ± 0.000002 h (~47 s), amplitude 0.34
P2 = 0.020735 ± 0.000002 h (~75 s), amplitude 0.28

The resulting lightcurves for this solution are labelled P1 and P2.

There are a number of other lesser minima in the period spectrum, all related to two other apparent periods, P3 = 0.016065 h (~58 s) and P4 = 0.009962 h (~36 s). However, P3 and P4 are both linearly related to the main frequencies of P1 and P2, where 1/P1 + 1/P2 = 2/P3 and 2/P1 + 1/P2 = 2/P4 and therefore, do not affect the conclusion that 2025 DJ22 is definitely tumbling. It is expected it may be rated as PAR = -3 on the scale defined in Pravec et al., (2005) (Petr Pravec, personal communication). During the time it was being observed, 246 rotations of the P1 period were completed and 155 of the P2 period. The NPAR lightcurves indicate that the full amplitude of the tumbling rotation was 0.6 mag. It is noted that the SBDB (JPL, 2025b) lists an approach to within ~6 LD of Earth on 2031 Sep 1.0 UTC when there may be short window to recover 2025 DJ22 at 19th mag with positional uncertainty < 3° but with interference from the full Moon.

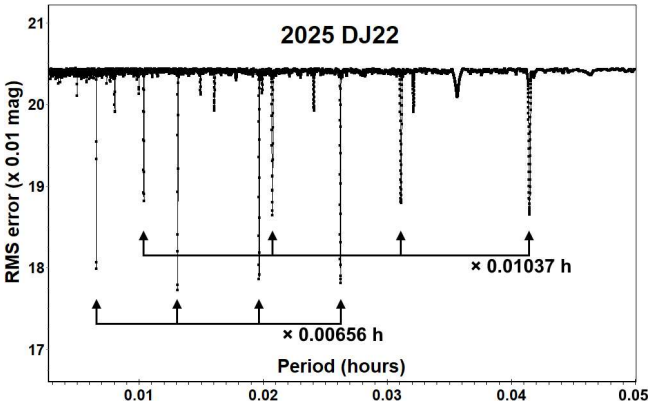

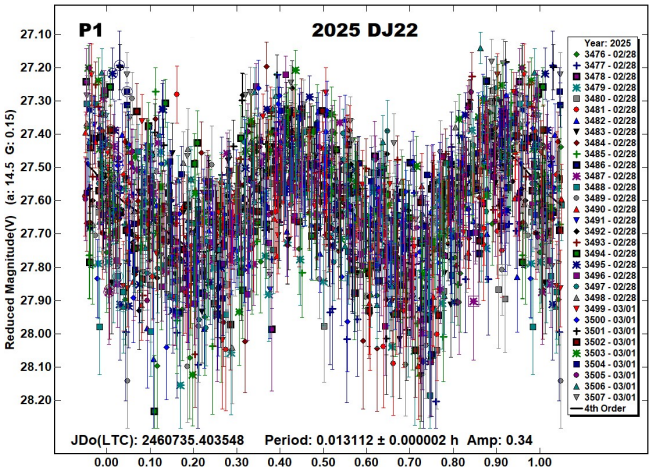

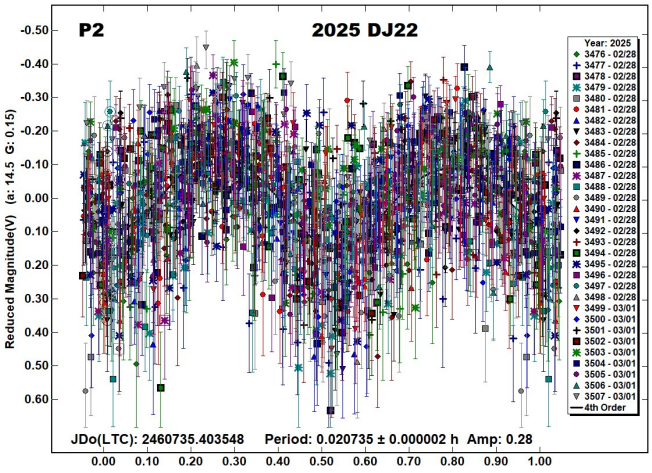

2025 FA. Another Apollo (*H = 22.5, D ~95 m*), discovered by the Catalina Sky Survey on 2025 Mar 16 and, 4 days later, made a relatively distant pass of Earth at 21 LD, 0.05 AU (Bacci et al., 2025). It was observed for 2.9 h starting on 2025 Mar 18.87 UTC and the best-fit solution indicates it has a slightly asymmetric lightcurve with a rotation period of 0.11282 ± 0.00003 h (~6.8 min) and amplitude of 0.9 mag. 2025 FA completed 25 rotations while under observation.

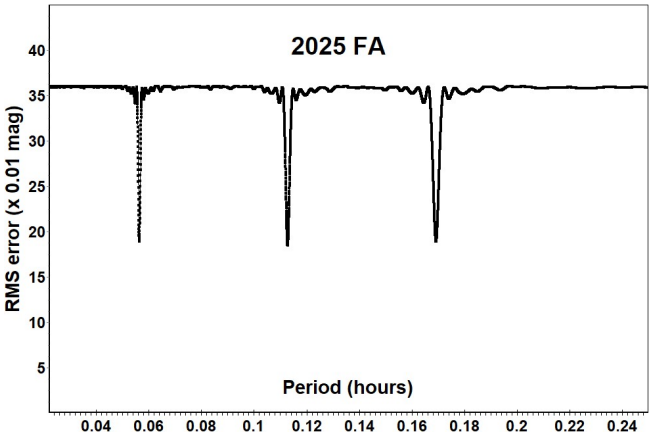

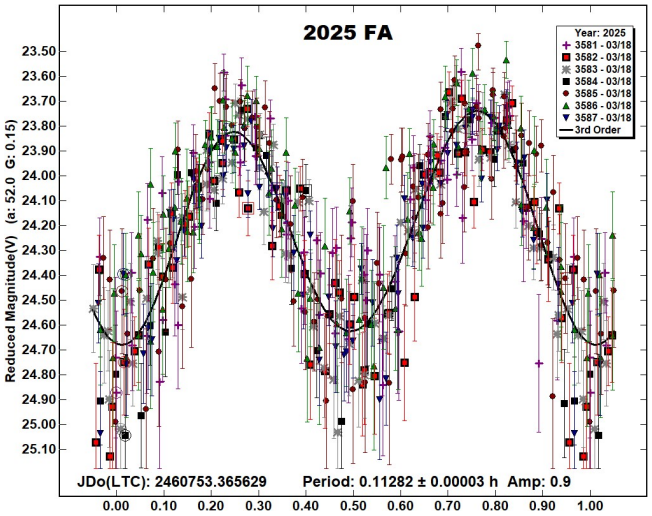

2025 GB. Discovered on 2025 Apr 01.3 UTC by ATLAS-HKO, Haleakala this Apollo (*H = 24.8, D ~33 m*) made an approach to 1.9 LD on 2025 Apr 3.06 UTC (Hoegner et al., 2025a). It was observed for 1.7 h starting on 2025 Apr 1.91 UTC and again for 2.1 h starting on 2025 Apr 2.91 UTC. Apparent speed limited exposure lengths to no more than 8.7 s on the first date and 4.2 s on the second to keep trailing within the measurement annulus used in *Astrometrica*. Analysis reveals a similar well-defined asymmetric bimodal lightcurve on both dates, the period spectrum for the second date is given. Amplitude reduced from 1.27 to 1.02 as the phase angle halved from 68° to 33°. While under observation 2025 GB completed 9 rotations on the first night and 12 on the second.

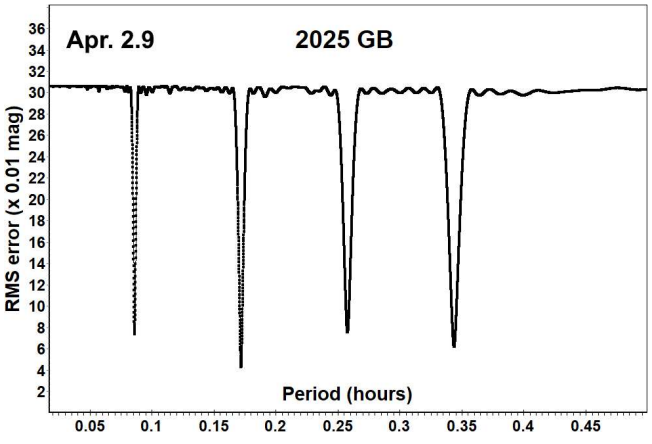

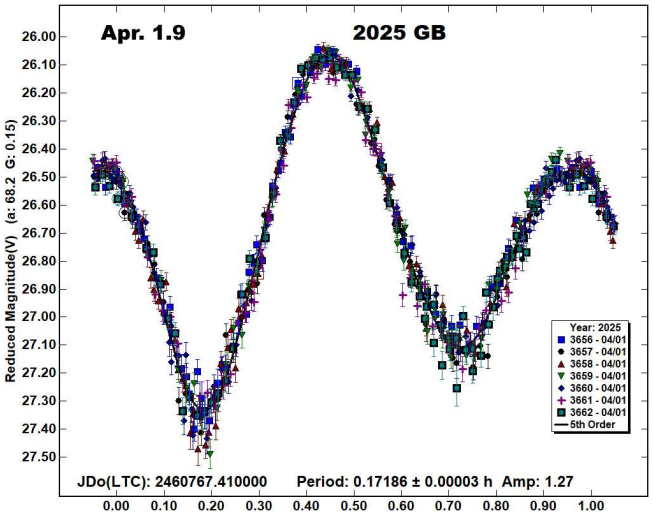

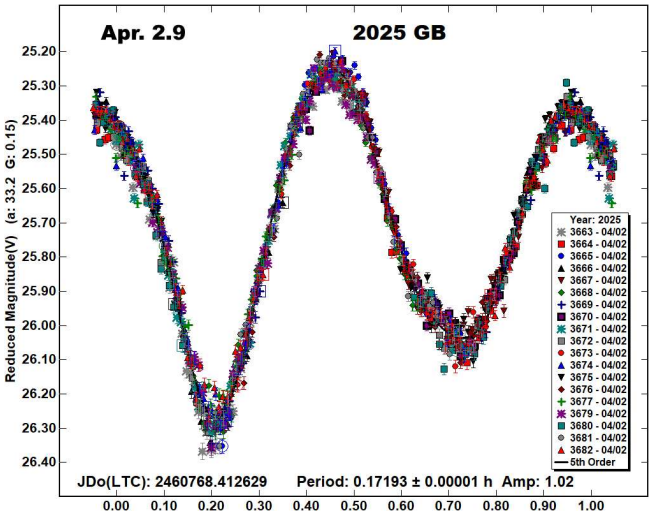

It is noted that the two lightcurves, with starting points 24.06 h apart appear to be aligned at approximately the same rotational phase. Using the better constrained period from the second date the number of rotations between the two dates is calculated to be 139.95, implying that the same features would be found approximately at the same phase on each plot. A check of the likely error in number of rotations ΔN between the two dates was made, derived from eq. (3) in Kwiatkowski et al. (2010):

$$\Delta N \approx \Delta t \, \Delta P / P^2$$

where Δt is the time interval separating two lightcurves, P is the period from one of the individual solutions and ΔP is the maximum period uncertainty, with Δt, ΔP and P expressed in the same units. This suggests an error of ≈ 0.01 rotation periods is to be expected between the two dates and therefore confirming features in the lightcurves are indeed likely to match at approximately the same phase in the two diagrams.

2025 GD. Discovered on 2025 Apr 01.4 UTC by ATLAS-MLO, Mauna Loa this Apollo (*H = 24.7, D ~34 m*) made an approach to 2.5 LD on 2025 Apr 5.86 UTC (Hoegner et al., 2025b). It was observed for 2.3 h starting on 2025 Apr 4.86 UTC and again for 2.5 h starting on 2025 Apr 5.83 UTC. Apparent speed limited exposure lengths to no more than 8 s on the first date and 3.8 s on the second. Period spectrum plots for both dates are very similar, the plot for the second date is given. All 12 minima are related, being integer multiples of either ⅓ or ½ of the best-fit period, which on both dates is 0.017624 ± 0.000002 h (~63.4 seconds) and represented by an asymmetric bimodal lightcurve. During the time it was under observation 2025 GD completed 128 rotations on Apr 4 and 141 on Apr 5.

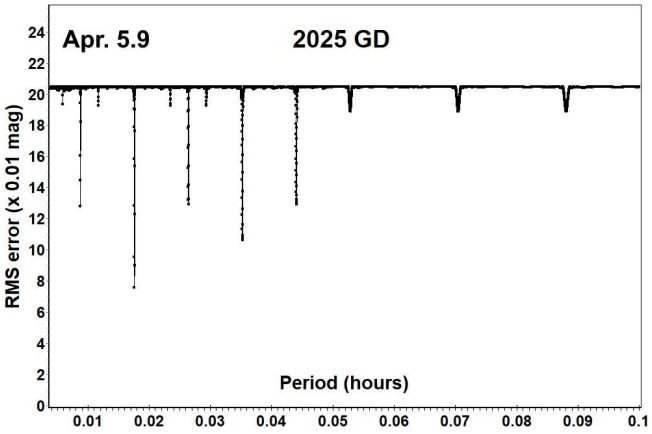

Similarly to 2025 GB, the 23.40 h between the start of the two phased lightcurve plots is equivalent to 1328.01 rotations, again implying that the same features would be found approximately at the same phase on each plot. In this case, the likely error in number of rotations ΔN between the two dates is determined using the same method used for 2025 GB to be ΔN ≈ 0.13 and so again confirming features in the lightcurves are likely to align at approximately the same phase in the two diagrams. It can be seen that as the phase angle increased from 44° to 54° the depth of the minima at phase ~ 0.25 increases significantly whereas the minima at phase ~ 0.75 reduces.

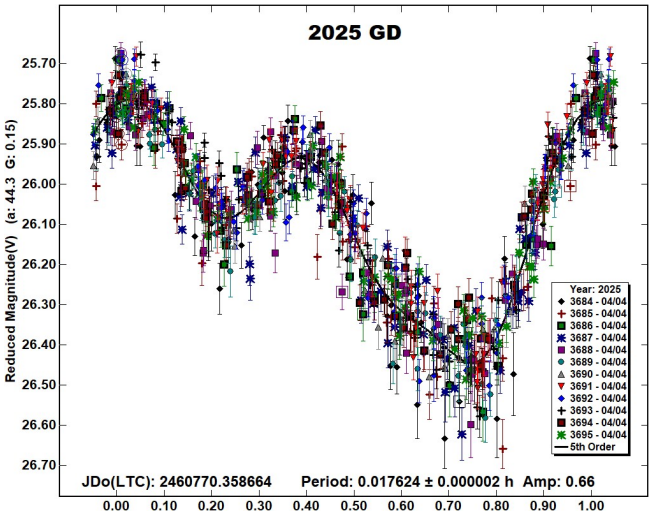

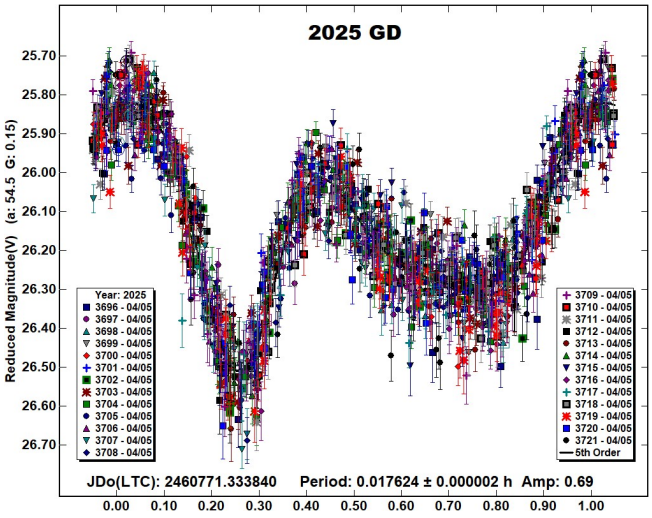

Number	Name	yyyy mm/dd	Phase	L_{PAB}	B_{PAB}	Period(h)	P.E.	Amp	A.E	PAR	H
484976	2009 UN3	2010 02/10-02/11	44.7,46.2	163	10	4.091	0.001	0.50	0.03		18.5
	2025 AB	2025 01/02-01/02	43.5,49.2	123	11	0.057151	0.000008	1.2	0.3	-3	27.1
						0.034019	0.000004	0.5	0.3		
	2025 AC	2025 01/02-01/02	13.9,23.1	103	9	0.0077818	0.0000003	0.4	0.1	-3	29.0
						0.0049569	0.0000001	0.3	0.1		
	2025 CF	2025 02/02-02/02	22.9,26.7	122	0	0.1062	0.0005	0.4	0.3		29.9
	2025 CQ1	2025 02/05-02/06	23.6,28.1	137	-13	0.406	0.002	0.3	0.2		26.2
	2025 DJ22	2025 02/28-03/01	14.8,20.4	167	-5	0.013112	0.000002	0.34	0.22	-3	27.0
						0.020735	0.000002	0.28	0.22		
	2025 FA	2025 03/18-03/18	52.1,51.3	156	18	0.11282	0.00003	0.9	0.3		22.5
	2025 GB	2025 04/01-04/01	68.3,66.7	171	27	0.17186	0.00003	1.27	0.07		24.8
	2025 GB	2025 04/02-04/02	33.0,29.3	191	16	0.17193	0.00001	1.02	0.05		24.8
	2025 GD	2025 04/04-04/04	44.2,44.0	177	13	0.017624	0.000002	0.66	0.10		24.7
	2025 GD	2025 04/05-04/05	54.4,58.1	170	-11	0.017624	0.000002	0.69	0.11		24.7

Table II. Observing circumstances and results. The phase angle is given for the first and last date. If preceded by an asterisk, the phase angle reached an extrema during the period. L_{PAB} and B_{PAB} are the approximate phase angle bisector longitude/latitude at mid-date range (see Harris et al., 1984). Amplitude error (A.E.) is calculated as √2 × (lightcurve RMS residual). PAR is the expected Principal Axis Rotation quality detection code (Pravec et al., 2005) and H is the absolute magnitude at 1 au from Sun and Earth taken from the Small-Body Database Lookup (JPL, 2025b).

Number	Name	Integration times	Max intg/Pd	Min a/b	Pts	Flds
484976	2009 UN3	4-6	0.000	1.2	1061	18
	2025 AB	2.3-3.9	0.032[1]	1.9*	1412	24
	2025 AC	1.4-1.6	0.090[1]	1.5	1388	35
	2025 CF	1.2-1.5	0.004	1.2	392	14
	2025 CQ1	2.4-2.6	0.002	1.2	813	17
	2025 DJ22	3.4-4.4	0.093[1]	1.5	1554	32
	2025 FA	9-20	0.049	1.4*	468	7
	2025 GB	4.1-8.7	0.014	1.6[2]	1614	26
	2025 GD	3.8-8	0.126	1.3*	2037	38

Table I. Ancillary information, listing the integration times used (seconds), the fraction of the period represented by the longest integration time (Pravec et al., 2000), the calculated minimum elongation of the asteroid (Zappala et al., 1990), the number of data points used in the analysis and the number of times the telescope was repositioned to different fields. Note: * = Value uncertain, based on phase angle > 40°, 1 = Calculated using the shorter of the NPAR periods, 2 = Calculated for 2025 Apr 2.9.

Acknowledgements

The author would like to thank Dr. Petr Pravec, Astronomical Institute, Czech Republic for his help with the data analysis of the tumbling asteroids reported in this paper. The author also gratefully acknowledges a Gene Shoemaker NEO Grant from the Planetary Society (2005) and a Ridley Grant from the British Astronomical Association (2005), both of which facilitated upgrades to observatory equipment used in this study. This work has made use of data from the European Space Agency (ESA) mission Gaia (*https://www.cosmos.esa.int/gaia*), processed by the Gaia Data Processing and Analysis Consortium (DPAC, *https://www.cosmos.esa.int/web/gaia/dpac/consortium)*. Funding for the DPAC has been provided by national institutions, in particular the institutions participating in the Gaia Multilateral Agreement.

References

ADS (2025). Astrophysics Data System. *https://ui.adsabs.harvard.edu/*

Bacci, P.; Maestripieri, M.; Tesi, L.; Fagioli, G.; Buzzi, L.; Pettarin, E.; Groeller, H.; Beuden, T.; Carvajal, V.F.; Fay, D.; Fazekas, J.B.; Fuls, D.C.; Gibbs, A.R.; Grauer, A.D.; Hogan, J.K. and 32 colleagues (2025). "2025 FA." MPEC 2025-F05. *https://minorplanetcenter.net/mpec/K25/K25F05.html*

Birtwhistle, P. (2021). "Ultra-Fast Rotators: Results and Recommendations for Observing Strategies." *Minor Planet Bull.* **48**, 346-352.

Coffano, A.; Marinello, W.; Micheli, M.; Pizzetti, G.; Soffiantini, A.; Bertolini, F.; Colzani, E.; Elli, F.; Redaelli, S.; Valli, E.; Ventre, G.; Sicoli, P.; Pettarin, E.; Beuden, T.; Carvajal, V.F. and 29 colleagues (2025). "2025 CF."" MPEC 2025-C15. *https://minorplanetcenter.net/mpec/K25/K25C15.html*

Fumagalli, A.; Testa, A.; Pittichova, J.; Dupouy, P.; della Vecchia, V.; Fazekas, J.B.; Hogan, J.K.; Gray, B.; Rankin, D.; Shelly, F.C.; Beuden, T.; Carvajal, V.F.; Fay, D.; Fuls, D.C.; Gibbs, A.R. and 15 colleagues (2025). "2025 DJ22." MPEC 2025-D236. *https://minorplanetcenter.net/mpec/K25/K25DN6.html*

Harris, A.W.; Young, J.W.; Scaltriti, F.; Zappala, V. (1984). "Lightcurves and phase relations of the asteroids 82 Alkmene and 444 Gyptis." *Icarus* **57**, 251-258.

Harris, A.W.; Young, J.W.; Bowell, E.; Martin, L.J.; Millis, R.L.; Poutanen, M.; Scaltriti, F.; Zappala, V.; Schober, H.J.; Debehogne, H.; Zeigler, K. (1989). "Photoelectric Observations of Asteroids 3, 24, 60, 261, and 863." *Icarus* **77**, 171-186.

Hicks, M.; Barajas, T.; Shitanishi, J. (2010) "Broadband Colors and Rotation Lightcurves of the Potentially Hazardous Asteroid 2009 UN3." *https://www.astronomerstelegram.org/?read=2449*

Hoegner, C.; Ludwig, F.; Hartmann, M.; Stecklum, B.; Dupouy, P.; Koch, B.; Urbanik, M.; Felber, T.; Losse, F.; Birtwhistle, P.; Remmel, P.; Gerhard, C.; Haeusler, B.; Duin, H.; Dekelver, P.-J. and 13 colleagues (2025a). "2025 GB." MPEC 2025-G32. *https://minorplanetcenter.net/mpec/K25/K25G32.html*

Hoegner, C.; Ludwig, F.; Hartmann, M.; Stecklum, B.; Bacci, P.; Maestripieri, M.; Tesi, L.; Fagioli, G.; Pettarin, E.; Robson, M.; Cloutier, W.; Dupouy, P.; Laborde, J.; Thinius, B.; Nevski, V. and 28 colleagues (2025b). "2025 GD." MPEC 2025-G39. *https://minorplanetcenter.net/mpec/K25/K25G39.html*

JPL (2025a). Sentry: Earth Impact Monitoring. *https://cneos.jpl.nasa.gov/sentry/*

JPL (2025b). Small-Body Database Lookup. *https://ssd.jpl.nasa.gov/tools/sbdb_lookup.html*

JPL (2025c). Small-Body Radar Astrometry *https://ssd.jpl.nasa.gov/sb/radar.html*

Kowalski, R.A.; Beuden, T.; Carvajal, V.F.; Fay, D.; Fazekas, J.B.; Fuls, D.C.; Gibbs, A.R.; Grauer, A.D.; Groeller, H.; Hogan, J.K.; Larson, S.M.; Leonard, G.J.; Rankin, D.; Seaman, R.L.; Shelly, F.C. and 16 colleagues (2025a). "2025 AB." MPEC 2025-A26. *https://minorplanetcenter.net/mpec/K25/K25A26.html*

Kowalski, R.A.; Gray, B.; Rankin, D.; Shelly, F.C.; Dupouy, P.; Laborde, J.; Holmes, R.; Linder, T.; Birtwhistle, P.; Tanasiychuk, Y.V.; Kozhukhov, A.M.; Brosio, A.; Denneau, L.; Siverd, R.; Tonry, J. and 5 colleagues (2025b). "2025 AC." MPEC 2025-A28. *https://minorplanetcenter.net/mpec/K25/K25A28.html*

Kwiatkowski, T.; Buckley, D.A.H.; O'Donoghue, D.; Crause, L.; Crawford, S.; Hashimoto, Y.; Kniazev, A.; Loaring, N.; Romero Colmenero, E.; Sefako, R.; Still, M.; Vaisanen, P. (2010). "Photometric survey of the very small near-Earth asteroids with the SALT telescope - I. Lightcurves and periods for 14 objects." *Astronomy & Astrophysics* **509**, A94.

Manca, F.; Testa, A.; Bressan, F.; Ierman, G.; Pettarin, E.; Dupouy, P.; de Vanssay, J.B.; della Vecchia, V.; Grazzini, L.; Losse, F.; Birtwhistle, P.; Demeautis, C.; Korlevic, K.; Poropat, L.; Denneau, L. and 8 colleagues (2025). "2025 CQ1." MPEC 2025-C58. *https://minorplanetcenter.net/mpec/K25/K25C58.html*

McNaught, R.H.; Beshore, E.C.; Boattini, A.; Garradd, G.J.; Gibbs, A.R.; Grauer, A.D.; Hill, R.E.; Kowalski, R.A.; Larson, S.M. (2009) "2009 UN3." MPEC 2009-U52. *https://minorplanetcenter.net/mpec/K09/K09U52.html*

MPC (2025a). MPC Orbit database MPCORB. *https://www.minorplanetcenter.net/iau/MPCORB/MPCORB.DAT*

MPC (2025b). Magnitude Band Conversion table. *https://www.minorplanetcenter.net/iau/info/BandConversion.txt*

NEODyS (2025). Near Earth Objects Dynamic Site. *https://newton.spacedys.com/neodys*

Polishook, D. (2012). "Lightcurves and Spin Periods of Near-Earth Asteroids, The Wise Observatory, 2005 - 2010." *Minor Planet Bull.* **39**, 187-192.

Pravec, P.; Hergenrother, C.; Whiteley, R.; Sarounova, L.; Kusnirak, P.; Wolf, M. (2000). "Fast Rotating Asteroids 1999 TY2, 1999 SF10, and 1998 WB2." *Icarus* **147**, 477-486.

Pravec, P.; Harris, A.W.; Scheirich, P.; Kušnirák, P.; Šarounová, L.; Hergenrother, C.W.; Mottola, S.; Hicks, M.D.; Masi, G.; Krugly, Y.N.; Shevchenko, V.G.; Nolan, M.C.; Howell, E.S.; Kaasalainen, M.; Galád, A. and 5 colleagues. (2005). "Tumbling Asteroids." *Icarus* **173**, 108-131.

Raab, H. (2024). Astrometrica software, version 4.15.0.460. *http://www.astrometrica.at/*

Warner, B.D.; Harris, A.W.; Pravec, P. (2009). "The Asteroid Lightcurve Database." *Icarus* **202**, 134-146. Updated 2023 Oct. *https://www.minorplanet.info/php/lcdb.php*

Warner, B.D. (2023). MPO Software, Canopus version 10.8.6.20. Bdw Publishing, Colorado Springs, CO.

Zappala, V.; Cellini, A.; Barucci, A.M.; Fulchignoni, M.; Lupishko, D.E. (1990). "An analysis of the amplitude-phase relationship among asteroids" *Astron. Astrophys*. **231**, 548-560.

LIGHTCURVES AND ROTATION PERIODS FOR SIX NEAR-EARTH ASTEROIDS

Daniel P. Bamberger
Northolt Branch Observatories
Alfred-Wegener-Straße 34
35039 Marburg, GERMANY
danielpeter1204@aol.com

Guy Wells
Northolt Branch Observatories
Northolt, ENGLAND

(Received: 2025 April 14)

Unfiltered CCD photometric observations of the near-Earth asteroids 2015 DP155, 2020 SW, 2020 UQ6, 2023 DZ2, 2025 GB, and 161989 Cacus have been made between 2018 and 2025. All but one of them have known rotation periods. We confirm those results, and find a new rotation period of 0.172 hours for 2025 GB.

All observations reported here were made with the 0.25-m Ritchey-Chretien telescope at Northolt Branch Observatory (MPC: Z80) in London, UK, on multiple nights between 2018 and 2025.

2015 DP155 is an Amor-type potentially hazardous asteroid with a diameter of about 160 meters. It made a close approach to Earth on 11 June 2018, at a distance of 0.023 au (JPL, 2025). We took photometric observations it on five nights around the date of the closest approach.

The lightcurve database includes three entries for this asteroid. Reshetnyk et al. (2018) found a rotation period of 3.105 ± 0.004 hours, with a maximum amplitude of 1.0 mag. Warner (2018) found a similar period, at 3.097 ± 0.001 hours. McGilvray et al. (2022) made use of our data for shape-modelling purposes.

We find a rotation period of 3.0945 ± 0.0005 hours, with a large amplitude of 1.16 mag. The period is unambigous. However, due to less-than-complete coverage, the shape of the lightcurve and the size of the amplitude are not well constrained.

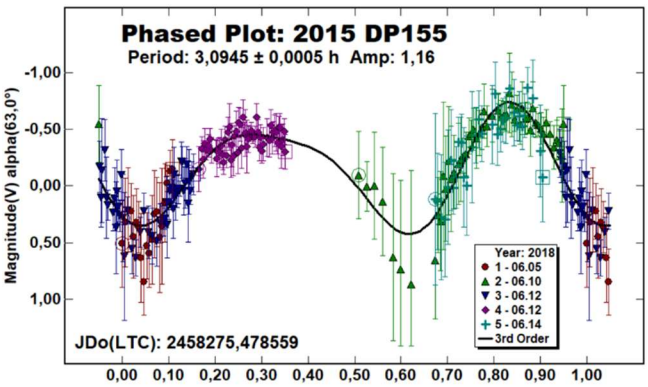

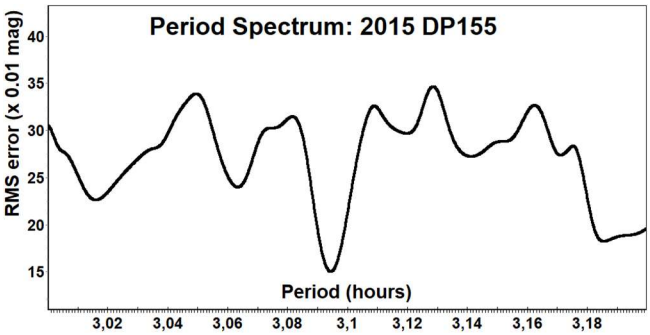

2020 SW is a small Aten-type asteroid with a diameter between 4 and 9 meters. On 24 September 2020, it came within 0.00019 au (just 28,000 km) of Earth (JPL, 2025). We observed it the night before, taking very short exposures that not only prevented trailing of the fast-moving asteroid, but also allowed us to search for very short periods.

A rotation period of 0.0079039 ± 0.0000001 hours, with a maximum amplitude of 0.73 mag, has been reported by Peter Birtwhistle (2021a). Birtwhistle's result references a previous version of our lightcurve, citing a post we had made on the platform Twitter (Wells et al., 2020). At the time, we gave a period of 0.00790 ± 0.00001 hours and an amplitude of 0.72 mag.

We have now re-analyzed that data, and find a rotation period of 0.007905 ± 0.000002 hours, with a slightly larger amplitude of 0.74 mag. The rotation period of 28.4 seconds is among the shortest of any asteroid in the lightcurve database.

The period spectrum has peaks at multiple alternative periods, all of which were manually ruled out as aliases.

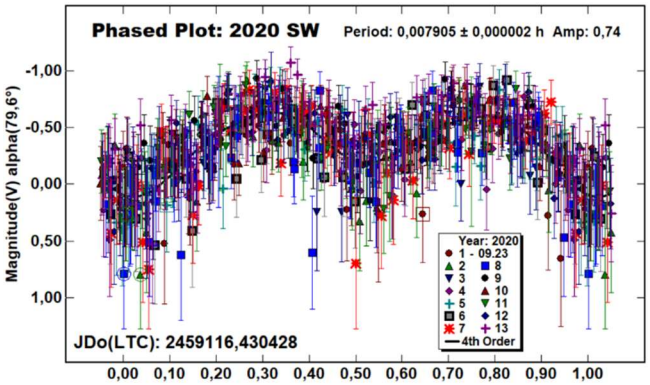

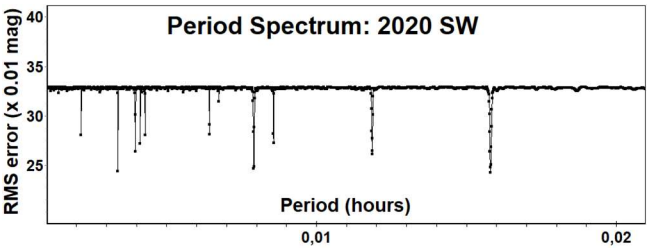

2020 UQ6 is an Apollo-type asteroid. Its absolute magnitude of 22.7 indicates that this is a relatively large Near-Earth asteroid, with a diameter between 90 and 170 meters. We observed it shortly after its close approach to Earth on 26 October 2020 at a distance of 0.01 au (JPL, 2025).

There are three results for this asteroid in the lightcurve database. Guido et al. (2021) found a period of 0.04521 ± 0.0001 hours, with an amplitude of 0.57 mag. Birtwhistle (2021b) gives 0.045210 ± 0.000002 hours, while Beniyama et al. (2022) found a period of 0.045228 ± 0.000008 hours, with a slightly larger amplitude of 0.82 mag.

We find a rotation period of 0.04518 ± 0.00004 hours, and an amplitude of 0.74 mag, slightly shorter than the period reported previously, but with a similar amplitude.

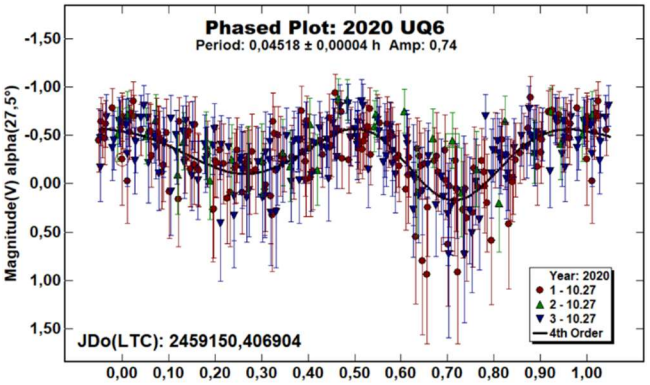

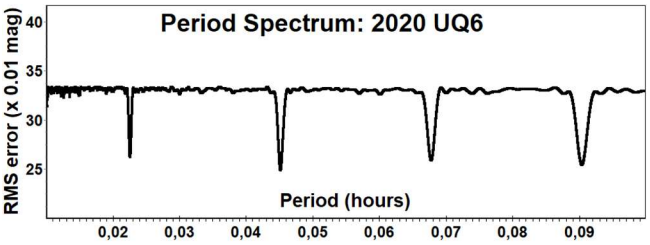

Number	Name	yyyy/mm/dd	Phase	L_{PAB}	B_{PAB}	Period(h)	P.E.	Amp	A.E.	Grp
	2015 DP155	2018/06/05-06/14	32.9,34.1	32	9	3.0945	0.0005	1.16	0.10	9101 NEA
	2020 SW	2020/09/23	15.9,16.4	5	7	0.007905	0.000002	0.74	0.02	9101 NEA
	2020 UQ6	2020/10/27	26.9,27.5	48	-4	0.04518	0.00004	0.74	0.03	9101 NEA
	2023 DZ2	2023/03/24	51.4,59.0	155	-1	0.10462	0.00009	0.38	0.02	9101 NEA
	2025 GB	2025/04/02	30.7,34.0	190	16	0.1720	0.0002	0.77	0.02	9101 NEA
161989	Cacus	2022/08/27-08/31	75.1,86.7	18	11	3.7594	0.0006	1.44	0.04	9101 NEA

Table I. Observing circumstances and results. The phase angle is given for the first and last date. If preceded by an asterisk, the phase angle reached an extrema during the period. L_{PAB} and B_{PAB} are the approximate phase angle bisector longitude/latitude at mid-date range (see Harris et al., 1984). Grp is the asteroid family/group (Warner et al., 2009).

2023 DZ2 is an Apollo-type asteroid. Its absolute magnitude of 24.3 suggests a diameter within a factor of two of 45 meters. It made a close approach to Earth on 25 March 2023, at a distance of 0.0011 au (JPL, 2025). We observed it about 20 hours before the closest approach.

The lightcurve database includes multiple results for this asteroid, all of which give rotation periods near 0.1045 hours, with amplitudes ranging from 0.33 to 0.64 mag.

Our result of 0.10462 ± 0.00009 hours, with an amplitude of 0.38 mag, is consistent with those.

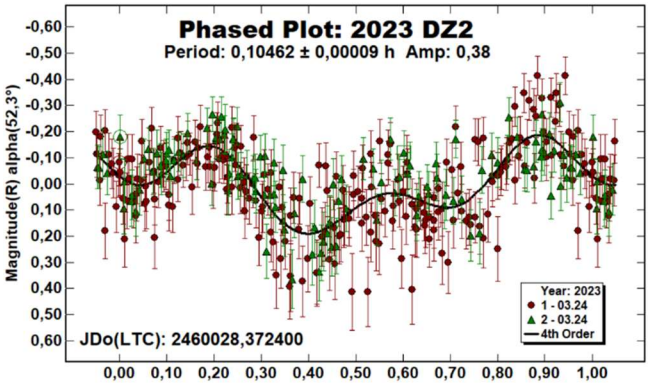

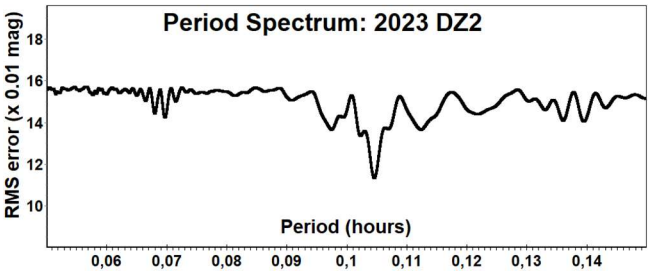

2025 GB is an Apollo-type asteroid with a diameter of about 45 meters. It was discovered on 1 April 2025. We observed it for several hours on the evening of April 2nd, shortly before its closest approach to Earth at a distance of 0.005 au (JPL, 2025). The asteroid's brightness was predicted to peak at 14.4 mag.

The lightcurve database contains no prior results for this asteroid, and we are not aware of any previously reported rotation periods. NASA/Goldstone have reported that the rotation period is probably faster than 30 minutes, based on radar images (Benner, 2025).

We can confirm their conclusion, finding a period of 0.1720 ± 0.0002 hours (10.32 ± 0.01 minutes), with an amplitude of 0.77 mag.

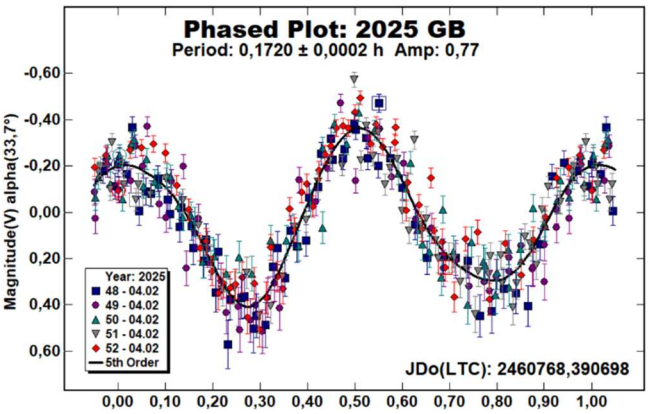

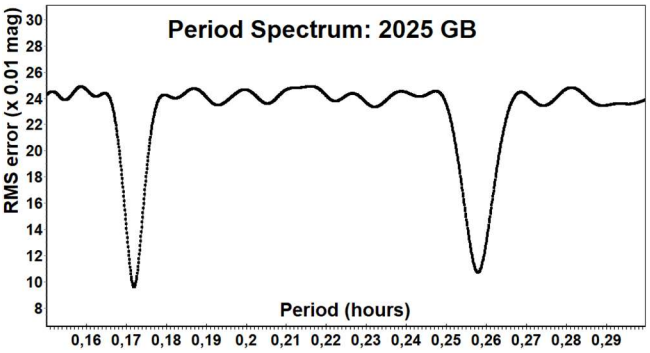

161989 Cacus is an Apollo-type potentially hazardous asteroid with a diameter of 1.9 km. We have observed this asteroid on three nights in late August 2022, shortly before its closest approach to Earth on September 1st at a distance of 0.058 au (JPL, 2025).

The lightcurve database includes multiple results for this asteroid, all with rotation periods near 3.75 hours and amplitudes ranging from 0.80 to 1.32 mag.

We find a similar period of 3.7594 ± 0.0006 hours, with a slightly larger amplitude of 1.44 mag.

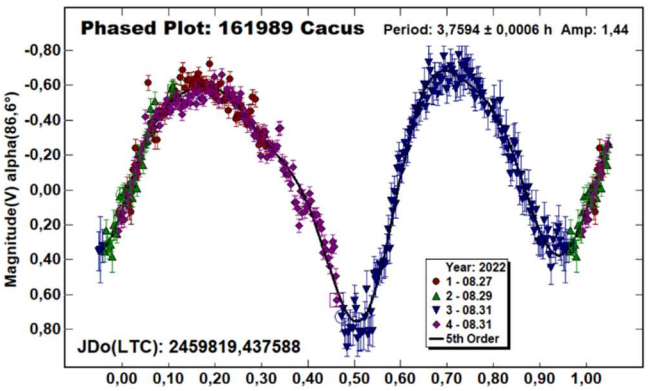

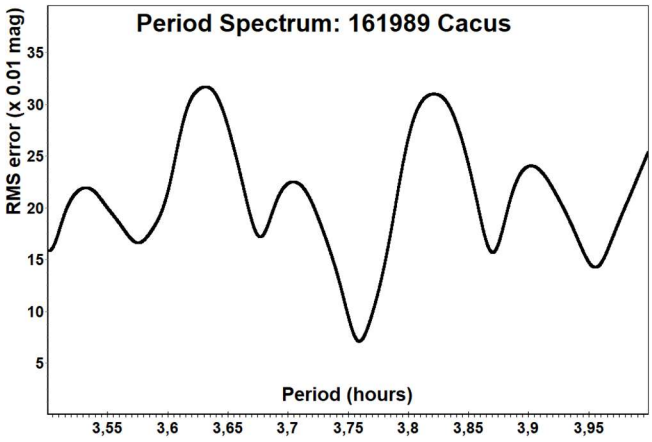

References

Beniyama, J.; Sako, S.; Ohsawa, R.; Takita, S.; Kobayashi, N.; Okumura, S.; Urakawa, S.; Yoshikawa, M.; Usui, F.; Yoshida, F.; Doi, M.; Niino, Y.; Shigeyama, T.; Tanaka, M.; Tominaga, N.; Aoki, T.; Arima, N.; Arimatsu, K.; Kasuga, T.; Kondo, S.; Mori, Y.; Takahashi, H.; Watanabe, J .(2022) "Video observations of tiny near-Earth objects with Tomo-e Gozen." *Publications of the Astronomical Society of Japan* **74**(4), 877-903.

Benner, L.A.M. (2025). "Goldstone Radar Observations of Asteroid 2025 GB." Updated 2025 Apr. 3. *https://echo.jpl.nasa.gov/asteroids/April2025.goldstone.planning.html*

Birtwhistle, P. (2021a). "Lightcurve Analysis for Four Near-Earth Asteroids." *Minor Planet Bulletin* **48**(1), 26-29.

Birtwhistle, P. (2021b). "Lightcurve Analysis for Ten Near-Earth Asteroids." *Minor Planet Bulletin* **48**(2), 180-186.

Guido, E.; Catapano, A.; Noschese, A. (2021). "Rotational Period and Lightcurve Determination of 2020 UQ6." *Minor Planet Bulletin* **48**(2), 105-106.

A NEW SATELLITE OF ASTEROID (6326) IDAMIYOSHI DISCOVERED FROM OCCULTATION OBSERVATION

Kazuhisa Miyashita
International Occultation Timing Association / East Asia
Nagano, JAPAN
k_miyash@nifty.com

Hayato Watanabe
International Occultation Timing Association / East Asia
Mie, JAPAN
starship@cty-net.ne.jp

Hidehito Yamamura
International Occultation Timing Association / East Asia
Shiga, JAPAN
h-yama81215211@mbox.biwako.ne.jp

Norihiro Manago
International Occultation Timing Association / East Asia
Wakayama, JAPAN
n_manago@nifty.com

(Received: 2025 March 12)

A highly probable satellite phenomenon was observed during the occultation of the star UCAC4 525-004262 by the asteroid (6326) Idamiyoshi on August 21, 2024 at 18.75 hr (UT).

(6326) Idamiyoshi is a main belt asteroid, and its known physical parameters are as follows: diameter is 6.856 km ± 0.156 km (Masiero et al., 2011), rotation period is 3.138 hours (Waszczak et al., 2015; Clark, 2016; Durech et al., 2020). The brightness of the asteroid during the occultation was 17.89 mag, and the brightness of the occulted star was 12.672 mag (V) and 11.77 mag (R), with an expected magnitude drop in stellar brightness of 5.5 mag. This phenomenon was reported by three observers. Hayato Watanabe at Nachikatsuura Wakayama, Japan (longitude 135°54'51.7", latitude 33°35'22.4", elevation 5m). Hidehito Yamamura at Taiji Wakayama, Japan (longitude 135°56'35.2", latitude 33°35'48.5", elevation 14m). Norihiro Manago at Kamitonda Wakayama, Japan (longitude 135°24'32.1", latitude 33°41'44.9", elevation 77m). This phenomenon was captured with astronomical CMOS cameras. The observation instruments and exposure times of the tree observers are listed in Table 1. Watanabe and Yamamura observed a disappearance and reappearance of the target star during the occultation event (see Figure 1). Meanwhile, Manago did not observe any decrease in the brightness of the target star due to the occultation phenomenon.

Observer	Telescope aperture	Camera	Frame exposure
Watanabe	20 cm	ZWO-ASI290MM	0.124 sec
Yamamura	20 cm	ZWO-ASI290MM	0.165 sec
Manago	35 cm	ZWO-ASI462MM	0.0358 sec

Table I. Observation instruments. These cameras are of rolling shutter type. The system time of the camera control PC was corrected by GPS and, in addition, the time of the lightcurve measurement was accurately corrected by 1PPS LED light, which was simultaneously recorded during observation.

Figure 1 shows the occultation lightcurve analyzed with the video measurement software *Limovie* (Miyashita et al., 2006). A main dip and a short dip (after the main dip) in the lightcurve is clearly observed in each observation. On the sky plane plot, the two observation sites are separated by 1.1 km in direction nearly perpendicular to the predicted path of the asteroid. The timing of the main dip and the short dip in the lightcurves are nearly identical at both sites. This strongly suggests that the short dip is not due to atmospheric variations or other factors, but rather to the occultation phenomenon.

Watanabe's observation: 2024 August 21, 18:45:23.932 UT: a major dimming lasting 1.053 seconds occurred and 0.39 seconds later, a second dimming was occurred. During the second dimming, the brightness of the target star decreased by 74% (see the top panel of Figure 1). This dimming corresponds to 6-sigma noise in the lightcurve (see Figure 2). The first dimming was deeper than the brightness of the faintest star in the frame (14.055 mag), and during the second dimming, the brightness of the target star decreased to 14.0 mag. If this phenomenon is caused by a double star, the total brightness of the first and second dimming events should be equal to the brightness of the star before the occultation. In this observation, the total brightness of the two dips in the lightcurve was 170% of the pre-occultation brightness of the star. This strongly suggests that the lightcurve obtained by Watanabe (including the two dips) is not caused by a double star.

Yamamura's observation: 2024 August 21, 18:45:24.250 UT: A major dimming occurred lasting 1.073 seconds, and 0.43 seconds later a second dimming occurred. The second dimming lasted for two frames. The maximum brightness drop is 33% depth (4-sigma noise, see Figure 2). Although the second dimming is shallower than Watanabe's observation, it is assumed that a short light drop occurred at near the boundary of frame-exposure and it was recorded into two frames divisionally. Thus, it is likely that this dimming was also caused by the occultation phenomenon.

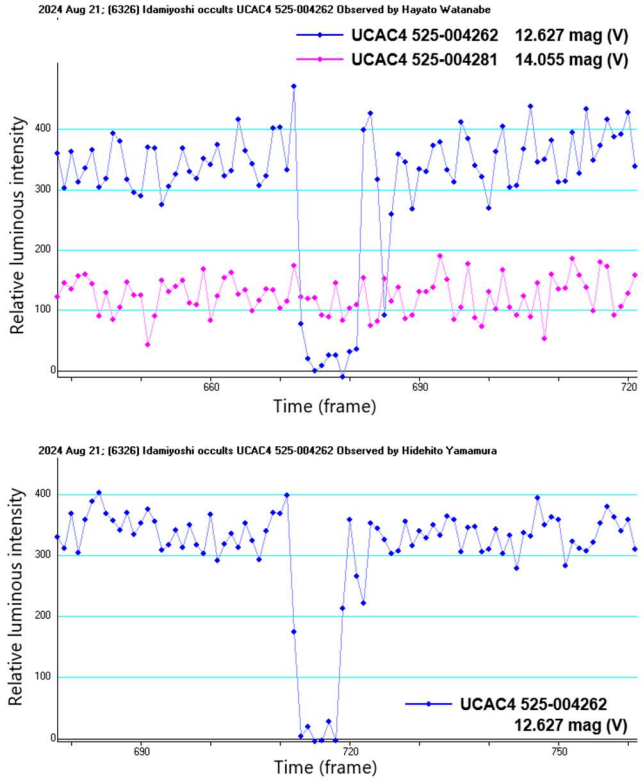

Figure 1. Lightcurves obtained from different observation sites. Top: Watanabe's observation. Bottom: Yamamura's observation.

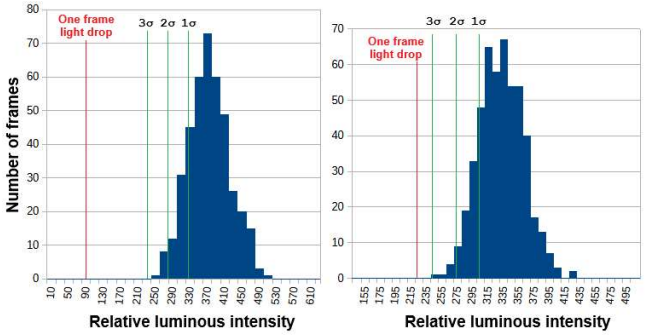

Figure 2. Noise distribution on the lightcurve. Left: Watanabe's observation. Right: Yamamura's observation.

The sky-plane plot (Figure 3) shows that the endpoints of the first long chords observed by Watanabe and Yamamura lie on a line perpendicular to or near the direction of motion of the target star. The same trend holds for the start and end points of the second chord. This indicates that the two observation points are close to the centerline of the shadow cast by the asteroid as it passed. The long chords of the Yamamura (9.0 km) and Watanabe (8.5 km) observations are 1.3 times the diameter of the asteroid as estimated by NEOWISE. The distance between the two dips is 2.7 km in both observations. It is unlikely that as a single asteroid it would have such a gap of 2.7 km as shown in the sky plot. We can exclude the possibility that a topographical effect on the graze occultation makes the two light dips.

There is a gradual change in brightness due to diffraction at the shadow edges of asteroids. In the case of asteroid which has large Fresnel number (almost larger than 10), the light change can be estimated by formula (1).

In the case of a half-plane with a straight edge, the luminous intensity at a distance x from the edge is expressed as follows.

$$I(\omega) = 0.5\, I_0[(0.5 + C(\omega))^2 + (0.5 + S(\omega))^2] \qquad (1)$$

where $C(\omega)$ and $S(\omega)$ are Fresnel integration defined as:

$$C(\omega)=\int_0^{\omega}\cos(\frac{\pi t^2}{2})\,dt\,, \quad S(\omega)=\int_0^{\omega}\sin(\frac{\pi t^2}{2})\,dt$$

when U_f is Fresnel scale unit as $U_f = \sqrt{\frac{\lambda d}{2}}$ then

ω (distance expressed in Fresnel units) is expressed as $\omega = \frac{x}{U_f}$.

The event time is obtained from that the light intensity is 25 % of no-occultation level. The Fresnel number of main body of (6326) Idamiyoshi is 60 in this phenomenon, therefore formula (1) can be applied.

However, in the case of occultation by small bodies as assumed in this second phenomenon, when the short light drop occurs near the boundary between the two frames, the light intensity of the frame may not show the maximum attenuation value. This is because the decrease in light intensity is divided and recorded in two frames. In addition, the Fresnel number will also be a small value, which means that the width of the shadow gradient will be larger, and it will not be possible to apply formula (1). Therefore, we calculated the light intensity distribution in shadow produced by small objects based on formula (2) (Trahan and Hyland, 2014; Roques et al., 1987) and compared the result of the diffraction simulation with the observed lightcurve.

$$I(P_{m.n}) = I(_0)|1 - \frac{1}{2i}\sum_{j,k}\Gamma(j,k)[F(v_2) - F(v_1)][F(w_2) - F(w_1)]|^2 \quad (2)$$

where I($p_{m,n}$): Light intensity on the site (m, n) on the observation plane. I(o) : Light intensity when there is no opaque object. $\Gamma(j,k)$: If a part of the object is contained in the micro-rectangle then this parameter is 1, if not then 0.

(v_1,ω_1), (v_2,ω_2) : Distance expressed in Fresnel units at two diagonal point of micro-rectangle.

$$F(x) = \int_0^x \exp\left(\frac{i\pi t^2}{2}\right)dt = C(x) - iS(x)$$

$C(x)$ and $S(x)$ are Fresnel integration.

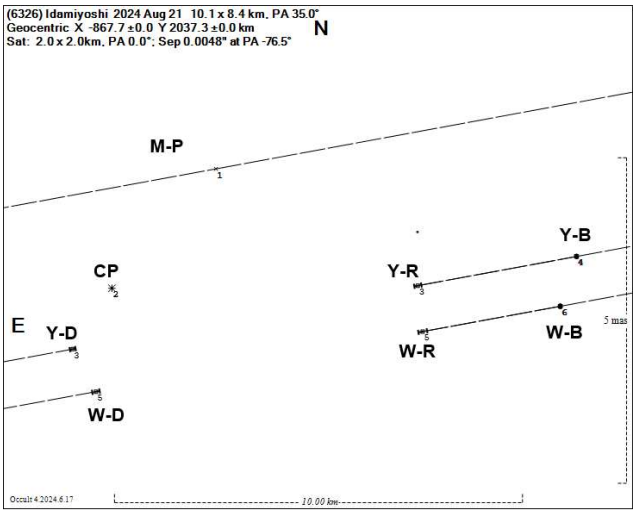

Figure 3. Sky-plane plot. Lines show the relative star's motion when no occulted. M-P: Manago (occultation phenomenon is not detected). Y-D, Y-R: disappearance and reappearance of main body observed by Yamamura. W-D, W-R: Main body phenomenon Watanabe observed. Y-B, W-B: the second dip at the frame middle time.

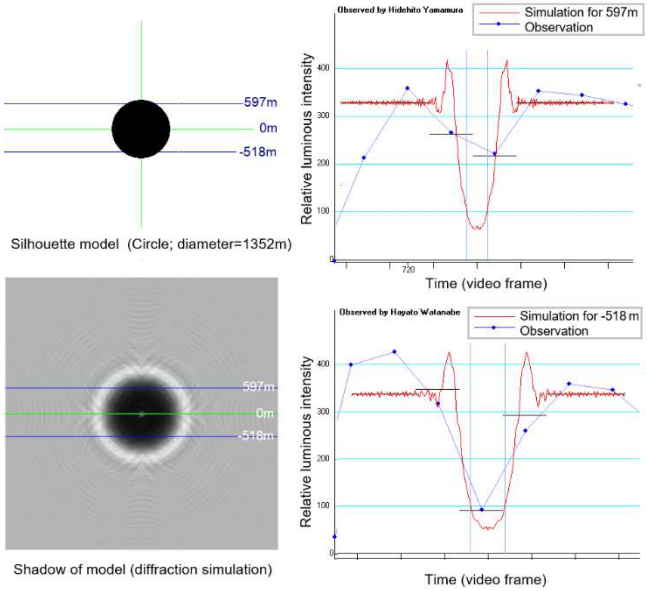

Figure 4. Comparison of the observed lightcurve with the simulated model. Left: Estimated circle silhouette model of the small object (top) and its diffraction-simulated shadow. Right: Most likely simulated lightcurve (red curve), and observed lightcurve. The blue vertical lines show the time of the geometric occultation phenomena.

Figure 4 shows the most likely size of the small object that caused the second light drop, assuming a circular profile. The estimated occultation times of two observers obtained from the diffraction simulation were plotted on the sky plane in a consistent manner (Figure 5). From the sky-plane plot, the size of the main body is given as 6.1 km × 8.7 km by an elliptical fit which does not occult the star at the Manago's observation site. The size of the satellite is estimated as 1.35 km × 1.35 km by diffraction simulation assuming a circular body. Assuming the above estimate, the position of the satellite relative to the main body is derived as: separation 4.8 mas in P.A. -82 degrees at 2024 Aug. 21.781527 UT. Note that no error has been added to the above values in this estimate because the uncertainty in the fit cannot be determined as only two observations were available to plot.

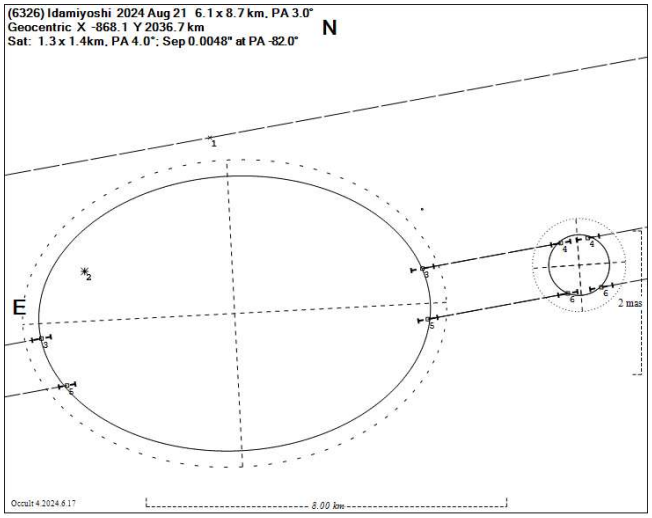

Figure 5. Sky-plane plot with estimated shape and size of the small object, with a possible satellite added. Error bars are given as 3 sigma estimates from the lightcurve noise. The ellipse drawn with dashed line indicates the peak of brightness caused by diffraction.

Conclusion

The observation of the stellar occultation caused by the asteroid (6326) Idamiyoshi was performed by Watanabe, Yamamura, and Manago in Japan on 2024 August 21 at 18.75 hr (UT).

The lightcurve obtained from Watanabe's observations showed a significant decrease in brightness (more than 1.4 magnitudes) during both the first and second dimming. Similar lightcurves were also obtained from Yamamura's observations. Furthermore, diffraction simulations yielded event times consistent with the observational results from the two different observing sites. Based on these results, it is very likely that a satellite has been discovered around the asteroid (6326) Idamiyoshi.

Acknowledgements

Miyoshi Ida (after whom the asteroid is named) provided a number of predictions for occultation phenomena, including this event. Tsutomu Hayamizu, Fumi Yoshida and others from the International Occultation Timing Association - East Asia (IOTA/EA) received the observation reports from the three observers and reduced the event time data. Dave Herald gave us valuable advice and discussion on whether this phenomenon was caused by an asteroidal satellite, and also advised us to publish the results. We thank them all.

References

Clark, M. (2016). "Asteroid photometry from the Preston Gott Observatory." *Minor Planet Bull.* **43**, 132-135. *https://articles.adsabs.harvard.edu/pdf/2016MPBu...43..132C*

Durech, J.; Tonry, J.; Erasmus, N.; Denneau, L. (2020). "Asteroid models reconstructed from ATLAS photometry." *Astron. Astrophys.* **643**, A59. *https://www.aanda.org/articles/aa/pdf/2020/11/aa37729-20.pdf*

Masiero, J.R.; Mainzer, A.K.; Grav, T.; Bauer, J.M.; Cutri, R.M.; Dailey, J.; Eisenhardt, P.R.M.; McMillan, R.S.; Spahr, T.B.; Skrutskie, M.F.; Tholen, D.; Walker, R.G.; Wright, E.L.; DeBaun, E.; Elsbury, D.; Gautier, T.; Gomillion, S.; Wilkins, A. (2011). "Main Belt Asteroids with WISE/NEOWISE. I. Preliminary Albedos and Diameters." *Astroph. J.* **741**, 68.

Miyashita, K.; Hayamizu, T.; Sôma, M. (2006). "LIMOVIE, a new light measurement tool for occultation observation using video recorded." *Rep. Natl. Astron. Obs. Jpn.* **9**, 1-26 (in Japanese).

Roques, F.; Moncuquet, M.; Sicardy, B. (1987). "Stellar occultations by small bodies: Diffraction effects." *The Astronomical Journal* **93**(6), 1549-1558. *https://adsabs.harvard.edu/full/1987AJ.....93.1549R*

Trahan, R.; Hyland, D. (2014). "Phase retrieval applied to stellar occultation for asteroid silhouette characterization." *Applied Optics* **53**(16), 3540-3547. *https://opg.optica.org/ao/abstract.cfm?uri=ao-53-16-3540*

Waszczak, A.; Chang, C.-K.; Ofek, E.O.; Laher, R.; Masci, F.; Levitan, D.; Surace, J.; Cheng, Y.-C.; Ip, W.-H.; Kinoshita, D.; Helou, G.; Prince, T.A.; Kulkarni, S. (2015). "Asteroid Light Curves from the Palomar Transient Factory Survey: Rotation Periods and Phase Functions from Sparse Photometry." *Astron. J.* **150**, A75.

GENERAL REPORT OF POSITION OBSERVATIONS BY THE ALPO MINOR PLANETS SECTION FOR THE YEAR 2024

Frederick Pilcher
4438 Organ Mesa Loop
Las Cruces, NM 88011 USA
fpilcher35@gmail.com

(Received: 2025 April 4)

Observations of positions of minor planets by members of the Minor Planets Section in calendar year 2024 are summarized.

During the year 2024 a total of 442 visual observations of 102 different minor planets were reported by members of the Minor Planets Section.

The summary lists minor planets in numerical order, the observer and telescope aperture (in cm), UT dates of the observations, and the total number of observations in that interval. When a significant departure from the predicted magnitude was noted, it is stated in the next line below the number of positions. The year is 2024 in each case.

Positional observations were contributed by the following observers:

Observer, Instrument	Location	Planets	Positions
Faure, Gérard		31	78
20 cm Celestron	Vaison la Romaine (France)		
35 cm Meade LX200	Col de L'Arzelier (France)		
45 cm Dobson Skywatcher	Vaison la Romaine (France)		
Harvey, G. Roger	Concord, North	74	364
81 cm Newtonian	Carolina, USA		
Rayon, Jean-Michel (with Gérard Faure)		5	11
45 cm Dobson Skywatcher	Vaison la Romaine (France)		

MINOR PLANET	OBSERVER & APERTURE (cm)	OBSERVING PERIOD (2024)	NO. OBS.
5 Astraea	Faure, 20	Apr 11	2
23 Thalia	Faure, 20	Apr 11-12	2
24 Themis	Harvey, 81	Feb 14	6
891 Gunhild	Harvey, 81	Mar 29	6
1036 Ganymed	Faure & Rayon, 45	Nov 3	2
1083 Salvia	Faure, 20	Apr 11-12	2
1201 Strenua	Faure, 35	Sep 1	2
1203 Nanna	Faure, 35	Oct 5	2
1313 Berna	Faure, 35	Sep 6-7	2
1367 Nongoma	Faure, 35	Aug 5	2
1394 Algoa	Faure, 35	Aug 31	2
1402 Eri	Harvey, 81	Jul 11	3
1779 Parana	Harvey, 81	Aug 26	3
1823 Gliese	Faure, 35	Aug 31	2
1833 Shmakova	Faure, 35	Jun 5	3
2445 Blazhko	Faure & Rayon, 45	Nov 3	3
2456 Palamedes	Harvey, 81	Feb 1	3
2571 Geisei	Faure, 35	Sep 7	2
2693 Yan'an	Faure & Rayon, 45	Nov 3	2
2994 Flynn	Harvey, 81	Sep 9	3
3028 Zhongguoxi	Faure, 35	Aug 1	2
3696 Herald	Harvey, 81	Sep 9	3
3775 Ellenbeth	Harvey, 81	Sep 9	3
4203 Brucato	Harvey, 81	Sep 9	3
4446 Carolyn	Faure, 35	Aug 2	2
4553 Doncampbell	Faure, 35	Aug 5	3
4764 Joneberhart	Faure, 35	Jul 9	3
4805 Asteropaios	Faure, 35	Sep 6	2
4836 Medon	Harvey, 81	Feb 3	3
4945 Ikenozenni	Faure, 35	Aug 2	3
4956 Noymer	Harvey, 81	Sep 3	6
5264 Telephus	Harvey, 81	Jan 8	3
5415 Lyanzuridi	Harvey, 81	Jan 8	3
5660 1974 MA	Harvey, 81	Aug 21	3
5661 Hildebrand	Harvey, 81	Aug 26	3
5996 Julioangel	Harvey, 81	Aug 27	3
6012 Williammurdoch	Harvey, 81	Jun 8	3
6460 Bassano	Harvey, 81	Jan 20	3
6537 Adamovich	Harvey, 81	Aug 26	3
6859 Datemasamune	Faure, 35	Aug 6	3
6874 1994 JO1	Faure, 35	Jun 5	4
7079 Baghdad	Faure, 35	Aug 1-2	2
7333 Bec-Borsenberger	Harvey, 81	Aug 27	3
7440 Zavist	Harvey, 81	Jan 30	3
7870 1987 UP2	Faure & Rayon, 45	Nov 2	2
8823 1987 WS3	Faure & Rayon, 45	Nov 2	2
8992 Magnanimity	Faure, 35	Aug 7	3
9175 Graun	Harvey, 81	Oct 23	3
			0.4f@16.1
9700 Paech	Harvey, 81	Oct 3	3
10487 Danpeterson	Faure, 20	Jul 4	4
	Harvey, 81	Jun 8	3
11018 1983 CZ2	Harvey, 81	Feb 1	3
12559 1998 QB69	Harvey, 81	Feb. 3	3
13474 V'yus	Harvey, 81	Oct 7	3
13502 1987 WD	Harvey, 81	Oct 3	6
14162 1998 TV1	Harvey, 81	Sep 23	3
17554 1993 VY	Harvey, 81	Nov 1	3
			0.5f@16.2
17662 1996 VG30	Harvey, 81	Feb 6	3
20231 1997 YK	Harvey, 81	Nov 1	6
21088 Chelyabinsk	Harvey, 81	Jul 11	6
21374 1977 WS22	Faure, 20	May 9	5
	Harvey, 81	May 10-11	12
21652 Vasishtra	Faure, 35	Aug 2	2
26110 1991 NK4	Harvey, 81	Jul 2	4
26916 1996 RR2	Harvey, 81	Feb 6	3
28188 1998 WV19	Harvey, 81	Feb 6	3
33323 Lucaspaganini	Harvey, 81	May 11	3
36183 1999 TX16	Harvey, 35	Nov 12	6
41074 1999 VL40	Harvey, 81	Jan 8	3
			0.5f@15.9
43028 1999 VE23	Harvey, 81	Nov 1	3
			0.5f@16.1
44700 1999 SG3	Harvey, 81	Nov 22	6
47834 2000 EN14	Harvey, 81	Nov 22	6
66251 1999 GJ2	Harvey, 81	Aug 27	6
			0.3f@16.3
93040 2000 SG	Harvey, 81	Jan 8	3
152787 1999 TB10	Harvey, 81	Mar 15	6
154589 2003 MX2	Harvey, 81	Oct 7	3
159399 1998 UL1	Harvey, 81	Apr 29	6
164217 2004 PT42	Harvey, 81	Aug 5	6
189099 2001 RO	Harvey, 81	Nov 22	6
219071 1997 US9	Harvey, 81	Oct 25	6
302523 2002 KH3	Harvey, 81	Jun 14	6
363027 1998 ST27	Harvey, 81	Oct 3-9	18
385268 2001 RC12	Harvey, 81	Oct 24	6
415029 2011 HL21	Fauare, 20	Sep 4	4
417264 2006 AT2	Harvey, 81	Feb 4	6
439437 2023 NK4	Harvey, 81	Apr 16	6
447755 2007 JX2	Harvey, 81	Nov 24	6
450649 2006 UY64	Harvey, 81	Oct 26	6
458122 2010 EW45	Harvey, 81	Dec 31	6
481032 2004 YZ23	Faure, 35	Jun 4	3
	Harvey, 81	Jun 11	6
482049 2009 XG8	Harvey, 81	May 10-11	12
523660 2012 KY41	Harvey, 81	Oct 23	6
2002 AY1	Harvey, 81	Jan 8	6
2006 WB	Harvey, 81	Nov 23	6
2008 OS7	Harvey, 81	Jan 30	6
2020 WG	Harvey, 81	Oct 29	6
2020 XR	Harvey, 81	Dec 3	6
2022 TN1	Harvey, 81	Apr 29	6
2023 SP1	Harvey, 81	Feb 8	6
2024 CR9	Harvey, 81	Jun 14	6
2024 MK	Harvey, 81	Jun 30	6
2024 PN3	Harvey, 81	Nov 22	6
2024 RZ5	Harvey, 81	Nov 24	6
2024 TX13	Harvey, 81	Nov 3	6

LIGHTCURVE PHOTOMETRY OPPORTUNITIES: 2025 JULY-OCTOBER

Brian D. Warner
Center for Solar System Studies (CS3)
446 Sycamore Ave.
Eaton, CO 80615 USA
brian@MinPlanObs.org

Alan W. Harris
Center for Solar System Studies (CS3)
La Cañada, CA 91011-3364 USA

Josef Ďurech
Astronomical Institute
Charles University
18000 Prague, CZECH REPUBLIC
durech@sirrah.troja.mff.cuni.cz

Lance A.M. Benner
Jet Propulsion Laboratory
Pasadena, CA 91109-8099 USA
lance.benner@jpl.nasa.gov

(Received: 2025 April 15)

We present lists of asteroid photometry opportunities for 2025 July-October. The extended four-month listing allows better observation planning, especially for those working in wide-spread collaborations. With the massive input of survey photometry, even if mostly sparse data, the small telescope researcher's role is moving away generic studies to those concentrating on specific needs and targets and so, we hope, leading to even more fulfilling and fruitful efforts.

We refer the reader to the lightcurve photometry opportunities article in *Minor Planet Bulletin* 51-4 (Warner et al., 2024) for a detailed discussion on the evolution of the lists presented here and the purpose behind each one. In addition, we refer the reader to other prior releases of this paper (e.g., Warner et al., 2023) for more detailed discussions about the requirements and considerations for the targets in the lists and to Warner et al. (2021a; 2021b).

On-Line Planning Tool

The ephemeris generator on the *https://MinorPlanet.info* web site allows creating custom lists for numbered objects reaching V ≤ 18.0 during a given month from 2020 through 2035 by setting search parameters based on a number of parameters.

https://www.minorplanet.info/php/callopplcdbquery.php

The updated page added data for the minimum phase angle of any object included in the search: the date (0.001 d), the minimum phase angle (0.1°), and the declination. Searches can limit results to a phase angle range between 0-120°. Also new is limiting the results to a range of rotation periods and so, for example, one can look for only long, or especially short, period objects.

Important and Useful Web Sites

The dates and values given on the MinorPlanet.info site are very good estimates in most cases. NEAs are sometimes an important exception. Use the site for preliminary planning for objects and then confirm those plans using the Minor Planet Center or JPL Horizons web sites.

MPC: *http://www.minorplanetcenter.net/iau/MPEph/MPEph.html*
JPL: *https://ssd.jpl.nasa.gov/sb/orbits.html*

Those doing work for modeling should contact Josef Ďurech at the email address above. If looking to add lightcurves for objects with existing models, visit the Database of Asteroid Models from Inversion Techniques (DAMIT) web site.

https://astro.troja.mff.cuni.cz/projects/damit/

to see what, if any, information it has on a chosen target.

For near-Earth asteroids in particular, check the list found on the Goldstone planned targets schedule at

http://echo.jpl.nasa.gov/asteroids/goldstone_asteroid_schedule.html

and keep in touch with Lance Benner at the email above. The radar team often needs updated astrometry and photometry (rotation period) prior to observing. Keep in mind as well that the *MinorPlanet.info* site opposition database includes only numbered objects. Keep a close eye on the MPC NEA pages.

Once you've obtained and analyzed your data, it's important to publish your results. Papers appearing in the *Minor Planet Bulletin* are indexed in the Astrophysical Data System (ADS) and so can be referenced by others in subsequent papers. It's also important to make the data available at least on a personal website or upon request. We urge you to consider submitting your raw data to the ALCDEF database. This can be accessed for uploading and downloading data at

http://www.alcdef.org

The database contains about 10.94 million observations for 24,639 objects (as of 2024 May 27), making it one of the more useful sources for raw data of *dense* time-series asteroid photometry.

The Planning Lists

The lists, excluding the one for NEAs, are usually restricted to objects reaching V ≤ 15.5 during the covered months. To include every object within a list that met this criterium alone resulted in far too many targets than the known community of asteroid photometrists could possibly handle, so only the "better" candidates are included. This is entirely subjective and the reader is encouraged to visit the *https://MinorPlanet.info* web site and use all the planning tools available there should our preferences not match yours.

Don't presume that something rated U ≥ 3– doesn't need more work nor, at the other end, that something not rated at all or 1– < U < 2+ or has a long period should be skipped in lieu of an "easier" project. The often-heard saying, "Past performance is not a guarantee of future results" should be part of your work ethic. Someone's "certain" result may not be so certain after all, especially if it's based on data that are minimal in quantity and/or quality.

Favorable Apparitions includes objects reaching one of the five brighter (favorable) apparitions from 1995 and 2050 and rated U < 3- in the LCDB (Warner et al., 2009).

No Pole Solutions includes objects rated U > 2+ but do not have a pole indicated on the LCDB summary line. This is list is the most likely needing further confirmation by checking the DAMIT web site, which grows in spurts large and small quite frequently and so the LCDB can lag considerably.

Poor Pole Solutions includes objects rated U < 3– that have a pole solution on the summary line. In this case, the period is often based on using sparse survey data, with or without support of dense lightcurve data. An additional set of dense data may help elevate both the U rating and the quality of the pole solution.

Low Phase Angles includes objects, regardless of U rating or even having a period, that reach a solar phase angle < 1°. You should refer to Warner et al. (2023) to review important information about low solar phase angle work.

Long Periods includes objects with $P \geq \sim 24$ hours. These are often overlooked because they are very difficult for a single-station campaign. However, they are ideal for collaborations, especially those with stations well-separated in longitude.

NEAs (aka Radar Target) is limited to *known* near-Earth asteroids that might be on the radar team's radar (pun intended). It is common for newly discovered objects to move into or out of the list. We recommend that you keep up with the latest discoveries by using the Minor Planet Center observing tools.

The List Data

If the list includes the "Fam" column, this is the orbital group (> 9000) using criteria from the LCDB or the collisional family (< 9000) based on Nesvorny et al. (2015) and Nesvorny (2015). To convert the number to a name, see the LCDB documentation on the LCDB web site or use the One Asteroid Lookup page on the site:

https://www.minorplanet.info/php/lcdb.php
https://minorplanet.info/php/oneasteroidinfo.php

Table Columns

Num	Asteroid number, if any.
Name	Name (or designation) assigned by the MPC.
Fam	Orbital group or collisional family.
BMD	Date of maximum brightness (to 0.1 d precision).
BMg	Approximate V magnitude at brightest.
BDC	Approximate declination at brightest.
PD	Date of minimum phase angle (to 0.001 d precision).
PMn	Phase angle at minimum (solar elongation > 90°).
PDC	Approximate declination at minimum phase angle.
P (h)	Synodic rotation period from summary line in the LCDB summary table. An * indicates a sidereal period.
U	LCDB solution quality (U) from 1 (probably wrong) to 3 (secure).
Notes	Comments about the object.

Some asteroids may appear in more than one list. The reader is referred to the latest LCDB release and, where and when necessary, the original reference source should be used. The Notes column is rarely used, for now, except for the NEAs list.

Calculations of brightest and minimum phase are by Brian D. Warner. For minimum phase, the observer should use the JPL Small Bodies Node Ephemeris site for more precise information. All periods are taken from the summary line of the LCDB. If needed, the LCDB should be checked to find the source of the summary line period.

Favorable Apparitions (U < 3-)

Num	Name	Fam	BMD	BMg	BDC	PD	PMn	PDC	P (h)	U	Notes
896	Sphinx	9104	07 11.3	13.5	-12	07 12.270	5.2	-12	21.038	2+	
2898	Neuvo	9104	07 15.5	14.8	-20	07 15.431	0.7	-20	13.83	2	
4826	Wilhelms	701	07 16.0	14.8	-39	07 14.779	9.8	-39	15.004	2	
1728	Goethe Link	9104	07 22.2	14.2	-10	07 22.169	4.7	-10	81	2	
6422	Akagi	502	07 25.4	14.8	-18	07 25.748	0.9	-18	7.74	2	
2865	Laurel	506	07 30.9	14.3	-24	07 31.204	2.5	-24	21.5	2	
3729	Yangzhou	502	08 02.9	14.6	-38	08 02.443	9.9	-38	29.158	2	
1606	Jekhovsky	9105	08 10.9	13.8	-3	08 09.641	7.4	-3	165.946	2	
1493	Sigrid	405	08 15.5	13.4	-15	08 15.166	0.4	-15	43.296	2	
3069	Heyrovsky	2004	08 17.3	14.8	-10	08 17.141	2.1	-10	6.6	2	
982	Franklina	9106	08 21.7	13.3	0	08 23.231	4.9	0	263.5	2	
7723	Lugger	9103	08 30.2	14.9	-19	08 27.856	6.1	-19	4.834	2	
3485	Barucci	2004	08 30.4	14.9	-8	08 30.837	0.6	-8	14.65	1	
2451	Dollfus	9106	09 02.4	14.5	-6	09 02.140	0.9	-6	48	1	
2097	Galle	9106	09 03.3	14.7	-5	09 03.300	1.2	-5	7.31	2	
4583	Lugo	9104	09 04.4	14.7	-7	09 05.025	0.1	-7	12	1	
1632	Siebohme	9105	09 11.1	14.5	0	09 11.345	2.3	0	56.65	2	
4257	Ubasti	9101	09 12.0	14.6	-4	09 11.931	0.6	-4	4.4	1	
1984	Fedynskij	9106	09 13.4	14.8	-2	09 14.010	0.7	-2	8.14	2	
994	Otthild	9104	09 19.5	12.6	-4	09 19.650	1.3	-4	5.95	2+	
2109	Dhotel	9105	09 28.5	14.1	-4	09 28.954	3.3	-4	32	1	
1475	Yalta	9104	10 02.5	14.3	5	10 02.285	0.9	5	70.77	2	
1615	Bardwell	602	10 07.5	14.6	4	10 06.828	0.7	4	17	2	
1024	Hale	9106	10 27.1	13.7	1	10 28.162	5.4	1	106.047	2+	
1555	Dejan	9105	10 28.0	13.8	25	10 29.650	5.7	24	16.96	2+	

Table I. A partial list of numbered asteroids reaching a favorable apparition and with an LCDB rating U < 3-.

Spin Axis and Modeling (Favorable Apparition, U > 2+, No LCDB pole, not in DAMIT)

Num	Name	Fam	BMD	BMg	BDC	PD	PMn	PDC	P (h)	U	Notes
1093	Freda	9106	05 18.5	12.3	-20	05 16.999	0.1	-20	19.670	3	
19261	1995 MB	9104	07 14.5	14.5	-5	07 14.923	8.8	-5	4.591	3	
1853	McElroy	9106	07 23.5	14.9	-20	07 21.728	0.1	-20	8.016	3-	
3578	Carestia	9106	08 17.3	14.2	+9	08 17.251	9.1	+9	9.974	3	
2408	Astapovich	9105	08 22.5	14.8	-4	08 23.869	3.8	-4	3.674	3	
379	Huenna	602	09 06.1	12.2	-7	09 05.144	0.2	-6	14.141	3	
3687	Dzus	9106	09 10.8	14.7	+17	09 11.998	10.9	+17	58.12	3-	
995	Sternberga	9105	09 11.0	12.8	+13	09 11.515	8.9	+13	11.191	3	
5567	Durisen	624	09 11.6	14.4	-14	09 12.558	4.2	-14	7.001	3	
1916	Boreas	NEA	09 14.7	14.7	+21	10 06.850	14.8	+26	3.475	3	
152664	1998 FW4	NEA	09 28.0	13.9	+39	09 17.927	10.9	+4	17.38	3	
477	Italia	9104	09 29.4	11.8	+2	09 30.157	0.4	+2	19.413	3	
4217	Engelhardt	4217	10 01.5	14.2	+18	10 03.211	7.9	+19	3.066	3	
1453	Fennia	9102	10 03.7	13.9	+8	10 03.884	1.9	+8	4.412	3	
1234	Elyna	606	10 06.1	14.8	+16	10 06.034	4.5	+16	5.422	3	
1346	Gotha	502	10 09.2	14.1	-5	10 08.283	5.6	-5	2.64	3	
1071	Brita	9106	10 31.5	13.7	+12	10 31.320	0.9	+12	5.817	3	

Table II. A partial list of numbered asteroids reaching a favorable apparition that have high-quality periods solutions but do not have a pole solution in the LCDB or DAMIT databases.

Spin Axis and Modeling (Any Apparition, U < 3–, Pole in LCDB)

Num	Name	Fam	BMD	BMg	BDC	PD	PMn	PDC	P (h)	U	Notes
1287	Lorcia	606	04 02.4	15.0	-7	04 02.576	0.9	-7	8.878	2	
2906	Caltech	9106	07 12.5	15.2	-43	07 11.024	6.9	-43	12.994	2+	
1913	Sekanina	605	07 24.5	15.2	-22	07 23.536	0.7	-22	14.035	2+	
1858	Lobachevskij	9106	08 07.4	15.0	-14	08 08.039	0.8	-14	5.413	2+	
982	Franklina	9106	08 21.7	13.3	0	08 23.231	4.9	+0	263.5	2	
3409	Abramov	605	09 07.5	15.5	-5	09 06.872	0.6	-5	7.791	2+	
926	Imhilde	639	09 10.1	15.4	-23	09 12.556	6.3	-23	25.977	2+	
470	Kilia	9104	09 10.4	13.0	-3	09 11.450	0.4	-4	296.2	2+	
1632	Siebohme	9105	09 11.1	14.5	0	09 11.345	2.3	+0	56.65	2	
1167	Dubiago	9106	09 16.4	14.5	3	09 16.625	1.9	+3	34.818	2	
994	Otthild	9104	09 19.5	12.6	-4	09 19.650	1.3	-4	5.95	2+	
1475	Yalta	9104	10 02.5	14.3	5	10 02.285	0.9	+5	70.77	2	
892	Seeligeria	9106	10 19.6	14.4	-5	10 18.793	5.2	-5	16.693	2+	
1118	Hanskya	2013	10 26.8	14.8	31	10 27.616	5.9	+31	25.31	2	
1555	Dejan	9105	10 28.0	13.8	25	10 29.650	5.7	+24	16.96	2+	

Table III. A partial list of numbered asteroids reaching brightest magnitude that have a reported pole position but the LCDB rating is U < 3-.

Low Phase Angle (V ≤ 15.0, phase angle α ≤ 1.0°)

Num	Name	Fam	BMD	BMg	BDC	PD	PMn	PDC	P (h)	U	Notes
551	Ortrud	9106	07 06.5	14.1	-23	07 04.323	0.2	-23	17.416	3	
295	Theresia	9106	07 08.5	14.1	-22	07 06.639	0.2	-22	10.702	3	
1853	McElroy	9106	07 23.5	14.9	-20	07 21.728	0.1	-20	8.016	3-	
390	Alma	9105	07 26.5	14.0	-19	07 28.418	0.2	-19	3.741	3	
3478	Fanale	9104	07 27.5	14.9	-19	07 27.092	0.2	-19	3.245	3	
522	Helga	9106	07 28.5	13.7	-20	07 26.068	0.2	-20	8.129	3	
30	Urania	9104	08 03.5	9.9	-18	08 02.101	0.1	-18	13.686	3	
62	Erato	602	08 03.5	12.9	-18	08 01.754	0.1	-18	9.221	3	
53	Kalypso	9105	08 12.5	12.7	-15	08 11.016	0.2	-15	9.036	3	
64	Angelina	9105	08 13.2	11.7	-15	08 12.493	0.2	-15	8.752	3	
609	Fulvia	9106	09 02.4	14.4	-7	09 03.577	0.2	-7	35.375	3	
379	Huenna	602	09 06.1	12.2	-7	09 05.144	0.2	-6	14.141	3	
2524	Budovicium	602	09 07.4	14.6	-5	09 08.926	0.2	-5	10.082	3	
1686	De Sitter	602	10 04.4	14.9	5	10 06.114	0.1	+5	11.292	3-	
697	Galilea	9106	10 06.4	12.4	5	10 07.802	0.2	+5	16.538	3	
1084	Tamariwa	9105	10 06.4	14.0	5	10 07.945	0.3	+5	6.196	3	
1207	Ostenia	606	10 12.5	14.6	7	10 11.503	0.2	+7	9.073	3	
1358	Gaika	9104	10 13.4	15.0	8	10 14.672	0.2	+8	10.1	3	
85	Io	502	10 16.4	10.3	9	10 16.939	0.1	+9	6.875	3	

Table IV. A partial list of numbered asteroids reaching a minimum phase angle α ≤ 1.0°. Bold indicates a favorable apparition.

Long Period (Favorable Apparition, $P \geq 24$ h, U < 3)

Num	Name	Fam	BMD	BMg	BDC	PD	PMn	PDC	P (h)	U	Notes
5438	Lorre	527	03 14.0	14.7	-40	03 13.600	20.1	-40	25.30	2+	
2045	Peking	401	03 21.5	14.6	+2	03 21.506	1.0	+02	158.7	2	
85953	1999 FK21	9101	04 05.0	14.6	+34	03 31.001	30.1	+11	28.08	2	
1512	Oulu	9107	04 08.5	14.3	-8	04 06.829	0.3	-08	132.3	2+	
1101	Clematis	2012	04 15.5	14.9	-8	04 13.453	0.3	-08	34.3	2	
6372	Walker	604	05 15.5	14.9	-15	05 15.378	1.7	-15	44.25	2	
1905	Ambartsumian	9104	05 16.8	14.1	-16	05 16.674	1.7	-16	92.153	2	
1457	Ankara	9105	06 09.5	13.5	-30	06 09.831	2.9	-30	35.54	2	
2660	Wasserman	502	06 14.0	14.9	-4	06 12.481	8.7	-04	527.991	2	
1728	Goethe Link	9104	07 22.2	14.2	-10	07 22.169	4.7	-10	81.	2	
3729	Yangzhou	502	08 02.9	14.6	-38	08 02.443	9.9	-38	29.158	2	
3009	Coventry	402	08 07.7	15.0	-25	08 07.489	5.0	-25	78.964	2-	
1606	Jekhovsky	9105	08 10.9	13.8	-3	08 09.641	7.4	-03	165.946	2	
5687	Yamamotoshinobu	9106	08 11.2	14.8	-18	08 11.093	1.1	-18	154.868	2	
1493	Sigrid	405	08 15.5	13.4	-15	08 15.166	0.4	-15	43.296	2	
982	Franklina	9106	08 21.7	13.3	+0	08 23.231	4.9	+00	263.5	2	
2451	Dollfus	9106	09 02.4	14.5	-6	09 02.140	0.9	-06	48.	1	
1632	Siebohme	9105	09 11.1	14.5	+0	09 11.345	2.3	+00	56.65	2	
2109	Dhotel	9105	09 28.5	14.1	-4	09 28.954	3.3	-04	32.	1	
1475	Yalta	9104	10 02.5	14.3	+5	10 02.285	0.9	+05	70.77	2	
1024	Hale	9106	10 27.1	13.7	+1	10 28.162	5.4	+01	106.047	2+	
2263	Shaanxi	606	10 28.8	15.0	+8	10 29.036	2.2	+08	272.2	2	
2490	Bussolini	502	11 09.2	14.8	+11	11 09.210	2.6	+11	24.	1	
1952	Hesburgh	9106	11 12.8	14.1	+7	11 12.767	4.1	+07	47.52	2	
1122	Neith	9105	11 14.9	13.3	+17	11 14.868	0.9	+17	25.11	2	
923	Herluga	9105	11 19.2	14.1	+3	11 20.538	8.2	+02	30.61	2	
3171	Wangshouguan	9106	12 06.6	15.0	+35	12 07.055	4.4	+35	43.548	2+	
4293	Masumi	9106	12 16.8	14.7	+31	12 16.358	3.6	+31	36.	2-	

Table V. A partial list of numbered asteroids reaching a favorable apparition and with a reported period $P \geq 24$ hours.

NEAs (aka Radar) Reaching Brightest for Year (Any Apparition, V ≤ 17.0, α ≤ 90°)

Num	Name	Fam	BMD	BMg	BDC	PD	PMn	PDC	P (h)	U	Notes
437844	1999 MN	9101	07 02.4	16.4	-32	07 01.890	8.6	-32	5.495	3	
348400	2005 JF21	9101	07 13.5	16.5	+9	12 07.061	14.2	-01	2.415	3	PHA
35107	1991 VH	9101	07 25.4	15.0	+56				2.624	3	PHA, BA, NHATS
442609	2012 KU42	9101	07 29.1	16.7	+5	12 20.839	23.4	-14			
613291	2005 YX128	9101	08 01.4	15.7	+46						
333284	1999 PJ1	9101	08 12.1	16.6	-14	08 12.296	0.8	-14	6.201	3	
2100	Ra-Shalom	9101	08 19.3	14.6	+32	08 30.500	43.3	+08	19.797	3	
1981	Midas	9101	09 09.4	17.0	+46	10 30.234	24.3	+51	5.220	3	PHA
89830	2002 CE	9101	09 10.6	16.7	+35				2.615	2-	
4257	Ubasti	9101	09 12.0	14.6	-4	09 11.931	0.6	-04	4.4	1	
1916	Boreas	9101	09 14.7	14.8	+21	10 06.850	14.8	+26	3.475	3	
162117	1998 SD15	9101	09 22.7	17.0	+17	10 03.340	46.4	-10	7.33	3-	
152664	1998 FW4	9101	09 28.0	13.9	+39	09 17.927	10.9	+04	17.38	3	PHA
219071	1997 US9	9101	09 28.4	16.8	+35	10 06.241	28.8	+26	3.319	3-	
443837	2000 TJ1	9101	10 03.7	16.9	+3	10 03.825	1.2	+03	14.09	3-	
461397	2001 SD170	9101	10 10.8	14.9	+5	10 09.982	5.4	+07			
112985	2002 RS28	9101	10 20.8	15.7	+31	10 26.971	18.7	+20	4.787	2	
144900	2004 VG64	9101	10 26.1	15.9	-5						
99907	1989 VA	9101	10 29.2	16.7	+40	11 12.914	54.7	+10	2.525	3	
164206	2004 FN18	9101	10 30.0	14.0	+8	10 27.947	6.0	+13			

Table VI. A list of near-Earth asteroids known as of 2025 April 14. Green bar lines are on the Goldstone list of planned targets. PHA: Potentially Hazardous Asteroid. NHATS: Near-Earth Object Human Space Flight Accessible Targets Study. BA: Binary asteroid. This is not necessarily a complete list of Goldstone targets. Check their web site.

References

Nesvorny, D. (2015). "Nesvorny HCM Asteroids Families V3.0." NASA Planetary Data Systems, id. EAR-A-VARGBET-5-NESVORNYFAM-V3.0.

Nesvorny, D.; Broz, M.; Carruba, V. (2015). "Identification and Dynamical Properties of Asteroid Families." In Asteroids IV (P. Michel, F. DeMeo, W.F. Bottke, R. Binzel, Eds.). Univ. of Arizona Press, Tucson, also available on astro-ph.

Warner, B.D.; Harris, A.W.; Pravec, P. (2009). "The Asteroid Lightcurve Database." *Icarus* **202**, 134-146. Updated 2023 Oct. *https://www.minorplanet.info/php/lcdb.php*

Warner, B.D.; Harris, A.W.; Ďurech, J.; Benner, L.A.M. (2021a). "Lightcurve Photometry Opportunities: 2021 January-March." *Minor Planet Bull.* **48**, 89-97.

Warner, B.D.; Harris, A.W.; Ďurech, J.; Benner, L.A.M. (2021b). "Lightcurve Photometry Opportunities: 2021 October-December." *Minor Planet Bull.* **48**, 406-410.

Warner, B.D.; Harris, A.W.; Ďurech, J.; Benner, L.A.M. (2023). "Lightcurve Photometry Opportunities: 2023 July - September." *Minor Planet Bull.* **50**, 240-244.

Warner, B.D.; Harris, A.W.; Ďurech, J.; Benner, L.A.M. (2024). "Lightcurve Photometry Opportunities: 2024 October - 2025 January." *Minor Planet Bull.* **51**, 379-384.

IN THIS ISSUE

This list gives those asteroids in this issue for which physical observations (excluding astrometric only) were made. This includes lightcurves, color index, and H-G determinations, etc. In some cases, no specific results are reported due to a lack of or poor-quality data. The page number is for the first page of the paper mentioning the asteroid. EP is the "go to page" value in the electronic version.

THE MINOR PLANET BULLETIN (ISSN 1052-8091) is the quarterly journal of the Minor Planets Section of the Association of Lunar and Planetary Observers (ALPO, http://www.alpo-astronomy.org). Current and most recent issues of the *MPB* are available on line, free of charge from:

https://mpbulletin.org/

The Minor Planets Section is directed by its Coordinator, Prof. Frederick Pilcher, 4438 Organ Mesa Loop, Las Cruces, NM 88011 USA (fpilcher35@gmail.com). Robert Stephens (rstephens@foxandstephens.com) serves as Associate Coordinator. Dr. Alan W. Harris (MoreData! Inc.; harrisaw@colorado.edu), and Dr. Petr Pravec (Ondrejov Observatory; ppravec@asu.cas.cz) serve as Scientific Advisors. The Asteroid Photometry Coordinator is Brian D. Warner (Center for Solar System Studies), Palmer Divide Observatory, 446 Sycamore Ave., Eaton, CO 80615 USA (brian@MinorPlanetObserver.com).

The Minor Planet Bulletin is edited by Professor Richard P. Binzel, MIT 54-410, 77 Massachusetts Ave, Cambridge, MA 02139 USA (rpb@mit.edu). Brian D. Warner (address above) is Associate Editor. Assistant Editors are Dr. David Polishook, Department of Earth and Planetary Sciences, Weizmann Institute of Science (david.polishook@weizmann.ac.il) and Dr. Melissa Hayes-Gehrke, Department of Astronomy, University of Maryland (mhayesge@umd.edu). The *MPB* is produced by Dr. Pedro A. Valdés Sada (psada2@ix.netcom.com).

Effective with Volume 50, the *Minor Planet Bulletin* is an electronic-only journal; print subscriptions are no longer available. In addition to the free electronic download of the *MPB* as noted above, electronic retrieval of all *Minor Planet Bulletin* articles (back to Volume 1, Issue Number 1) is available through the Astrophysical Data System:

http://www.adsabs.harvard.edu/

Authors should submit their manuscripts by electronic mail (rpb@mit.edu). Author instructions and a Microsoft Word template document are available at the web page given above. All materials must arrive by the deadline for each issue. Visual photometry observations, positional observations, any type of observation not covered above, and general information requests should be sent to the Coordinator.

* * * * *

The deadline for the next issue (52-4) is July 15, 2025. The deadline for issue 53-1 is October 15, 2025.

THIS PAGE IS INTENTIONALLY LEFT BLANK